Secondary Metabolites from Fungi *Coniella fragariae* and *Phomopsis* sp. D15a2a

Inaugural dissertation

for the attainment of the title of doctor
in the Faculty of Mathematics and Natural Sciences
at the Heinrich Heine University Düsseldorf

presented by

Haiqian Yu
from Shandong, P. R. China

Düsseldorf, 10, 2019

from the Institute of Pharmaceutical Biology and Biotechnology at the
Heinrich Heine University Düsseldorf

Published by permission of the
Faculty of Mathematics and Natural Sciences at
Heinrich Heine University Düsseldorf

Supervisor: Prof. Dr. Dres. h.c. Peter Proksch
Co-supervisor: Prof. Dr. Rainer Kalscheuer

Date of the oral examination: 18.12.2019

Erklärung

Hiermit erkläre ich ehrenwörtlich, dass ich die vorliegende Dissertation mit dem Titel „Sekundärmetaboliten aus den Pilzen *Coniella fragariae* und *Phomopsis* sp. D15a2a“ selbst angefertigt habe. Außer den angegebenen Quellen und Hilfsmitteln wurden keine weiteren verwendet. Diese Dissertation wurde weder in gleicher noch in abgewandelter Form in einem anderen Prüfungsverfahren vorgelegt. Weiterhin erkläre ich, dass ich früher weder akademische Grade erworben habe, noch dies versucht habe.

Düsseldorf, den 25.10.2019

Haiqian Yu

CONTENTS

ABSTRACT **1**

ZUSAMMENFASSUNG **3**

1 INTRODUCTION **5**

1.1 FUNGI AND THEIR METABOLITES 5

1.2 FUNGI: *CONIELLA* AND *PHOMOPSIS* 6

1.2.1 Fungi of the Genus Coniella *6*

1.2.2 Fungi of the Genus Phomopsis *7*

1.3 METABOLITES FROM *PHOMOPSIS* (*DIAPORTHE*) REPORTED DURING 2013-2018 7

1.3.1 Xanthone Derivatives *8*

1.3.2 Other Polyketide Metabolites *13*

1.3.3 Lipids *22*

1.3.4 Cytochalasins *23*

1.3.5 Peptides *25*

1.3.6 Terpenoids and Steroids *25*

1.4 AZAPHILONES, A GROUP OF BIOACTIVE POLYKETIDE METABOLITES (A REVIEW COVERING THE YEARS 2013-2018) 29

1.4.1 Classical Azaphilones *30*

1.4.2 Classical Azaphilones with Oxygen Linked Side Chains *34*

1.4.3 Unusual Azaphilones *37*

1.4.4 7, 8 - Lactone Ring Azaphilones and Their Derivatives *40*

1.4.5 Nitrogenous Azaphilones *44*

1.5 AIMS OF THE STUDY 47

2 AZAPHILONE DERIVATIVES FROM THE FUNGUS *CONIELLA FRAGARIAE* INHIBIT NF-*K*B ACTIVATION AND REDUCE TUMOR CELL MIGRATION **48**

3* AZAPHILONE PIGMENTS AND MACRODIOLIDES FROM THE COPROPHILOUS FUNGUS *CONIELLA FRAGARIAE **92**

4 POLYKETIDES AND NITROGENOUS METABOLITES FROM THE ENDOPHYTIC FUNGUS *PHOMOPSIS* SP. D15A2A **114**

5 DISCUSSION **161**

5.1 CHEMICAL CONSTITUENTS OF THE FUNGUS *CONIELLA FRAGARIAE* 161

5.1.1 Macrodiolides *161*
5.1.2 Azaphilones *163*
5.1.2.1 Structures of Azaphilones 163
5.1.2.2 Azaphilone Pigments 163
5.1.2.3 Bioactivities of Azaphilones 165
5.2 CHEMICAL CONSTITUENTS OF THE FUNGUS *PHOMOPSIS* SP. D15A2A 166
5.2.1 Koninginin Derivatives *166*
5.2.2 Pantothenic Acid Derivatives *167*
5.2.3 Tentoxin Derivatives *168*
5.3 CONCLUSION 169
6 REFERENCES 170
7 LIST OF ABBREVIATIONS 185
8 ACKNOWLEDGEMENTS 187
9 CURRICULUM VITAE 189

Abstract

Fungi and their secondary products play an important part in our daily life, not only in the field of pharmacy, but also in agriculture and in food industry. Their chemical constituents, especially secondary metabolites are important for drug discovery, pesticide discovery, and fermented food safety evaluations. This dissertation describes the chemical constituents of two fungal strains: *Coniella fragariae* and *Phomopsis* sp. D15a2a. In order to obtain crude extracts, fungi were fermented individually on rice media following by chromatographic workup. After successful isolation of compounds, NMR and HRMS were used to elucidate their structures. In addition, ECD spectroscopy, X-ray diffraction and chemical reactions were used to determine the absolute configurations of chiral compounds. All compounds were investigated for their bioactivity.

The coprophilous fungus *Coniella fragariae* was isolated from goose (*Anser anser*) dung, collected at northern Germany's seacoast. It produced a group of new azaphilones together with two known macrolides and other metabolites. The endophytic fungus *Phomopsis* sp. D15a2a was isolated from leaves of *Alternanthera bettzickiana* collected in Nigeria. The rice fermentation extract lead to the isolation of three types of new metabolites including koniginin derivatives, pantothenic acid derivatives and one tentoxin derivative. This dissertation consists of the following three manuscripts.

Azaphilone Derivatives from the Fungus *Coniella fragariae* Inhibit NF-κB Activation and Reduce Tumor Cell Migration

Seven new azaphilones, coniellins A−G, were obtained. TDDFTECD calculation was used to determine the absolute configuration of coniellin A, while Mosher's method was applied to determine the absolute configuration of coniellin E. Coniellin A exhibited significant inhibition of NF- κB activation in the triple negative breast cancer cell line MDAMB- 231 with an IC_{50} value of 4.4 μM. Moreover, coniellin A, D and E clearly reduced tumor cell migration. Coniellin A was the most active derivative tested in this assay and displayed 60% inhibition of tumor cell migration at a dose of 5 μM and 98% inhibition at 10 μM after 24 h.

Azaphilone pigments and macrodiolides from the coprophilous fungus *Coniella fragariae*

In continuation of the study on *Coniella fragariae*, two azaphilone pigments, two dihydrobenzofurans, two macrodiolides, and a dimeric alkyl aromatic constituent were isolated. Two azaphilone pigments and one dihydrobenzofuran proved to be new natural products. The crystal structure of pyrenophorin is reported for the first time. Pyrenophorin showed strong cytotoxicity against several cancer cell lines with IC_{50} values ranging from 0.07 to 7.8 μM.

Polyketides and Nitrogenous Metabolites from The Endophytic Fungus *Phomopsis* sp. D15a2a

Three new polyketides, phomopones A−C, one new cyclic tetrapeptide, 18-hydroxydihydrotentoxin, and a new amide, 6-hydroxyenamidin together with a known derivative, enamindin were obtained from the endophytic fungus *Phomopsis* sp. D15a2a. The structures of the new compounds were elucidated by 1D, 2D NMR and HRMS data. The absolute configurations of the isolated metabolites were determined either by X-ray crystallography, Marfey's method or by converting the compounds to Mosher esters.

Zusammenfassung

Pilze und ihre Sekundärmetaboliten spielen eine wichtige Rolle in unserem alltäglichen Leben. Dies bezieht sich nicht ausschließlich auf die pharmazeutische Verwendung, sondern ebenfalls auf die Nutzung in der Landwirtschaft und der Lebensmittelindustrie. Ihre Inhaltsstoffe, insbesondere ihre Sekundärmetaboliten, stellen eine wichtige Quelle für die Entdeckung neuer Arzneimittel und Pestizide dar und sind maßgeblich für die Sicherheitseinstufung fermentierender Lebensmittel. Diese Dissertation widmet sich der Untersuchung von Inhaltsstoffe, die von den beiden Pilzstämme *Coniella fragariae* und *Phomopsis sp.* D15a2a produziert werden. Zur Gewinnung von Rohextrakten wurden diese Pilze einzeln auf Reismedium kultiviert und im Anschluss chromatographisch aufbereitet. Nach erfolgreicher Isolation der Inhaltstoffe wurde deren chemische Struktur mittels Kernspinresonanzspektroskopie (NMR) und Massenspektrometrie (MS) aufgeklärt. Zusätzlich wurde die absolute Konfiguration chiraler Verbindungen durch den Einsatz von elektronischem Circulardichroismus (ECD), Röntgenkristallographie und stereospezifischer chemischer Reaktionen ermittelt. Alle Verbindungen wurden auf ihre biologische Aktivität untersucht.

Der koprophile Pilze *Coniella fragariae* wurde aus einer Gänsekotprobe (*Anser anser*) isoliert, welche an der Meeresküste in Norddeutschland gesammelt wurde. Er produzierte eine Serie neuer Azaphilone, neben zwei bekannten Makroliden und einigen anderen Metaboliten. Der endophytische Pilz *Phomopsis sp.* D15a2a wurde aus den Blättern der Pflanze *Alternathera bettzickiana* isoliert, welche in Nigeria gesammelt wurden. Die Fermentation von Reismedium führte zur Isolation neuer Metaboliten aus den drei Klassen der Koniginin-, Pantothensäure- und Tentoxin-Derivate. Diese kummulative Dissertation besteht aus den drei folgenden Manuskripten.

Azaphilonderivate des Pilzes *Coniella fragariae* inhibieren die Aktivierung von NF-κB und reduzieren Tumorzellmigration

Die sieben neuen Azaphilone Coniellin A-G wurden isoliert. Die absolute Konfiguration von Coniellin A wurde durch TDDFT-ECD Berechnungen bestimmt,

während die absolute Konfiguration von Coniellin E über die Mosher Methode bestimmt wurde. Coniellin A zeigte eine signifikante Inhibition der NF-κB Aktivierung in der tripelnegativen Brustkrebszelllinie MDAMB- 231 mit einem IC_{50}-Wert von 4,4 µM. Außerdem reduzierten Coniellin A, D und E eindeutig die Tumorzellmigration. Coniellin A war in diesem Testsystem das aktivste Derivat. Es zeigte nach 24 Stunden eine Inhibitionsrate der Tumorzellmigration von 60% bei einer Dosis von 5 µM und 98% bei 10 µM.

Azaphilonpigmente und Makrolide aus dem koprophilen Pilz *Coniella fragariae*

Bei weiterführenden Untersuchungen von *Coniella fragariae* wurden zwei Azaphilonpigmente, zwei Dihydrobenzofurane, zwei Makrodiolide und eine dimere Alkylarylverbindung isoliert. Die beiden Azaphilonpigmente und ein Dihydrobenzofuran wurden als neue Naturstoffe identifiziert. Die Kristallstruktur von Pyrenophorin wurde hierbei zum ersten Mal veröffentlicht. Pyrenophorin zeigte starke Zytotoxizität gegenüber mehreren Krebszelllinien mit IC_{50} Werten zwischen 0,07 und 7,8 µM.

Polyketide und stickstoffhaltige Metaboliten des endophytischen Pilzes *Phomopsis* sp. D15a2a

Die drei neuen Polyketide Phomopon A−C, das neue zyklisches Tetrapeptid 18-Hydroxydihydrotentoxin und das neue Amid 6-Hydroxyenamidin wurden zusammen mit dem bekannten Derivat Enamindin aus einer Fermentation des endophytischen Pilzes *Phomopsis* sp. D15a2a isoliert. Die Strukturen der neuen Verbindungen wurden anhand ihrer ein- und zweidimensionalen NMR Spektren, sowie ihrer MS Daten ermittelt. Die absoluten Konfigurationen. der Verbindungen wurde jeweils entweder durch Röntgenkristallographie, Marfey Analyse oder durch Umsetzung zu Mosher Estern bestimmt.

1 Introduction

1.1 Fungi and Their Metabolites

Fungi are an important part of the ecosystem (Gadd 2007) and are found in almost all corners of the world, even in extreme environments, such as deserts, (Grishkan, Zaady et al. 2006) the deep sea, (Le Calvez, Burgaud et al. 2009) and polar regions. (Ruisi, Barreca et al. 2006) As heterotrophic organisms, fungi can grow on almost any conceivable organic substrate and are usually classified by source, namely, as endophytic fungi, (Kui-Wu, Shi-Wei et al. 2014) coprophilous fungi, (Sarrocco 2016) soil fungi, (Bridge and Spooner 2001) and others. However, the relationships between endophytes and their hosts are not yet fully understood. Some reports have shown mutualistic relationships between fungi and their host plants. For example, the grass *Leymus mollis* from coastal and geothermal regions depends on its symbiotic fungal endophytes for salt and heat tolerance. (Rodriguez, Henson et al. 2008) Hot springs panic grass (*Dichanthelium lanuginosum*) can grow on geothermal soil, but it requires a fungal endophyte to do so. (Roossinck 2011) Endophytic fungi can produce secondary metabolites for plant growth regulation, such as indole-3-acetic acid, cytokines, or other plant growth-promoting substances. (Zhou, MacKenzie et al. 1999) Fungi also contribute secondary metabolites to the host plant's defense against herbivores. For example, ergot alkaloids are fungal secondary metabolites from genus *Claviceps* that affect animals and humans after consumption in the form of "St. Anthony's fire", which characterized by vasoconstriction of the extremities that cases swelling with a violent, burning pain in the hands, feet, and whole limbs. (Schiff 2006) Ergot-derivatives have a long history of being used medically for the treatment of a number of diseases and symptoms. (Haarmann, Rolke et al. 2009) For example, in 550 BC, the Hearst Papyrus of Egypt described a preparation of ergot with oil and honey that was used as a treatment for inhibiting hair growth, and, in 370 BC, Hippocrates described ergot use to halt postpartum hemorrhage. (Schiff 2006) Furthermore, although the widely used naturally derived anticancer drug taxol was initially isolated from a yew tree (*Taxus brevifolia*), over 50 species of endophytic fungi have been reported to be potential producers of taxol. (Deshmukh, Gupta et al. 2019)

Fungi are capable of producing numerous chemically diverse secondary metabolites with a wide range of bioactivities. (Aly, Debbab et al. 2011) Since Sir Alexander Fleming

isolated penicillin from *Penicillium notatum* and its derivatives were adapted to be the first broadly used class of antibiotics, a large number of fungal metabolites have been identified as potential drug candidates. (Aly, Debbab et al. 2011) Plinabulin, a clinical phase III anticancer drug candidate, is based on phenylahistin from *Aspergillus ustus*. (Kanoh, Kohno et al. 1997, Greve, Mohamed et al. 2010) The first immunosuppressive drug used for the prevention of organ transplant rejection, the cyclopeptide cyclosporine A, was isolated from the soil fungus *Tolypocladium inflatum*. (Tribe 1998, Butler 2004) In agriculture, fungicidal strobilurins based on a fungal metabolite from *Strobilurus tenacellus* have been developed by AstraZeneca, BASF, and others and are widely used in agriculture. (2007) In the food industry, fungal colorants from *Monascus* are widely used in Asia but are still forbidden in Europe and the USA due to safety concerns. However, these compounds show potential for the development of natural colorants. (Caro, Anamale et al. 2012) In the flavoring agent market, a variety of aromatic flavors produced by white-rot basidiomycetes are in development as "natural food flavoring". (Lomascolo, Stentelaire et al. 1999) To summarize, fungal metabolite studies form the basis for drug development, food additive development, and other uses.

1.2 Fungi: *Coniella* and *Phomopsis*

1.2.1 Fungi of the Genus *Coniella*

Coniella is a fungal genus of the Schizoparmaceae family, which contains 65 species recorded in the database Mycobank. (Mycobank) The first fungus belonging to *Coniella* genus was *Coniella pulchella,* established by Von Hoehnel in 1918. (Von Höhnel 1918) Alvarez, regarded genera *Pilidiella* and *Schizoparme* together with *Coniella* as synonyms. (Alvarez, Groenewald et al. 2016) As typical plant pathogenic fungi and due to globalization, *Coniella* occur worldwide as plant pathogens. *Coniella vitis* and *Coniella diplodiella* are two common pathogens that cause white rot disease in grapevines. (Chethana, Zhou et al. 2017) *Coniella granati* induces crown rot and fruit rot in pomegranates in Central Asia. (Çeliker, Uysal et al. 2012) In northern Australia, several species of *Coniella* have been reported to cause foliage blight on eucalyptus trees. (Griffiths, Wylie et al. 2004) Several *Coniella* fungi from South Africa are harmful for grapevine cultivation. (Van Niekerk, Groenewald et al. 2004) In 2015, *Coniella fragariae* was reported as the causal agent for strawberry crown rot in Latvia. (Grantina-Ievina and Kalniņa 2016) Fewer reports about *Coniella*

come from north and south America, but *Coniella lustricola* was isolated as a new species from submerged detritus in Black Moshannon State Park in Pennsylvania, USA. (Raudabaugh, Iturriaga et al. 2018) Considerable research on this genus of fungi has been published in the field of agriculture and biology but there are far few reports about the secondary metabolites of *Coniella*.

1.2.2 **Fungi of the Genus *Phomopsis***

Fungi of the genus *Phomopsis* or their teleomorph *Diaporthe* are distributed globally as endophytic fungi and include saprobes and pathogens of plants, animals and humans. (Gomes, Glienke et al. 2013) The genus *Diaporthe* should be used as the taxonomic name for all *Phomopsis* (first recorded in 1905) species due to *Diaporthe* (1870) being the first taxonomic classification. However, the name *Phomopsis* is more commonly used. (Udayanga, Liu et al. 2011)

Numerous reports have been published about the biology, taxonomy, and secondary metabolite diversity of *Phomopsis*. From 2013 to 2018, around 100 articles were published about secondary metabolites, including their bioactivity from the database of Sci-Finder. (Sci-Finder) For example, phomoxanthone A (PXA), a metabolite from a *Phomopsis* fungus, is a prime example of a fungal secondary metabolite that shows potential for further development as an anticancer drug because PXA exhibits selective activity against different cancer cells. (Frank, Niemann et al. 2015) Mechanistic research showed that PXA strongly induces apoptosis in cisplatin-resistant solid cancer cells. (Wang, Engelke et al. 2019) Nectriapyrone, macrosporin, and alternasolanol A are also examples of anticancer drug candidates isolated from *Phomopsis*. (Evidente, Kornienko et al. 2014) Numerous metabolites from this genus, such as dinemasone A, microsphaeropsone A, and cytosporone D, have also shown promising antibiotic activities. (Deshmukh, Verekar et al. 2014)

1.3 Metabolites from *Phomopsis* (*Diaporthe*) Reported During 2013-2018

A general review of reported new secondary metabolites and their bioactivities from *Phomopsis* from 2013 to 2018 is given in Chapter 1.3. Many polyketide metabolites and other kinds of secondary metabolites have been isolated from this genus and the compounds are grouped by structural characteristics.

1.3.1 **Xanthone Derivatives**

Xanthones are the main metabolites of *Phomopsis* fungi. These compounds have a high possibility of showing cytotoxicity. (Barbero, Artuso et al. 2018) Xanthone dimers, reported during the past six years, are shown below. The complex bisanthraquinone cytoskyrin C (**1**) was isolated from *Diaporthe* sp., a fungus isolated from *Anoectochilus roxburghii* which is a regional herb in Fujian Province, P. R. China. The ECD calculations were carried out and the absolute configuration was established. (Tian, Liao et al. 2018) Phomoxanthones C–E (**2-4**) were produced by endophytic fungus *Phomopsis* sp. xy21, isolated from *Xylocarpus granatum,* a Mangrove plant from Trang, Thailand. The absolute configuration of compound **2** was established via X-ray measurements. The ECD spectra of compounds **2** and **3** showed high similarity. (Wang, Luo et al. 2018) Diaporthemins A and B (**5** and **6**) were isolated from the fungus *Diaporthe melonis*, which was obtained from *Annona squamosa* (Annonaceae) collected in Kupang, Eastern Indonesia. Both compounds had the same planar structure and were elucidated as mirror image structures via ECD spectroscopic analysis. (Ola, Debbab et al. 2014) Two 12-deacetylphomoxanthone A derivatives (**7** and **8**) which had the same planar structure were isolated from two fungi strains *Phomopsis* sp. IM 41-1 and *Phomopsis longicolla. Phomopsis* sp. IM 41-1 was isolated from the Mangrove plant *Rhizhopora mucronate* collected from Jakarta, Indonesia. (Shiono, Sasaki et al. 2013) *Phomopsis longicolla* was isolated from the Mangrove plant *Sonneratia caseolaris* in Hainan Island, P. R. China. (Ronsberg, Debbab et al. 2013) Roensberg *et al.* clearly declared the absolute configurations of phomoxanthone derivatives including compound **7** via ECD calculation and X-ray measurements in the paper which studied metabolites of *Phomopsis longicolla*. (Ronsberg, Debbab et al. 2013) Monodeacetylphomoxanthone B (**9**) was isolated from *Phomopsis longicolla* S1B4*,* an endophytic fungus isolated from a plant sample collected in Hadong–gun Kyungnam Province, South Korea. (Choi, Kim et al. 2013) Phomolactonexanthones A (**10**), B (**11**) and deacetylphomoxanthone C (**12**) were isolated from a *Phomopsis* sp., which was derived from the Mangrove plant *Acanthus ilicifolius* collected in the South China Sea. (Ding, Yuan et al. 2013)

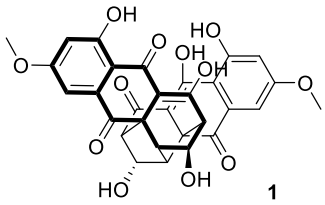

1

(Tian, Liao et al. 2018)

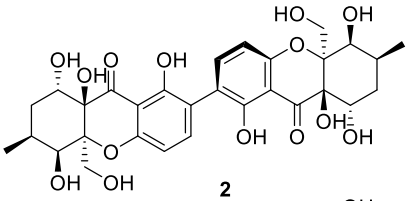

2

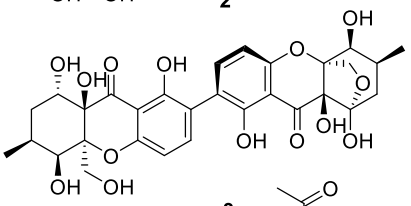

3

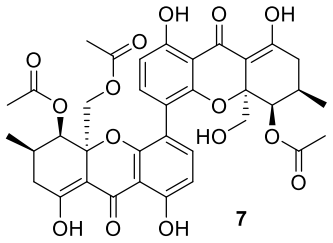

7

(Shiono, Sasaki et al. 2013)

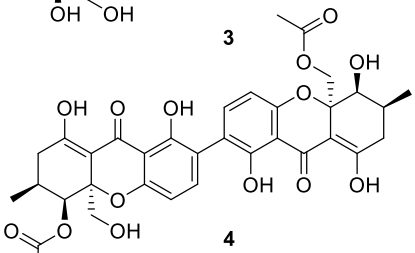

4

(Wang, Luo et al. 2018)

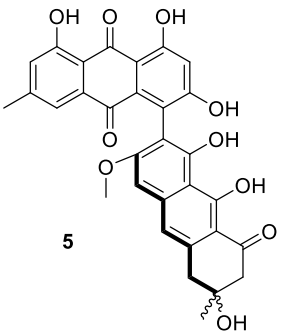

5

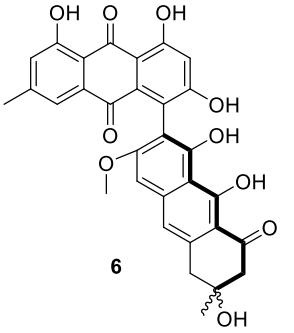

6

(Ola, Debbab et al. 2014)

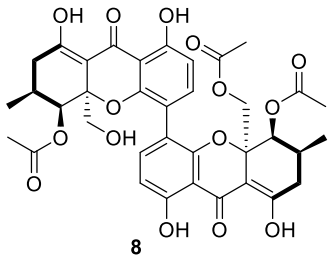

8

(Roensberg, Debbab et al. 2013)

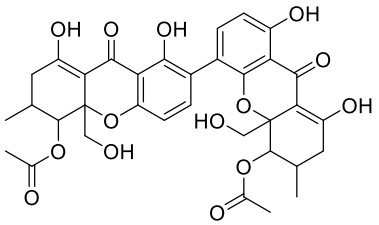

9

(Choi, Kim et al. 2013)

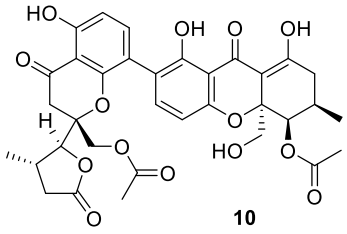

10

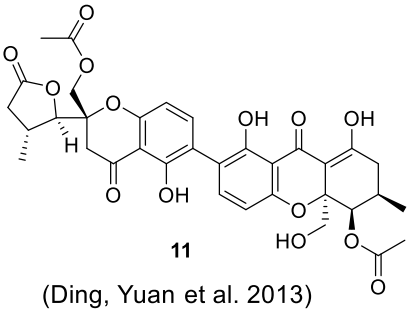

11

(Ding, Yuan et al. 2013)

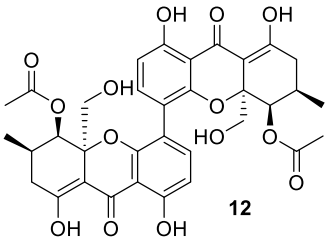

12

Monomeric xanthone derivatives are shown below. Chaetochromones A–C (**13-15**) were first reported from *Phomopsis* sp. SCSIO 41006, isolated from Mangrove-derived fungus *Rhizophora stylosa* collected in Hainan Island, P. R. China, were reported as new secondary metabolites. The configuration of compound **13** was determined via ECD calculation. (Ju, Lin et al. 2017) *Phomopsis* sp. HNY29-2B, an endophytic fungus of the Mangrove plant *Acanthus ilicifolius* Linn., collected from Hainan, P. R. China, yield phomochromenones A-C (**16-18**). The absolute configurations for compounds **17** and **18** were elucidated by ECD calculations. Compound **18** is an alkaloid processing a unique chromeno pyridine nucleus. (Ding, Wang et al. 2017) Phomopsichins A–D (**19-22**) were

isolated from *Phomopsis* sp. 33#, an endophytic fungus of the Mangrove plant *Rhizophora stylos* collected in Guangdong Province, P. R. China. ECD calculations determined the configurations for compounds **19**–**22**. Besides, the structure of phomopsichin A (**19**) was confirmed by X-ray measurement. (Huang, Li et al. 2016) A series of xanthones, diaporchromanones A–D (**23**-**26**), (-)-phomopsichin A (**27**), (+)-phomopsichin B (**28**), and (±)-diaporchromone A (**29**) were isolated from the fungus *Diaporthe phaseolorum* SKS019*,* an endophyte of the Mangrove plant *Acanthus ilicifolius* from Guangxi Province, P. R. China. The absolute configurations of compounds **23**–**28** were elucidated via ECD calculation. (Cui, Ding et al. 2017) Two xanthones (**30**, **31**) with highly oxygenated side chains were isolated from *Phomopsis amygdali,* an endophytic fungus of *Paris axialis* from Yunnan, P. R. China. Both compounds showed cytotoxic activity with IC_{50} values ranging from 3.6 to 8.7 μM against A549 and SHSY5Y cell lines. (Hu, Yang et al. 2015) *Phomopsis amygdali* KF308686, (Yang, Yang et al. 2014) *Phomopsis amygdali* (without accession number), (Li, Wang et al. 2014) and *Phomopsis* sp. KF609280 (Yang, Gao et al. 2013) were isolated from the plant *Paris polyphylla* var. *yunnanensis* collected from Yunnan Province, P. R. China. One xanthone (**32**) was produced by an endophyte *Phomopsis amygdali* KF308686, which showed cytotoxicity against A549 and PC3 cell lines with IC_{50} values of 5.8 and 3.6 μM. (Yang, Yang et al. 2014) From *Phomopsis* sp. KF609280, three xanthone compounds (**33**–**35**) were obtained. Compounds **33** and **35** showed cytotoxicity against several cell lines, especially against A549 cells with IC_{50} values of 3.6 and 2.5 μM respectively. (Yang, Gao et al. 2013)

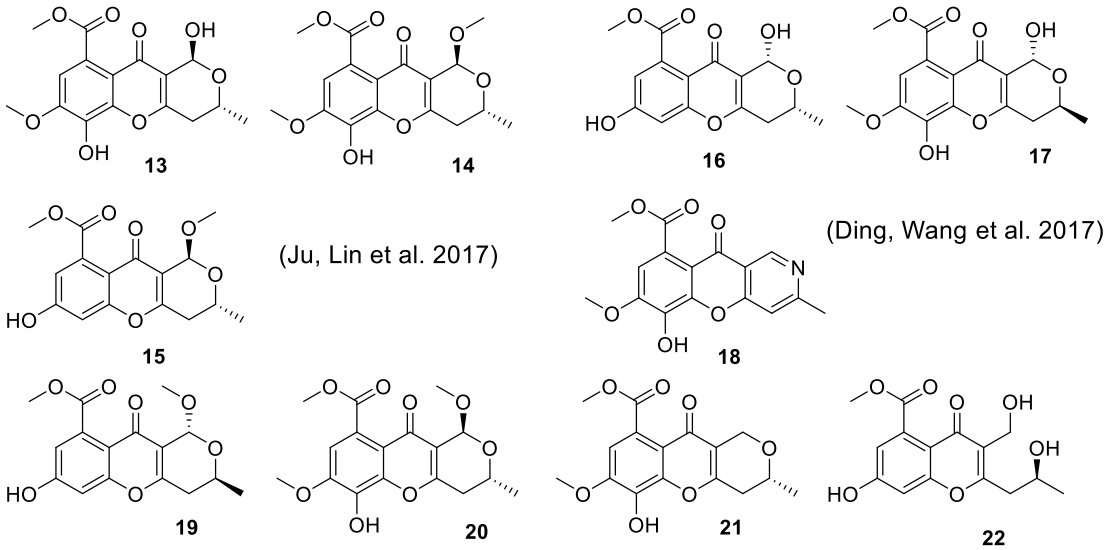

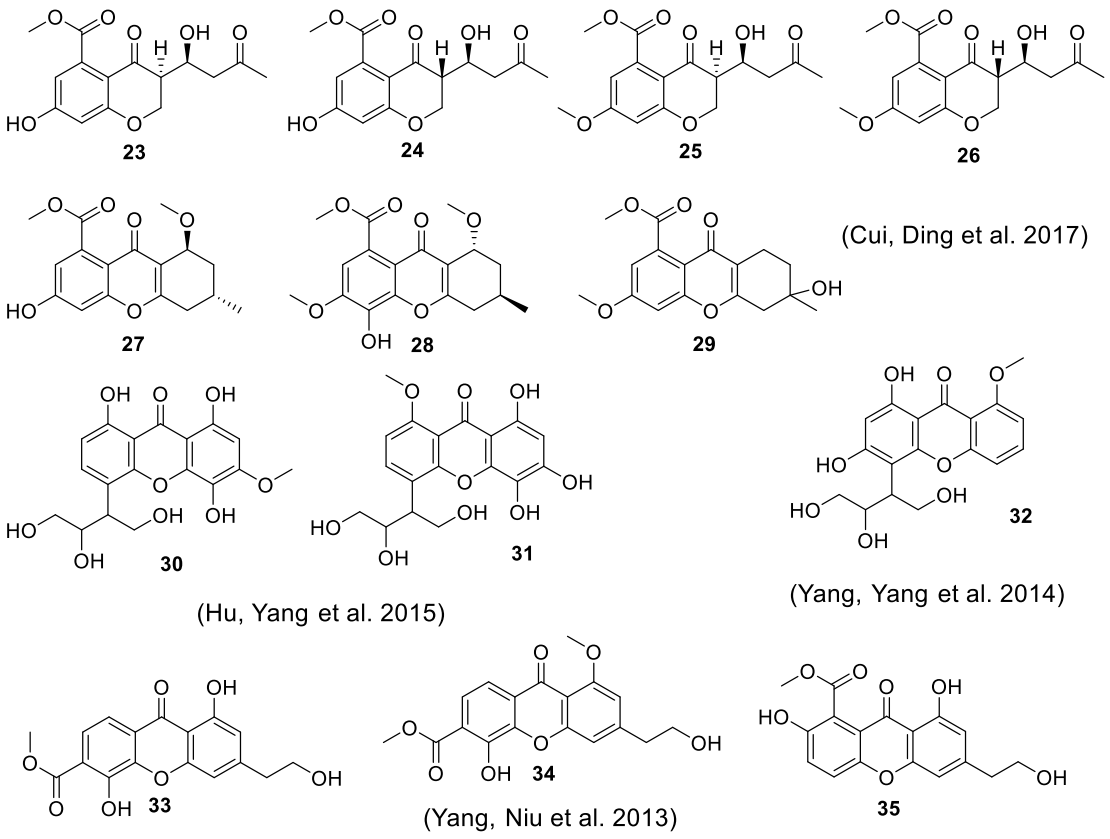

From another strain of *Phomopsis amygdali* without accession number, a xanthone (**36**) was obtained which showed high cytotoxicity against NB4 and PC3 cells with IC_{50} values of 4.5 and 3.8 µM, respectively. (Li, Wang et al. 2014) Two xanthones (**37** and **38**) with ethanol side chains were isolated from the fungus *Phomopsis amygdali*, which was derived from the plant *Paris axialis* collected from Yunnan Province, P. R. China. (Yuan, Huang et al. 2015) The Mangrove derived endophytic fungus *Phomopsis* sp. SK7RN3G1 from the South China Sea produced a xanthone (**39**) which showed cytotoxicity against HEp-2 and HepG2 cell lines with IC_{50} values of 8 and 9 µg/mL. (Yang, Qiu et al. 2013) An O-glycosidic xanthone (**40**) was isolated from *Phomopsis* sp., an endophytic fungus of the Mangrove plant *Excoecaria agallocha* in Hainan Island, P. R. China. The compound showed weak cytotoxicity against HEp-2 and HepG2 cells with IC_{50} values of 9 and 16 µM. (Huang, Yang et al. 2013) *Phomopsis* sp. xy21, an endophytic fungus of the Thai Mangrove plant *Xylocarpus granatum* from Trang Province, Thailand, produced phomoxanthones F-K (**41**–**46**). The X-ray measurement elucidated the structures of compounds **41** and **42**. The configuration of compound **44** was elucidated via ECD calculation. (Hu, Luo et al. 2018) Four chromeno [3,2-c] pyridines, diaporphasines A–D (**47**–**50**) and two isoindolinones, meyeroguillines C and D (**51** and **52**) were isolated from *Diaporthe phaseolorum* SKS019 an endophytic fungus of the Mangrove plant *Acanthus ilicifolius*.

(Cui, Yu et al. 2017) The natural product α-mangostin (**53**) from *Garcinia mangostana* was added to a fermentation of the fungi *Colletotrichum* sp. MT02 and *Phomopsis euphorbiae* K12, which resulted in the production of five new derivatives (**54**–**58**). (Arunrattiyakorn, Suwannasai et al. 2014)

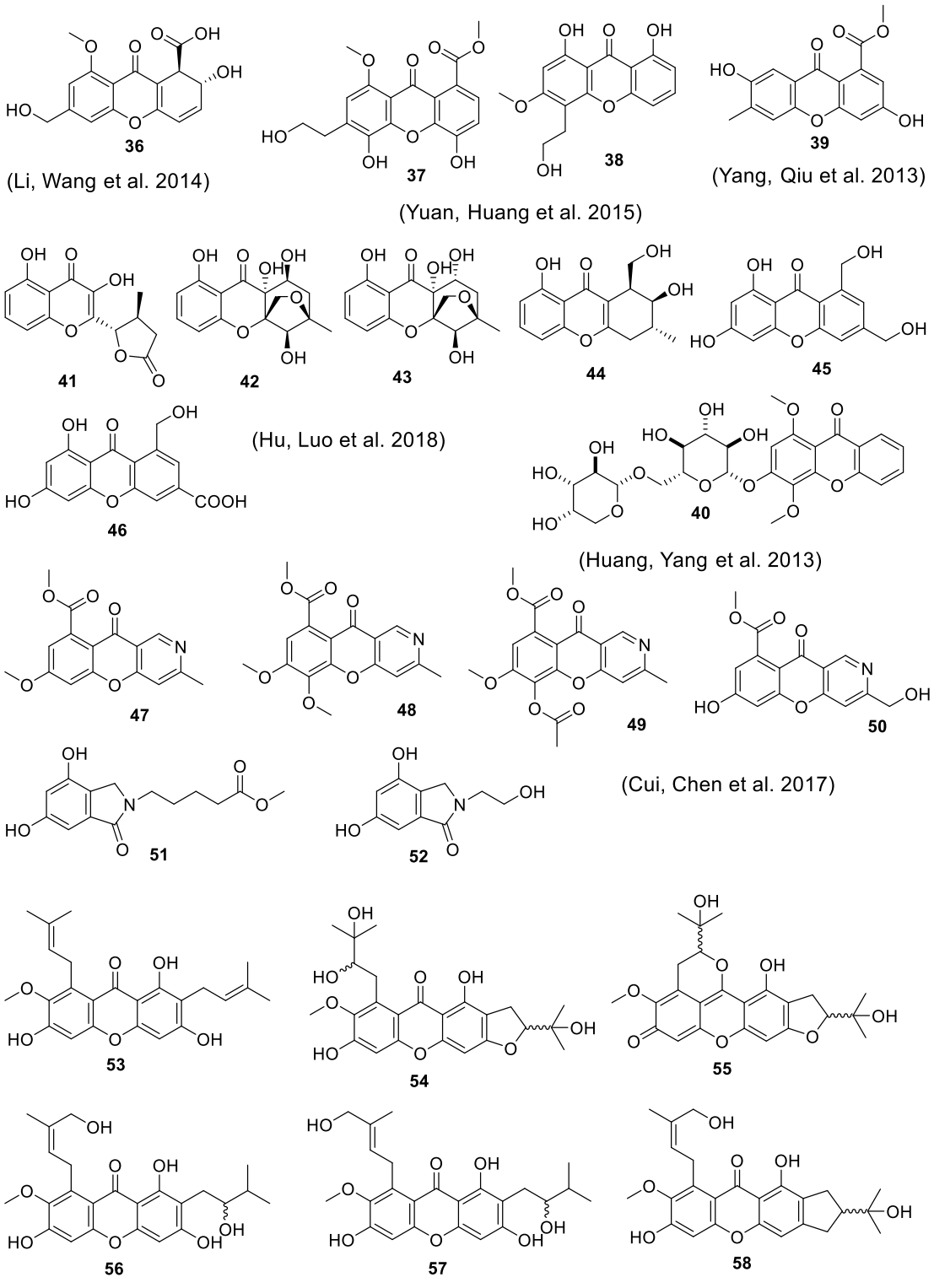

1.3.2 **Other Polyketide Metabolites**

Other structurally complex polyketide metabolites such as azaphilones, tenellone-macrolides and others are shown below.

Six chloroazaphilones isochromophilones A−F (**59**–**64**) were isolated from *Diaporthe* sp. SCSIO 41011 an endophytic fungus of the Mangrove plant *Rhizophora stylosa* collected from Hainan Island, P. R. China. The absolute configurations for the six compounds were deduced by ECD calculation and comparison with known congeners. (Luo, Lin et al. 2018) Four structurally interesting tenellone-macrolides conjugated [4+2] hetero-adducts lithocarpins A–D (**65**–**68**), were discovered from *Phomopsis lithocarpus* FS508, a deep-sea fungus from the Indian Ocean. The configurations of lithocarpins C and D (**67** and **68**) were determined via X-ray measurement. These compounds all showed weak cytotoxicity against SF-268, MCF-7 and HepG-2 cell lines with IC_{50} values more than 10 μM. (Xu, Tan et al. 2018) Diaporisoindoles A–C (**69**–**71**), and tenellone C (**72**) were produced by *Diaporthe* sp. SYSU-HQ3, an endophyte from a fresh branch of the Mangrove plant *Excoecaria agallocha*. The configurations of diaporisoindoles A and B (**69** and **70**) were determined via X-ray measurement together with ECD calculation. Diaporisoindole A (**69**) and tenellone C (**72**) exhibited strong inhibitory effects against *Mycobacterium tuberculosis* protein tyrosine phosphatase B with IC_{50} values 4.2 and 5.2 μM respectively, even stronger than the positive control oleanolic acid with an IC_{50} value of 22.1 μM. (Cui, Lin et al. 2017)

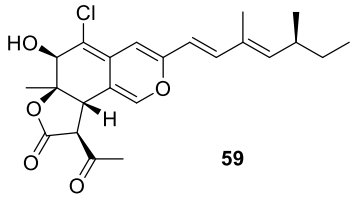

59

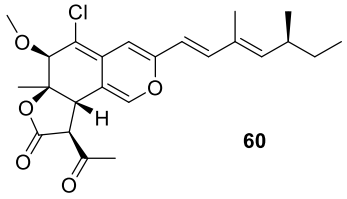

60

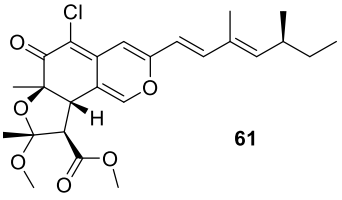

61

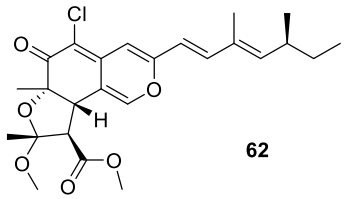

62

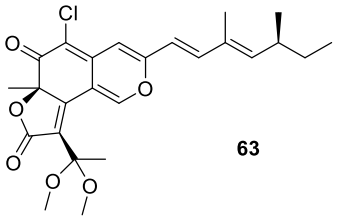

63

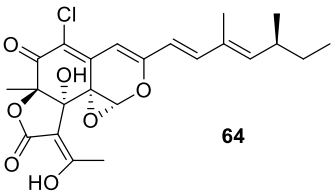

64

(Luo, Lin et al. 2018)

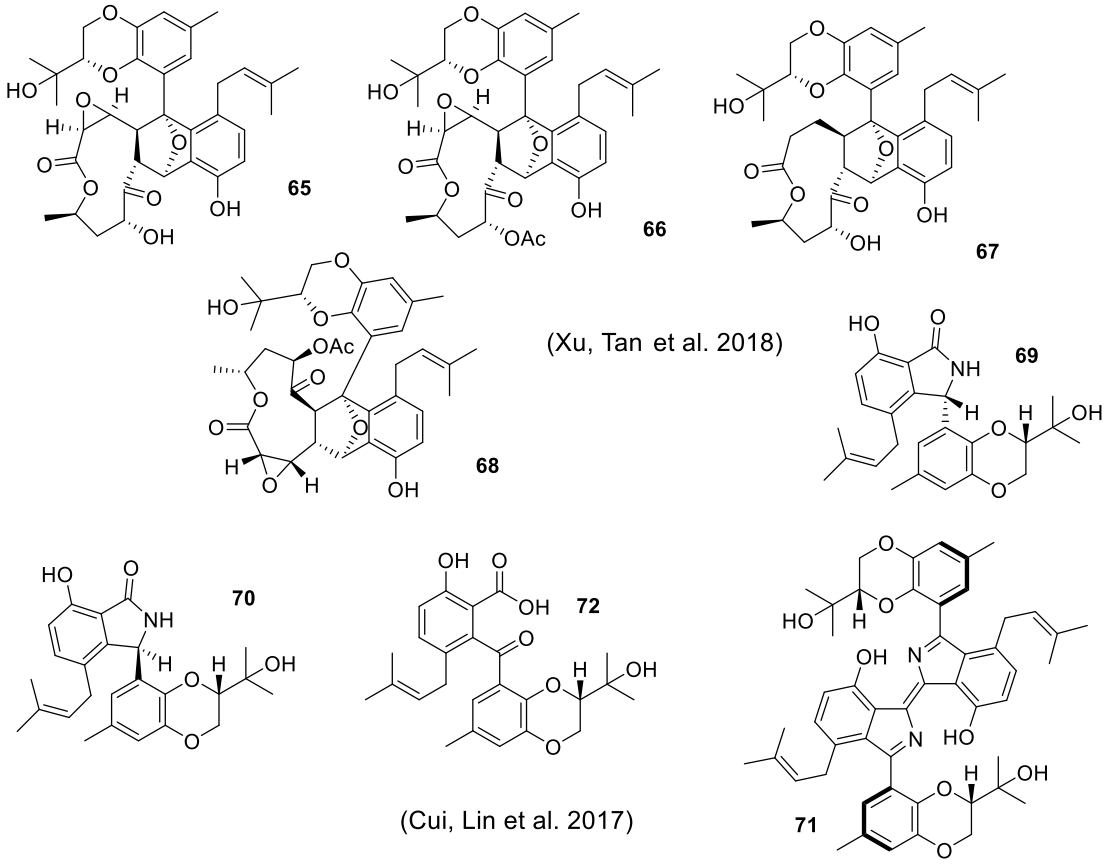

Later, from the same fungus *Diaporthe* sp. SYSU-HQ3, diaporindenes A–D (**73**–**76**), isoprenylisobenzofuran A (**77**), and two isoprenylisoindole alkaloids diaporisoindoles D and E (**78** and **79**) as well as the new benzophenone derivative tenellone D (**80**) were isolated by same research group. The absolute configurations of the compounds were elucidated via ECD calculation. Diaporindene A (**73**) and isoprenylisobenzofuran A (**77**) were also defined by a single crystal X-ray analysis. Compounds **73–77** exhibited significant inhibition of NO production in RAW 264.7 cells with IC_{50} values lower than 10 μM, and compounds **78**–**80** with IC_{50} value ranging between 10 to 20 μM. However, the positive control indomethacin showed an IC_{50} value of 37.5 μM. (Cui, Liu et al. 2018) Two diphenyl ether derivatives, diaporthols A and B (**81** and **82**), were produced by the fungus *Diaporthe* sp., which was isolated from leaves of *Phellodendron amurens* collected from Gifu, Japan. X-ray diffraction confirmed the structure of diaporthol B (**82**). The bioassay showed anti-migration activities in TGF-β1-elicited MDA-MB-231 cells at a concentration of 20 μM. (Nakashima, Tomida et al. 2018) The fungus *Phomopsis* sp. A123, which was isolated from the Mangrove plant *Kandelia candel (L.)* Druce collected in Fujian, P. R. China, produced the depsidone compound phomopsidone A (83). (Zhang, Xu et al. 2014) Four nitrogen containing chromenopyridines, phochrodines A–D (**84**–**87**) were isolated from *Phomopsis* sp. 33#. The fungus had been obtained from the

bark of the Mangrove plant *Rhizophora stylosa* collected from the South China Sea. (Chen, Huang et al. 2018)

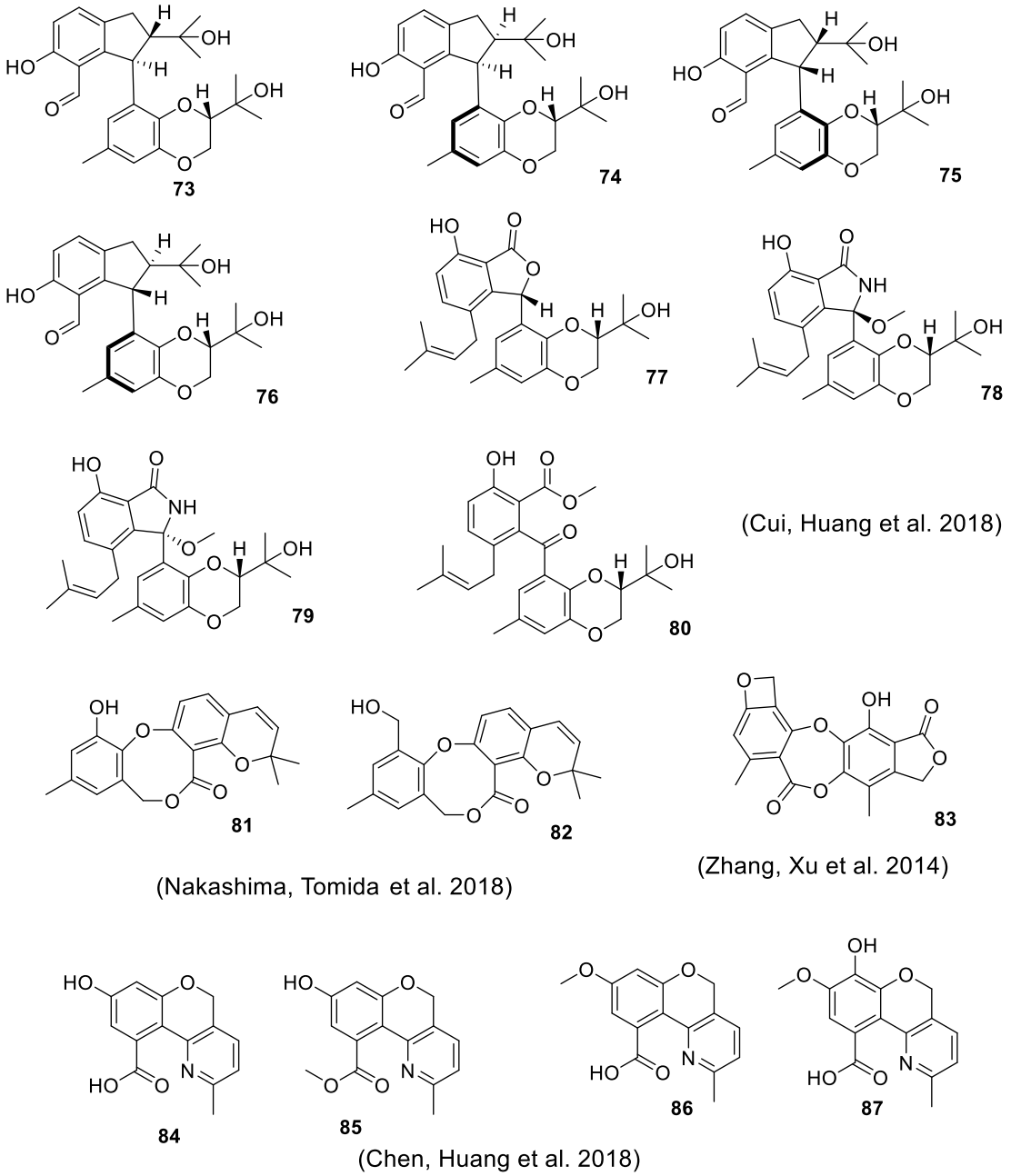

(Cui, Huang et al. 2018)

(Nakashima, Tomida et al. 2018)

(Zhang, Xu et al. 2014)

(Chen, Huang et al. 2018)

Compounds in this group mainly consist of an aromatic system coupled with terpenoid or fatty acid side chains. Three naphthalenes (**88**–**90**) isolated from *Phomopsis fukushii* showed activity against MRSA with MIC values ranging from 4 to 6 mg/mL. This fungus had been isolated from rhizomes of *Paris polyphylla* var. *yunnanensis,* collected from Yunnan Province, P. R. China. (Yang, Duan et al. 2017) *Diaporthe* sp. F2934, an endophytic fungus from leaves of *Siparuna gesnerioides* collected in the Chagres National Park, Panama, yielded three polyketide metabolites (**91**–**93**). (Sousa, Aguilar-Pérez et al. 2016) Phomopsiketones AC (**9496**), (10*S*)-10-O-*β*-D-40-

methoxymannopyranosyldiaporthin (**97**) and clearanol H (**98**), were discovered via OSMAC (One Strain Many Compounds) experiments. *Phomopsis* sp. sh917 was isolated from the plant *Isodon laxiflora* in Yunnan Province, P. R. China. The configurations of compounds **94**, **96,** and **97** were determined by single crystal X-ray diffraction experiments. The absolute configuration of compound **95** was elucidated by ECD and comparison to compound **94**. (Tang, Wang et al. 2017) Phomonaphthalenone A (**99**), a dihydronaphthalenone with an oxygen bridge between C-3 and C-5, was produced by *Phomopsis* sp. HCCB04730, an endophytic fungus of *Stephaniae japonicae,* collected from Zhejiang Province, P. R. China. The configuration was deduced from X-ray measurement. The bioassay showed moderate anti-HIV activities with an IC_{50} value of 11.6 μg/mL and relative low cytotoxicity with IC_{50} values 52.7, 64.2 and 92.5 μg/mL against PANC-1, MDA-MB-231 and A549 cell lines respectively. (Yang, Ding et al. 2013) *Senna spectabilis* (Fabaceae) collected in São Paulo, Brazil obtained endophytic fungus *Phomopsis* sp. which produced 2-hydroxy-alternariol (**100**). (Chapla, Zeraik et al. 2014) The fungus *Diaporthe* sp. LG23, an endophytic fungus isolated from leaves of *Datura inoxia* Mill produced xylarolide A (**101**), diportharine A (**102**) and xylarolide B (**103**). In the bioactivity studies, xylarolide A (**101**) showed growth inhibition against MIAPaCa-2 and PC-3 cancer cells with IC_{50} values of 20 and 14 μM, respectively, whereas it displayed antioxidant activity with an EC_{50} value of 27.5 mM, while the positive control ascorbic acid had an EC_{50} value of 6.2 mM. (Sharma, Singamaneni et al. 2018) The isochroman (3*R*,4*S*)-3,4-dihydro-8-hydroxy-4-methoxy-3-methylisocoumarin (**104**) was produced by the endophytic fungus *Phomopsis* sp. Gx-4, which was isolated from a South China Sea Mangrove plant. (Yang, Qiu et al. 2014) Two dimeric xanthones 12-deacetylphomoxanthone A (**8**) derivatives, homo-2,3-dihydrochromone (**105**) and isomonodictyphenone (**106**) were isolated from *Phomopsis longicolla*. (Ronsberg, Debbab et al. 2013) An endophytic fungus *Phomopsis* sp. isolated from *Morus cathayana* collected in West Java, Indonesia yielded epoxyquinophomopsin (**107**). (Hermawati, Juliawaty et al. 2017)

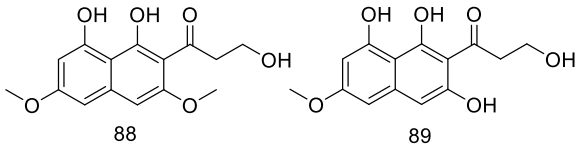

88

89

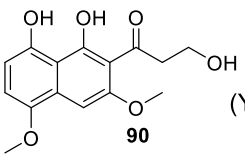

90

(Yang, Duan et al. 2017)

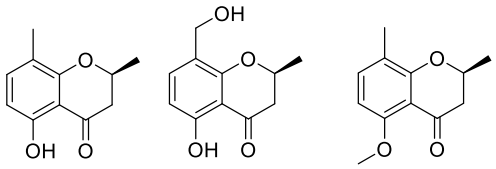

91 **92** **93**

(Sousa, Aguilar-Pérez et al. 2016)

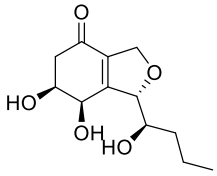

94

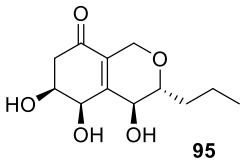

95

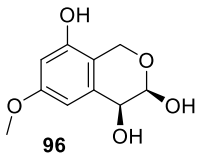

96

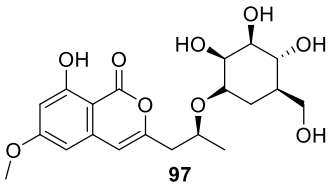

97

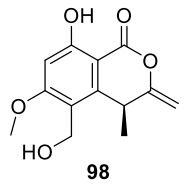

98

(Tang, Wang et al. 2017)

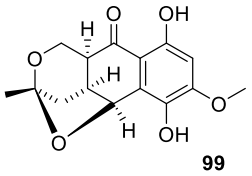

99

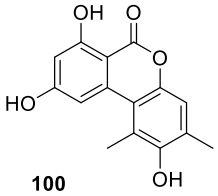

100

(Yang, Ding et al. 2013)

(Chapla, Zeraik et al. 2014)

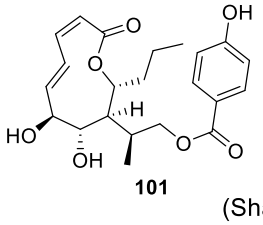

101

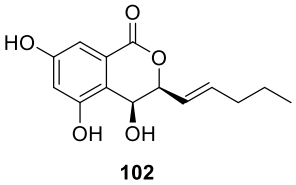

102

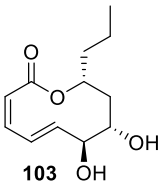

103

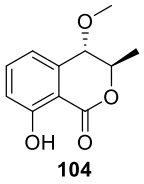

104

(Sharma, Sharma et al. 2018)

(Yang, Qiu et al. 2014)

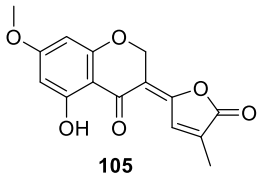

105

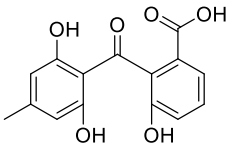

106

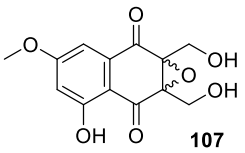

107

(Roensberg, Debbab et al. 2013)

(Hermawati, Juliawaty et al. 2017)

Acetoxydothiorelone B (**108**), (15*S*)-acetoxydothiorelone A (**109**), dothiorelone K (**110**), dothiorelone L (**111**), dothiorelone M (**112**), dothiorelone N (**113**), 5-hydroxy-7-methoxy-4,6-dimethyl-2-phenylisoindoline-1,3-dione (**114**), (13*R*)-diaporphthalide A (**115**), and (9*S*, 17*R*, 19*S*, 6*Z*, 10*E*, 14*E*)-diaporlactone A (**116**) were isolated from *Diaporthe pseudomangiferaea*. This fungus had been obtained from the famous Chinese folk medicinal plant *Tylophora ouata* collected in Guangxi Province, P. R. China. The absolute configurations of these metabolites were established by comparing the specific optical rotation to known compounds or determined by ECD spectrum. (Liu, Zhao et al. 2018) A group of compounds including the benzophenones tenellones D–H (**117**-**121**) with terpenoid side chain and the eremophilane lithocarin A (**122**) were discovered from *Phomopsis lithocarpus* FS508, a fungus from a deep-sea sediment sample, collected in the Indian Ocean. The structure of tenellone D (**117**) was further confirmed via X-ray crystallographic measurement. In the bioactivity test, tenellone H (**121**) showed weak cytotoxicity with an IC_{50} value ranging from 16 to 25 μM against HepG-2, MCF-7, SF-268, and A549 cell lines. (Xu, Liu et al. 2018)

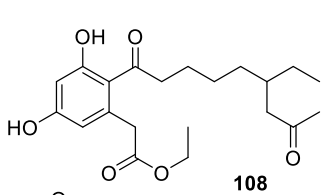

108

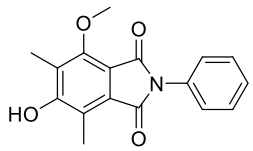

114

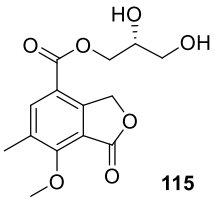

115

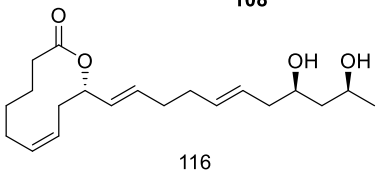

116

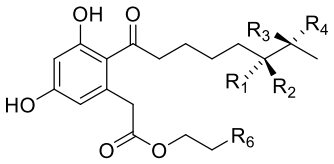

	R1	R2	R3	R4	R5	R6
109:	H	H	OCOCH3	H	CH3	H
110:	H	H	H	H	COOCH3	H
111:	OH	OH	H	H	CH3	H
112:	H	H	H	H	CH3	P-OH-Ph
113:	H	H	H	H	CH2OCOCH3	P-OH-Ph

(Liu, Zhao et al. 2018)

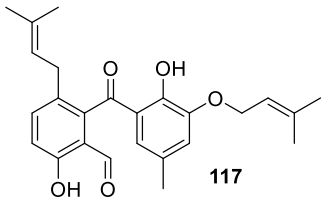

117

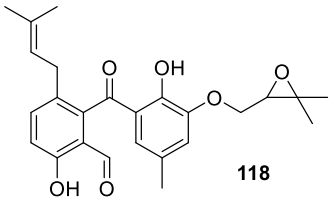

118

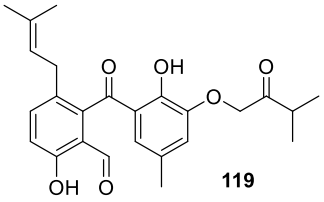

119

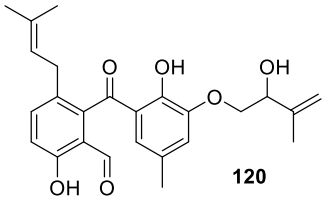

120

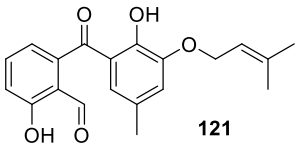

121

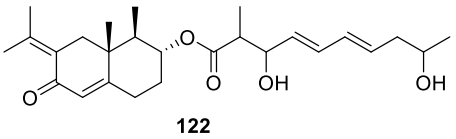

122

(Xu, Liu et al. 2018)

Six new polyketides dothiorelone O (**123**), (15*R*)-acetoxydothiorelone A (**124**), pestalotiopsone H (**125**), (±)-microsphaerophthalide H (**126**), microsphaerophthalide I (**127**) and methyl convolvulopyrone (**128**) were produced by *Diaporthe* sp. SCSIO 41011, which has also been reported to produce isochromophilones A−F (**59–64**). (Luo, Lin et al. 2018) The configuration of microsphaerophthalide I (**127**) was established via ECD calculation.(Luo, Yang et al. 2018) The plant *Paris polyphylla* var. *yunnanensis* from Yunnan Province, P. R. China, was collected by different research groups and yielded endophytic fungi *Phomopsis fukushii* KP068615, (Li, Yang et al. 2018) *Phomopsis fukushii* KP068682, (Gao, Zheng et al. 2018) and *Phomopsis* sp. KF609280. (Li, Yang et al. 2018) From *Phomopsis fukushii* KP068615, three isopentylated diphenyl ethers (**129**–**131**) were isolated and showed strong activity against MRSA with diameters of inhibition zone of 15-21 mm, compared to the positive control tetracycline with 32 mm. (Li, Yang et al. 2018) Three arylbenzofurans derivatives (**132**–**134**) with terpenoid side chains were isolated from the endophyte *Phomopsis* sp. KF609280. In the activity test against tobacco

mosaic virus, all three compounds showed strong inhibition rates between 23.6 to 35.2%, equal to the positive control ningnanmycin with an inhibition rate of 31.8%. (Du, Wang et al. 2017) From *Phomopsis fukushii* KP068682, three diphenyl ethers (**135**–**137**) were isolated. Compounds **135**–**137** showed strong activity in the anti-MRSA test with inhibition zones of 15.2 - 20.2 mm, while the positive control erythromycin showed an inhibition zone of 21.9 mm. (Gao, Zheng et al. 2018) *Diaporthe cryptica,* a fungus isolated from a cankered branch of *Corylus avellana* L. in Sardinia, Italy, produced three phytotoxic metabolites, namely crypticins A–C (**138–140**). The configurations of all three compounds was elucidated via ECD calculation and comparison with known compounds. (Cimmino, Nocera et al. 2018)

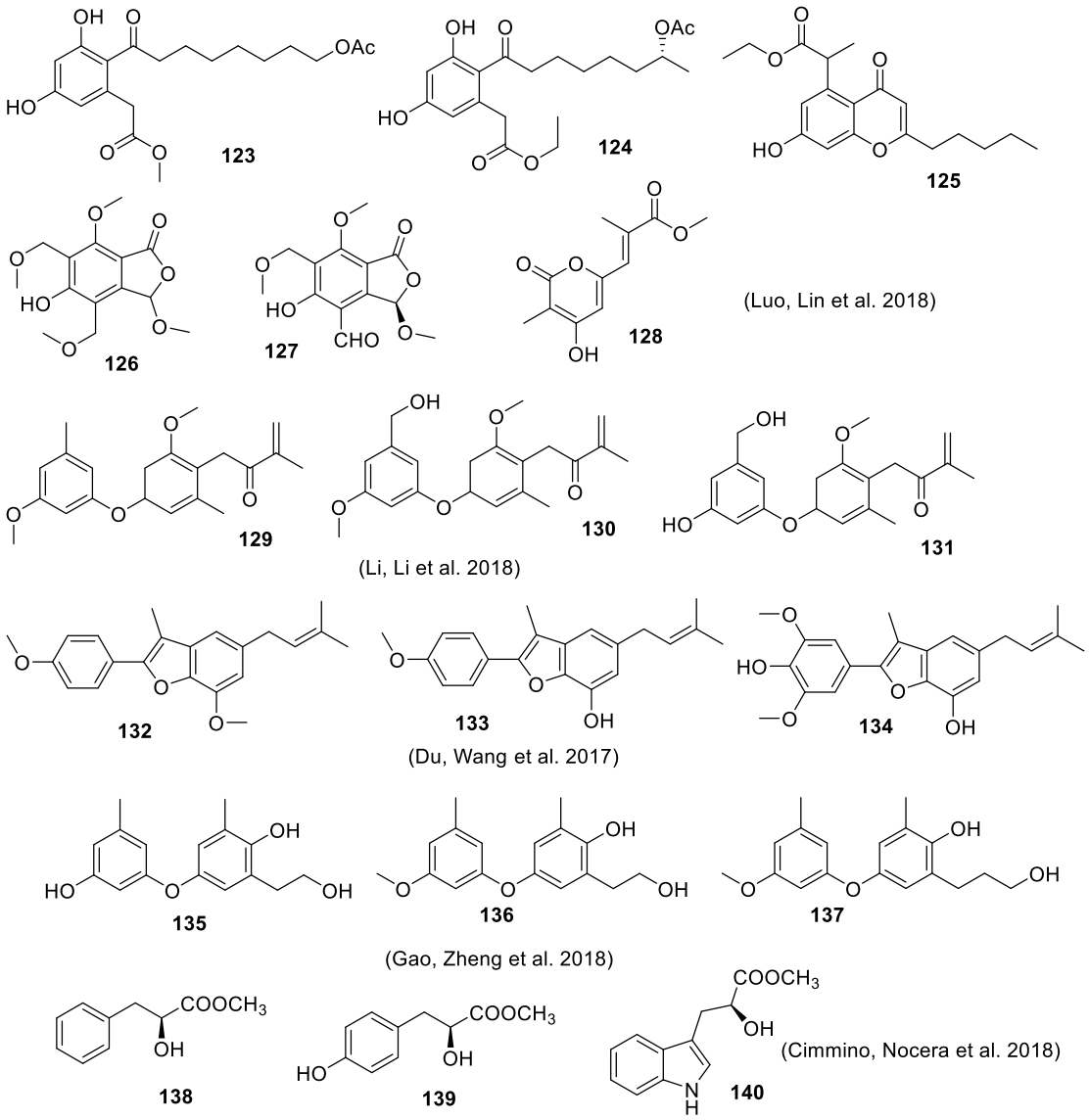

Kongiidiazadione (**141**) was obtained from *Diaporthe kongii*, a fungus isolated from *Carthamus lanatus* L. ssp. *lanatus* collected in Australia. The absolute configuration was elucidated via ECD calculation. (Evidente, Boari et al. 2015) Phomopyrone A (**142**) was

isolated from *Phomopsis* sp. HNY29-2B, an endophytic fungus derived from the Mangrove plant *Acanthus ilicifolius,* collected from Hainan Island, P. R. China. The structure was further confirmed by X-ray diffraction. (Cai, Chen et al. 2017) Phomobutenolide (**143**) was obtained from the endophytic fungus *Phomopsis* sp. 11F0023, which was isolated from *Eragrostis amabilis* collected in Hsinchu, Taiwan.(Cheng, Wu et al. 2015) From *Phomopsis* sp. 10F0011, an endophytic fungus of *Peperomia sui* collected from Pingtung County, Taiwan, phomopsuidiol (**144**) was obtained. (Cheng, Wu et al. 2018) The virulent fungus *Diaporthe gulyae* isolated from *Carthamus lanatus* L. ssp. *lanatus,* collected in Australia, yielded gulypyrones A and B (**145** and **146**), phomentrioloxins B and C (**147** and **148**). The Mosher's reaction was carried out to obtain the absolute configuration of gulypyrones A (**145**). (Andolfi, Boari et al. 2015) Two cytosporones (**149** and **150**) were isolated from *Phomopsis* sp. PSU-H188, an endophytic fungus of *Hevea brasiliensis*, collected from Trang Province, Thailand. (Kongprapan, Xu et al. 2017) Compounds (**150)** also been reported from *Phomopsis* sp. YM355364. (Ma, Shen et al. 2014) Dothiorelones I and J (**151** and **152**) were isolated from fungus *Phomopsis* sp. BCC 45011 which was isolated from a *Xylocarpus granatum* leaf, collected in Nakhon Si Thammarat Province, Thailand. (Kornsakulkarn, Somyong et al. 2015) *Phomopsis* sp. IFB-ZS1-S4 produced cytosporone T and U (**153** and **154**) and the fungus was isolated from a healthy stem of *Scaevola hainanensis* Hance, collected in Hainan Island, P. R. China. (Wu, Guo et al. 2013) Phomentrioloxin (**155**) was produced by the fungus *Diaporthe gulyae,* which was isolated from *Carthamus lanatus* L. (Cimmino, Andolfi et al. 2013)

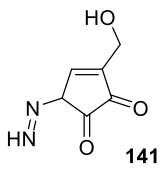

141

(Evidente, Boari et al. 2015)

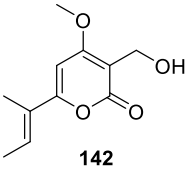

142

(Cai, Chen et al. 2017)

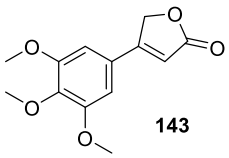

143

(Cheng, Wu et al. 2015)

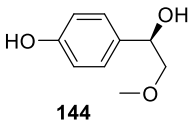

144

(Cheng, Wu et al. 2018)

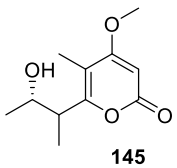

145

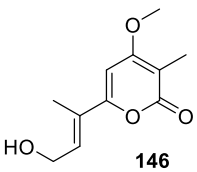

146

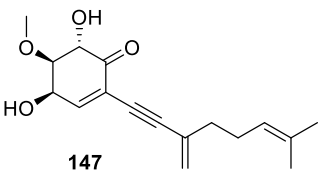

147

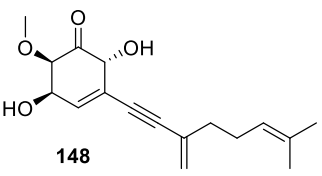

148

(Andolfi, Evidente et al. 2015)

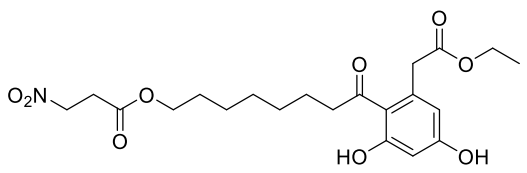

149

(Kongprapan, Xu et al. 2017) and (Ma, Shen et al. 2014)

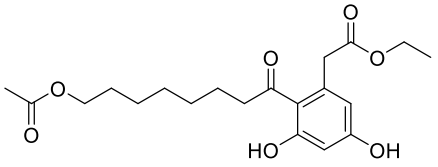

150

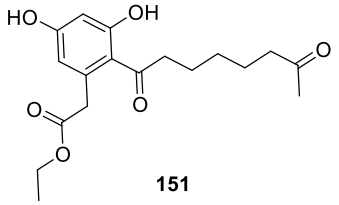

151

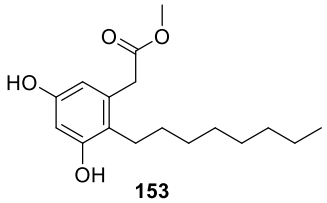

153

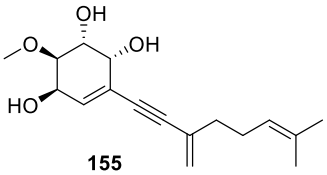

155

(Cimmino, Andolfi et al. 2013)

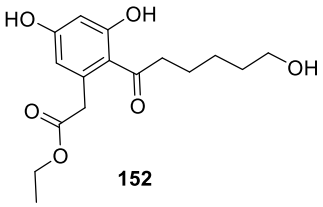

152

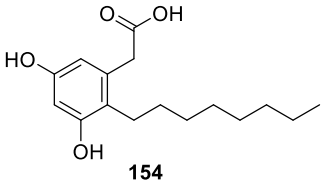

154

(Wu, Guo et al. 2013)

(Kornsakulkarn, Somyong et al. 2015)

Seven polyoxygenated cyclohexenoids phomopoxides A−G (**156**–**162**) were obtained from *Phomopsis* sp. YE3250. The fungus was isolated from *Paeonia delavayi* collected in Yunnan Province, P. R. China. The X-ray crystallographic analysis determined the configuration for phomopoxide A (**156**). Compounds **156**–**162** displayed weak cytotoxic, weak antifungal. In the test of *α*-glycosidase inhibitory activities, compounds **156-162** showed IC_{50} value ranging 1.47-2.88 mM, while the positive control acarbose displayed an IC_{50} value of 1.22 mM. (Huang, Jiang et al. 2018) *Diaporthe* sp. SXZ-19 an endopyte of *Camptotheca acuminate* collected from Fujian Province, P. R. China, yielded a new polyketide (**163**). (Liu, Hu et al. 2013) Four similar polyketide phomopsolidones A–D (**164**–**167**) were isolated from *Phomopsis* sp. DC275, a fungus obtained from *Vitis vinifera* from Ticino, Switzerland. (Goddard, Mottier et al. 2014) Diaporthacol (**168**) was discovered from *Diaporthe* sp. PSU-SP2/4. This fungus was isolated from a sponge collected in Trang Province, Thailand. (Khamthong, Rukachaisirikul et al. 2014) 5,6-Dihydro-2-pyrone (**169**) was produced by *Phomopsis amygdali,* an endophytic fungus from *Corylus avellana,* collected in Turkey. (Akay, Ekiz et al. 2014) Three oxygen-bridged cyclooctadiene phomoxydienes A–C (**170**–**172**) together with compounds **151** and **152**were isolated from *Phomopsis* sp. BCC 45011. (Kornsakulkarn, Somyong et al. 2015) *Phomopsis* sp. CMU-LMA, isolated from *Alpinia malacensis,* yielded three compounds (**173**–**175**). (Adelin, Martin et al. 2013)

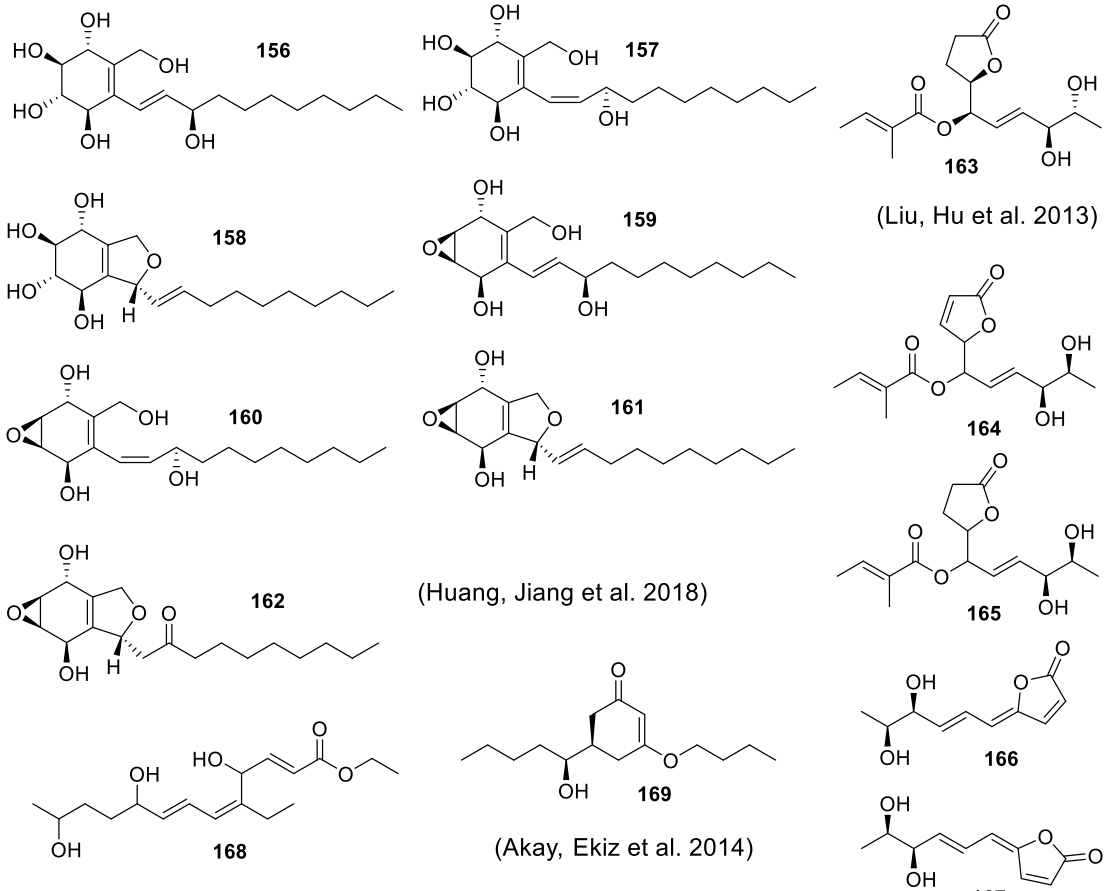

(Liu, Hu et al. 2013)

(Huang, Jiang et al. 2018)

(Akay, Ekiz et al. 2014)

(Khamthong, Rukachaisirikul et al. 2014)

(Goddard, Mottier et al. 2014)

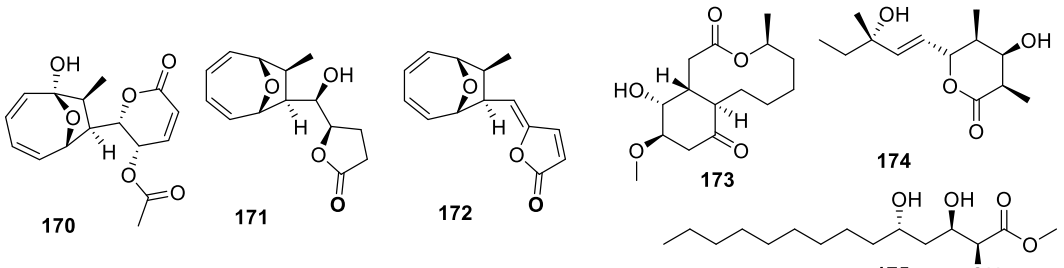

(Kornsakulkarn, Somyong et al. 2015)

(Adelin, Martin et al. 2013)

1.3.3 **Lipids**

Two fatty acids (**176** and **177**) were isolated from *Diaporthe terebinthifolii,* a fungal endophyte from *Glycyrrhiza glabra* Linn. (Yedukondalu, Arora et al. 2017) *Diaporthe* sp. JC-J7, isolated from *Dendrobium nobile,* collected in Yunnan Province, P. R. China, yielded a group of compounds, namely diaporthsins A–K (**178**–**188**). All compounds are fatty acid derivatives. (Hu, Yang et al. 2018)

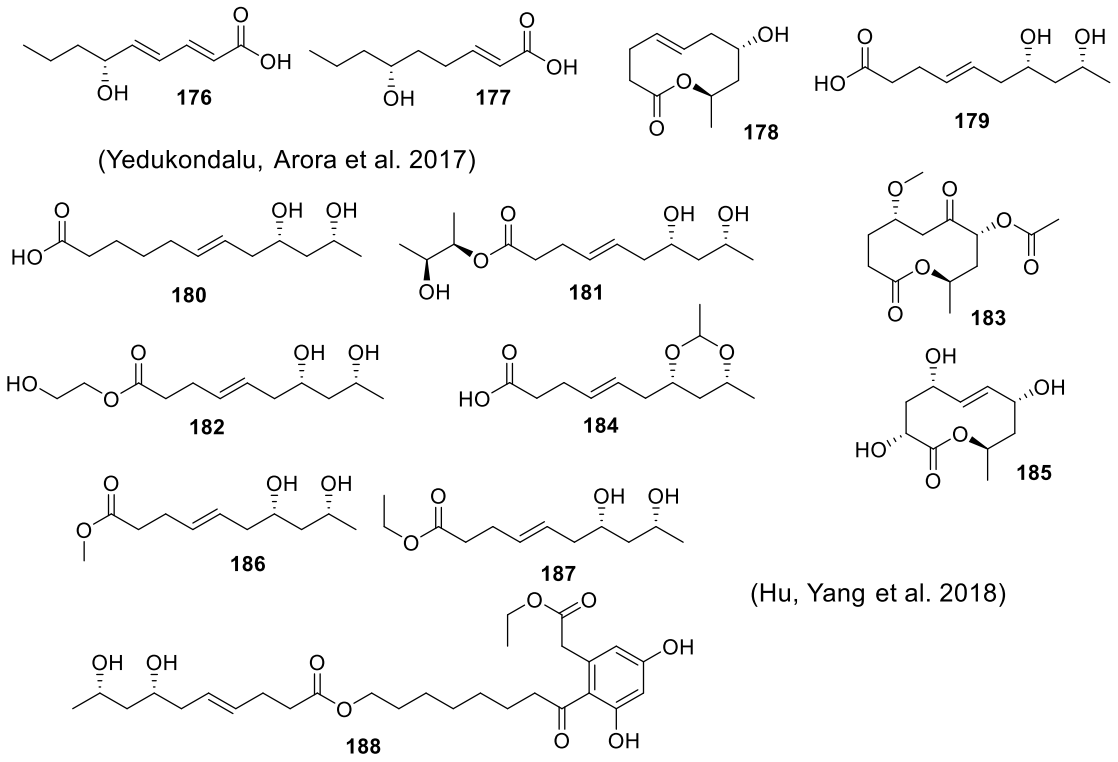

1.3.4 **Cytochalasins**

Cytochalasins are structurally diverse polyketide-non ribosomal peptide fungal secondary metabolites. The characteristic structural feature is a substituted isoindole scaffold with a macrocyclic ring which is derived from a highly reduced polyketide backbone and an amino acid. (Skellam 2017) Phomopsichalasins D–G (**189**–**192**) were isolated from *Phomopsis* sp. xy21. The fungus was obtained as Mangrove endophyte from *Xylocarpus granatum,* collected in Trang, Thailand. (Luo, Zhang et al. 2016) *Phomopsis* sp. shj2 yielded three cytochalasins, phomopchalasins A–C (**193**–**195**). The configurations of phomopchalasins A and B (**193** and **194**) were determined via ECD calculation and comparison with known compounds. The X-ray measurement for phomopchalasins A and C (**193** and **195**) confirmed the structures. (Yan, Wang et al. 2016) Phomocytochalasin A (**196**) was isolated from *Phomopsis asparagi*, an endophyte of the plant *Peperomia sui* collected from Pingtung County, Taiwan. *(Chang, Peng et al. 2018)* 18-Methoxycytochalasin J (**197**) was produced by *Phomopsis* sp. IFB-E060. The fungus was isolated from plant *Vatica mangachapoi* collected from Guangdong Province, P. R. China. (Shen, Luo et al. 2014) *Phomopsis theicola* obtained from leaves of *Litsea hypophaea* collected in Pingtung County, Taiwan, yielded phomocytochalasin (**198**). (Hsiao, Chang et al. 2016) Cytochalasin R1 (**199**) was isolated from *Phomopsis* sp. CIB-109, a plant

pathogenic fungus collected from Sichuan Province, P. R. China. (Zhan, Li et al. 2013) Cytochalasins J1–J3, H1, and H2 (**200–204**) were isolated from the marine sediment derived fungus *Phomopsis* sp. CMB-M0042F collected in Queensland, Australian. (Shang, Raju et al. 2017) Diaporthalasin (**205**), an interesting pentacyclic lactam cytochalasin, was isolated from *Diaporthe* sp. PSU-SP2/4 together with compound **164** which had been described before. (Khamthong, Rukachaisirikul et al. 2014)

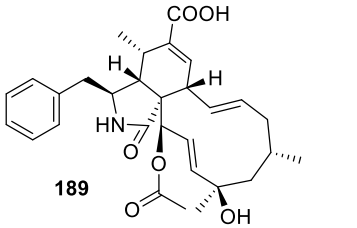

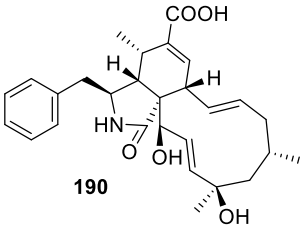

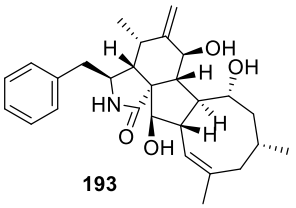

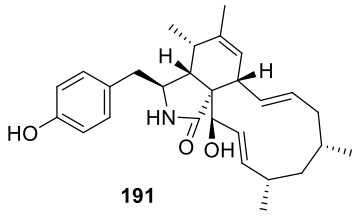

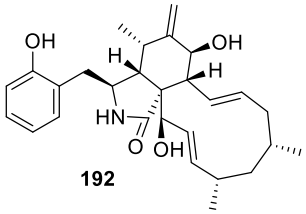

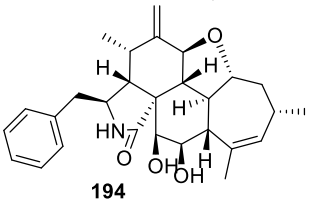

(Luo, Zhang et al. 2016)

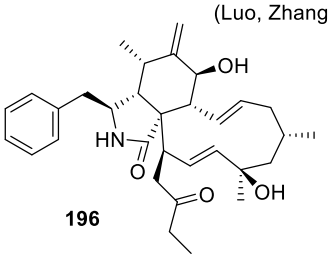

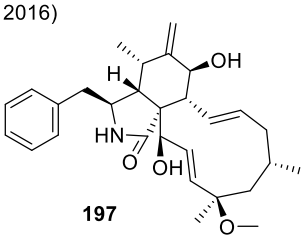

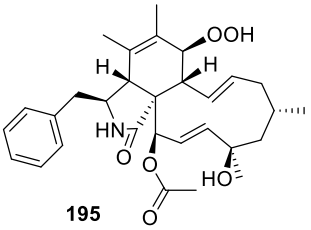

(Chang, Peng et al. 2018)

(Shen, Luo et al. 2014)

(Yan, Wang et al. 2016)

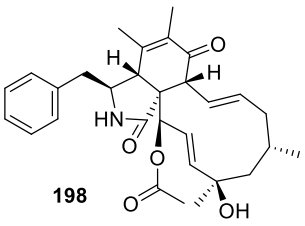

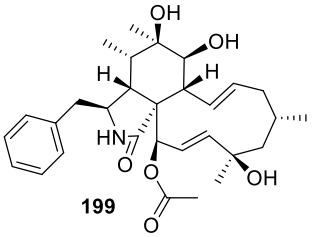

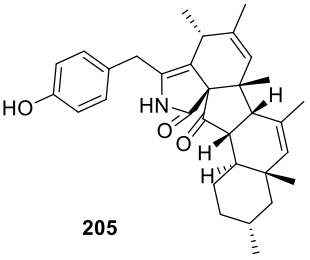

(Hsiao, Chang et al. 2016)

(Zhan, Li et al. 2013)

(Khamthong, Rukachaisirikul et al. 2014)

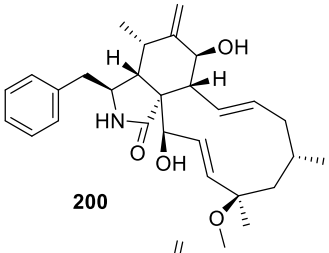

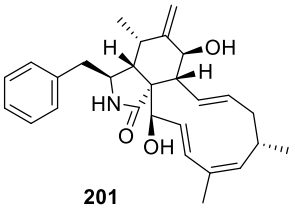

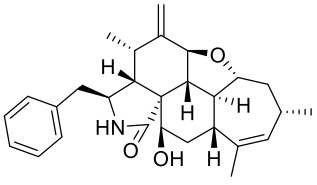

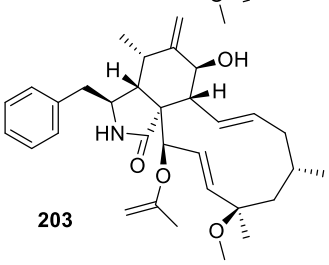

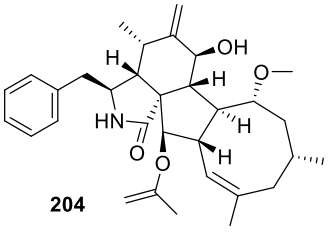

(Shang, Raju et al. 2017)

1.3.5 **Peptides**

Two cyclopeptides (**206** and **207**) were isolated from a co-culture of *Phomopsis* sp. K38 and *Alternaria* sp. E33. Those soil-derived fungi were obtained from a Mangrove area in Guangdong Province, P. R. China. In the antifungal activity test against plant pathogenic fungi *Gaeumannomyces graminis, Rhizoctonia cerealis, Helminthosporium sativum,* and *Fusarium graminearum*, both compounds showed activity with MIC values range from 150 to 400 μg/mL, while the positive control triadimefon had a MIC of 100-150 μg/mL. (Shi, Yuan et al. 2016) A methylated derivative of phomopsin A (**208**) was isolated from lupin seeds fermented by *Diaporthe toxica*. It showed cytotoxicity against HepG2 cells with an IC_{50} value of 6.1 μM. (Schloss, Hackl et al. 2017) The fungus *Phomopsis glabrae* isolated from leaves of the Mangrove plant *Pongamia pinnata*, collected in Maharashtra, India, produced the depsipeptide PM181110 (**209**) with a fatty acid moiety. (Verekar, Mishra et al. 2014)

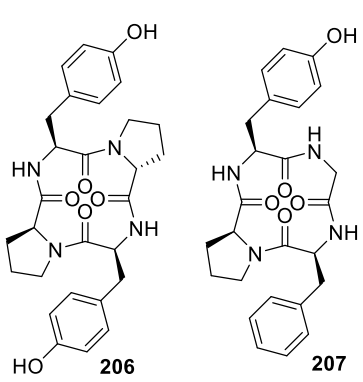

206 **207**

(Shi, Yuan et al. 2016)

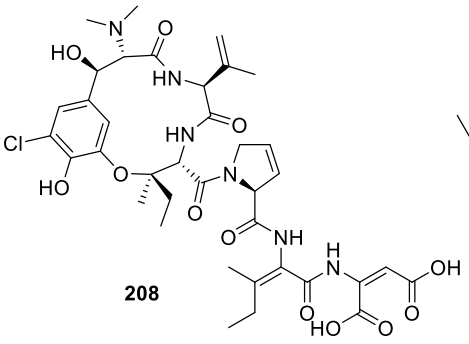

208

(Schloss, Hackl et al. 2017)

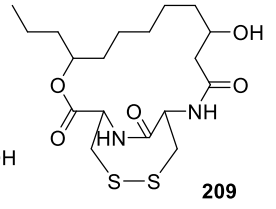

209

(Verekar, Mishra et al. 2014)

1.3.6 **Terpenoids and Steroids**

Terpenoids are also a major class of secondary metabolites from *Phomopsis* and are derived from the isoprene biosynthesis pathway. (Schmidt-Dannert 2015) Phomophyllins A–N (**209**–**223**) were isolated from *Phomopsis* sp. TJ507A. The fungus was obtained as an endophytic fungus of the medicinal plant *Phyllanthus glaucus* collected in Jiangxi Province, P. R. China. The absolute configurations of all compounds were elucidated based on ECD calculation or X-ray measurement together with Mosher's reactions. Compounds **209–215** and **217** showed inhibitory activity ranging from 19.4% to 43.8% at a dose of 40 μM against the *β*-site amyloid precursor protein cleaving enzyme 1 (BACE1). The BACE1 inhibitor LY2811376 (0.5 μM) was used as the positive control

with an inhibitory rate of 38.6%. (Xie, Wu et al. 2018) Ten sesquiterpenoids diaporols J-S (**224**–**233**) were isolated from the fungus *Diaporthe* sp. IFB-3lp-10. The fungus was obtained from leaves of *Rhizophora sutylosa,* a Mangrove plant collected from Hainan Island, P. R. China. The absolute configurations of compounds **224, 225, 232**, and **233** were elucidated via X-ray measurements, and absolute configurations for compounds **224** and **230** were determined via ECD calculation and comparison with known compounds. (Chen, Liu et al. 2015)

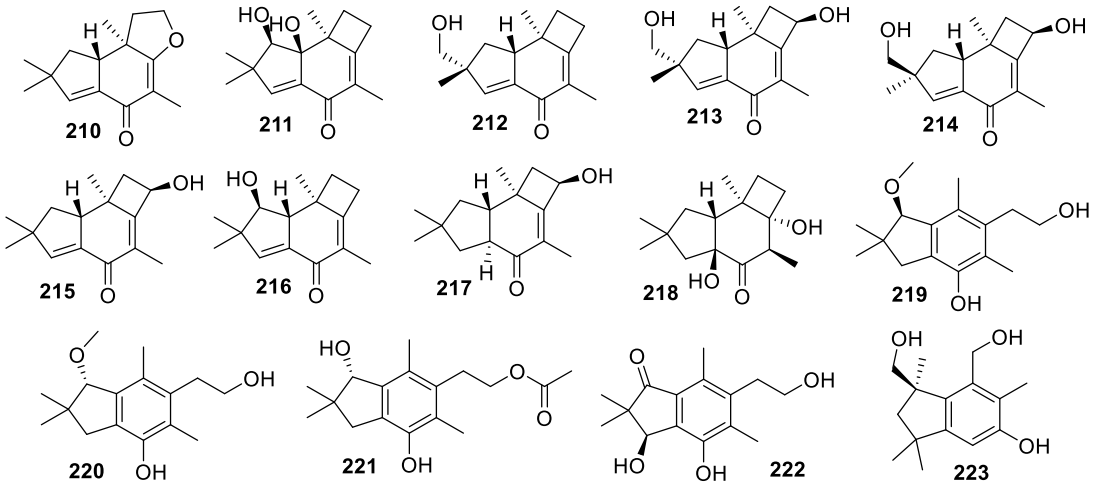

(Xie, Wu et al. 2018)

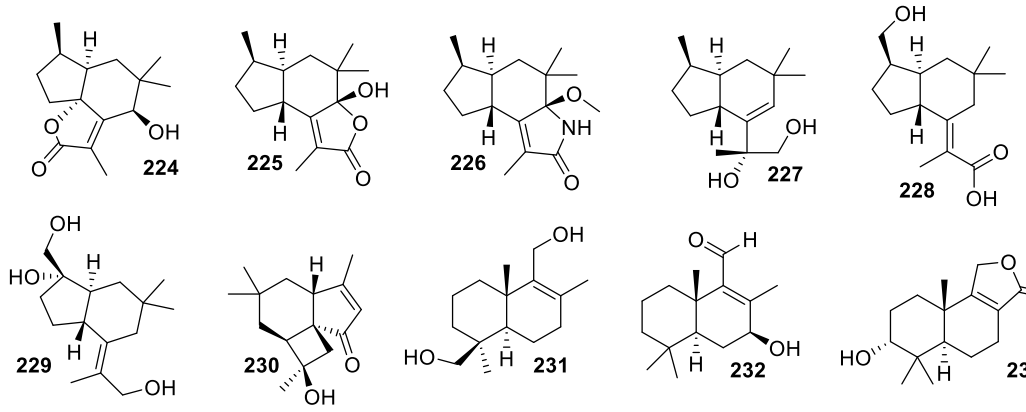

(Chen, Liu et al. 2015)

Myrocin E (**234**), tellenone J (**235**) and libertellenone K (**236**) were isolated from *Phomopsis* sp. S12. The fungus was obtained from seeds of *Illigera rhodantha,* collected in Hainan Island, P. R. China. The structures of tellenone J (**235**) and libertellenone K (**236**) were confirmed by X-ray measurement. In the bioactivity test, tellenone J (**235**) showed significant immunosuppressive activities and reduced LPS-induced NO, IL-1β, IL-6 and TNF-α production with an IC_{50} value ranging from 2.2 to 10.2 μM. It furthermore inhibited activation of MAP kinase and NF-κB pathway. (Wei, Gao et al. 2014) A lanostanoid (**237**) with a structurally interesting aromatic B-ring was

isolated from *Diaporthe* sp. LG23, an endophytic fungus of *Mahonia fortune,* collected in Shanghai, P. R. China. The bioassay showed antibiotic activity with MIC value ranging from 0.1 to 5.0 µg/mL against the bacterial strains *Staphylococcus aureus* (DSM 799), *Escherichia coli* (DSM 682), *Bacillus subtilis* (DSM 1088), *Pseudomonas aeruginosa* (DSM 22644), and *Streptococcus pyogenes* (DSM 11728), while the positive controls streptomycin and gentamicin had MIC values of 1-10 µg/mL. (Li, Kusari et al. 2015) An euphane triterpenoid (**238**) was produced by *Phomopsis chimonanthi,* an endophytic fungus of *Tamarix chinensis* from Shandong Province, P. R. China. The absolute configurations were determined via Mosher's reaction (Zhang, Hao et al. 2013) Two steroids (**239** and **240**) were isolated from *Phomopsis* sp. YM 355364, an endophytic fungus of *Aconitum carmichaeli* from Yunnan Province, P. R. China. (Wu, Huang et al. 2013) Two ergostane-type steroids, namely phomopsterones A and B (**241** and **242**) were isolated from *Phomopsis* sp. TJ507A, an endophytic fungus of the medicinal plant *Phyllanthus glaucus*. The bioassay indicated that phomopsterone B (**242**) exhibited anti-inflammatory activity and caused iNOS enzyme inhibition as well as inhibed nitric oxide (NO) production. (Hu, Wu et al. 2017) *Diaporthe* sp. SNB-GSS10, an endophytic fungus from leaves of *Sabicea cinereal*, collected in Roura, French Guiana, produced enamidin (**243**) and eremofortin F (**244**). (Mandavid, Rodrigues et al. 2015) Eremophil-9-ene-11,12,13-triol (**245**) and oxazole, 4-(2-hydroxyethyl)-5-methyloxazole (**246**) were isolated from the endophytic fungus *P*homopsis sp. A240. The fungus was obtained from *Taxus chinensis* var. *mairei* collected in Guangdong Province, P. R. China. (Tao, Chen et al. 2014) (+)-*S*-1-Methyl-abscisic-6-acid (**247**), a new abscisic acid congener, was isolated from the entomogenous fungus *Phomopsis amygdali* No. RAXL Y-6. The fungus was isolated from Cecidomyiidae Gall midges collected from Ai Sha forest farm, Guangxi Province, P. R. China. (Ma, Wang et al. 2016) Homopetasinic acid (**248**), consisting the moieties of an ester of a fatty acid and a sesquiterpene was isolated from *Diaporthe* sp. The ECD calculation established the configuration. (Ito, Kumagai et al. 2016)

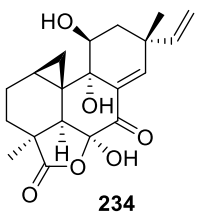

234

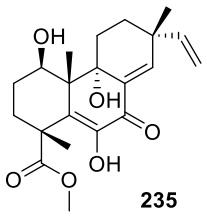

235

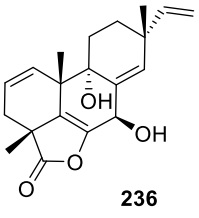

236

(Wei, Gao et al. 2014)

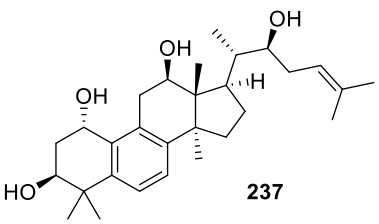

237

(Li, Kusari et al. 2015)

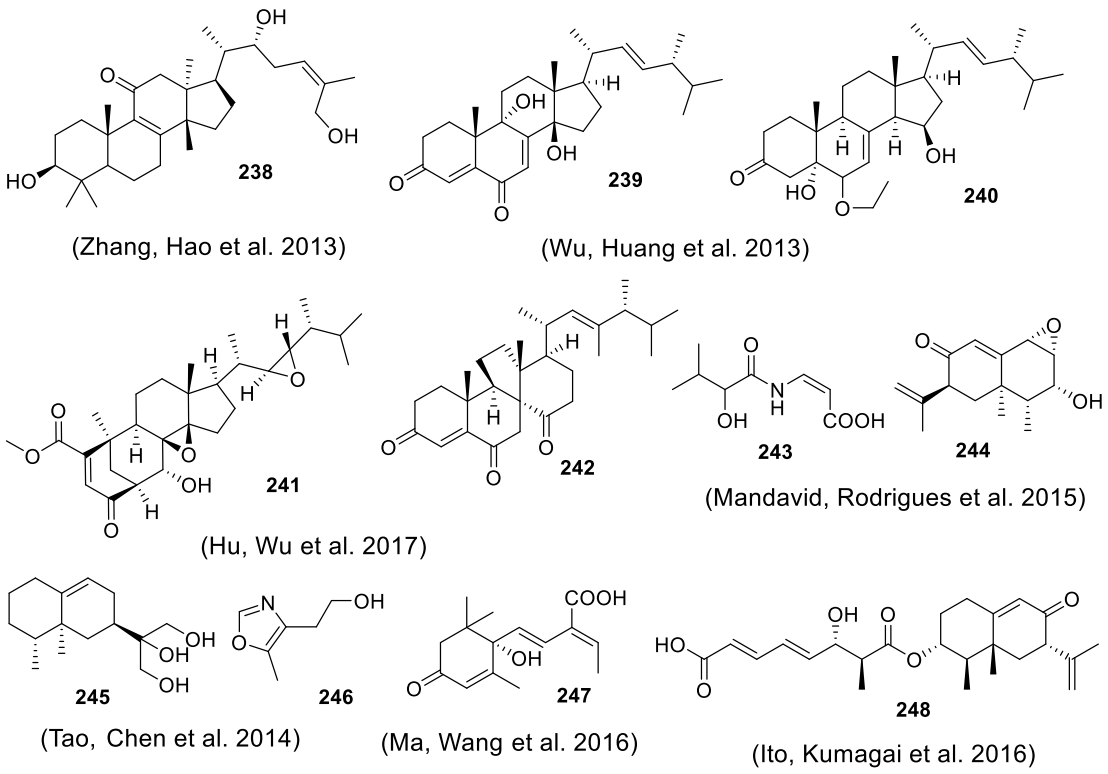

In total, 248 new metabolites were reported from the genus *Phomopsis* in the past six years. Most of the producers were endophytic fungi, especially from medicinal plants such as *Paris polyphylla* and from Mangrove plants. Based on the structural characteristics, polyketide-derived metabolites are the largest group.

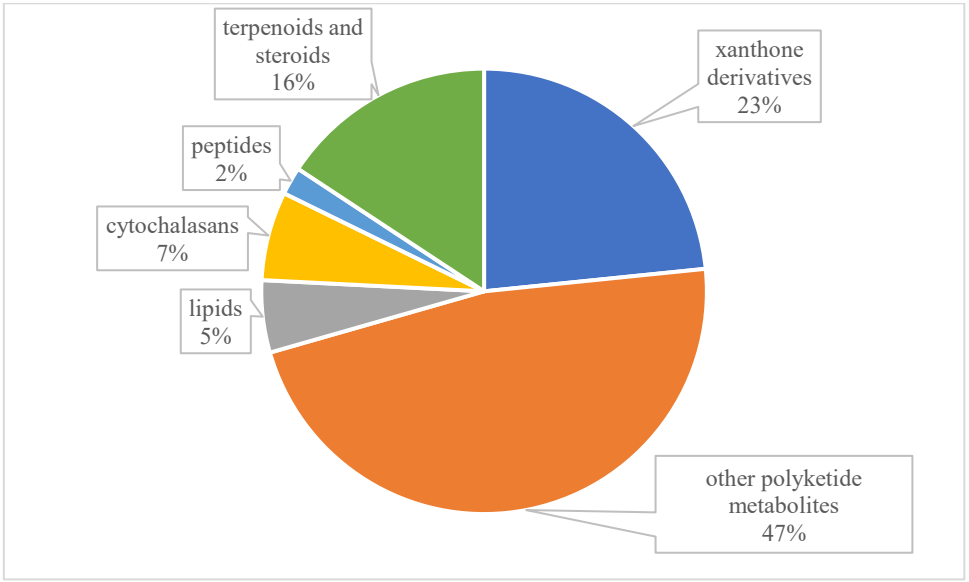

1.4 Azaphilones, a Group of Bioactive Polyketide Metabolites (a Review Covering the Years 2013-2018)

In this chapter, azaphilones are summarized by their structures to better understand the main compounds isolated from *Coniella fragariae* as presented in this thesis. The first reported azaphilone was citrinin, which was isolated from *Penicillium citrinum* in 1931. (Hetherington and Raistrick 1931) The core structure of the azaphilones is based on a highly oxygenated bicyclical core containing oxygen or nitrogen at position 2. (Gao, Yang et al. 2013) The side chains or methyl groups are preferentially linked to positions 3 and 8. At position 8, a saturated side chain usually forms a five-membered lactone ring. The unsaturated side chain is preferably linked to position 3. The oxygen prefers positions 6, 7, and 8 and to be in the form of hydroxyl or carbonyl groups. Some compounds will form an ester bridge with a fatty acid. Additionally, azaphilones were isolated from a fungal-fungal co-culture of *Nigrospora oryzae* and *Beauveria bassiana*, (Zhang, Yang et al. 2018) and also during several OSMAC (one strain many compounds) experiments. Interestingly, only the OSMAC-obtained azaphilones have a side chain at the unusual C-5 position. (Hewage, Aree et al. 2014, Wijesekera, Mahidol et al. 2017)

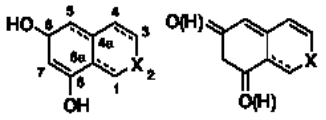

X=O or N

Azaphilones are typical fungal polyketide metabolites, that have mainly been reported from the fungal genera *Penicillium, Aspergillus, Talaromyces, Monascus,* and *Chaetomium*. (Gao, Yang et al. 2013) The compounds can be considered as taxonomic markers. (Chen, Chen et al. 2017) Depending on the chemical structures, different kinds of activities of azaphilones have been described. Furthermore, numerous publications exist reporting the biosynthesis of azaphilones as well as their chemical synthesis. Until 2012, 373 azaphilones had been reported according to a review by Gao *et al.*. (Gao, Yang et al. 2013) Between 2013 and 2018, 50 additional papers were published reporting 153 azaphilones as new natural products. These azaphilones are grouped by chemical structures as classical azaphilones, classical azaphilones with oxygen side chains, unusual azaphilones, 7,8-lactone ring azaphilones, and nitrogenous azaphilones.

1.4.1 **Classical Azaphilones**

Compounds **1–17** were reported as new compounds without side chains. Annulohypoxylomans A−C (**1–3**), annulohypoxylomanols A and B (**4** and **5**) and annulohypoxyloside (**6**) were isolated from *Annulohypoxylon truncatum* JS540, which is an endophytic fungus of the plant *Zizania caduciflora* collected from Suncheon, South Korea. Annulohypoxyloside (**6**) is the only glucosidic azaphilone published between the year 2013 and 2018 (Li, Lee et al. 2017) From an unidentified marine bryozoan, the entomopathogenic fungus *Beauveria felina* EN-135 was isolated and produced felinones A and B (**7** and **8**). The absolute configuration of felinone A (**7**) was determined by the application of ECD and comparison with known compound pestafolide A. (Du, Li et al. 2014) Xylariphilone (**9**) was isolated from a seagrass-derived fungus *Xylariales* sp. PSU-ES163. The seagrass *Halophila ovalis* was collected from Trang Province, Thailand. The absolute configuration was only proposed by ECD spectrum analysis and comparison with a similar known compound. (Arunpanichlert, Rukachaisirikul et al. 2016) Hypoillexidiol only with relative configuration with same planner structure of xylariphilone (**9**) also reported from *Hypoxylon* sp. 12F 0687. The fungus was obtained as endophytic fungus from roots of *Ilex formosana* collected in Yilan County, Taiwan. Hypoillexidiol showed potent anti-NO production activity with an IC_{50} value of 17.5 μM, while the positive control quercetin had an IC_{50} value of 35.9 μM. (Chen, Cheng et al. 2015) Aspergillusone C (**10**) was isolated from the fungus *Aspergillus clavatus,* an endophytic fungus isolated from leaves of *Tripterygium hypoglaucum* (Levl.) Hutch. (Wang, Bai et al. 2015) Felinone A (**7**), xylariphilone (**9**), and aspergillusone C (**10**), share the same planar structure with different configurations at position 6 and 7. Perangustols A and B (**11** and **12**) only the relative configuration were isolated from the marine sediment-derived fungus *Cladosporium perangustm* FS62, which collected at a depth of 955 m in the South China Sea. (Fan, Sun et al. 2016) From the fungus *Aspergillus fumigatus,* which was isolated from the fruiting body of *Cordyceps sinensis* collected from Gansu Province, P. R. China, five azaphilones (**13–17**) were isolated. The first two compounds **13** and **14** were mixtures of enantiomers, which was separated by chiral HPLC. ECD calculations were used to determine the absolute configurations for compounds **13** and **14**. (Li, Han et al. 2018)

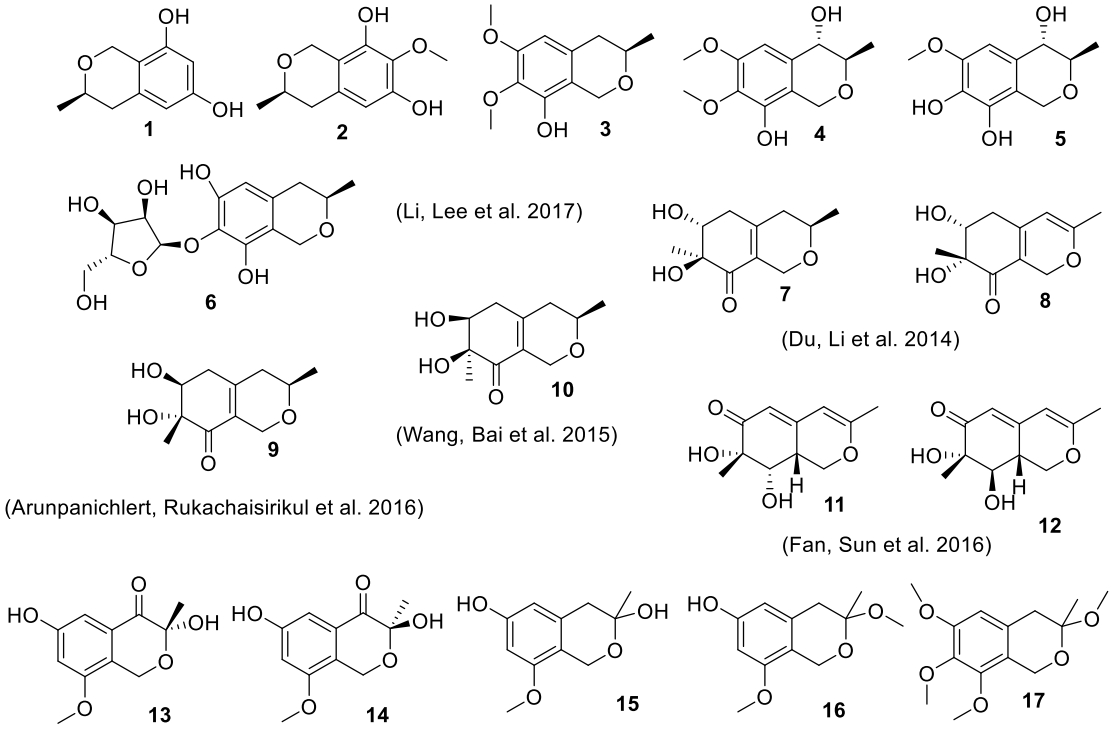

This group of classical azaphilones shares a carbon scaffold and a side chain connected to carbon-3. Nigirpexins A–D (**18–21**) are four pulvilloric acid-type azaphilones, which isolated from a *Nigrospora oryzae* co-culture with *Irpex lacteus*. Furthermore, the authors also investigated the interactions of between *N. oryzae* and *I. lacteus*. Both endophytic fungi were isolated from seeds of *Dendrobium officinale*, which were collected from Yunnan Province, P. R. China. The authors suggested that azaphilones were produced by *N. oryzae*, while *I. lacteus* induced their production. (Zhou, Yang et al. 2018) Nigbeauvins A–E (**22**–**26**) were also obtained from a co-culture of *Nigrospora oryzae* with *Beauveria bassiana*. Both fungi were isolated form seeds of *Dendrobium officinale* collected from Yunnan Province, P. R. China. Interestingly, nigirpexin B (**23**) displayed an unprecedented skeleton with a bicyclic oxygen bridge at carbons 3 and 1. Nigbeauvins A and B (**22** and **23**) showed pronounced NO inhibitory activity with ratios at 37% and 39% at 50 μM, respectively, while the positive control NG-monomethyl-L-arginine (L-NMMA) showed an inhibition ratio of 50 % at 50 μM. (Zhang, Yang et al. 2018) Peniazaphilin A (**27**), an azaphilone with a tetrahydrofuran moiety was isolated from soil derived *Penicillium* sp. CPCC 400786 collected from Chongqing City, P. R. China. The absolute configuration was determined by ECD spectrum comparison to known compounds. This compound showed weak anti-HIV activity with an IC_{50} value of 60.4 μM. (Zhang, Zhao et al. 2018) The structure of pleosporalone A (**28**) was elucidated as an

azaphilone with an aromatic moiety at carbon-3. It was obtained from a marine derived *Pleosporales* sp. CF09-1, which was isolated from sediment collected from Bohai Sea, P. R. China. Pleosporalone A (**28**) showed stronger antifungal activity against plant pathogenic *Botrytis cinereal* (IC_{50} 0.39 μM), *Rhizopus oryzae* (IC_{50} 0.78 μM) and *Phytophthora capsici* (IC_{50} 0.78 μM), compared to the positive control carbendazim with IC_{50} values 0.78, 1.56 and 1.56 μM, respectively. (Cao, Yang et al. 2016) An unnamed azaphilone (**29**), with a rare hydroxyl group connected to carbon-5, was isolated from *Penicillium* 303#. The fungus was obtained from sea water collected in a Mangrove reserve area in Guangdong Province, P. R. China. The compound **29** reported only with relative configuration showed weak cytotoxicity with IC_{50} values ranging of 11.09-24.62 μM against MDA-MB-435, HepG2, HCT-116, and A549 cell lines.(Li, Yang et al. 2014) Geumsanols A and C–E (**30–33**) were produced by a soil derived *Penicillium* sp. KCB11A109 together with several chlorinated known compounds. The fungus was isolated from a soil sample collected in Geumsan, Korea. Geumsanol E (**33**) exhibited phenotypic effects in zebrafish development. (Son, Ko et al. 2016)

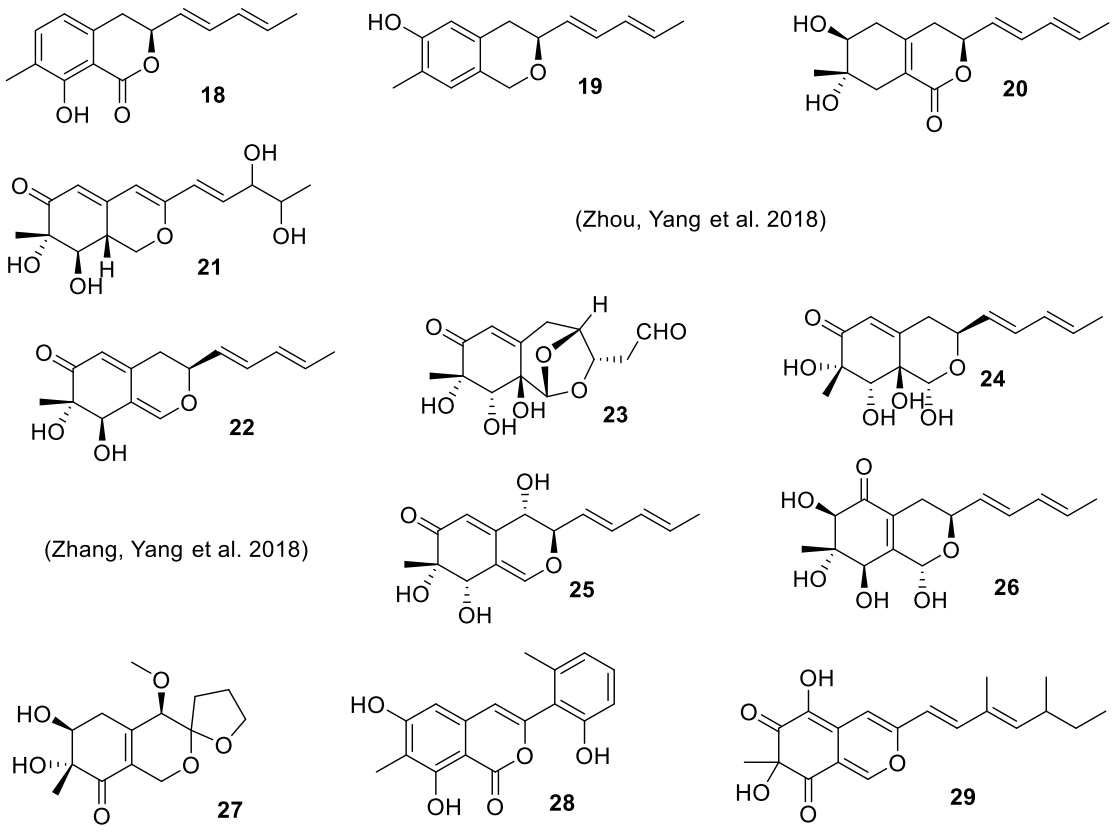

(Zhou, Yang et al. 2018)

(Zhang, Yang et al. 2018)

(Zhang, Zhao et al. 2018)

(Cao, Yang et al. 2016)

(Li, Yang et al. 2014)

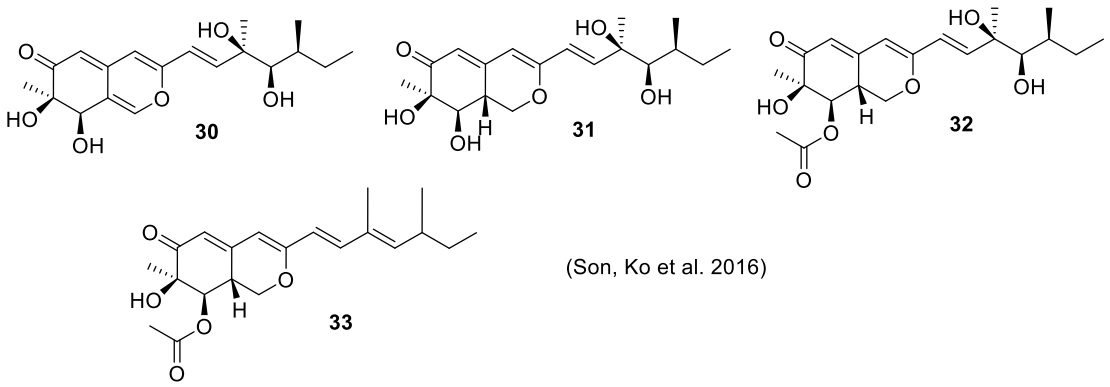

(Son, Ko et al. 2016)

The azaphilones depicted below are halogenated and contain a chloride moiety at position 5. Penicilazaphilones D and E (**34** and **35**) are two chlorinated azaphilones, isolated from *Penicillium sclerotiorum*. The fungus was obtained from the inner tissue of an unidentified sponge collected from a coral reef at a depth of 10 m in the sea area of Guangdong Province, P. R. China. Penicilazaphilone E (**35**) exhibits an interesting side chain at carbon-3, derived from a tetrahydrofuran ring. The absolute configuration of compound **34** was determined via X-ray measurement together with ECD calculations. (Wang, Hao et al. 2018) Penicilazaphilone C (**36**) was isolated from the marine fungus *Penicillium sclerotiorum*. The fungus was isolated from a rotten leaf sample collected near the sea coast at Hainan Island, P. R. China. The compound showed selective antiproliferative activity against B-16 and SGC-7901 cells, but weak effects against normal M-10 cells. In the antibacterial activity test, it showed activity with IC_{50} values ranging from 0.037 to 0.150 mM against *Staphylococcus aureus*, *Pseudomonas aeruginosa*, *Klebsiella pneumonia*, and *Escherichia coli*. (Zhou, Wang et al. 2016) Eupenicilazaphilones A–C (**37**–**39**) were isolated from *Eupenicillium* sp. 6A-9, which was isolated from the sponge *Plakortis simplex* collected from Yongxing island, P. R. China. The configurations of compounds (**37**–**39**) were elucidated via ECD calculation and comparison to known compounds. In the cytotoxicity test, all compounds showed weak cytotoxicity with IC_{50} value ranging from 36.88 to 49.95 μM against the MCF7 cell line, and compounds **38** and **39** showed cytotoxicity with IC_{50} values 63.32 and 43.96 μM against the A459 cell line. (Gu, wu et al. 2018) *Epi*-isochromophilone III (**40**) were isolated from soil derived fungus *Penicillium multicolor* CM01 collected from Chiang Mai Province, Thailand, and showed cytotoxicity against KB, MCF-7 and NCI-H187 cell lines with IC_{50} values of 6.9, 10.6 and 6.2 μg/mL. (Hemtasin, Kanokmedhakul et al. 2016) Penidioxolanes A and B (**41** and **42**), with interesting 1,3-dioxolane containing side chains, were discovered from a marine sediment derived *Penicillium* sp. KCB12C078

collected in Anmyeon Island of South Korea, however, only with relative configuration were reported. (Kim, Son et al. 2015)

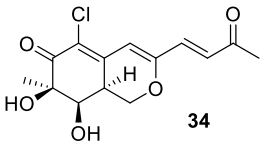

34

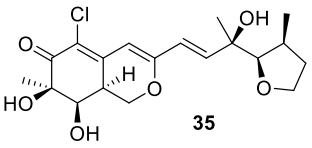

35

(Wang, Hao et al. 2018)

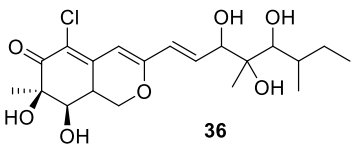

36

(Zhou, Wang et al. 2016)

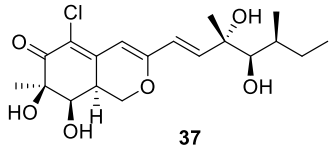

37

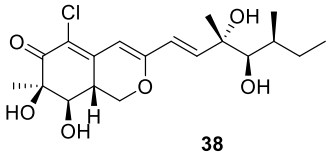

38

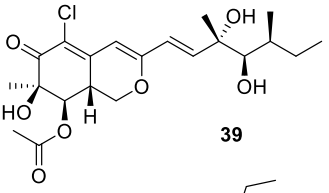

39

(Gu, wu et al. 2018)

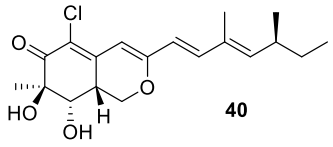

40

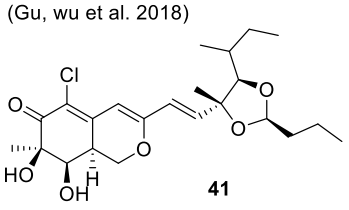

41

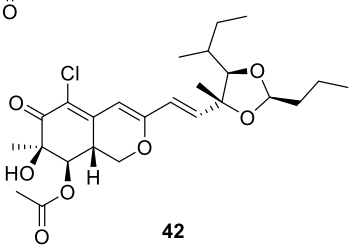

42

(Hemtasin, Kanokmedhakul et al. 2016)

(Kim, Son et al. 2015)

1.4.2 **Classical Azaphilones with Oxygen Linked Side Chains**

This group of azaphilones is characterized by oxygen linked side chains. Usually the side chain prefers to form an ester bridge at position 6, 7, or 8. Based on their chemical structures, most of these side chains are derived from the polyketide/fatty acid pathway. Compounds **43-51** shown below exhibit fatty acid side chains at position 7. Phialomustins A, C and D (**43**–**45**) were isolated from the endophytic fungus *Phialophora mustea,* derived from the plant *Crocus sativus*. The configurations for compounds **43**–**45** were established by comparison of measured ECD spectra with known structures. Phialomustins C and D (**44** and **45**) showed antifungal activity against *Candida albicans* with IC_{50} values of 14.3 and 73.6 μM. (Nalli, Mirza et al. 2015) Penicilones A–D (**46**–**49**) were isolated from *Penicillium janthinellum* HK1-6, which had been obtained from Mangrove rhizosphere soil collected in Hainan Island, P. R. China. All compounds exhibit a six-membered ring at carbon-3 and an ester linked fatty acid side chain at carbon-7. The absolute configuration of penicilone A (**46**) was established via ECD spectrum comparison and Mosher's reaction. Penicilones B–D (**47–49**) showed similar anti-MRSA activities with MIC values ranging from 3.13-6.25 μg/mL, compared to the positive control vancomycin·HCl with 0.39-6.25 μg/mL. (Chen, Shen et al. 2017) Helicusin E (**50**) and isochromophilone XI (**51**), two chloroazaphilones,

were isolated from the fungus *Bartalinia robillardoides* LF550, which had been obtained from the Mediterranean sponge *Tethya aurantium*. The ester side chain at position 7 is derived from the polyketide pathway. The absolute configurations of both compounds were determined by ECD calculation and comparison to known compounds. (Jansen, Ohlendorf et al. 2013)

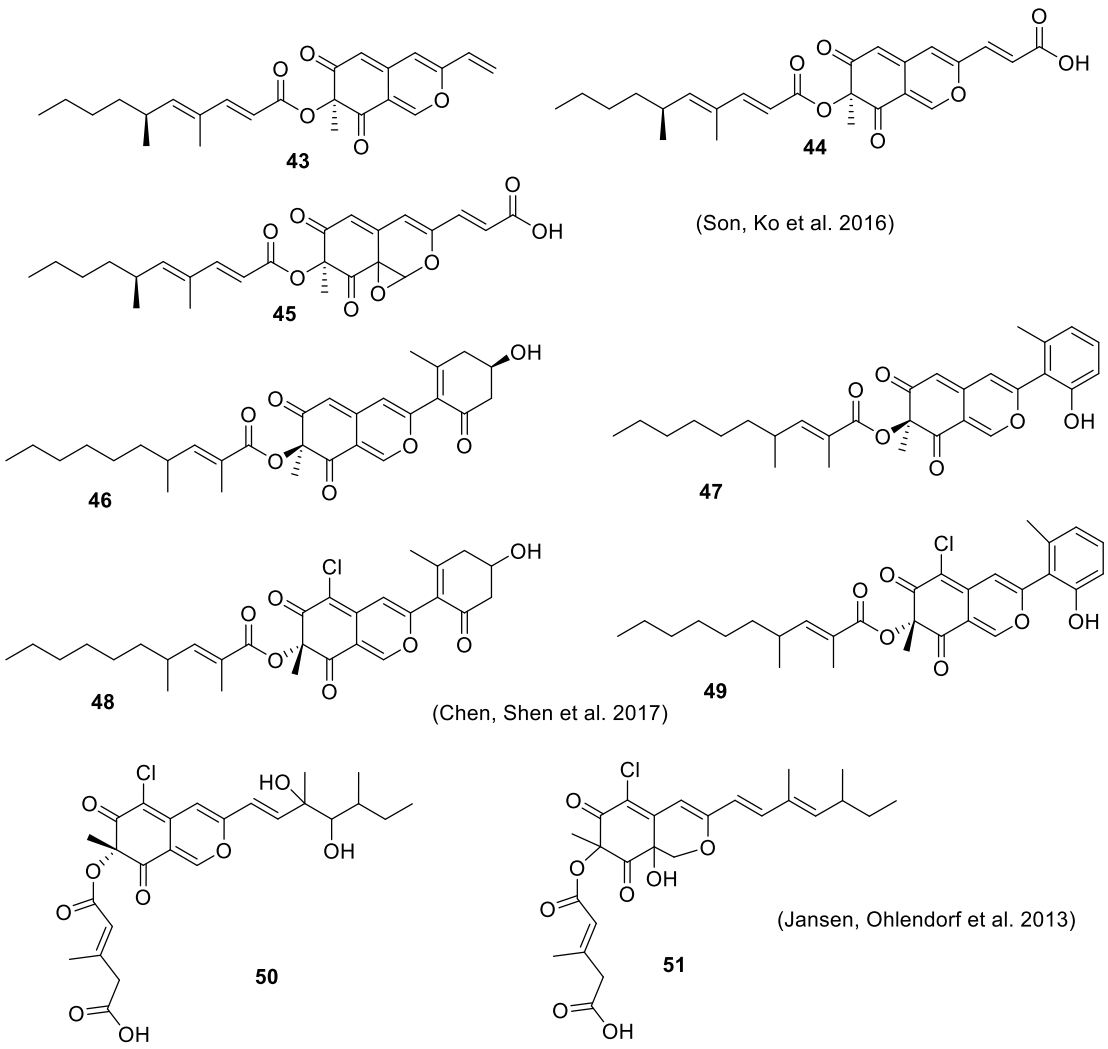

In this group, azaphilones (**52–69**) are connected to an orsellinic acid moiety at position 6, 7, or 8. The azaphilone core structure and orsellinic acid both originate through the polyketide pathway. (Sanchez, Chiang et al. 2010) Montagnuphilones A–G (**52–58**) were published with relative configurations and isolated from the endophytic fungus *Montagnulaceae* sp. DM0194. This fungus was obtained from submerged roots of *Persicaria amphibia* collected from shallow water in Arizona, USA. Montagnuphilones B and E (**53** and **56**) showed NO inhibitory effects without cytotoxicity on lipopolysaccharide activated RAW264.7 cells. The NO inhibition activities are stronger

than that of the positive control with IC_{50} values of 25.5, and 39.6 μM respectively, compared to the positive control, NG-nitro-L-arginine methyl ester (L-Name), which showed an IC_{50} value of 30.6 μM. (Luo, Xu et al. 2017) Pinophilins D–F (**59–61**) were obtained from a gorgonian-derived fungus *Penicillium pinophilum* XS-20090E18, collected from a coral reef in the South China Sea. The absolute configurations for compounds **59–61** were elucidated via ECD calculations. (Zhao, Shao et al. 2015) 6''-Hydroxy-(*R*)-mitorubrinic acid (**62**) and purpurquinone D (**63**) were isolated from the fungus *Aspergillus* sp16-5C, which is an endophyte of the Mangrove plant *Sonneratia apetala* collected in Hainan island, P. R. China. The absolute configurations of compounds **62** and **63** were determined by comparing the optical rotation and ECD spectra to similar known compounds. (Xiao, Lin et al. 2015) Talaraculones A–F (**64–69**), all exhibiting interesting different side chains at carbon-3, were isolated from the saline soil-derived fungus *Talaromyces aculeatus* from Shandong Province, P. R. China. Talaraculones A and B (**64** and **65**) exhibited α-glucosidase inhibition activity with IC_{50} values of 78.6 and 22.9 μM, which are stronger than the positive control acarbose with an IC_{50} value of 101.5 μM. (Ren, Ding et al. 2017)

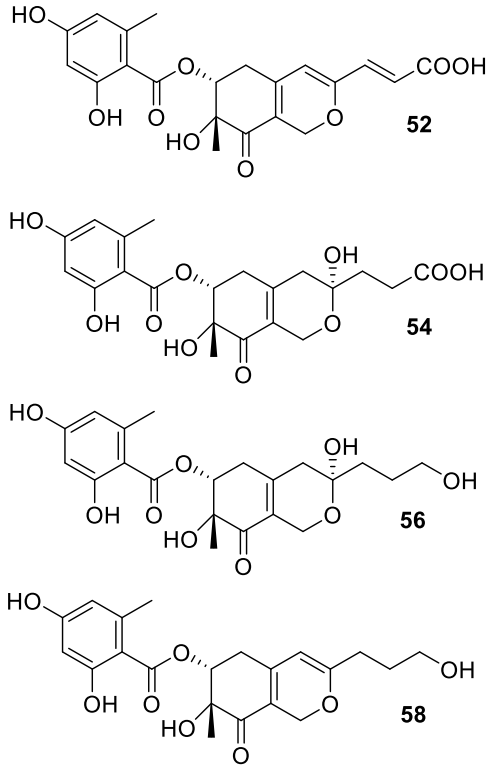

(Luo, Xu et al. 2017)

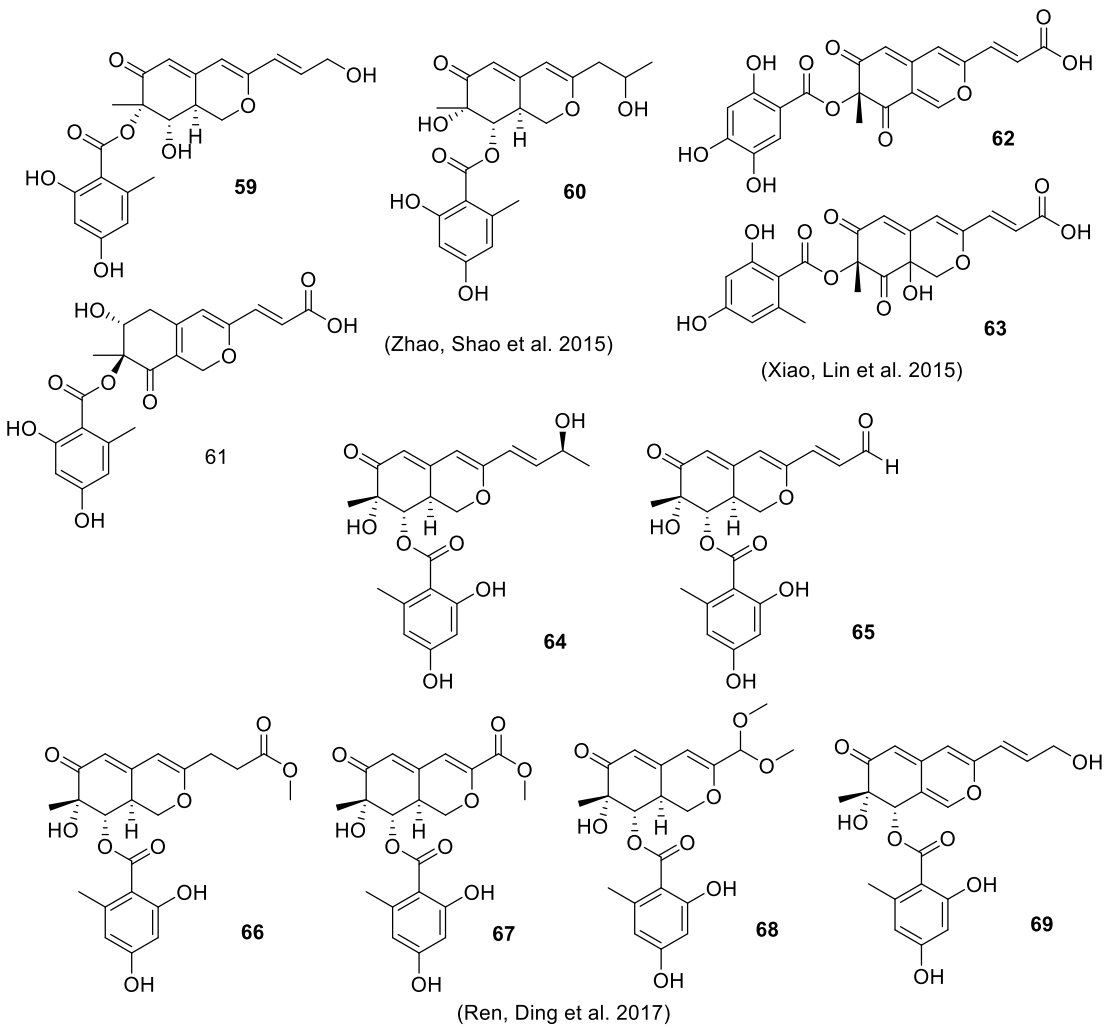

1.4.3 **Unusual Azaphilones**

This group consists of unusual azaphilones. Carbon linked side chains or methyl groups are normally connected to positions C-3, 7 or 8. However, some azaphilones show interesting structures which defy these norms and exhibit unusual side chains or additional ring systems.

Peyronellones A–F (**70–75**) were isolated from the endophytic fungus *Peyronellaea glomerate* and show rare methyl groups at carbon-4. This fungus was obtained from fresh bark of *Ilex cornuta* collected in Jiangsu Province, P. R. China. The absolute configurations of peyronellone A and B (**70** and **71**) could not be identified due to their complex structures. The configurations for the remaining compounds **72**–**75** were all established via ECD calculations. The structure of peyronellone F (**75**) was confirmed by X-ray measurement. Peyronellone A and B (**70** and **71**) improved the survival rate of hypoxia/reoxygenation-treated human umbilical vein endothelial cells from 35% to

70% similar to the positive control verapamil. (Li, Liu et al. 2018) Thielavialides A–E (**76–80**) were isolated from *Thielavia* sp. PA0001, which was obtained from leaf tissue of aeroponically grown *Physalis alkekengi* collected from Arizona, USA. Considering the structural similarity to the known azaphilone pestafolide, they are also be considered as azaphilone class. (Wijeratne, Espinosa-Artiles et al. 2014) Two interesting azaphilones, dothideomynone A (**81**) with methyl groups at C-4 and 5, and dothideomynone C (**82**) which is dimer azaphilone linked by C-5, were isolated from *Dothideomycete* sp. CRI7 through OSMAC methods. The fungus was isolated from the Thai medicinal plant, *Tiliacora triandra* collected from Nakhonsawan Province, Thailand. The configuration of dothideomynone A (**81**) was identified by single crystal X-ray analysis. In cytotoxicity tests against HuCCA-1, MOLT-3, and HepG2 cell lines, dothideomynone C (**82**) exhibited weak cytotoxic activity against MOLT-3 cell lines with an IC_{50} value of 17.4 μg/mL. (Hewage, Aree et al. 2014)

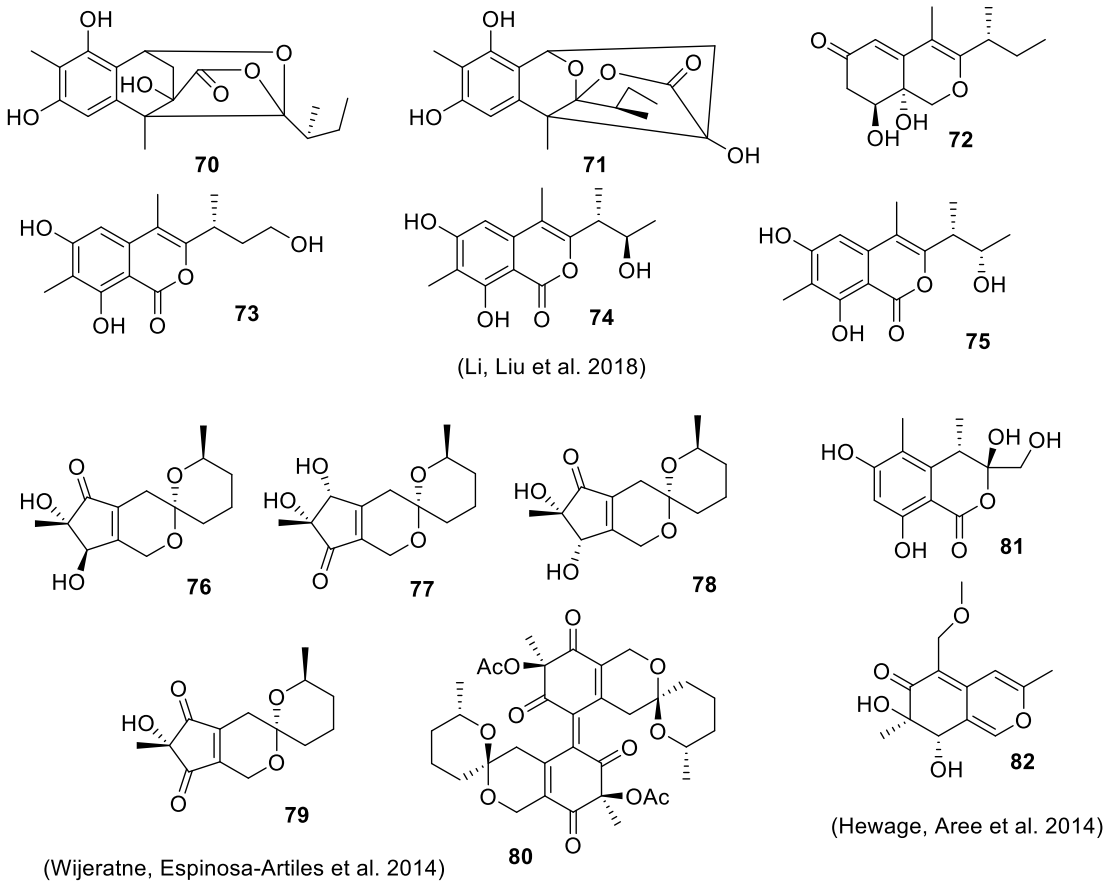

Citrifurans A–D (**83**–**86**), four dimerized azaphilones and furanones with unusual carbon-1 linked cyclic side chain were obtained from a centipede intestine derived

fungus *Aspergillus* sp. from Jiangsu Province, P. R. China. The configurations of citrifurans A and D (**83** and **86**) were established via X-ray measurement and ECD calculation. Citrifurans A–C (**83–85)** were published as new scaffolds, and showed inhibition of LPS-induced NO production in macrophages of RAW 246.7 cells with IC_{50} values of 18.3, 22.6, and 25.3 μM, respectively. (Yin, Wu et al. 2017) Dothideomynone B (**87**) was reported as the first hybrid azaphilone-pyrone, which was isolated together with dothideomynone A and C (**81** and **82**). (Hewage, Aree et al. 2014) Dothideomynones D–F (**88**–**90**), three interesting azaphilones with carbon-5 side chains, together with compounds **81, 82** and **87**, were published from the same fungus *Dothideomycete* sp. CRI7. The configuration of compound **88** was established based on Mosher's reaction and energy minimization. (Wijesekera, Mahidol et al. 2017) Mycoleptones A–C (**91**–**93**), three dimeric azaphilones, were isolated from *Mycoleptodiscus indicus*. The fungus was described as an endophyte of the medicinal plant *Borreria verticillata* (L.) G. F. W. Meyer collected from Recife, Brazil. All dimeric azaphilones are linked via a methylene group at carbon-5. The configurations of three compounds were elucidated via ECD calculation. (Andrioli, Conti et al. 2014) Monapilosusazaphilone (**94**) was isolated from the pigment producing fungus *Monascus pilosus* which is used for food fermentation of red yeast rice. This compound was isolated as yellowish optically inactive oil but not as a pigment. (Cheng, Wu et al. 2013) The fungus *Epicoccum nigrum* which was derived from an unspecified green alga collected in Cabrera, Spain, yielded acetosellin (**95**) and 5', 6'-dihydroxyacetosellin (**96**) which have a carbon-side chain at carbon-6 that forms a lactone ring. Compound **95** formed an aromatic ring at the side chain with carbon-6. (Hufendiek, Stoelben et al. 2017)

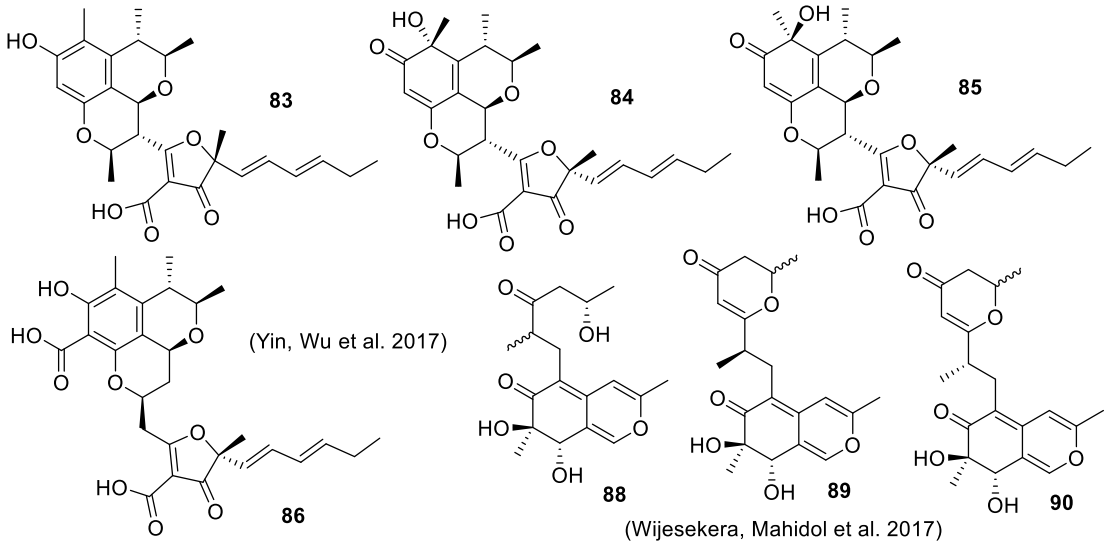

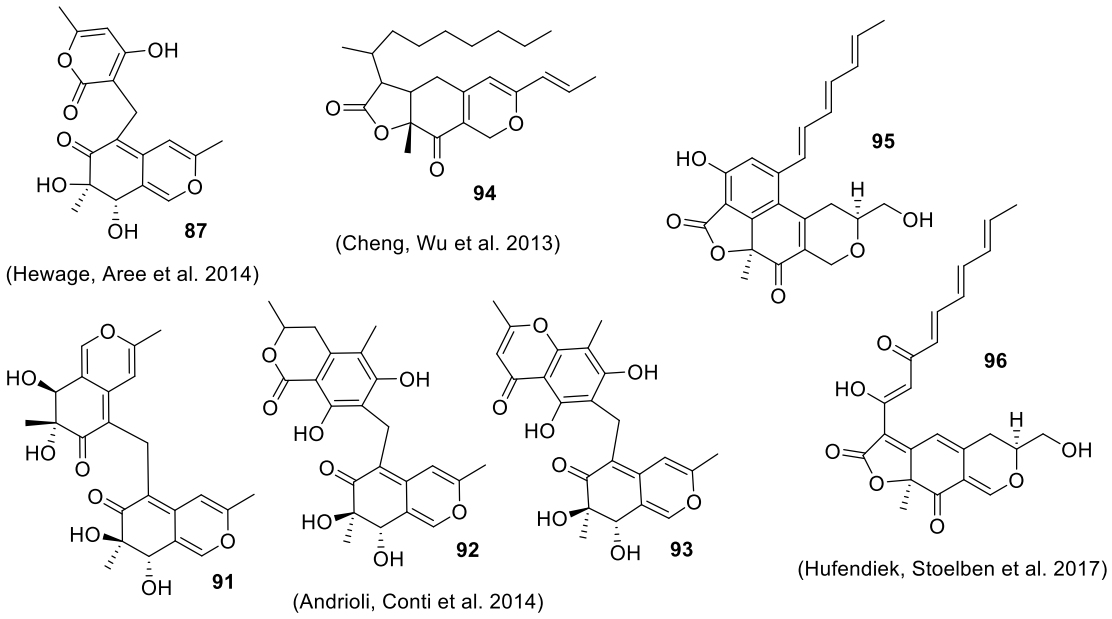

1.4.4 **7, 8 - Lactone Ring Azaphilones and Their Derivatives**

The side chains linked to carbon 8 are mainly derived from fatty acid biosynthesis and may form five-membered lactone rings. Most of these compounds exhibit lactone rings at position 7 and 8. Some compounds, which are proposedly derived from decarboxylation, are also included.

Colletotrichones A–C (**97**–**100**) were isolated from the endophytic fungus *Colletotrichum* sp.. The fungus was obtained from leaves of the traditional Chinese medicinal plant *Buxus sinica* collected from Guangdong Province, P. R. China. The configurations of all compounds were elucidated via ECD calculation and comparison to known compounds. The structure of colletotrichone A (**97**) was confirmed by X-ray measurement. Colletotrichones A, B_a and C (**97, 98** and **100**) showed antibacterial activity without significant cytotoxic effects. Especially compound **97** showed strong inhibitory against *Escherichia coli* and *Bacillus subtilis* with MIC values of 1.0 and 0.1 µg/mL compared to the positive control gentamicin with a MIC value of 1.0 µg/mL against both bacterial strains. (Wang, Kusari et al. 2016) Coniellins A–G (**101**–**107**) were isolated from the fungus *Coniella fragariae*, which obtained from goose drug collected at the North Sea coast close to Garding, Germany. The compounds exhibit rare aldehyde moieties at carbon-5. The configuration of coniellin A (**101**) was determined via ECD calculation. The compounds showed potent NF-κB inhibition and tumor cell migration inhibition at a concentration of 5 µM. (Yu, Sperlich et al. 2018) Minutellins A–D (**108**–**111**),

four azaphilones isolated from the endophyte *Annulohypoxylon minutellum* from stromata (fruiting bodies) of A*nnulohypoxylon minutellum* collected from the Canary Island La Palma, Spain, act as valuable chemotaxonomic markers. The configuration of minutellin A (**108**) was determined by Mosher's reaction together with ECD spectrum comparison to known compounds. (Kuhnert, Surup et al. 2017)

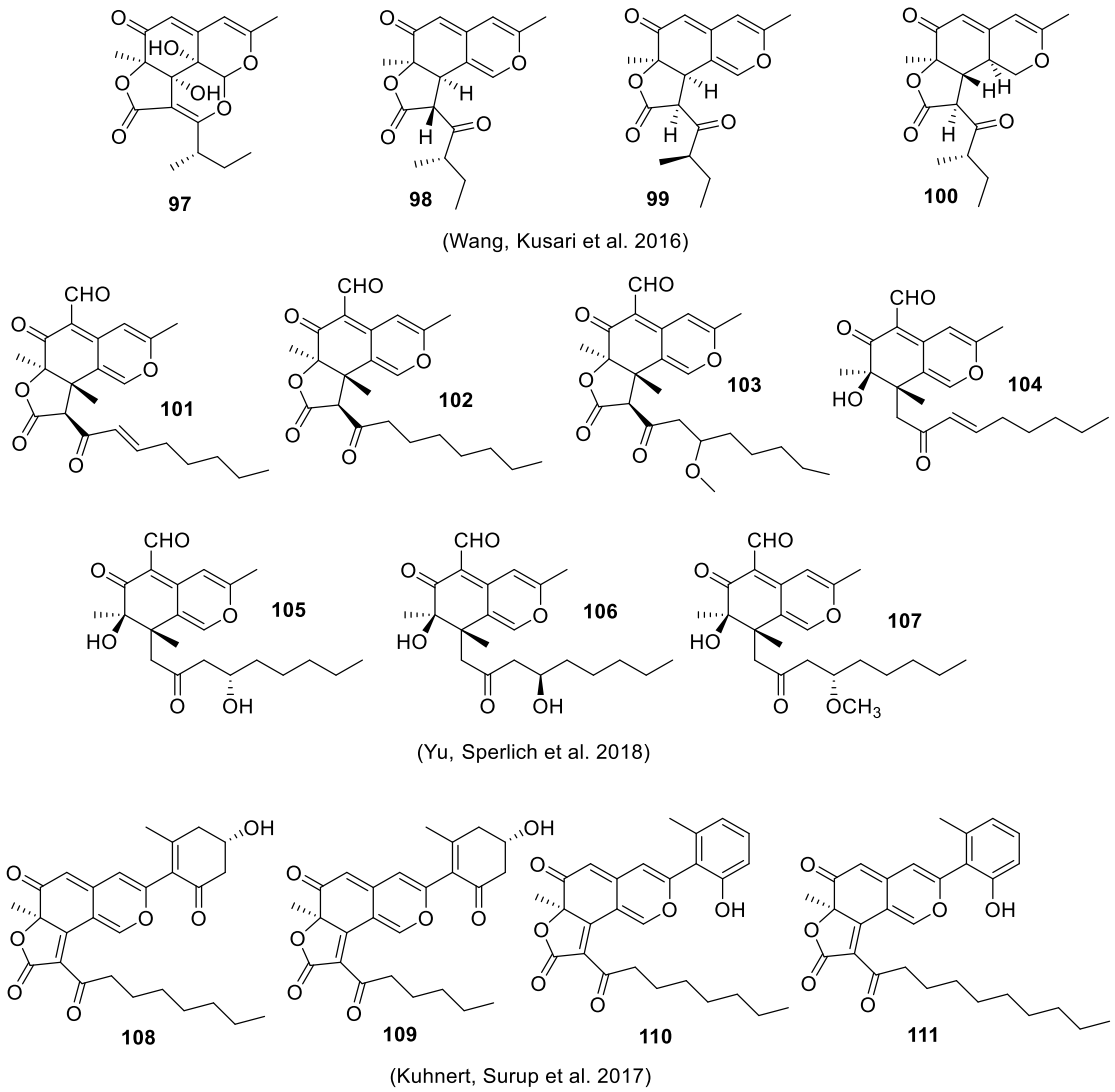

Geumsanol B (**112**), with a side chain at carbon-3, together with geumsanols A and C–E (**30–33**) which had been introduced before, were isolated from the soil derived fungus *Penicillium* sp. KCB11A109. (Son, Ko et al. 2016) The soil derived fungus *Penicillium multicolor* CM01 produced dechloroisochromophilone II (**113**) together with *epi*-isochromophilone III (**40**). The compounds **40** and **113** exhibit a short side chains at carbon-8. (Hemtasin, Kanokmedhakul et al. 2016) Berkchaetoazaphilones A–C (**114–116**) were

isolated from an acid mine extremophile strain of *Pleurostomophora* sp. from Berkeley Pit, USA. Berkchaetoazaphilones B (**115**) showed cytotoxicity with an IC_{50} value of 1.1 µM against the Y79 cell line. It furthermore inhibited the production of interleukin 6 (IL-6) and IL-33, and mitigated production of TNF-α and IL-1β by 95% at the concentration of 10 µM in THP-1 cells. The publication also discussed the similarity of the ECD data related to other azaphilones. (Stierle, Stierle et al. 2015) Cohaerins G–K (**117**–**121**) were isolated from the fungus *Annulohypoxylon cohaerens*. The fungus was obtained from a dead *Fagus sylvatica* trunk in Rheinland-Pfalz, Germany. (Surup, Mohr et al. 2013) A pigment, acetyl-monasfluol B (**122**), was isolated from a conditional culture of fungus *Monascus ruber* after treatment with dihydrocoumarin which is a NAD^+-dependent deacetylases inhibitor. (Hu, Zhou et al. 2017) Monascusazaphilones A–C (**123**–**125**) were isolated from *Monascus purpureus* BCRC 38108. All three compounds showed strong inhibition of NO production with IC_{50} values ranging from 4.60 to 8.88 µg/mL, compared to the positive control quercetin with an IC_{50} value of 8.49 µg/mL against RAW264.7 cell line. (Wu, Cheng et al. 2013) Monascuskaodione (**126**) was isolated from the fungus *Monascus kaoliang* (Cheng, Wu et al. 2015) and monascuspurone (**127**) was from the fungus *Monascus ruber*. (Cheng, Wu et al. 2016) The only differences of both structures are the side chain length at carbon-8. The biosynthesis study at gene level confirmed azaphilones as marker metabolites for fungi of the genus *Monascus*. *(Chen, Chen et al. 2017)*

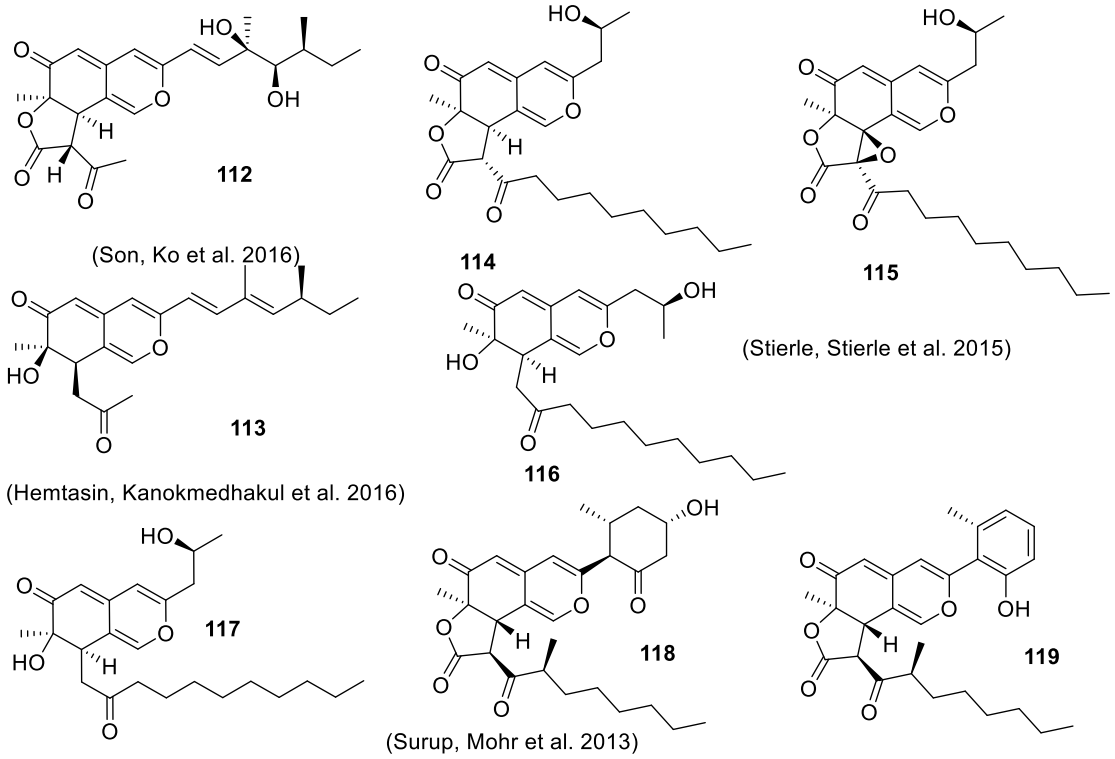

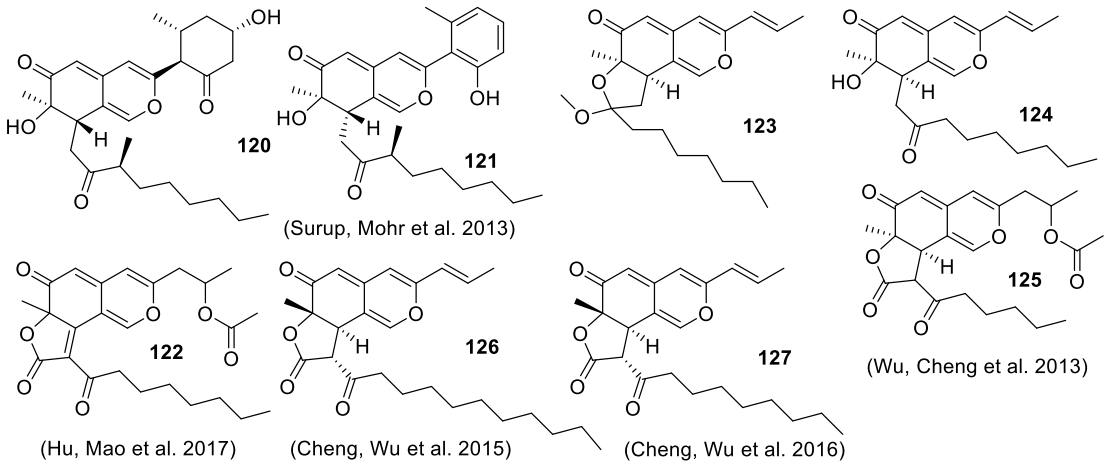

Compounds **128–140** shown below are chlorinated-lactone azaphilones and their derivatives. Similar to chlorinated classical azaphilones, the chloride atom is usually located at position 5. Isochromophilones A–F (**128–133**), six chlorinated azaphilones, were isolated from the endophytic fungus *Diaporthe* sp. SCSIO 41011. The fungus was derived from the Mangrove plant *Rhizophora stylosa* collected in Hainan Island, P. R. China. The configurations of all compounds **128**–**133** were elucidated via ECD calculation and comparison to known compounds. Isochromophilones D and F (**131** and **133**) showed cytotoxicity against ACHN, 786-O, OS-RC-2 cell lines with IC_{50} values ranging from 10 to 38 μM, the positive control sorafenib had IC_{50} values ranging from 3.4 to 7.0 μM. (Luo, Lin et al. 2018) Two chlorinated azaphilones, chaephilones A and B (**134** and **135**), were isolated from *Chaetomium globosum,* an endophyte of *Armadillidium vulgare* TW1-1 collected from Hubei Province, P. R. China. Both compounds showed interesting side chains at carbon-8. (Chen, Wang et al. 2016) Chaephilone C (**136**), a chlorinated azaphilone, was isolated from the deep-sea water derived fungus *Chaetomium* sp. NA-S01-R1. The fungus was obtained from the seawater sample at a depth of 4050 m in the West Pacific Ocean. (Wang, Liao et al. 2018) Iso-chromophilonol (**137**) and ochrephilonol (**138**) were discovered from fermentation of the fungus *Chaetomium cupreum*. The fungus was collected from a pineapple plantation at Rayong province, Thailand. (Panthama, Kanokmedhakul et al. 2015) Chaetoviridins J and K (**139** and **140**) were isolated from the fungus *Chaetomium globosum,* which was described as an endophyte of leaves of *Wikstroemia uvaursi* collected from Hawaii, USA. The configuration of chaetoviridin J (**139**) was determined via Mosher's reaction together with comparison of the ECD spectrum to known compounds. The X-ray measurement confirmed the structure of chaetoviridin K (**140**) (Youn, Sripisut et al. 2015)

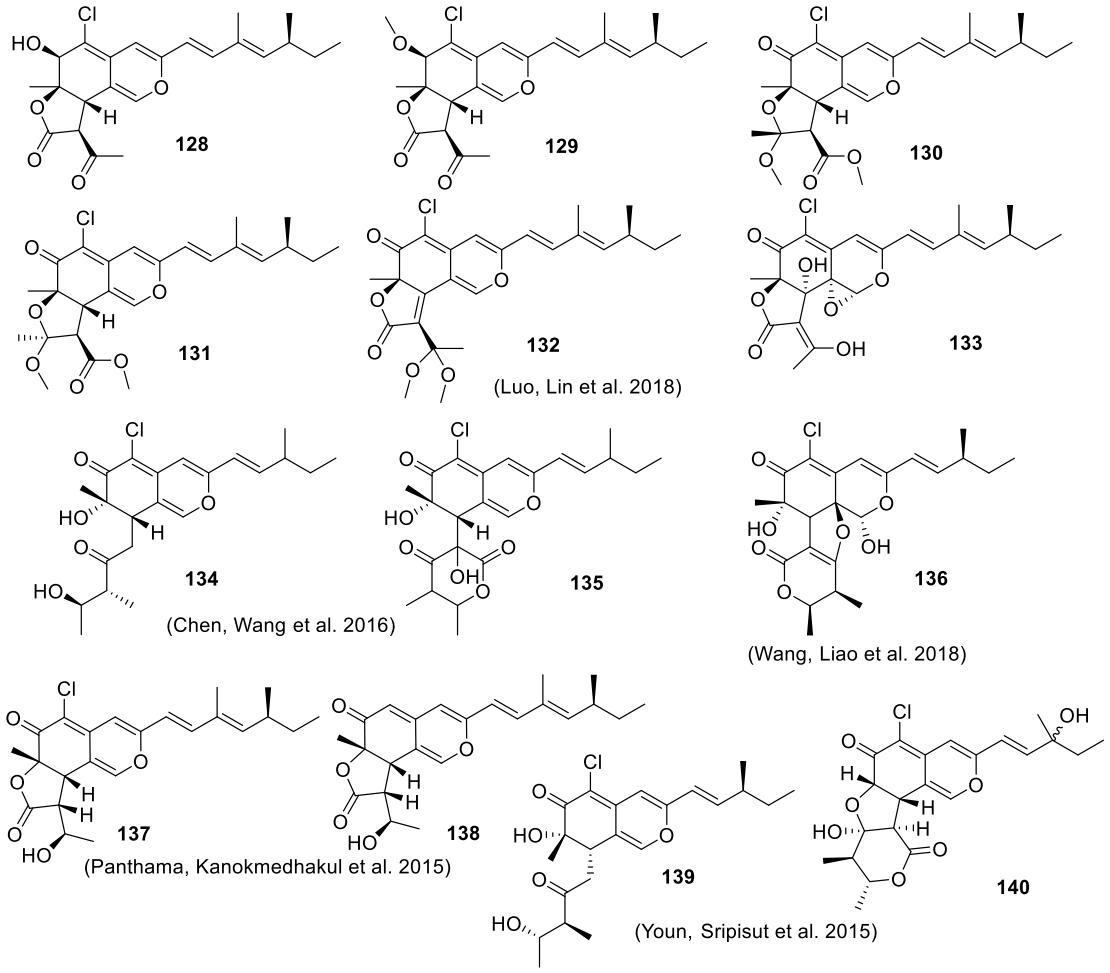

1.4.5 **Nitrogenous Azaphilones**

This class contains azaphilones with nitrogen replacing oxygen at position 2 in the core structure. Nitrogenous azaphilones are proposed to be generated by the same biosynthetic pathway as their oxygen counterparts, because some fungi can produce both kinds of azaphilones. *Chaetomium* fungi are able to produce a great number of nitrogenous azaphilones. (Zhang, Li et al. 2012) Nitrogenous azaphilones are more brightly colored than their oxygen containing counterparts. (Chen, Chen et al. 2017) The nitrogenous azaphilones published in the past six years are shown below.

Peniazaphilones A–D (**141**–**144**) are nitrogenous azaphilones, which were isolated from an alga derived *Penicillium* sp. ZJ-27 collected in Guangdong Province, P. R. China. The configurations for compounds **141** and **142** were determined based on ECD calculation. (Zhang, Long et al. 2016) The red pigment berkchaetorubramine (**145**), which carries a side chain at carbon-6 that forms an aromatic lactone ring was isolated together with berkchaetoazaphilones A–C (**114–116**) from an acid mine extremophile strain

Pleurostomophora sp.. (Stierle, Stierle et al. 2015) Chaetomugilides A–C (**147**–**149**) were isolated from *Chaetomium globosum* TY1, an endophytic fungus of *Ginkgo biloba* collected from Shandong Province, P. R. China. Chaetomugilide A (**147**) exhibited cytotoxicity against the human cancer cell line HePG2 with an IC_{50} value of 1.7 μM, while the positive control camptothecin showed an IC_{50} value of 32.3 μM. (Li, Tian et al. 2013) N-2-Butyric-azochaetoviridin E (Chaetomugilide A) (**147**), isochromophilone XIII (**146**), and 4'-*epi*-N-2-hydroxyethyl-azachaetoviridin A (Chaetomugilide C) (**149**) were isolated from *Chaetomium globosum* DAOM 240359 isolated from an indoor air sample in Ontario, Canada. (McMullin, Sumarah et al. 2013) Isochromophilone X (**150**), a nitrogenous azaphilone with a polyketide side chain, was isolated from *Bartalinia robillardoides* together with two oxygen containing azaphilones helicusin E (**50**) and isochromophilone XI (**51**). (Jansen, Ohlendorf et al. 2013) Chaetoviridides A–C (**151**–**153**) and chaephilone C (**135**), were obtained from the same *Chaetomium* sp. NA-S01-R1. Chaetoviridides A–C (**151**–**153**) with yellow or red color all showed antibiotic and cytotoxic activity. Especially chaetoviridide A (**151**) showed strong antimicrobial activity with an IC_{50} value of 7.3 μg/mL against *Vibrio rotiferianus*, while the positive control erythromycin showed an IC_{50} value of 3.9 μg/mL. In the cytotoxicity test, compound **151** showed an IC_{50} value of 3.9 μM against Hep G2 cells, and the positive control doxorubincin showed an IC_{50} value of 1.1 μM. (Wang, Liao et al. 2018)

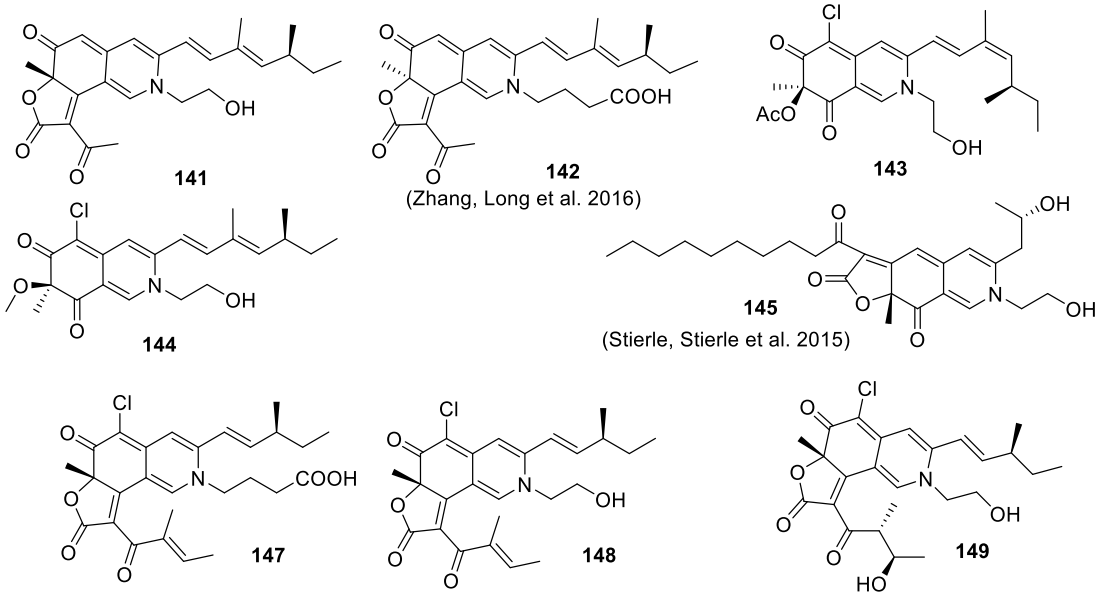

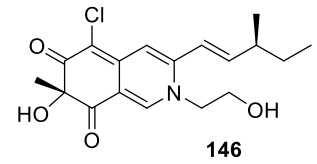

146

(McMullin, Sumarah et al. 2013)

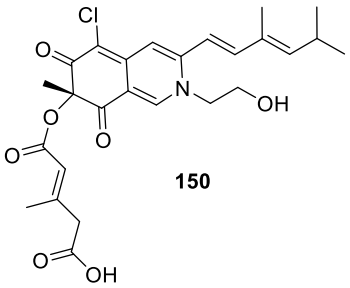

150

(Jansen, Ohlendorf et al. 2013)

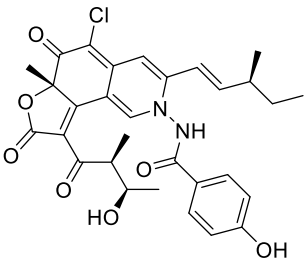

151

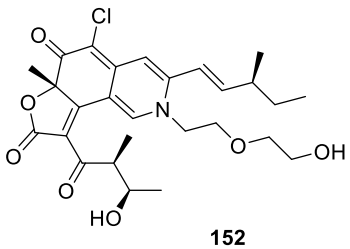

152

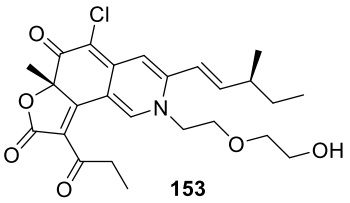

153

(Wang, Liao et al. 2018)

From 2013 to 2016, 153 azaphilones were published from 50 fungal strains belonging to 26 genera. From the genus *Penicillium,* 25 azaphilones were isolated while, 14 compounds were isolated from *Annulohypoxylon* and, 14 from *Chaetomium*. From the 153 azaphilones, 102 compounds were isolated from endophytic fungi from plants, algae, sponges, or animals. From plant endophytes, including Mangrove plants, 77 azaphilones have been reported. The marine-associated fungi, including from Mangrove environments contributed 41 azaphilones.

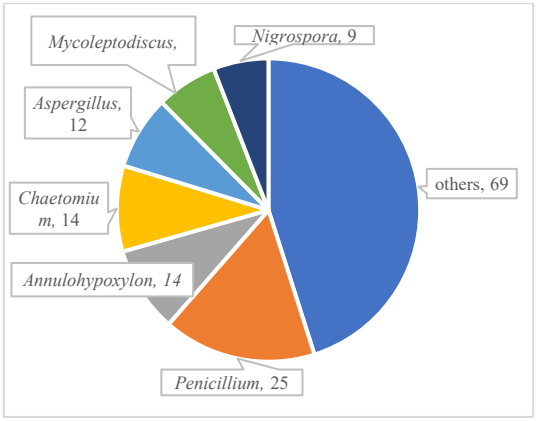

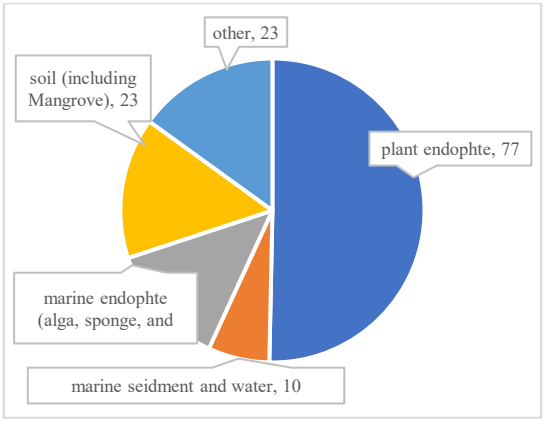

1.5 Aims of the Study

The aim of this study is focused on the discovery of new natural products from fungi and the elucidation of their various bioactivities. In order to enhance the possibility to find novel metabolites, less investigated fungi and talented fungi were chosen for this investigation. Firstly, fungi from less investigated habitats have a higher chance for producing novel compounds. Coprophilous fungi, which exist in animal dung are under investigated and offer a high chance to find new and interesting compounds. (Sarrocco 2016) Secondly, some well-investigated fungi, which have shown a large number of new compounds already in the past, can also be of interest for further studies especially if new methods for fermentation such as the OSMAC approach or co-cultivation are employed. (Marmann, Aly et al. 2014, Romano, Jackson et al. 2018)

In this thesis goose (*Anser anser*) dung, collected near the seacoast of North Germany, was used as a special source for the isolation of several fungi, including *Coniella fragariae*. Fungi isolated from dung may not be exclusively coprophilous fungi, but may also originate from food that the animal ate. The latter seems to be the case for *Coniella fragariae* which is a known strawberry pathogen. As a less investigated fungus, its extract obtained following fermentation on solid rice medium proved to be rich in new metabolites.

Phomopsis sp. D15a2a was isolated as an endophytic fungus from the plant *Alternanthera bettzickiana*. As mentioned in the Introduction, a large number of publications reporting new compounds was already known for this fungus. Nevertheless, also in this case new compounds could be obtained from this well investigated source.

The results obtained during my PhD studies are compiled as a cumulative dissertation which is based on three original publications.

.

2 Azaphilone Derivatives from the Fungus *Coniella fragariae* Inhibit NF-κB Activation and Reduce Tumor Cell Migration

Published in: "Journal of Natural Products"

Contribution: first author, conducting most of the experiments, literature research, manuscript writing.

JOURNAL OF NATURAL PRODUCTS

Article

Cite This: *J. Nat. Prod.* 2018, 81, 2493−2500

pubs.acs.org/jnp

Azaphilone Derivatives from the Fungus *Coniella fragariae* Inhibit NF-κB Activation and Reduce Tumor Cell Migration

Haiqian Yu,[†] Julia Sperlich,[‡] Attila Mándi,[§] Tibor Kurtán,[§] Haofu Dai,[⊥] Nicole Teusch,[‡] Zhi-Yong Guo,[#] Kun Zou,[#] Zhen Liu,*[,†] and Peter Proksch*[,†]

[†]Institute of Pharmaceutical Biology and Biotechnology, Heinrich-Heine-Universität Düsseldorf, Universitätsstrasse 1, 40225 Düsseldorf, Germany

[‡]Bio-Pharmaceutical Chemistry and Molecular Pharmacology, Faculty of Applied Natural Sciences, Technische Hochschule Köln, Chempark, 51368 Leverkusen, Germany

[§]Department of Organic Chemistry, University of Debrecen, P.O. Box 400, H-4002 Debrecen, Hungary

[⊥]Key Laboratory of Biology and Genetic Resources of Tropical Crops, Ministry of Agriculture, Institute of Tropical Bioscience and Biotechnology, Chinese Academy of Tropical Agricultural Sciences, Haikou 571101, People's Republic of China

[#]Hubei Key Laboratory of Natural Product Research and Development, College of Biological and Pharmaceutical Sciences, China Three Gorges University, Yichang 443002, People's Republic of China

Supporting Information

ABSTRACT: Seven new azaphilones, coniellins A−G (**1**−**7**), were obtained from the fungus *Coniella fragariae* that had been isolated from goose dung. Their structures were elucidated by analysis of 1D and 2D NMR as well as HRESIMS data. TDDFT-ECD calculation was used to determine the absolute configuration of **1**, while Mosher's method was applied to determine the absolute configuration of **5**. While displaying only moderate cytotoxicity, compound **1** exhibited significant inhibition of NF-κB activation in the triple negative breast cancer cell line MDA-MB-231 with an IC_{50} value of 4.4 μM. Moreover, compounds **1**, **4**, and **5** clearly reduced tumor cell migration. Compound **1** was the most active derivative tested in this assay and displayed 60% inhibition of tumor cell migration at a dose of 5 μM and 98% inhibition at 10 μM after 24 h.

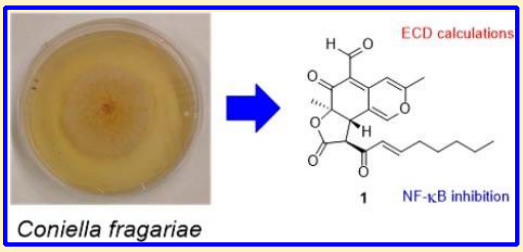

Fungi are an important source of secondary metabolites with a variety of chemical structures and diverse biological activities.[1] Investigation of fungi from hitherto less investigated habitats such as animal dung is expected to enhance the discovery rate of new secondary metabolites. Dung-inhabiting fungi, known as coprophilous fungi, have already been shown to produce an impressive number of bioactive natural products with antibacterial and antifungal activities.[2,3] These fungi and their metabolites play an important ecological role in decomposing and recycling nutrients from animal dung.[4]

In our continuous studies on new bioactive fungal natural products,[5−7] the fungus *Coniella fragariae* was isolated from goose dung, which was collected near the sea coast in North Germany. Fungi from the genus *Coniella* are generally known as phytopathogens. For example, *C. granati* is the causative agent of pomegranate disease in Greece, Israel, Turkey, and Italy.[8−11] *C. diplodiella* is known to cause white rot in grapes[12] and crown rot in strawberries.[13] In Australia, *C. fragariae* was found to cause foliage blight in *Eucalyptus pellita*.[14] In the present study, plants that had been eaten by geese are expected to be the true source of *C. fragariae*.

No report on natural products from fungi of the genus *Coniella* has been published so far. Investigation of *C. fragariae* yielded seven new azaphilone derivatives, coniellins A−G (**1**−**7**). The isolation and structure elucidation of the new compounds as well as their cytotoxic and NF-κB inhibitory activities are reported herein.

RESULTS AND DISCUSSION

Compound **1** was isolated as a yellow powder. It had the molecular formula $C_{22}H_{24}O_6$ with 11 degrees of unsaturation as deduced from the HRESIMS data. The ^{13}C NMR data of **1** (Table 1) showed the presence of three carbonyls at δ_C 191.1 (C-6), 190.2 (C-13), and 190.0 (C-10), an ester carbonyl at δ_C 168.8 (C-21), and eight olefinic carbons at δ_C 165.4 (C-3), 153.0 (C-15), 149.5 (C-4a), 148.5 (C-1), 127.3 (C-14), 117.9 (C-8a), 110.0 (C-5), and 108.0 (C-4), accounting for eight degrees of unsaturation. Thus, compound **1** was suggested to be tricyclic. The ^1H NMR spectrum displayed an aldehyde group signal at δ_H 10.18 (H-10), two olefinic proton singlets at

Received: July 3, 2018
Published: October 24, 2018

ACS Publications © 2018 American Chemical Society and American Society of Pharmacognosy

DOI: 10.1021/acs.jnatprod.8b00540
J. Nat. Prod. 2018, 81, 2493−2500

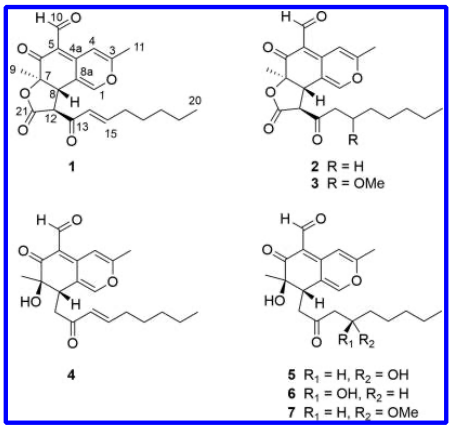

δ_H 8.40 (H-4) and 7.49 (H-1), and two methyl group singlets at δ_H 2.42 (Me-11) and 1.36 (Me-9). HMBC correlations from H-1 to C-3, C-4a, and C-8 (δ_C 43.1), from Me-11 to C-3 and C-4, from H-4 to C-5 and C-8a, from H-10 to C-4a and C-5, from Me-9 to C-6, C-7 (δ_C 81.0), and C-8, and from H-8 (δ_H 3.90) to C-6 established the pyranoquinone bicyclic core with an aldehyde group at C-5 and two methyl groups at C-3 and C-7, respectively (Figure 1). Apart from these signals, two olefinic protons at δ_H 7.13 (H-15) and 6.58 (H-14), a methyl group at δ_H 0.89 (Me-20), a methine group at δ_H 4.16 (H-12), and four methylene groups were observed in the ^{1}H NMR data of **1**. COSY correlations between H-8/H-12, between H-14/H-15/H_2-16 (δ_H 2.31)/H_2-17 (δ_H 1.51)/H_2-18 (δ_H 1.34), and

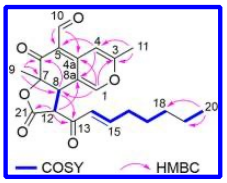

Figure 1. COSY and key HMBC correlations of compound **1**.

between H_2-19 (δ_H 1.34)/Me-20, together with HMBC correlations from Me-20 to C-18 (δ_C 31.4) and C-19 (δ_C 22.4), from H-8 to C-13, and from H-12 to C-8a, C-13, and C-21, indicated the presence of an ester bridge between C-7 and C-21 to form the third ring and a 1-oxooct-2-en-1-yl side chain at C-12. Thus, the planar structure of compound **1** was elucidated as shown, representing a new azaphilone derivative, for which the name coniellin A is proposed. The double bond at C-14/C-15 was determined to be *E* configured based on the large coupling constants between H-14 and H-15 (15.6 Hz). In the ROESY spectrum, an NOE correlation between H-12 and Me-9 was observed, suggesting that H-12 and Me-9 were on the same face of the lactone ring, while H-8 was on the opposite face. The chemical shifts of H-8, H-12, and Me-9 of compound **1** also supported this assignment of the relative configuration after comparison with similar tricyclic azaphilones reported in the literature.[15] In addition, cohaerins G and H exhibited similar ECD data (+350, −272 nm) when compared to those of coniellin A (Figure 2), suggesting they shared the same absolute configuration.[15]

To elucidate the absolute configuration of **1**, the solution time-dependent density functional theory/electronic circular

Table 1. ^{1}H and ^{13}C NMR Data of Compounds 1−3

	1[a]		**2**[b]		**3**[a]	
position	δ_C, type	δ_H (J in Hz)	δ_C, type	δ_H (J in Hz)	δ_C, type	δ_H (J in Hz)
1	148.5, CH	7.49, d (1.5)	148.4, CH	7.46, d (1.7)	148.7, CH	7.44, d (1.7)
3	165.4, C		165.6, C		165.5, C	
4	108.0, CH	8.40, s	108.1, CH	8.41, s	108.1, CH	8.39, s
4a	149.5, C		149.5, C		149.5, C	
5	110.0, C		109.8, C		109.9, C	
6	191.1, C		191.1, C		191.2, C	
7	81.0, C		80.9, C		81.0, C	
8	43.1, CH	3.90, dd (12.7, 1.5)	42.8, CH	3.81, dd (12.8, 1.7)	42.3, CH	3.89, dd (12.7, 1.7)
8a	117.9, C		117.8, C		117.9, C	
9	18.3, CH_3	1.36, s	18.3, CH_3	1.34, s	18.4, CH_3	1.34, s
10	190.0, CH	10.18, s	190.0, CH	10.19, s	190.1, CH	10.19, s
11	20.4, CH_3	2.42, s	20.4, CH_3	2.43, s	20.5, CH_3	2.42, s
12	51.6, CH	4.16, d (12.7)	53.1, CH	3.95, d (12.8)	55.0, CH	4.15, d (12.7)
13	190.2, C		202.3, C		202.1, C	
14	127.3, CH	6.58, d (15.6)	42.2, CH_2	3.07, dt (18.2, 7.2)	46.9, CH_2	3.23, dd (14.4, 10.3)
				2.76, dt (18.2, 7.2)		2.76, dd (14.4, 3.4)
15	153.0, CH	7.13, dt (15.6, 7.0)	23.2, CH_2	1.65, m	79.5, CH	3.78, m
16	32.8, CH_2	2.31, q (7.0)	28.9, CH_2	1.31, m	32.4, CH_2	1.70, m
						1.54, m
17	27.5, CH_2	1.51, m	29.0, CH_2	1.31, m	24.1, CH_2	1.32, m
18	31.4, CH_2	1.34, m	31.6, CH_2	1.27, m	31.8, CH_2	1.31, m
19	22.4, CH_2	1.34, m	22.6, CH_2	1.28, m	22.6, CH_2	1.33, m
20	13.9, CH_3	0.89, t (7.0)	14.0, CH_3	0.88, t (6.9)	14.0, CH_3	0.90, t (6.9)
21	168.8, C		168.7, C		168.7, C	
15-OMe					56.4, CH_3	3.35, s

[a]Recorded at 600 MHz (^{1}H) and 150 MHz (^{13}C) in $CDCl_3$. [b]Recorded at 300 MHz (^{1}H) and 75 MHz (^{13}C) in $CDCl_3$.

DOI: 10.1021/acs.jnatprod.8b00540
J. Nat. Prod. 2018, 81, 2493−2500

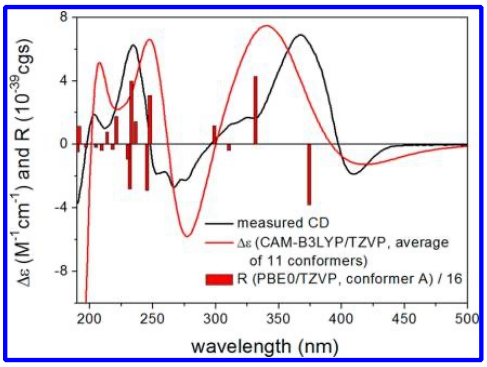

Figure 2. Experimental ECD spectrum of **1** compared with the Boltzmann-weighted CAM-B3LYP/TZVP (PCM/MeCN) ECD spectrum of (7*R*,8*S*,12*S*)-**1**. Level of optimization: B97D/TZVP PCM/MeCN. Bars represent the rotatory strength values of the lowest-energy conformer.

dichroism (TDDFT-ECD) method was applied on the arbitrarily chosen (7*R*,8*S*,12*S*) enantiomer.[16,17] Merck Molecular Force Field (MMFF) conformational search with a 21 kJ/mol energy window resulted in 395 conformers, which were reoptimized at the B3LYP/6-31G(d), the B97D/TZVP[18,19] PCM/MeCN, and the CAM-B3LYP/TZVP[20] PCM/MeCN levels of theory. To decrease the number of computed conformers, the orientation of the last four carbons of the C-12 substituent was neglected by reclustering after DFT optimizations.[21] ECD spectra computed at various levels (B3LYP, BH&HLYP, CAM-B3LYP, and PBE0 with the TZVP basis set) for all sets of conformers gave moderate to good agreement, suggesting the 7*R*,8*S*,12*S* absolute configuration (Figure 2). In order to further verify the absolute configuration, specific rotation values were also computed for the (7*R*,8*S*,12*S*) B3LYP conformers, resulting in the same positive sign as the experimental value for all the low-energy conformers, supporting the ECD results.[22,23] The Boltzmann-averaged values (+373, +350, and +374 at the B3LYP/TZVP, BH&HLYP/TZVP, and PBE0/TZVP levels, respectively) are also in good agreement with the experimental specific rotation (+371). Thus, the absolute configuration of **1** was unambiguously elucidated as (7*R*,8*S*,12*S*).

The molecular formula of coniellin B (**2**) was determined to be $C_{22}H_{26}O_6$ by HRESIMS, containing two additional hydrogen atoms compared to **1**. The NMR data of compound **2** (Table 1) resembled those of **1** except for the replacement of the double bond in the side chain by two methylene groups at δ_H 3.07 (H_a-14), 2.76 (H_b-14), and 1.65 (H_2-15), which was confirmed by COSY correlations between H_{ab}-14/H_2-15/H_2-16 (δ_H 1.31) and HMBC correlations from H-8 (δ_H 3.81), H-12 (δ_H 3.95), H_{ab}-14, and H_2-15 to the downfield-shifted C-13 (δ_C 202.3). The remaining substructures and the relative configuration of **2** were determined to be identical to those of **1** by detailed analysis of the 2D NMR spectra of **2**.

Coniellin C (**3**) had the molecular formula $C_{23}H_{28}O_7$ as determined by the HRESIMS data. Comparison of its ^{1}H and ^{13}C NMR data with those of compound **2** showed the presence of an additional methoxy group (δ_H 3.35 and δ_C 56.4) and an

Table 2. ^{1}H and ^{13}C NMR Data for Compounds 4−7

	4[a]		5[b]		6[b]		7[a]	
position	δ_C, type	δ_H (*J* in Hz)	δ_C, type	δ_H (*J* in Hz)	δ_C, type	δ_H (*J* in Hz)	δ_C, type	δ_H (*J* in Hz)
1	150.9, CH	7.61, d (1.7)	150.4, CH	7.57, d (1.8)	150.6, CH	7.55, d (1.9)	150.8, CH	7.55, d (1.9)
3	165.1, C		165.0, C		165.0, C		165.1, C	
4	107.7, CH	8.43, s	107.6, CH	8.44, s	107.6, CH	8.44, s	107.7, CH	8.42, s
4a	151.1, C		150.9, C		151.0, C		151.1, C	
5	108.4, C		108.5, C		108.4, C		108.3, C	
6	198.9, C		198.8, C		198.9, C		198.9, C	
7	71.8, C		71.7, C		71.5, C		71.5, C	
8	40.3, CH	3.33, dt (10.2, 1.7)	39.7, CH	3.37, ddd (9.4, 2.6, 1.8)	39.6, CH	3.39, ddd (9.8, 2.1, 1.9)	39.3, CH	3.37, dt (10.0, 1.9)
8a	121.9, C		121.6, C		121.5, C		121.7, C	
9	20.6, CH_3	1.11, s	20.6, CH_3	1.09, s	20.7, CH_3	1.08, s	20.7, CH_3	1.07, s
10	190.2, CH	10.20, s	190.1, CH	10.20, s	190.2, CH	10.20, s	190.2, CH	10.18, s
11	20.2, CH_3	2.38, s	20.1, CH_3	2.39, s	20.1, CH_3	2.38, s	20.1, CH_3	2.38, s
12	36.3, CH_2	3.50, dd (16.7, 1.7)	39.4, CH_2	3.28, dd (17.6, 2.6)	40.7, CH_2	3.31, dd (18.4, 2.1)	39.7, CH_2	3.27, dd (18.0, 1.9)
		2.82, dd (16.7, 10.2)		2.86, dd (17.6, 9.4)		2.87, dd (18.4, 9.8)		2.85, dd (18.0, 10.0)
13	198.7, C		209.3, C		209.4, C		207.9, C	
14	129.4, CH	6.17, dt (15.9, 1.5)	49.7, CH_2	2.74, dd (16.0, 3.0)	49.3, CH_2	2.70, dd (15.6, 9.9)	46.9, CH_2	2.68, dd (14.8, 5.3)
				2.62, dd (16.0, 9.4)		2.61, dd (15.6, 2.7)		2.66, dd (14.8, 7.1)
15	150.1 CH	7.06, dt (15.9, 6.9)	68.5 CH	4.14, m	69.0 CH	4.14, m	77.8 CH	3.74, m
16	32.6, CH_2	2.25, q (7.0)	37.1, CH_2	1.54, m	37.2, CH_2	1.54, m	32.9, CH_2	1.62, m
				1.47, m		1.48, m		1.48, m
17	27.7, CH_2	1.48, m	25.2, CH_2	1.45, m	25.0, CH_2	1.43, m	24.7, CH_2	1.30, m
				1.34, m		1.33, m		
18	31.4, CH_2	1.30, m	31.7, CH_2	1.31, m	31.7, CH_2	1.31, m	31.8, CH_2	1.30, m
19	22.4, CH_2	1.32, m	22.6, CH_2	1.32, m	22.6, CH_2	1.32, m	22.5, CH_2	1.31, m
20	13.9, CH_3	0.90, t (7.0)	14.0, CH_3	0.90, t (7.0)	13.9, CH_3	0.90, t (7.0)	14.0, CH_3	0.89, t (6.9)
15-OMe							56.2, CH_3	3.33, s

[a]Recorded at 300 MHz (^{1}H) and 75 MHz (^{13}C) in $CDCl_3$. [b]Recorded at 600 MHz (^{1}H) and 150 MHz (^{13}C) in $CDCl_3$.

DOI: 10.1021/acs.jnatprod.8b00540
J. Nat. Prod. 2018, 81, 2493−2500

additional methine (δ_H 3.78 and δ_C 79.5, CH-15). The attachment of the methoxy group at C-15 was confirmed by the HMBC correlation from the protons of the methoxy group to C-15 and the COSY correlations between H_{ab}-14 (δ_H 3.23 and 2.76)/H-15/H_{ab}-16 (δ_H 1.70 and 1.54). Thus, compound **3** was a 15-methoxy derivative of coniellin B (**2**). The relative configuration of the methoxy group at C-15 could not be assigned.

Coniellin D (**4**) was isolated as a yellow powder. The molecular formula of $C_{21}H_{26}O_5$ was deduced from the HRESIMS data of **4**, differing from **1** by the loss of a carbonyl group and the addition of two extra protons. The NMR data of **4** (Table 2) were similar to those of **1** including signals for the pyranoquinone bicyclic ring, the aldehyde group, and the 1-oxooct-2-en-1-yl side chain. However, an additional methylene group at δ_H 3.50 and 2.82 (H_{ab}-12) was observed in **4** in addition to the absence of the ester carbonyl at C-21. The COSY correlation between H_{ab}-12/H-8 (δ_H 3.33) and the HMBC correlations from H_{ab}-12 and H-8 to C-13 (δ_C 198.7) confirmed the location of the additional methylene at C-12 and the disappearance of the lactone carbonyl group in **4**. The NOE cross-peaks from Me-9 (δ_H 1.11) to H_{ab}-12 suggested a *trans* relationship between Me-9 and H-8, as already confirmed in compounds **1**–**3**. Thus, the structure of compound **4** was elucidated as shown.

The molecular formula of compound **5** was elucidated as $C_{21}H_{28}O_6$ based on the HRESIMS data, containing an additional oxygen atom and two additional protons when compared to **4**. Comparison of the NMR data of **5** with those of **4** revealed the presence of an additional oxygenated methine group at δ_H 4.14 and δ_C 68.5 (CH-15). The attachment of a hydroxy group at C-15 was confirmed by the COSY correlations between H_{ab}-14 (δ_H 2.74 and 2.62)/H-15/H_{ab}-16 (δ_H 1.54 and 1.47) and the HMBC correlations from H_{ab}-14 to C-13 (δ_C 209.3). The remaining structure of **5** was shown to be identical to that of **4** after analysis of the 2D NMR data. The NOE relationships from Me-9 (δ_H 1.09) to H_{ab}-12 (δ_H 3.28 and 2.86) indicated the same *trans* configuration between Me-9 and H-8 as that in **4**. The absolute configuration at C-15 in **5** was determined to be *S* using Mosher's method (Figure 3).

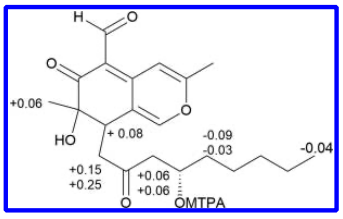

Figure 3. $\Delta\delta^{SR}$ ($\delta_S - \delta_R$) values of (*S*)- and (*R*)-MTPA esters of **5**.

Detailed analysis of the HRESIMS and 2D NMR data of coniellin F (**6**) revealed that it shared the same planar structure as that of **5**. In the ROESY spectrum of **6**, Me-9 (δ_H 1.08) showed NOE correlations to H_{ab}-12 (δ_H 3.31 and 2.87) suggesting that the relative configuration at C-7 and C-8 was identical to that of **5**. Meanwhile, the different coupling constants between H-15 and H_{ab}-14 in compounds **5** ($J_{Ha\text{-}14/H\text{-}15}$ = 3.0 Hz, $J_{Hb\text{-}14/H\text{-}15}$ = 9.4 Hz) and **6** ($J_{Ha\text{-}14/H\text{-}15}$ = 9.9 Hz, $J_{Hb\text{-}14/H\text{-}15}$ = 2.7 Hz) suggested that these two compounds are 15-epimers.

The molecular formula of coniellin G (**7**) was determined to be $C_{22}H_{30}O_6$ on the basis of the HRESIMS data. The NMR data of **7** (Table 2) were similar to those of compounds **5** and **6** except for signals indicating the presence of an additional methoxy group. HMBC correlations from the methoxy singlet to the downfield-shifted C-15 (δ_C 77.8) and COSY correlations between H_{ab}-14 (δ_H 2.68 and 2.66)/H-15/H_{ab}-16 (δ_H 1.62 and 1.48) indicated the methoxy group to be located at C-15. Detailed analysis of the 2D NMR spectra of **7** confirmed the compound to be identical to **5** and **6** with the exception of the methoxy substituent at C-15. The chemical shifts and coupling constants of CH_2-14 in **7** (δ_H 2.68, dd, J = 14.8, 5.3 Hz, and 2.66, dd, J = 14.8, 7.1 Hz) were comparable to those in **5** (δ_H 2.74, dd, J = 16.0, 3.0 Hz, and 2.62, dd, J = 16.0, 9.4 Hz), but differed from those in **6** (δ_H 2.70, dd, J = 15.6, 9.9 Hz, and 2.61, dd, J = 15.6, 2.7 Hz), suggesting that **5** and **7** share the same configuration.

Azaphilones possessing a highly oxygenated bi- or tricyclic core have hitherto mainly been reported from the fungal genera *Penicillium*, *Aspergillus*, *Talaromyces*, *Monascus*, and *Chaetomium*.[24] Some of these compounds may be considered as important taxonomic marker metabolites. Azaphilones are biogenetically derived from the polyketide pathway giving rise to the cyclized core structure and from fatty acid metabolism yielding the side chain. The aldehyde group at C-5 in the azaphilone derivatives isolated in this study is unusual. Few azaphilones with an aliphatic side chain at C-5 have been reported in the literature including austdiol from *Aspergillus ustus*[25] and helotialins A and C from *Helotiales* sp.[26] Due to the deshielding effect of the aldehyde group in coniellins and austdiol or the carboxylic acid group in helotialins A and C, the signals of H-4 of those compounds are around δ_H 8.5, whereas the signals of H-4 of azaphilone derivatives with a proton at C-5 appear at δ_H 5.9–6.5.

Azaphilones were previously reported to possess cytotoxicity against various tumor cell lines.[27,28] However, to date, effects of azaphilones on triple negative breast cancer cell lines have not been evaluated. Noteworthy, triple negative breast cancer (TNBC) represents the most aggressive form of breast cancer with currently no targeted therapy available and a significantly reduced overall survival rate.[29] Thus, the effects on viability of the triple negative breast cancer cell line MDA-MB-231 of compounds **1**–**7** were tested. Among them, compounds **1**–**5** and **7** displayed weak cytotoxic activities, with IC_{50} values ranging between 18.6 μM (**4**) and 79.3 μM (**5**). Compound **6** displayed no activity (IC_{50} > 100 μM) after 24 h of compound incubation (Table 3).

Various studies have suggested that several azaphilones exhibit anti-inflammatory activity by inhibiting nitric oxide production.[30,31] Furthermore, Youn et al. reported inhibition of tumor necrosis factor alpha (TNFα)-induced nuclear factor-kappa B (NF-κB) in RAW 264.7 cells with IC_{50} values ranging between 0.9 and 11.6 μM.[32] In our study, compounds **1** and **4**–**7** displayed inhibition of NF-κB, with compound **1** as the most active analogue (IC_{50} value of 4.4 μM). Noteworthy, based on the short compound incubation time of 2 h used for this assay, NF-κB inhibition effects of azaphilones can be clearly distinguished from their cytotoxicity (Table 3). NF-κB activity is involved in epithelial-to-mesenchymal transition in breast cancer, thereby enhancing invasion and metastasis.[33] Thus, to explore the potential of azaphilone derivatives on tumor cell migration, we further analyzed the NF-κB inhibitor **1** at concentrations of 1, 5, and 10 μM and compounds **4**, **5**

DOI: 10.1021/acs.jnatprod.8b00540
J. Nat. Prod. 2018, 81, 2493–2500

Table 3. Cell Viability and NF-κB Inhibition Assessment of Azaphilone Derivatives

compound	cell viability,[a] IC_{50} (μM)	NF-κB inhibition,[b] IC_{50} (μM)
1	21.5 ± 9.5	4.4 ± 2.3
2	19.6 ± 10.0	>100
3	21.0 ± 3.7	>100
4	18.6 ± 4.7	37.8 ± 3.2
5	79.3 ± 0.8	29.4 ± 2.2
6	>100	70.7 ± 7.8
7	21.6 ± 3.0	11.3 ± 0.5

[a]Cell viability of MDA-MB-231 cells was measured 24 h after compound treatment. As a positive control, cells were incubated with a concentration of 5 μM staurosporine normalized to 1% DMSO, the latter equaling 100% cell viability; 5 μM staurosporine reduced cell viability to 10.9%. [b]To determine NF-κB inhibition, compounds were incubated for 20 min followed by treatment with 20 ng/mL TNFα for 2 h. TNFα alone served as positive control, inducing NF-κB activation by 5.3-fold at a concentration of 20 ng/mL.

and **7** at a concentration of 10 μM each in a 2D scratch wound assay, respectively (Figures 4 and 5). Compound **1** displayed 60% inhibition of tumor cell migration at 5 μM and 98% inhibition at 10 μM after 24 h. Furthermore, compounds **4** and **5** blocked migration by 78% and 83% at 10 μM, respectively. In contrast, compounds **6** and **7** did not exhibit significant cell migration inhibition when tested at a concentration of 5 μM. Furthermore, we evaluated compound **1** in a 3D invasion assay at a concentration of 10 μM. After 24 h, compound **1** reduced invasion of triple negative breast cancer cells into the surrounding extracellular matrix by 52%.

Comparison of the structure of **1** with those of **2** and **3** indicated that the presence of a double bond at C-14/C-15 is important for NF-κB inhibition. Compared to **1**, the loss of the lactone ring in **4** significantly decreased the inhibitory activity. For the 15-epimers **5** and **6**, the 15*S* isomer **5** was more active than the 15*R* isomer **6**, while methylation at 15-OH (**7** vs **5**) increased NF-κB inhibitory activity, perhaps due to increased lipophilicity and enhanced diffusion across membranes.

EXPERIMENTAL SECTION

General Experimental Procedures. NMR spectra were recorded on Bruker Avance III 300 or Bruker Avance III 600 spectrometers. HRESIMS data were obtained on a Bruker Daltonics UHR-QTOF Maxis 4G mass spectrometer. Optical rotations were measured with a JASCO P-2000 polarimeter. ECD spectra were recorded on a J-810 spectropolarimeter. HPLC analysis was carried out using a Dionex UltiMate-3400SD system (an LPG-3400SD pump and a DAD3000RS photodiode array detector) coupled with a Knauer Eurospher C_{18} analytical column (125 × 4 mm, 5 μm). Semi-preparative HPLC was performed on a Lachrom-Merck Hitachi system (an L-7100 pump and an L-7400 UV detector) using a 300 × 8 mm Knauer Eurospher C_{18} column. For TLC, plates precoated with Merck silica gel F254 were used with detection under 254 and 365 nm or by spraying the plates with anisaldehyde reagent followed by heating.

Fungal Material and Identification. The fungus was isolated from goose (*Anser anser*) dung collected at the North Sea coast close to Garding, Germany, in September 2016. The fungus was identified as *C. fragariae* (GenBank accession number KJ710465.1) by DNA amplification and sequencing of its ITS region as described before.[34]

Fermentation, Extraction, and Isolation. The fungus was cultivated on rice medium in 50 Erlenmeyer flasks (1 L each, 100 g of rice and 110 mL of demineralized water per flask, autoclaved at 121 °C for 20 min before inoculation). After 14 days of fermentation at 20 °C under static conditions, 500 mL of EtOAc was added to each flask, followed by shaking at 150 rpm for 8 h. The solvent was evaporated to dryness to give 52 g of crude extract. Liquid−liquid separation between *n*-hexane and MeOH was performed. The obtained MeOH-soluble fraction (27 g) was separated by vacuum liquid chromatography on an RP-18 column (60 × 200 mm) using a solvent gradient (from 100% H_2O to 100% MeOH) to give seven fractions (Fr.1 to Fr.7). Fr.5 (1.6 g) was subjected to a Sephadex LH-20 column (20 × 1000 mm) with MeOH, followed by separation on a silica gel column (30 × 500 mm) eluted with a gradient of *n*-hexane and EtOAc (from 9:1 to 1:2) to afford five subfractions (Fr.5.1 to Fr.5.5). Fr.5.3 contained compound **1** (1.1 g). Fr.5.4 was separated by semi-preparative HPLC using 60% MeOH−H_2O to give compounds **2** (6.1 mg) and **3** (5.6 mg). Fr.4 (0.9 g) was fractionated on a silica gel column (30 × 300 mm) with *n*-hexane and EtOAc as mobile phase to give three subfractions (Fr.4.1 to Fr.4.3). Fr.4.1 and Fr.4.2 were separated by semipreparative HPLC with 60% MeOH−H_2O to afford compounds **4** (5.5 mg) and **7** (6.9 mg), respectively. Following the same procedure, Fr.3 (0.8 g) was subjected to a silica column (30 × 300 mm) using a gradient of *n*-hexane and EtOAc, followed by purification with semipreparative HPLC using 50% MeOH−H_2O to give compounds **5** (3.4 mg) and **6** (2.9 mg).

Coniellin A (1): yellow powder; $[\alpha]_D^{20}$ +371 (*c* 0.1, $CHCl_3$); UV (CH_3OH) λ_{max} 255, 382 nm; ECD (MeCN, λ [nm] (Δε), *c* 0.163 mM) 410 (−1.87), 368 (+6.92), 326sh (+1.70), 313sh (+1.30),

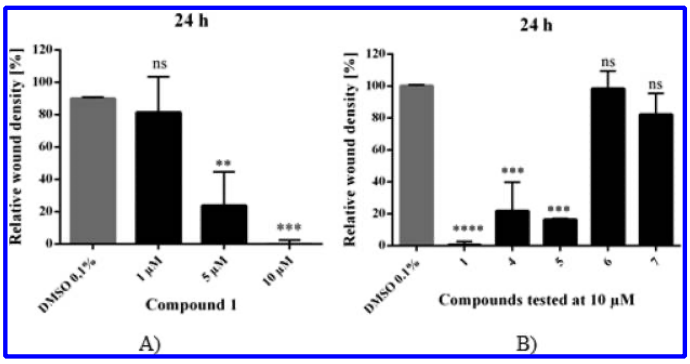

Figure 4. Inhibition of tumor cell migration in a scratch wound assay. Compound **1** was (A) tested at the concentrations of 1, 5, and 10 μM, respectively, or (B) evaluated at 10 μM in comparison with derivatives **4**−**7**. Data represent increasing relative wound density in percentage calculated with the IncuCyte ZOOM software. Error bars show ± SEM. Four stars represent a significance of $p < 0.0001$, three stars of $p < 0.001$, and two stars of $p < 0.01$. "Ns" means not significant.

DOI: 10.1021/acs.jnatprod.8b00540
J. Nat. Prod. 2018, 81, 2493−2500

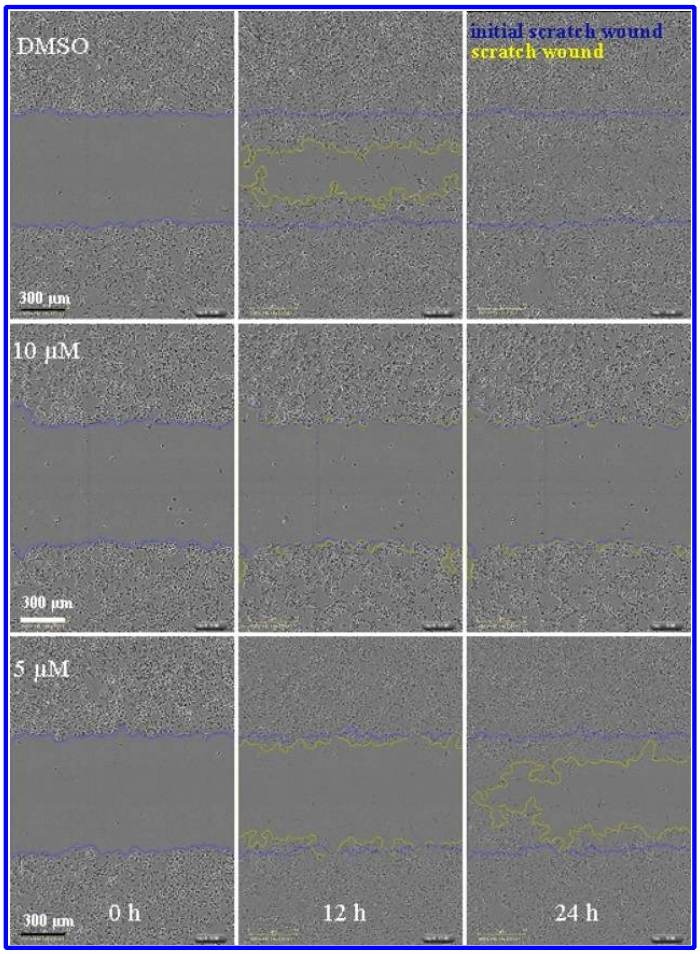

Figure 5. Images of the scratch wound assay after 0, 12, and 24 h of incubation with compound **1**. Compound **1** was tested at concentrations of 5 and 10 μM, respectively. Whereas the cells in the controls migrate and cover the clear zone of the scratch wound completely after 24 h, treatment with compound **1** inhibits cell migration.

276sh (−2.27), 267 (−2.72), 253sh (−1.85), 235 (+6.27), 204sh (+1.88); ^{1}H and ^{13}C NMR data, Table 1; HRESIMS *m*/*z* 385.1650 [M + H]$^+$ (calcd for $C_{22}H_{25}O_6$, 385.1646).

*Coniellin B (**2**):* yellow powder; $[\alpha]_D^{20}$ +417 (*c* 0.1, $CHCl_3$); UV (CH_3OH) λ_{max} 257, 379 nm; ^{1}H and ^{13}C NMR data, Table 1; HRESIMS *m*/*z* 387.1802 [M + H]$^+$ (calcd for $C_{22}H_{27}O_6$, 387.1802).

*Coniellin C (**3**):* yellow powder; $[\alpha]_D^{20}$ +400 (*c* 0.1, $CHCl_3$); UV (CH_3OH) λ_{max} 257, 379 nm; ^{1}H and ^{13}C NMR data, Table 1; HRESIMS *m*/*z* 417.1903 [M + H]$^+$ (calcd for $C_{23}H_{29}O_7$, 417.1908).

*Coniellin D (**4**):* yellow powder; $[\alpha]_D^{20}$ +124 (*c* 0.1, $CHCl_3$); UV (CH_3OH) λ_{max} 271, 379 nm; ^{1}H and ^{13}C NMR data, Table 2; HRESIMS *m*/*z* 359.1853 [M + H]$^+$ (calcd for $C_{21}H_{27}O_5$, 359.1853).

*Coniellin E (**5**):* yellow powder; $[\alpha]_D^{20}$ +171 (*c* 0.1, $CHCl_3$); UV (CH_3OH) λ_{max} 258, 378 nm; ^{1}H and ^{13}C NMR data, Table 2; HRESIMS *m*/*z* 377.1957 [M + H]$^+$ (calcd for $C_{21}H_{29}O_6$, 377.1959).

*Coniellin F (**6**):* yellow powder; $[\alpha]_D^{20}$ +97 (*c* 0.1, $CHCl_3$); UV (CH_3OH) λ_{max} 252, 377 nm; ^{1}H and ^{13}C NMR data, Table 2; HRESIMS *m*/*z* 377.1959 [M + H]$^+$ (calcd for $C_{21}H_{29}O_6$, 377.1959).

*Coniellin G (**7**):* yellow powder; $[\alpha]_D^{20}$ +225 (*c* 0.1, $CHCl_3$); UV (CH_3OH) λ_{max} 269, 379 nm; ^{1}H and ^{13}C NMR data, Table 2; HRESIMS *m*/*z* 391.2111 [M + H]$^+$ (calcd for $C_{22}H_{31}O_6$, 391.2115).

Cell Culture and Reagents. MDA-MB-231 cells, obtained from European Collection of Authenticated Cell Cultures (Salisbury, UK), were cultured in RPMI medium supplemented with 15% fetal calf serum (FCS), 100 U/mL penicillin, and 100 U/mL streptomycin at 37 °C in the presence of 5% CO_2. Stable transfected NF-κB-MDA-MB-231 cells were cultured with Dulbecco's modified Eagle's medium supplemented with 10% FCS, 450 μg/mL hygromycin B (Sigma, Munich, Germany), 100 U/mL penicillin, and 100 μg/mL streptomycin at 37 °C in the presence of 5% CO_2. Media and antibiotics were purchased from Gibco (Life Technologies, Carlsbad, CA, USA). Matrigel was obtained from Corning (New York, USA), and collagen R solution (0.2%) was purchased from Serva Electrophoresis GmbH (Heidelberg, Germany).

Cell Viability Assay. Cytotoxicity of test compounds was determined 24 h after compound treatment with the CellTiter-Glo Luminescent Cell Viability Assay (Promega, Madison, WI, USA) according to the manufacturer's instructions. A total of 5600 cells/well were seeded in white 384-well plates using the CyBi-Well 96-channel simultaneous pipettor (Analytic Jena, Jena, Germany) and cultured overnight at 37 °C before compound addition.

NF-κB Reporter Gene Assay. Stable NF-κB-MDA-MB-231 cells were generated as described previously.[35] The cells were seeded at a

DOI: 10.1021/acs.jnatprod.8b00540
J. Nat. Prod. 2018, 81, 2493−2500

densitiy of 20 000 cells/well in white 96-well plates (Greiner Bio-One, Kremsmuenster, Austria). After 24 h, cells were treated with indicated compounds for 20 min followed by incubation of 20 ng/mL TNFα (Peprotech, Rocky Hill, NJ, USA) for 2 h. Luminescence was determined using NanoGlo reagent from Promega (Madison, WI, USA).

2D Scratch Wound Assay. MDA-MB-231 cells were seeded in an ImageLock 96-well plate (Sartorius, Goettingen, Germany) at a density of 50 000 cells/well. After 24 h a scratch was made with the IncuCyte WoundMaker. Compounds were added at different concentrations, and images were taken every 2 h for a time range of 24 h with the IncuCyte ZOOM Imager.

3D Invasion Assay. Spheroids were generated with 3000 cells/well of MDA-MB-231 cells supplemented with 0.25% matrigel in an ultralow-attachment (ULA) plate (Corning, NY, USA). The cells were centrifuged for 10 min at 1000 rpm at 4 °C. After 72 h of spheroid formation, a mixture of matrigel and collagen R solution (ratio of 1:1) was used for embedding the spheroids. Polymerization of matrigel−collagen solution was allowed for 1 h at 37 °C. Invasion of cells into the surrounding matrix was recorded every day for a time range of 3 days and analyzed with ImageJ Fiji.

Computational Section. Mixed torsional/low-mode conformational searches were carried out by means of the Macromodel 10.8.011 software[36] using the MMFF with an implicit solvent model for $CHCl_3$ applying a 21 kJ/mol energy window. Geometry reoptimizations of the resultant conformers [B3LYP/6-31G(d) level in vacuo, B97D/TZVP with PCM solvent model for MeCN, and CAM-B3LYP/TZVP with PCM solvent model for MeCN], OR, and ECD calculations were performed with Gaussian 09.[37] Chiroptical values were computed using various functionals (B3LYP, BH&HLYP, CAM-B3LYP, PBE0) and the TZVP basis set. ECD spectra were generated as the sum of Gaussians[38] with 3900 cm^{-1} half-height width (corresponding to ca. 28 at 270 nm), using dipole-velocity-computed rotational strength values. Boltzmann distributions were estimated from the ZPVE-corrected B3LYP/6-31G(d) energies in the gas-phase calculations and from the B97D/TZVP and CAM-B3LYP/TZVP energies in the PCM model ones. The MOLEKEL[39] software package was used for visualization of the results.

Chiral Derivatization. Compound **5** (1.0 mg) dissolved in deuterated pyridine (1.5 mL) was added to two dry and clean NMR tubes in equal parts. Then 10 μL of (*R*)- or (*S*)-MTPA (α-methoxy-α-(trifluoromethyl)phenylacetyl) chloride was added separately under argon protection. The tubes were shaken to mix the samples and MTPA chloride. After 8 h of incubation at room temperature, ^{1}H NMR spectra were measured in order to detect the reaction products. Then the reaction products were purified by semipreparative HPLC with MeOH−H_2O as mobile phase.

■ ASSOCIATED CONTENT

Supporting Information

The Supporting Information is available free of charge on the ACS Publications website at DOI: 10.1021/acs.jnatprod.8b00540.

HRESIMS, UV, and NMR spectra of compounds **1**−**7** as well as ECD calculations, cell viability, and NF-κB inhibitory assay for compound **1** (PDF)

■ AUTHOR INFORMATION

Corresponding Authors

*Tel: +49 211 81 15979. Fax: +49 211 81 11923. E-mail: zhenfeizi0@sina.com (Z. Liu).

*Tel: +49 211 81 14163. Fax: +49 211 81 11923. E-mail: proksch@uni-duesseldorf.de (P. Proksch).

ORCID

Attila Mándi: 0000-0002-7867-7084

Zhen Liu: 0000-0003-3314-7853

Notes

The authors declare no competing financial interest.

■ ACKNOWLEDGMENTS

We thank the DFG (GRK 2158) and the Manchot Foundation for support. The research project was further supported by a grant to N.T. provided by the Ministry of Culture and Science of the federal state of North Rhine-Westphalia, Germany. The research of the Hungarian authors was supported by the EU and cofinanced by the European Regional Development Fund under the project GINOP-2.3.2-15-2016-00008. The Governmental Information-Technology Development Agency (KIFÜ) is acknowledged for CPU time.

■ REFERENCES

(1) Bills, G. F.; Gloer, J. B. [redacted] **2016**, *4*, 1−32.

(2) Jayanetti, D. R.; Yue, Q.; Bills, G. F.; Gloer, J. B. [redacted] **2015**, *78*, 396−401.

(3) Jayanetti, D. R.; Li, Y.; Bartholomeusz, G. A.; Bills, G. F.; Gloer, J. B. [redacted] **2017**, *80*, 707−712.

(4) Sarrocco, S. [redacted] **2016**, *72*, 643−652.

(5) Liu, S.; Dai, H.; Makhloufi, G.; Heering, C.; Janiak, C.; Hartmann, R.; Mándi, A.; Kurtán, T.; Müller, W. E. G.; Kassack, M. U.; Lin, W.; Liu, Z.; Proksch, P. [redacted] **2016**, *79*, 2332−2340.

(6) Elnaggar, M. S.; Ebrahim, W.; Mándi, A.; Kurtán, T.; Müller, W. E. G.; Kalscheuer, R.; Singab, A.; Lin, W.; Liu, Z.; Proksch, P. *RSC Adv.* **2017**, *7*, 30640−30649.

(7) Wang, H.; Eze, P. M.; Hofert, S.-P.; Janiak, C.; Hartmann, R.; Okoye, F. B. C.; Esimone, C. O.; Orfali, R. S.; Dai, H.; Liu, Z.; Proksch, P. *RSC Adv.* **2018**, *8*, 7863−7872.

(8) Tziros, G. T.; Tzavella-Klonari, K. [redacted] **2008**, *57*, 783.

(9) Levy, E.; Elkind, G.; Ben-Arie, R.; Ben-Ze'ev, I. S. [redacted] **2011**, *39*, 403−405.

(10) Çeliker, N. M.; Uysal, A.; Çetinel, B.; Poyraz, D. [redacted] **2012**, *7*, 161−162.

(11) Pollastro, S.; Dongiovanni, C.; Gerin, D.; Pollastro, P.; Fumarola, G.; De Miccolis Angelini, R. M.; Faretra, F. *Plant Dis.* **2016**, *100*, 1498.

(12) Han, J.; Chen, D.; Huang, J.; Li, X.; Zhou, W.-W.; Gao, W.; Jia, Y. [redacted] **2015**, *25*, 1120−1132.

(13) Grantina-Ievina, L.; Kalniņa, I. *Environ. Exp. Biol.* **2016**, *14*, 51−52.

(14) Griffiths, M.; Wylie, R.; Lawson, S.; Pegg, G.; McDonald, J. In *Prospects for High-Value Hardwood Timber Plantations in the 'Dry' Tropics of Northern Australia*; Academic Press: Mareeba, Australia, 2004; p 15.

(15) Stierle, A. A.; Stierle, D. B.; Girtsman, T.; Mou, T. C.; Antczak, C.; Djaballah, H. [redacted] **2015**, *78*, 2917−2923.

(16) Superchi, S.; Scafato, P.; Górecki, M.; Pescitelli, G. *Curr. Med. Chem.* **2017**, *25*, 287−320.

(17) Mándi, A.; Mudianta, I. W.; Kurtán, T.; Garson, M. J. *J. Nat. Prod.* **2015**, *78*, 2051−2056.

(18) Grimme, S. [redacted] **2006**, *27*, 1787−1799.

(19) Sun, P.; Xu, D. X.; Mándi, A.; Kurtán, T.; Li, T. J.; Schulz, B.; Zhang, W. [redacted] **2013**, *78*, 7030−7047.

(20) Yanai, T.; Tew, D. P.; Handy, N. C. [redacted] **2004**, *393*, 51−57.

(21) Zhou, Z. F.; Kurtán, T.; Yang, X. H.; Mándi, A.; Geng, M. Y.; Ye, B. P.; Taglialatela-Scafati, O.; Guo, Y. W. [redacted] **2014**, *16*, 1390−1393.

(22) Polavarapu, P. L. *Chirality* **2008**, *20*, 664−672.

(23) Sun, P.; Yu, Q.; Li, J.; Riccio, R.; Lauro, G.; Bifulco, G.; Kurtán, T.; Mándi, A.; Tang, H.; Zhuang, C. L.; Gerwick, W. H.; Zhang, W. [redacted] **2016**, *79*, 2552−2558.

(24) Gao, J.-M.; Yang, S.-X.; Qin, J.-C. [redacted] **2013**, *113*, 4755−4811.

DOI: 10.1021/acs.jnatprod.8b00540
J. Nat. Prod. 2018, 81, 2493−2500

(25) Vleggaar, R.; Steyn, P. S.; Nagel, D. W. [redacted] **1974**, *1*, 45−−49.
(26) Zou, X.-W.; Sun, B.-D.; Chen, X.-L.; Liu, X.-Z.; Che, Y.-S. [redacted] **2009**, *7*, 140−144.
(27) Panthama, N.; Kanokmedhakul, S.; Kanokmedhakul, K.; Soytong, K. [redacted] **2011**, *74*, 2395−2399.
(28) Zhou, S.-L.; Wang, M.; Zhao, H.-G.; Huang, Y.-H.; Lin, Y.-Y.; Tan, G.-H.; Chen, S.-L. [redacted] **2016**, *39*, 1621−1627.
(29) Pal, S. K.; Childs, B. H.; Pegram, M. [redacted] **2011**, *125*, 627−636.
(30) Luo, J.-G.; Xu, Y.-M.; Sandberg, D. C.; Arnold, A. E.; Gunatilaka, A. A. L. [redacted] **2017**, *80*, 76−81.
(31) Cheng, M.-J.; Wu, M.-D.; Su, Y.-S.; Yuan, G.-F.; Chen, Y.-L.; Chen, I.-S. [redacted] **2012**, *5*, 262−266.
(32) Youn, U. J.; Sripisut, T.; Park, E. J.; Kondratyuk, T. P.; Fatima, N.; Simmons, C. J.; Wall, M. M.; Sun, D.; Pezzuto, J. M.; Chang, L. C. [redacted] *Lett.* **2015**, *25*, 4719−4723.
(33) Pires, B. R. B.; Mencalha, A. L.; Ferreira, G. M.; de Souza, W. F.; Morgado-Díaz, J. A.; Maia, A. M.; Corrêa, S.; Abdelhay, E. S. F. W. [redacted] **2017**, *12*, e0169622.
(34) Kjer, J.; Debbab, A.; Aly, A. H.; Proksch, P. [redacted] **2010**, *5*, 479−490.
(35) Sperlich, J.; Kerr, R.; Teusch, N. [redacted] **2017**, *15*, 262.
(36) *MacroModel*; Schrödinger LLC: New York, 2015, https://www.schrodinger.com/macromodel.
(37) Frisch, M. J.; Trucks, G. W.; Schlegel, H. B.; Scuseria, G. E.; Robb, M. A.; Cheeseman, J. R.; Scalmani, G.; Barone, V.; Mennucci, B.; Petersson, G. A.; Nakatsuji, H.; Caricato, M.; Li, X.; Hratchian, H. P.; Izmaylov, A. F.; Bloino, J.; Zheng, G.; Sonnenberg, J. L.; Hada, M.; Ehara, M.; Toyota, K.; Fukuda, R.; Hasegawa, J.; Ishida, M.; Nakajima, T.; Honda, Y.; Kitao, O.; Nakai, H.; Vreven, T.; Montgomery, J. A., Jr.; Peralta, J. E.; Ogliaro, F.; Bearpark, M.; Heyd, J. J.; Brothers, E.; Kudin, K. N.; Staroverov, V. N.; Kobayashi, R.; Normand, J.; Raghavachari, K.; Rendell, A.; Burant, J. C.; Iyengar, S. S.; Tomasi, J.; Cossi, M.; Rega, N.; Millam, J. M.; Klene, M.; Knox, J. E.; Cross, J. B.; Bakken, V.; Adamo, C.; Jaramillo, J.; Gomperts, R.; Stratmann, R. E.; Yazyev, O.; Austin, A. J.; Cammi, R.; Pomelli, C.; Ochterski, J. W.; Martin, R. L.; Morokuma, K.; Zakrzewski, V. G.; Voth, G. A.; Salvador, P.; Dannenberg, J. J.; Dapprich, S.; Daniels, A. D.; Farkas, Ö.; Foresman, J. B.; Ortiz, J. V.; Cioslowski, J.; Fox, D. J. *Gaussian 09*, Revision E.01; Gaussian, Inc.: Wallingford, CT, 2013.
(38) Stephens, P. J.; Harada, N. [redacted] **2010**, *22*, 229−233.
(39) Varetto, U. *MOLEKEL 5.4*; Swiss National Supercomputing Centre: Manno, Switzerland, 2009.

DOI: 10.1021/acs.jnatprod.8b00540
J. Nat. Prod. 2018, 81, 2493−2500

Supporting Information

Azaphilone Derivatives from the Fungus Inhibit NF-κB Activation and Reduce Tumor Cell Migration

Haiqian Yu,[†] Julia Sperlich,[‡] Attila Mándi,[§] Tibor Kurtán,[§] Haofu Dai,[⊥] Nicole Teusch,[‡] Zhi-Yong Guo,[#] Kun Zou,[#] Zhen Liu,*[,†] Peter Proksch*[,†]

[†]Institute of Pharmaceutical Biology and Biotechnology, Heinrich-Heine-Universität Düsseldorf, Universitätsstrasse 1, 40225 Düsseldorf, Germany

[‡]Bio-Pharmaceutical Chemistry and Molecular Pharmacology, Faculty of Applied Natural Sciences, Technische Hochschule Köln, Chempark, 51368 Leverkusen, Germany

[§]Department of Organic Chemistry, University of Debrecen, P.O. Box 400, H-4002 Debrecen, Hungary

[⊥]Key Laboratory of Biology and Genetic Resources of Tropical Crops, Ministry of Agriculture, Institute of Tropical Bioscience and Biotechnology, Chinese Academy of Tropical Agricultural Sciences, Haikou 571101, China

[#]Hubei Key Laboratory of Natural Product Research and Development, College of Biological and Pharmaceutical Sciences, China Three Gorges University, Yichang 443002, China

Table of Contents

Figure S1. The HRESIMS of compound 1 4
Figure S2. The ^{1}H NMR (600 MHz, $CDCl_3$) spectrum of compound 1 4
Figure S3. The ^{13}C NMR (150 MHz, $CDCl_3$) spectrum of compound 1 5
Figure S4. The COSY (600 MHz, $CDCl_3$) spectrum of compound 1 5
Figure S5. The HSQC (600 MHz, $CDCl_3$) spectrum of compound 1 6
Figure S6. The HMBC (600 MHz, $CDCl_3$) spectrum of compound 1 6
Figure S7. The ROESY (600 MHz, $CDCl_3$) spectrum of compound 1 7
Figure S8. The UV spectrum of compound 1 7
Figure S9. The HRESIMS of compound 2 8
Figure S10. The ^{1}H NMR (300 MHz, $CDCl_3$) spectrum of compound 2 8
Figure S11. The ^{13}C NMR (75 MHz, $CDCl_3$) spectrum of compound 2 9
Figure S12. The COSY (300 MHz, $CDCl_3$) spectrum of compound 2 9
Figure S13. The HSQC (300 MHz, $CDCl_3$) spectrum of compound 2 10
Figure S14. The HMBC (300 MHz, $CDCl_3$) spectrum of compound 2 10
Figure S15. The ROESY (300 MHz, $CDCl_3$) spectrum of compound 2 11
Figure S16. The UV spectrum of compound 2 11
Figure S17. The HRESIMS of compound 3 12
Figure S18. The ^{1}H NMR (600 MHz, $CDCl_3$) spectrum of compound 3 12
Figure S19. The ^{13}C NMR (150 MHz, $CDCl_3$) spectrum of compound 3 13
Figure S20. The COSY (600 MHz, $CDCl_3$) spectrum of compound 3 13
Figure S21. The HSQC (600 MHz, $CDCl_3$) spectrum of compound 3 14
Figure S22. The HMBC (600 MHz, $CDCl_3$) spectrum of compound 3 14
Figure S23. The ROESY (600 MHz, $CDCl_3$) spectrum of compound 3 15
Figure S24. The UV spectrum of compound 3 15
Figure S25. The HRESIMS of compound 4 16
Figure S26. The ^{1}H NMR (300 MHz, $CDCl_3$) spectrum of compound 4 16
Figure S27. The ^{13}C NMR (75 MHz, $CDCl_3$) spectrum of compound 4 17
Figure S28. The COSY (300 MHz, $CDCl_3$) spectrum of compound 4 17
Figure S29. The HSQC (300 MHz, $CDCl_3$) spectrum of compound 4 18
Figure S30. The HMBC (300 MHz, $CDCl_3$) spectrum of compound 4 18
Figure S31. The ROESY (300 MHz, $CDCl_3$) spectrum of compound 4 19
Figure S32. The UV spectrum of compound 4 19
Figure S33. The HRESIMS of compound 5 20
Figure S34. The ^{1}H-NMR (600 MHz, $CDCl_3$) spectrum of compound 5 20
Figure S35. The ^{13}C NMR (150 MHz, $CDCl_3$) spectrum of compound 5 21
Figure S36. The COSY (600 MHz, $CDCl_3$) spectrum of compound 5 21
Figure S37. The HSQC (600 MHz, $CDCl_3$) spectrum of compound 5 22
Figure S38. The HMBC (600 MHz, $CDCl_3$) spectrum of compound 5 22
Figure S39. The ROESY (600 MHz, $CDCl_3$) spectrum of compound 5 23
Figure S40. The UV spectrum of compound 5 23
Figure S41. The HRESIMS of compound 6 24
Figure S42. The ^{1}H NMR (600 MHz, $CDCl_3$) spectrum of compound 6 24

Figure S43. The ^{13}C NMR (150 MHz, $CDCl_3$) spectrum of compound 6 25
Figure S44. The COSY (600 MHz, $CDCl_3$) spectrum of compound 6 25
Figure S45. The HSQC (600 MHz, $CDCl_3$) spectrum of compound 6 26
Figure S46. The HMBC (600 MHz, $CDCl_3$) spectrum of compound 6 26
Figure S47. The ROESY (600 MHz, $CDCl_3$) spectrum of compound 6 27
Figure S48. The UV spectrum of compound 6 27
Figure S49. The HRESIMS of compound 7 28
Figure S50. The ^{1}H NMR (300 MHz, $CDCl_3$) spectrum of compound 7 28
Figure S51. The ^{13}C NMR (75 MHz, $CDCl_3$) spectrum of compound 7 29
Figure S52. The COSY (300 MHz, $CDCl_3$) spectrum of compound 7 29
Figure S53. The HSQC (300 MHz, $CDCl_3$) spectrum of compound 7 30
Figure S54. The HMBC (300 MHz, $CDCl_3$) spectrum of compound 7 30
Figure S55. The ROESY (300 MHz, $CDCl_3$) spectrum of compound 7 31
Figure S56. The UV spectrum of compound 7 31
Figure S57. Structure and population of the low-energy B97D/TZVP PCM/MeCN conformers (> 1%) of (7*R*,8*S*,12*S*)-1 32
Table S1. Boltzmann populations and optical rotations of the low-energy conformers of (7*R*,8*S*,12S)-1 computed at various levels for the B3LYP/6-31G(d) reoptimized MMFF conformers. 32
Figure S58. Time course of tumor cell migration in the presence of 1. 33
Figure S59. Compound 1 inhibits invasion into the 3D extracellular matrix. 34

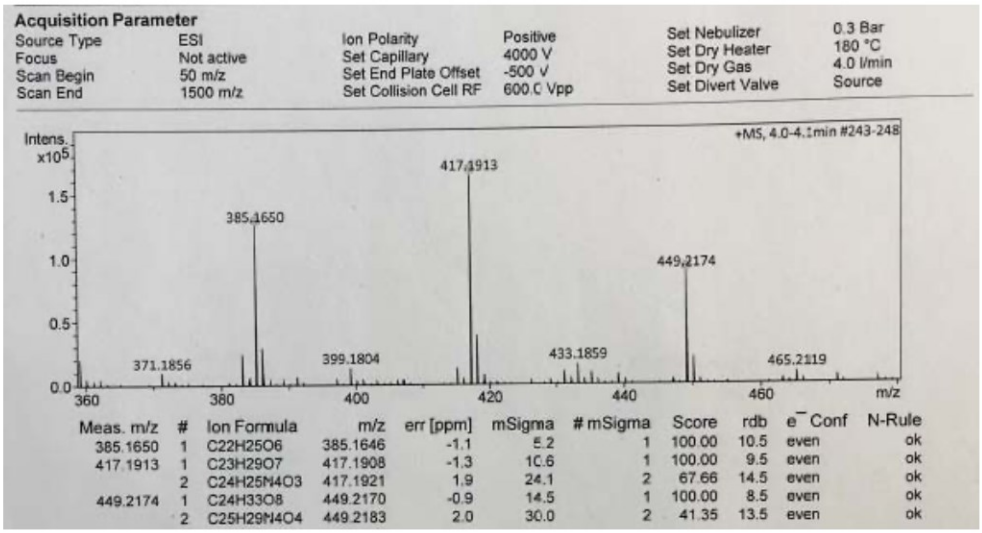

Figure S1. The HRESIMS of compound 1

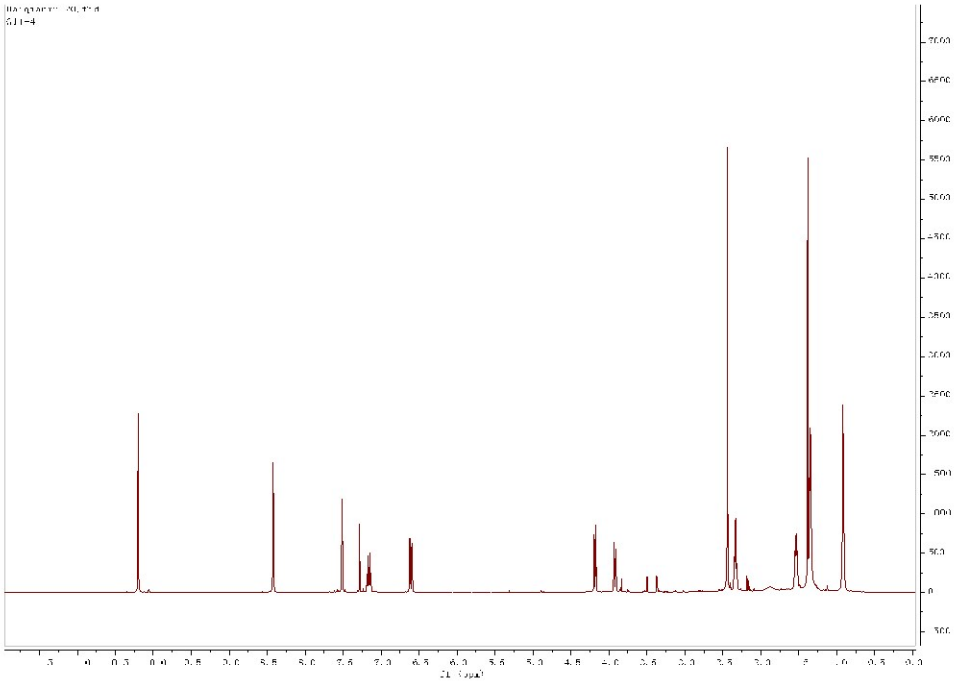

Figure S2. The ^{1}H NMR (600 MHz, $CDCl_3$) spectrum of compound 1

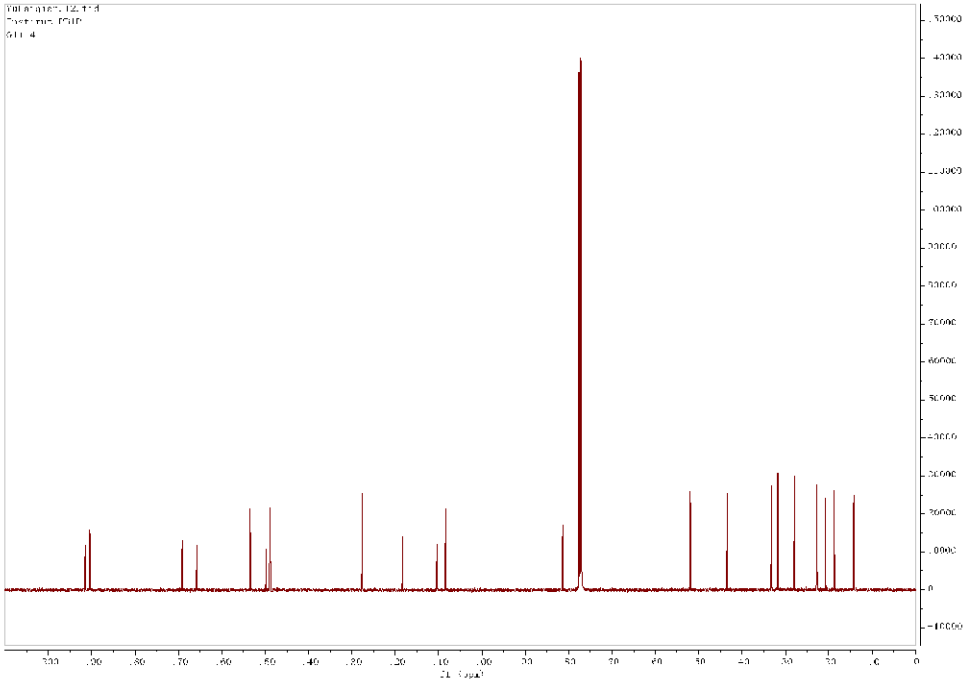

Figure S3. The ^{13}C NMR (150 MHz, $CDCl_3$) spectrum of compound 1

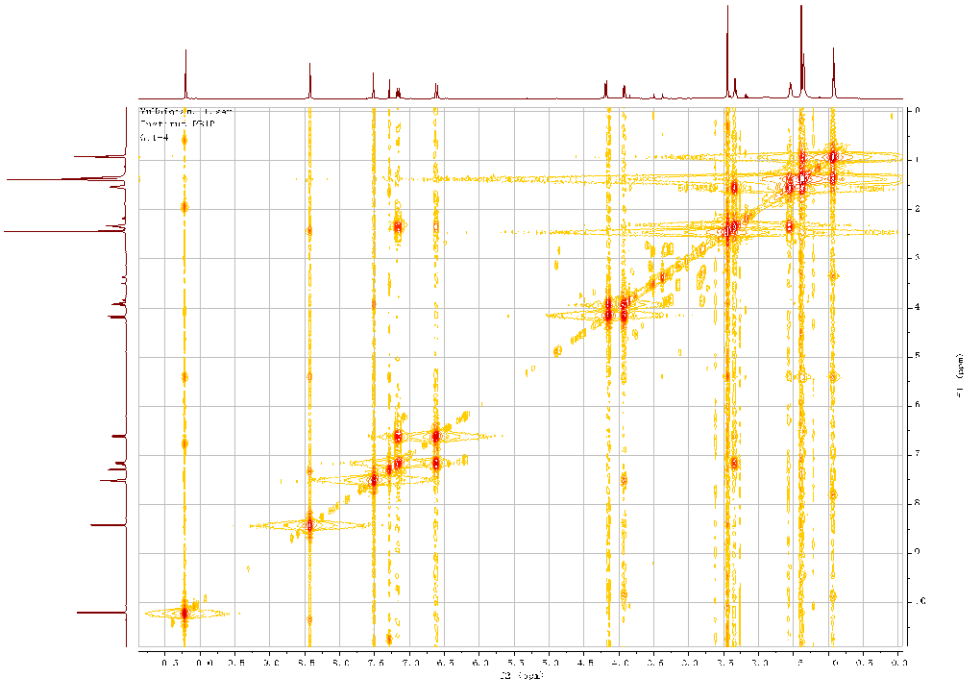

Figure S4. The COSY (600 MHz, $CDCl_3$) spectrum of compound 1

Figure S5. The HSQC (600 MHz, $CDCl_3$) spectrum of compound 1

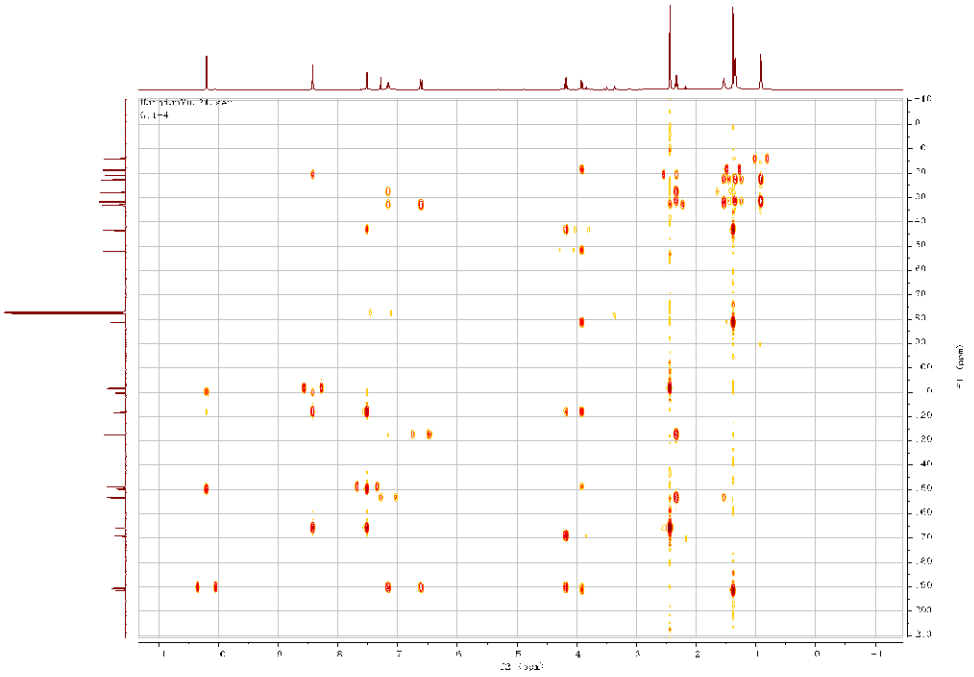

Figure S6. The HMBC (600 MHz, $CDCl_3$) spectrum of compound 1

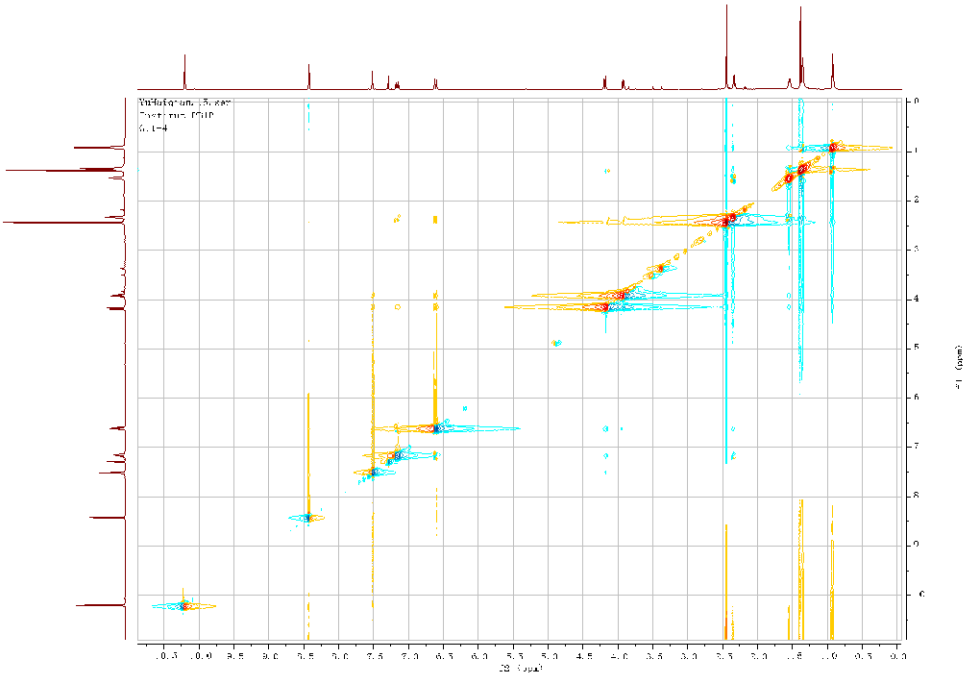

Figure S7. The ROESY (600 MHz, $CDCl_3$) spectrum of compound 1

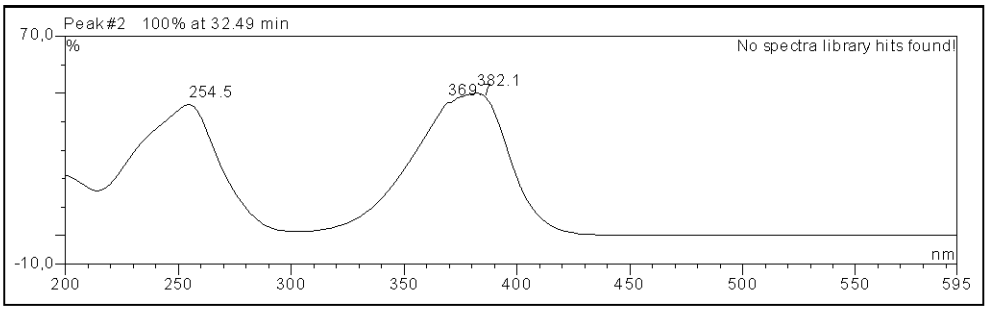

Figure S8. The UV spectrum of compound 1

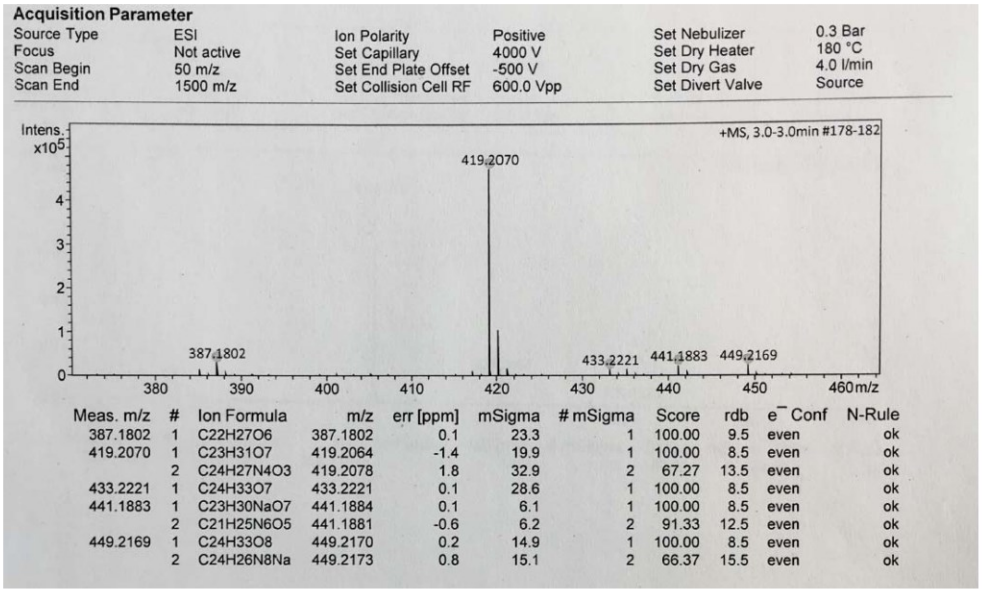

Meas. m/z	#	Ion Formula	m/z	err [ppm]	mSigma	# mSigma	Score	rdb	e⁻ Conf	N-Rule
387.1802	1	C22H27O6	387.1802	0.1	23.3	1	100.00	9.5	even	ok
419.2070	1	C23H31O7	419.2064	-1.4	19.9	1	100.00	8.5	even	ok
	2	C24H27N4O3	419.2078	1.8	32.9	2	67.27	13.5	even	ok
433.2221	1	C24H33O7	433.2221	0.1	28.6	1	100.00	8.5	even	ok
441.1883	1	C23H30NaO7	441.1884	0.1	6.1	1	100.00	8.5	even	ok
	2	C21H25N6O5	441.1881	-0.6	6.2	2	91.33	12.5	even	ok
449.2169	1	C24H33O8	449.2170	0.2	14.9	1	100.00	8.5	even	ok
	2	C24H26N8Na	449.2173	0.8	15.1	2	66.37	15.5	even	ok

Figure S9. The HRESIMS of compound 2

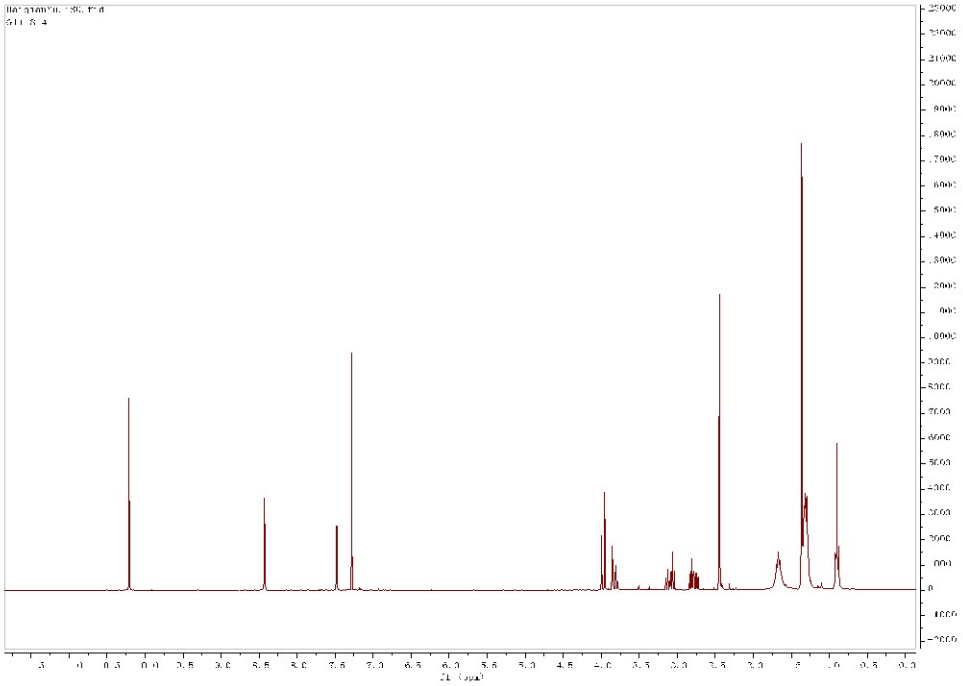

Figure S10. The ^{1}H NMR (300 MHz, $CDCl_3$) spectrum of compound 2

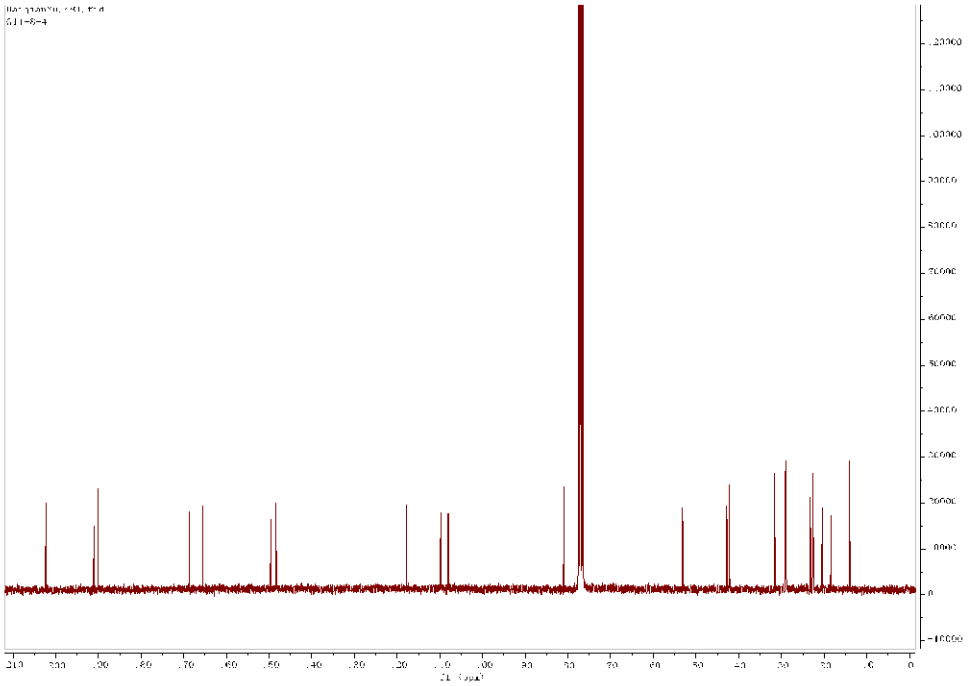

Figure S11. The ^{13}C NMR (75 MHz, $CDCl_3$) spectrum of compound 2

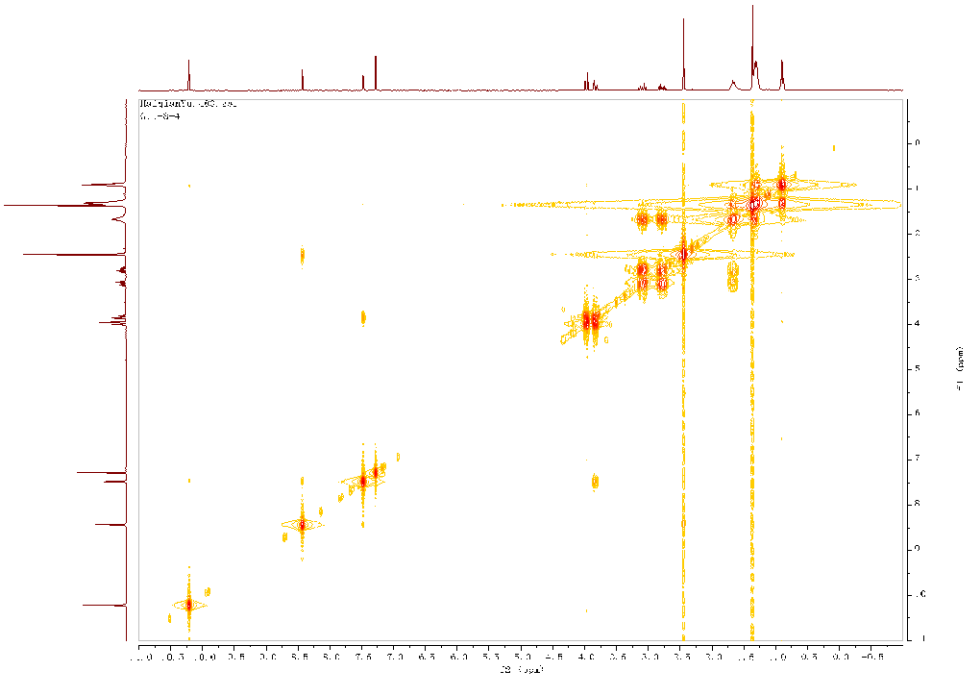

Figure S12. The COSY (300 MHz, $CDCl_3$) spectrum of compound 2

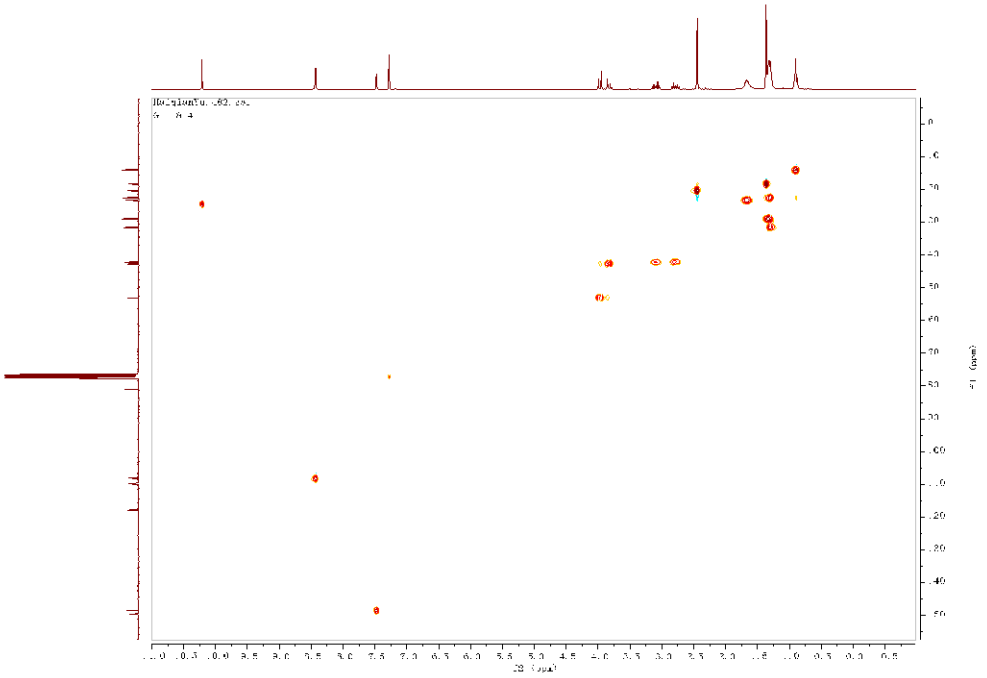

Figure S13. The HSQC (300 MHz, $CDCl_3$) spectrum of compound 2

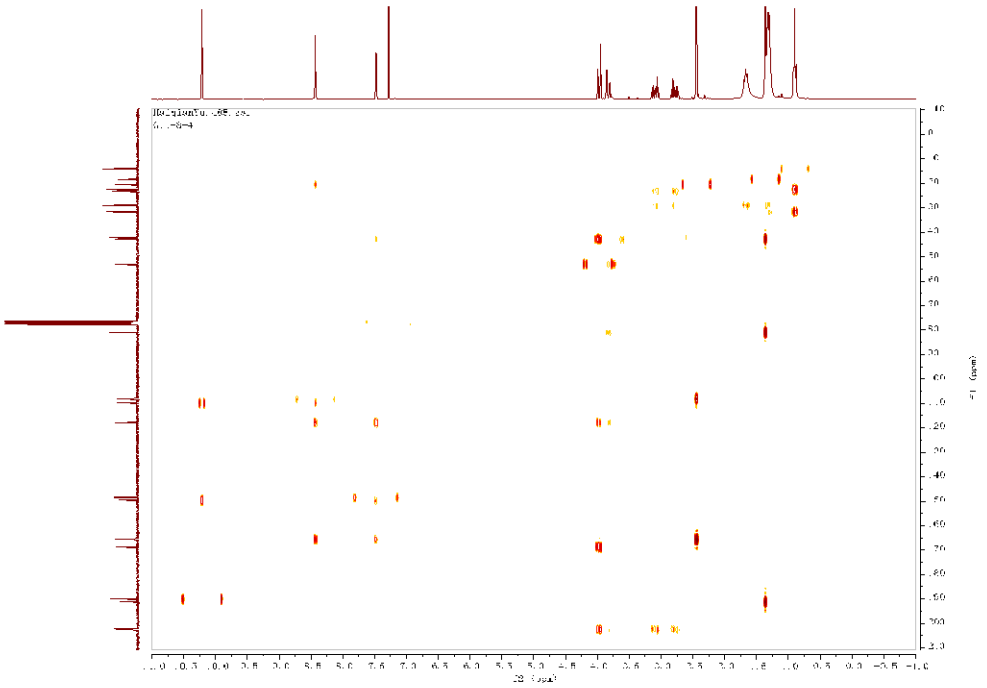

Figure S14. The HMBC (300 MHz, $CDCl_3$) spectrum of compound 2

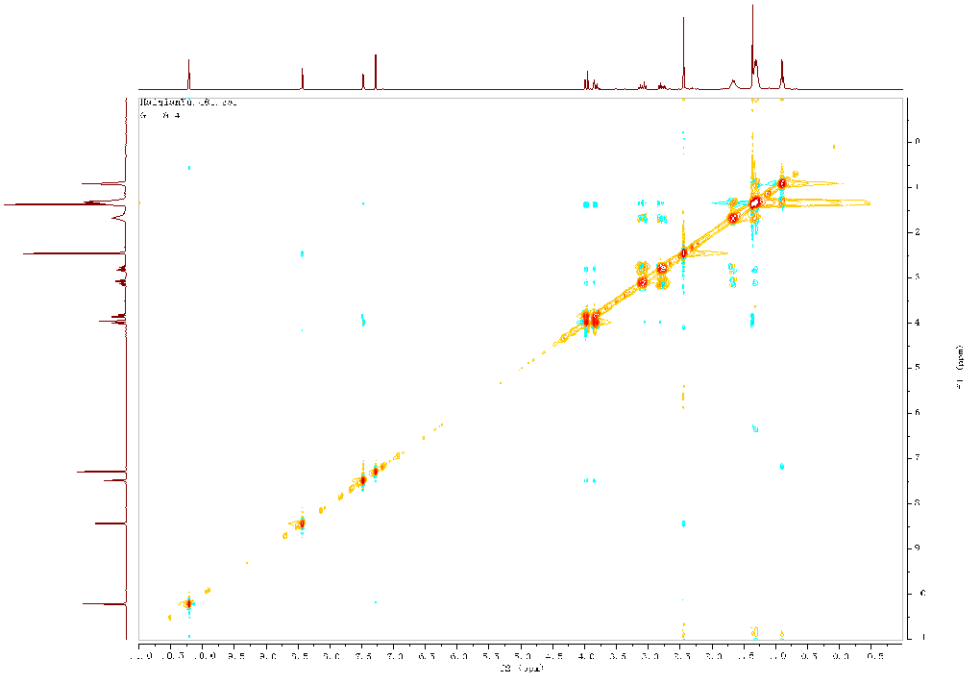

Figure S15. The ROESY (300 MHz, $CDCl_3$) spectrum of compound 2

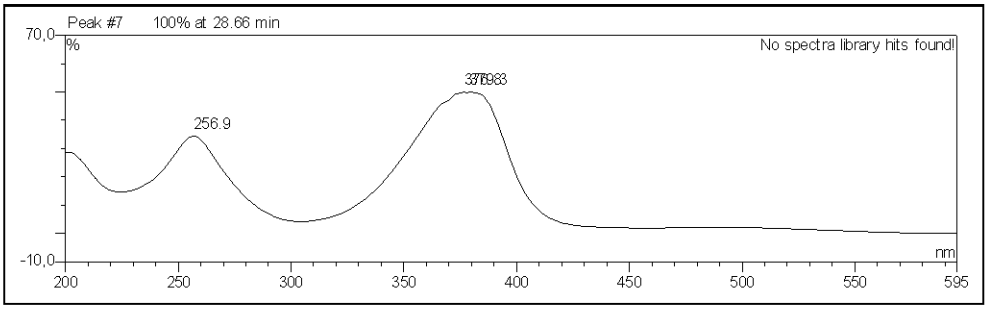

Figure S16. The UV spectrum of compound 2

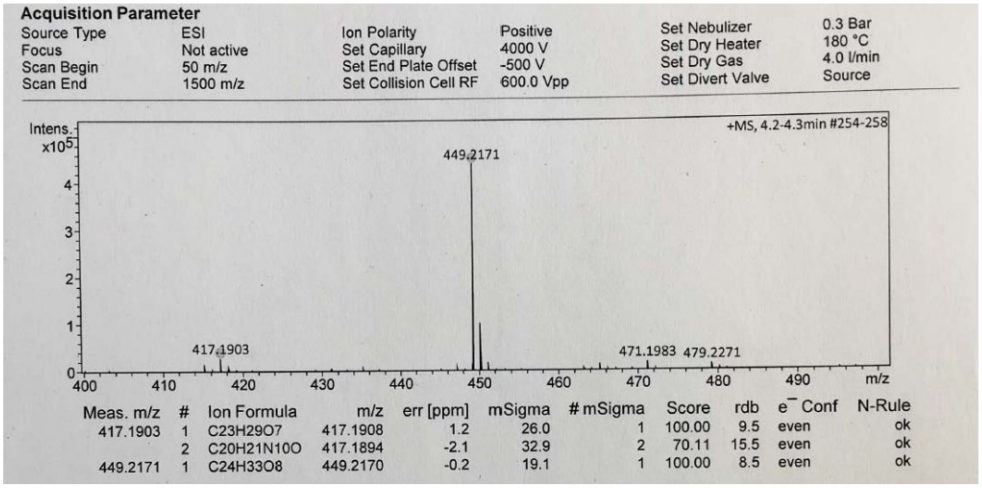

Figure S17. The HRESIMS of compound 3

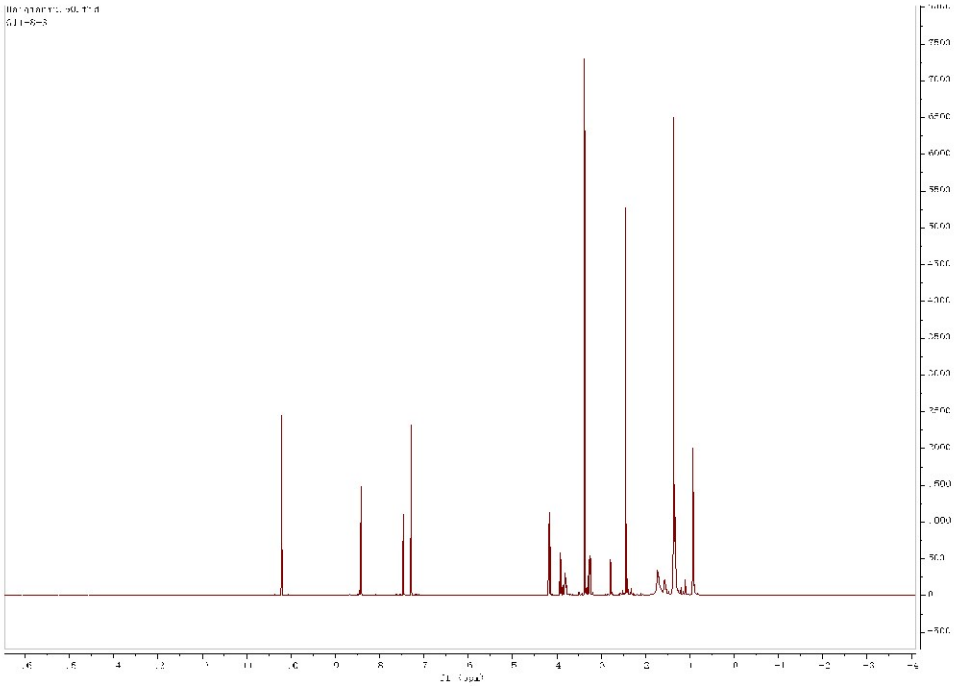

Figure S18. The ^{1}H NMR (600 MHz, $CDCl_3$) spectrum of compound 3

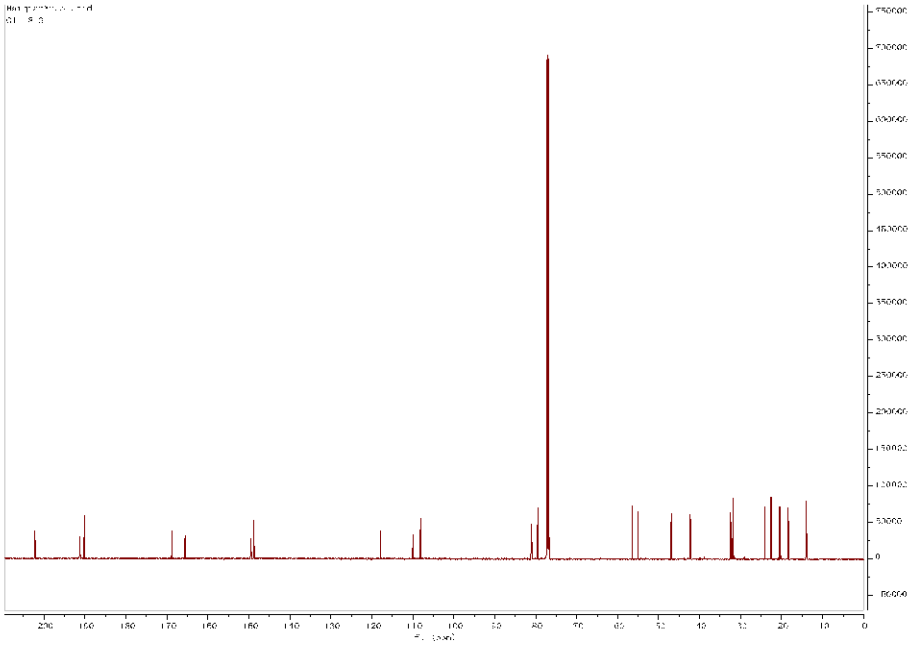

Figure S19. The ^{13}C NMR (150 MHz, $CDCl_3$) spectrum of compound 3

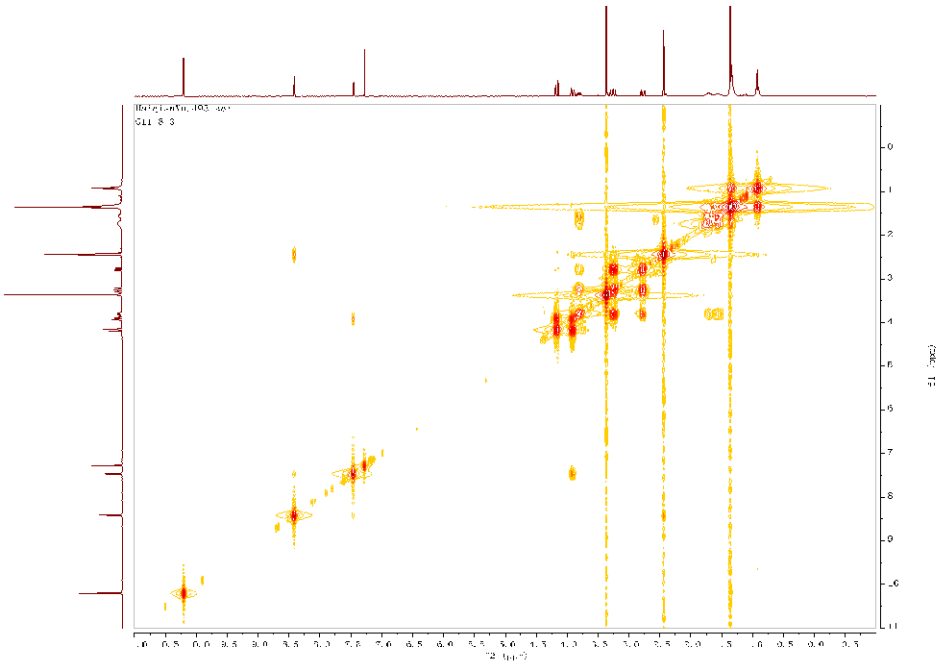

Figure S20. The COSY (600 MHz, $CDCl_3$) spectrum of compound 3

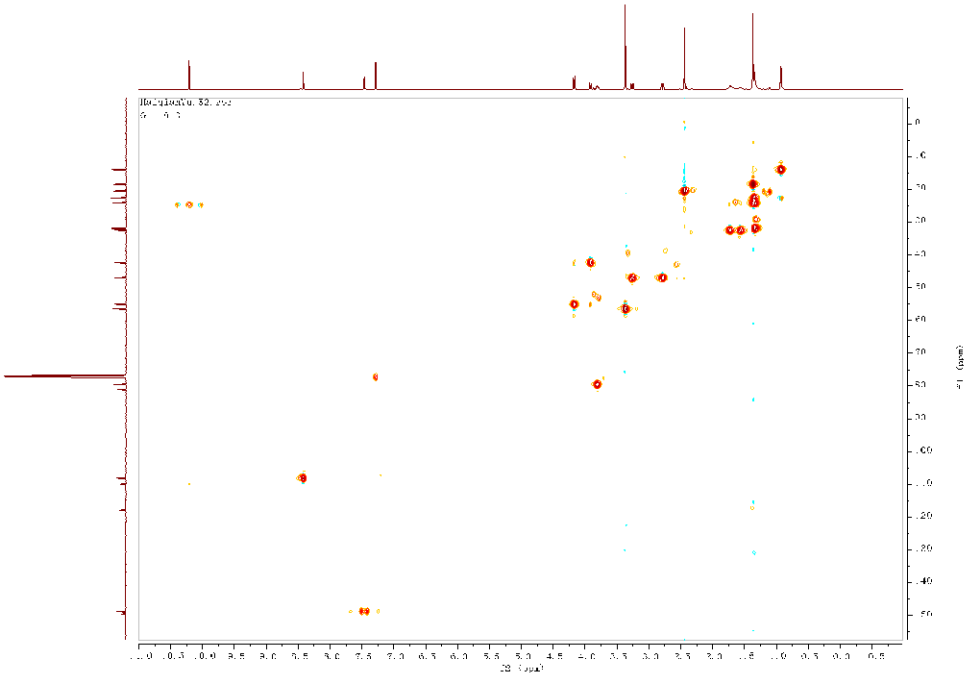

Figure S21. The HSQC (600 MHz, $CDCl_3$) spectrum of compound 3

Figure S22. The HMBC (600 MHz, $CDCl_3$) spectrum of compound 3

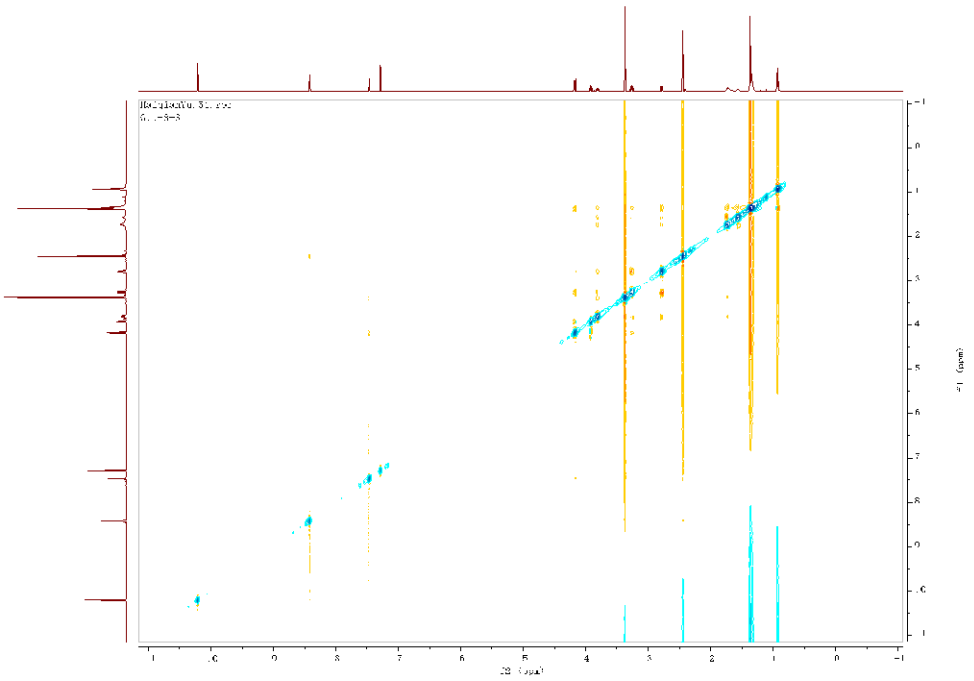

Figure S23. The ROESY (600 MHz, $CDCl_3$) spectrum of compound 3

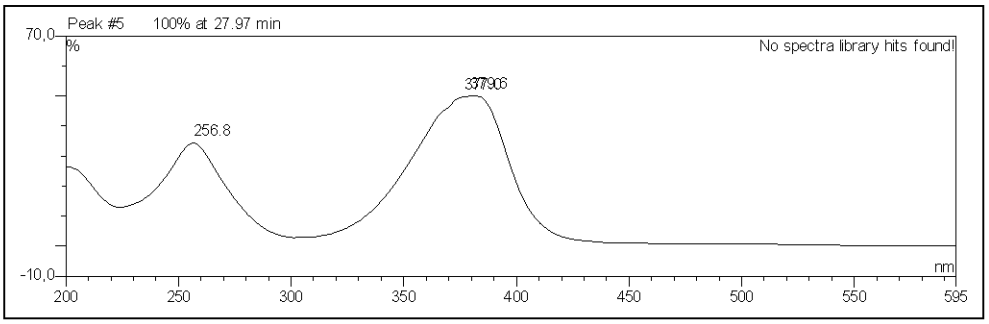

Figure S24. The UV spectrum of compound 3

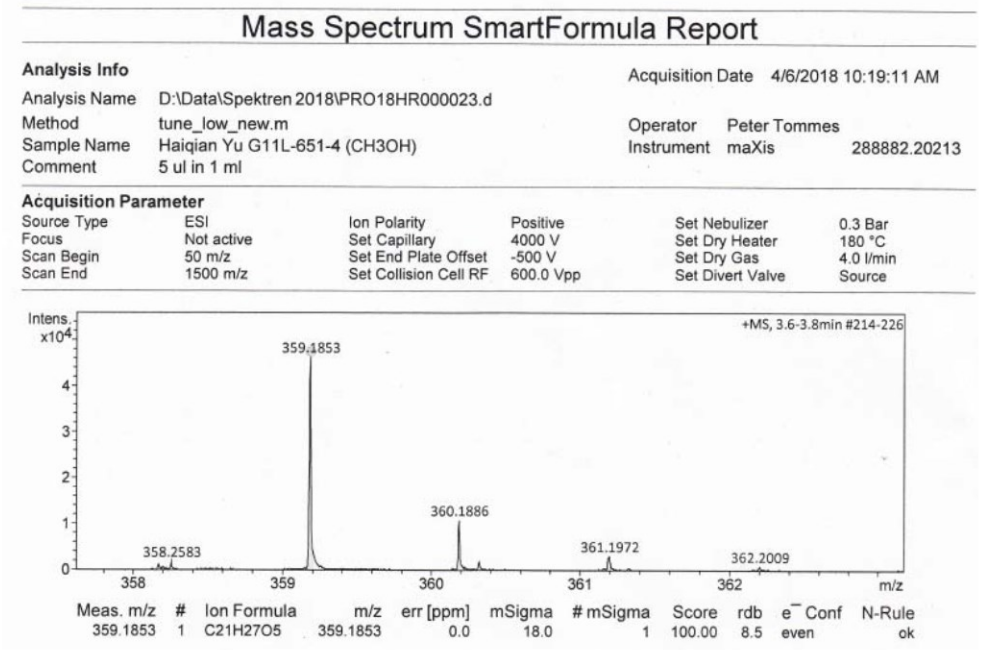

Figure S25. The HRESIMS of compound 4

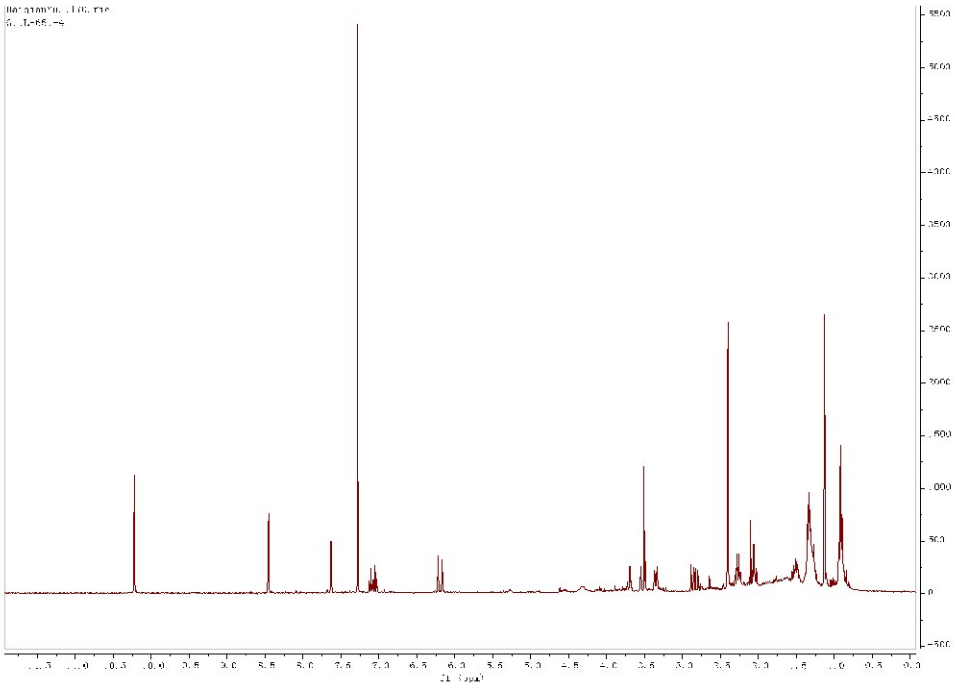

Figure S26. The ^{1}H NMR (300 MHz, $CDCl_3$) spectrum of compound 4

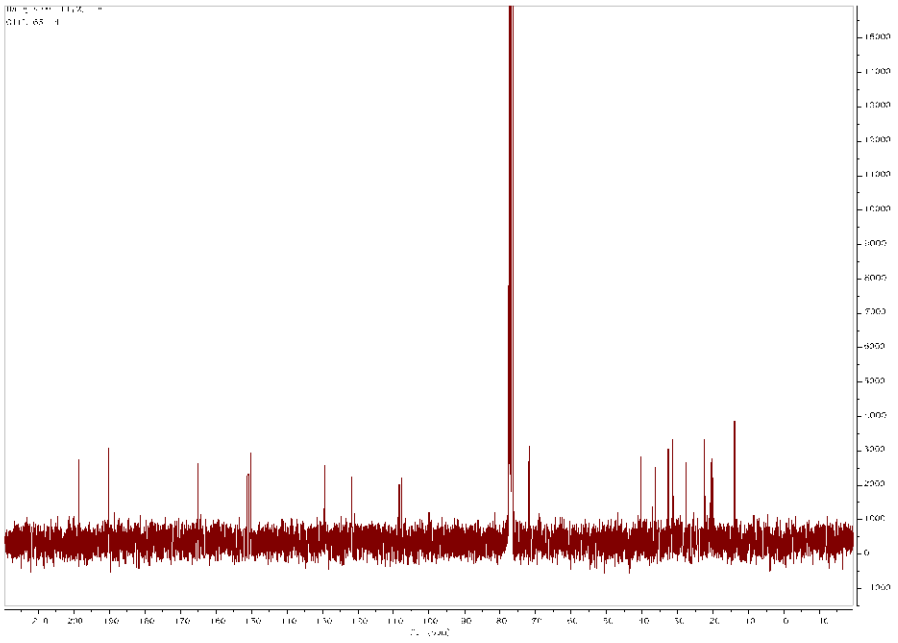

Figure S27. The ^{13}C NMR (75 MHz, $CDCl_3$) spectrum of compound 4

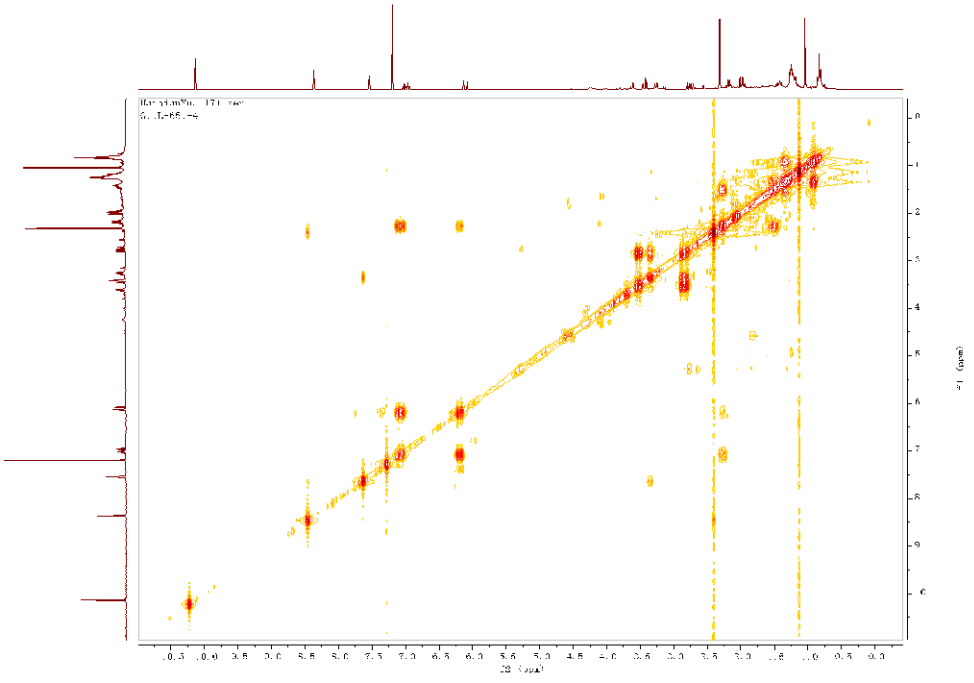

Figure S28. The COSY (300 MHz, $CDCl_3$) spectrum of compound 4

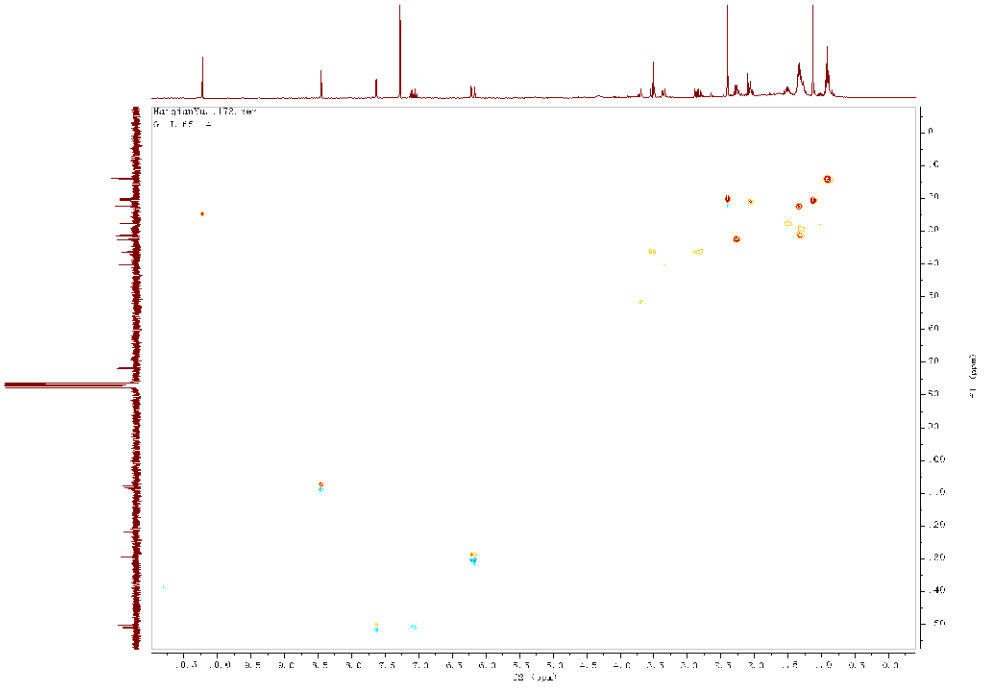

Figure S29. The HSQC (300 MHz, $CDCl_3$) spectrum of compound 4

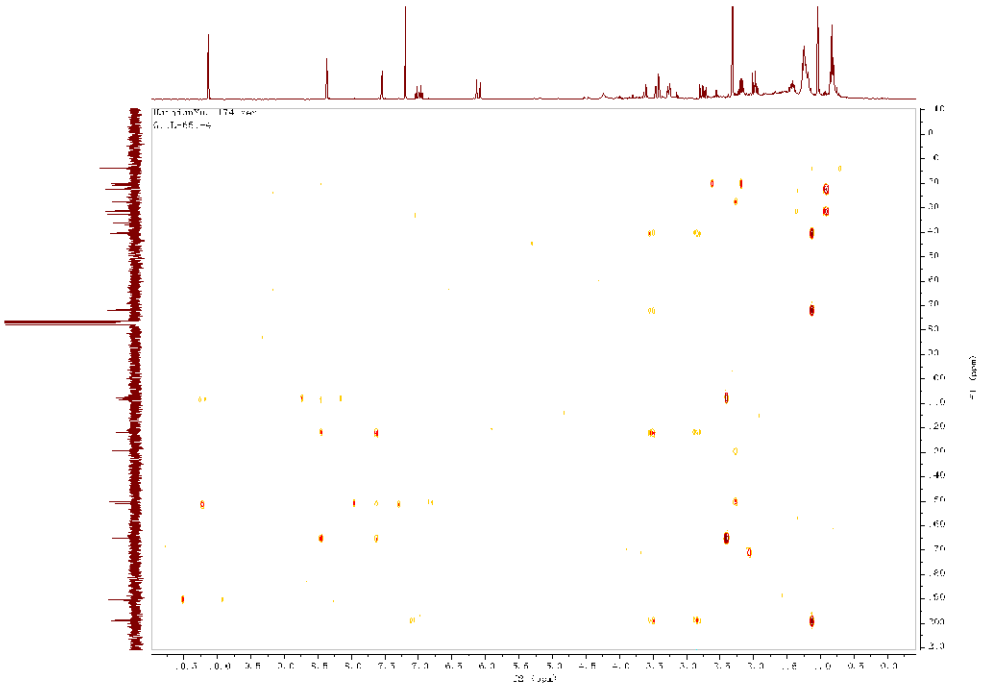

Figure S30. The HMBC (300 MHz, $CDCl_3$) spectrum of compound 4

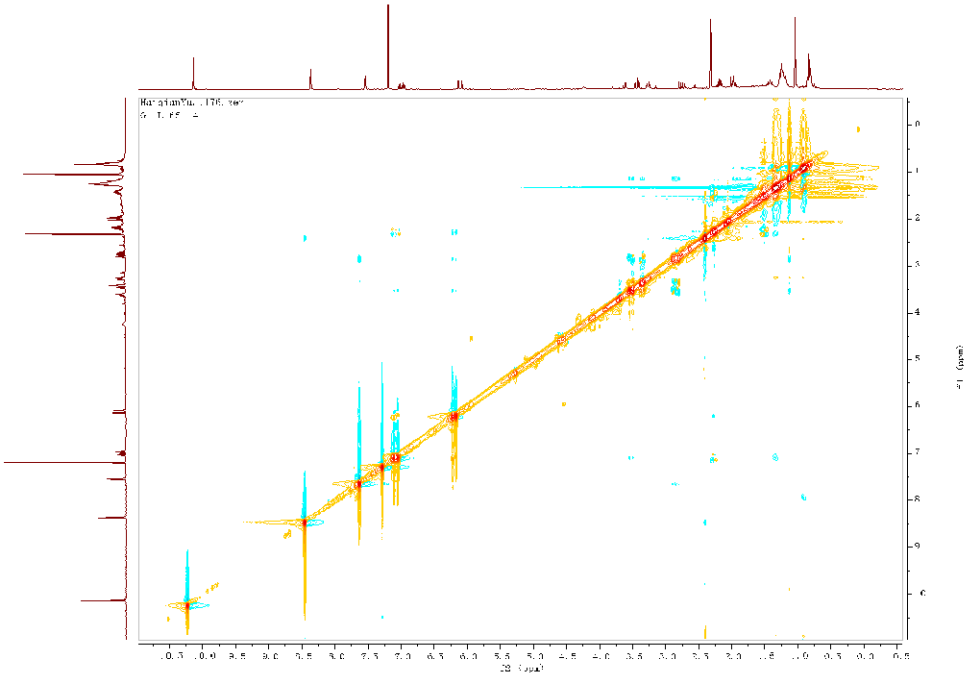

Figure S31. The ROESY (300 MHz, $CDCl_3$) spectrum of compound 4

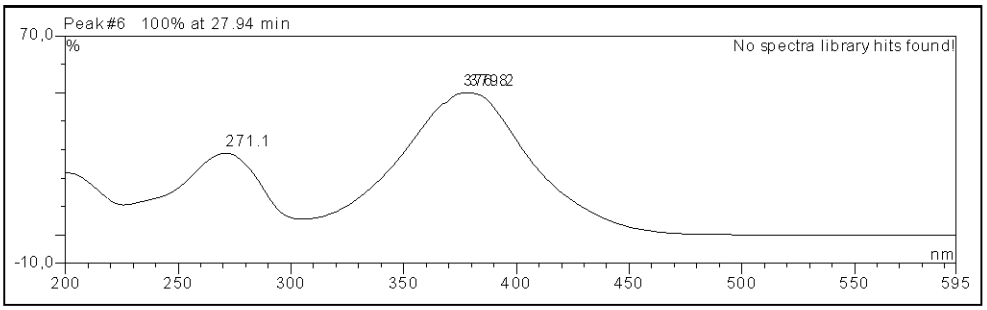

Figure S32. The UV spectrum of compound 4

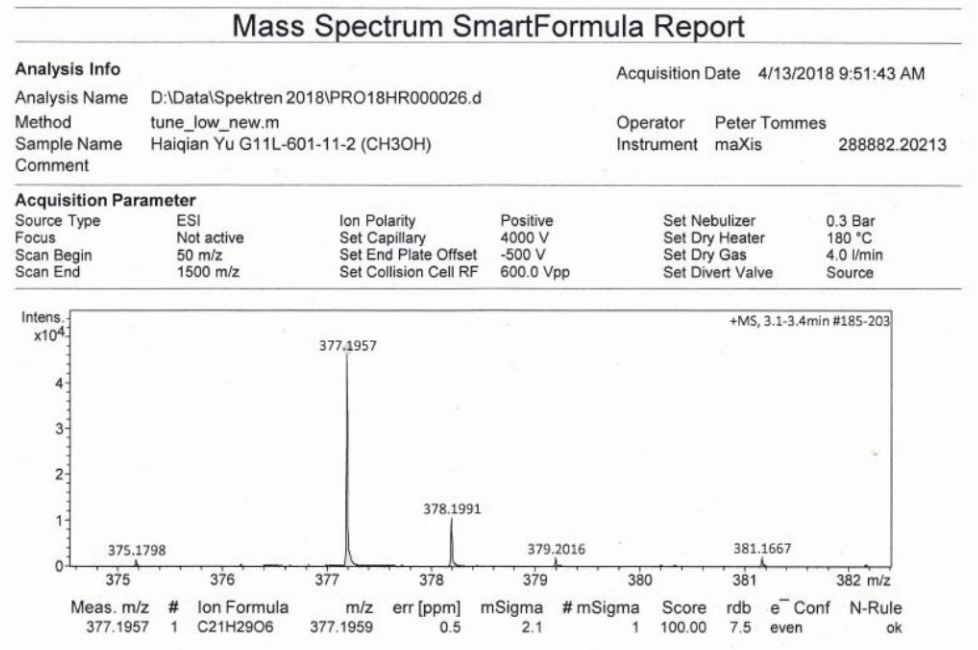

Figure S33. The HRESIMS of compound 5

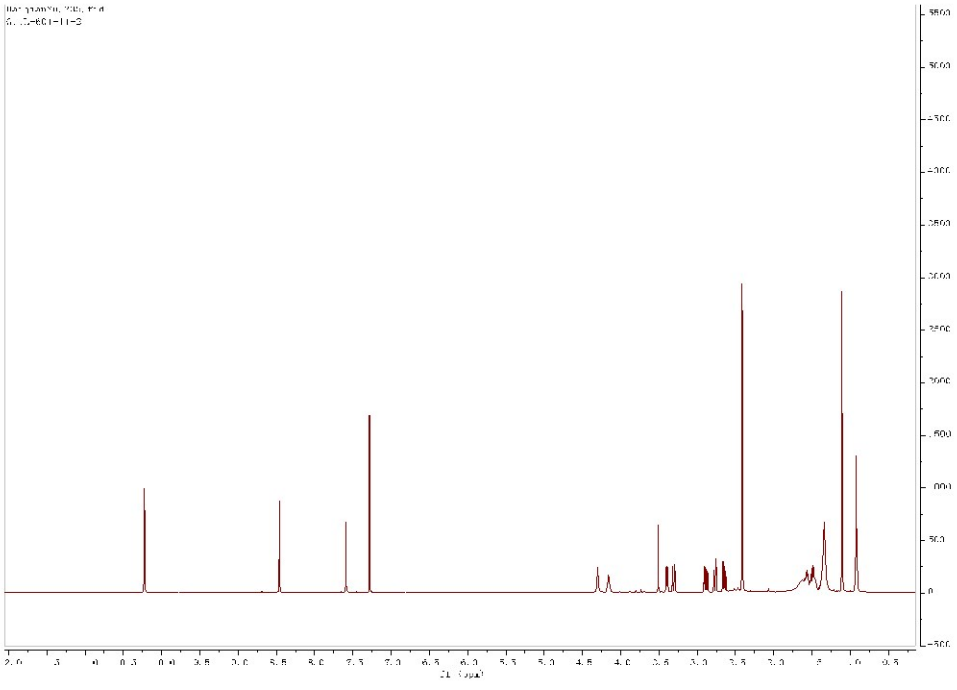

Figure S34. The ^{1}H-NMR (600 MHz, $CDCl_3$) spectrum of compound 5

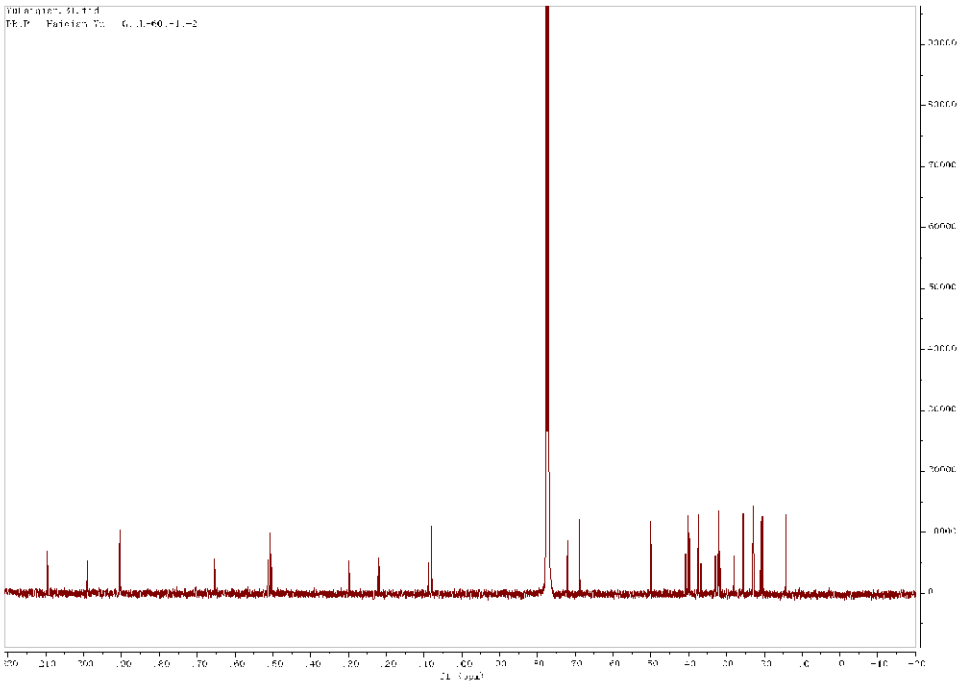

Figure S35. The ^{13}C NMR (150 MHz, $CDCl_3$) spectrum of compound 5

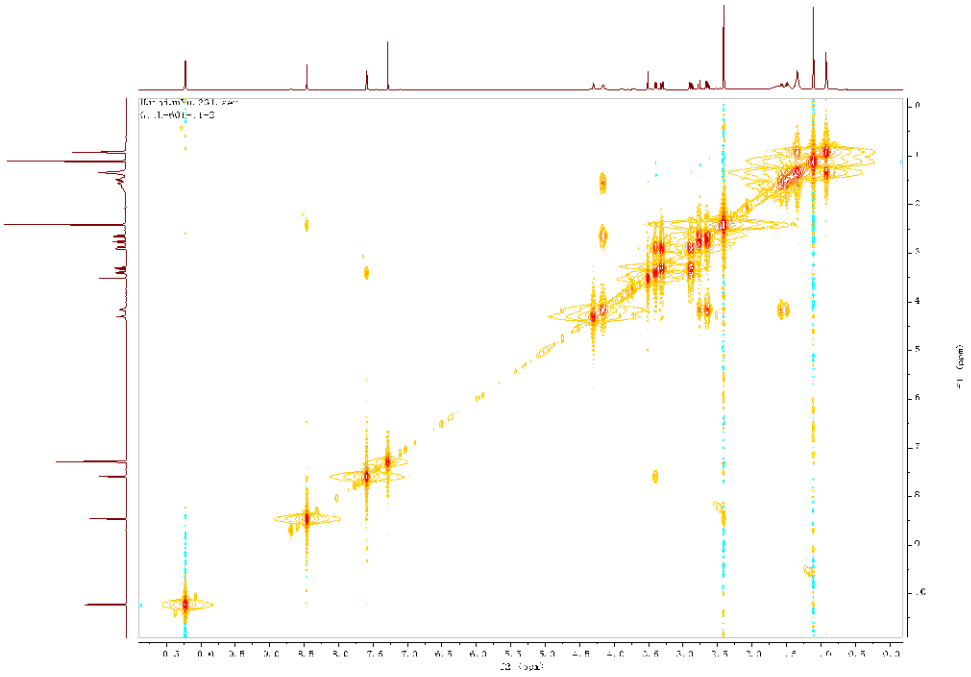

Figure S36. The COSY (600 MHz, $CDCl_3$) spectrum of compound 5

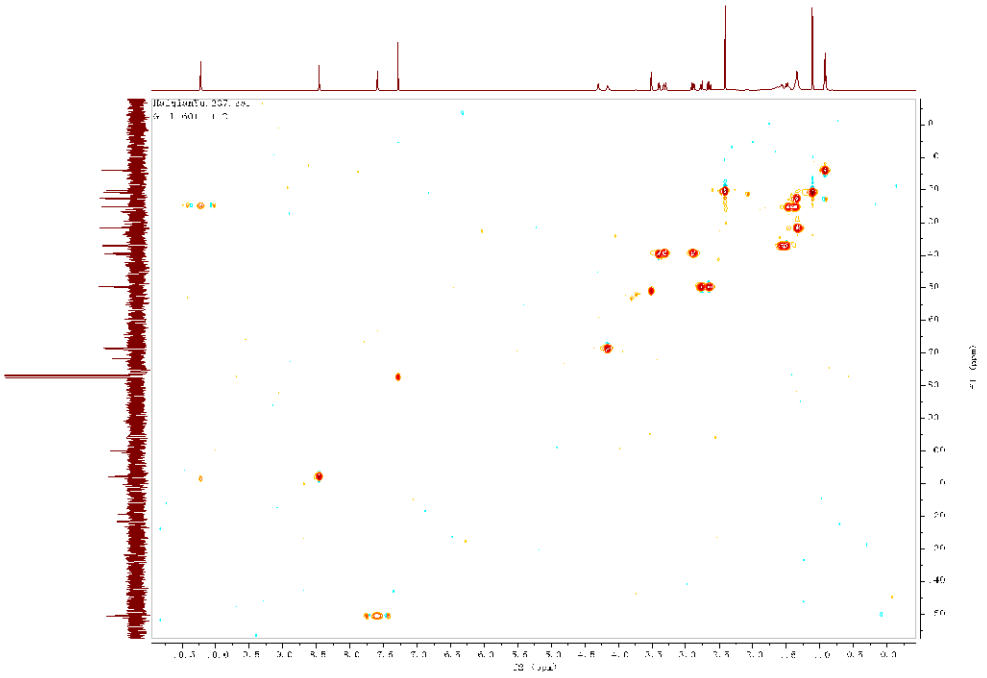

Figure S37. The HSQC (600 MHz, $CDCl_3$) spectrum of compound 5

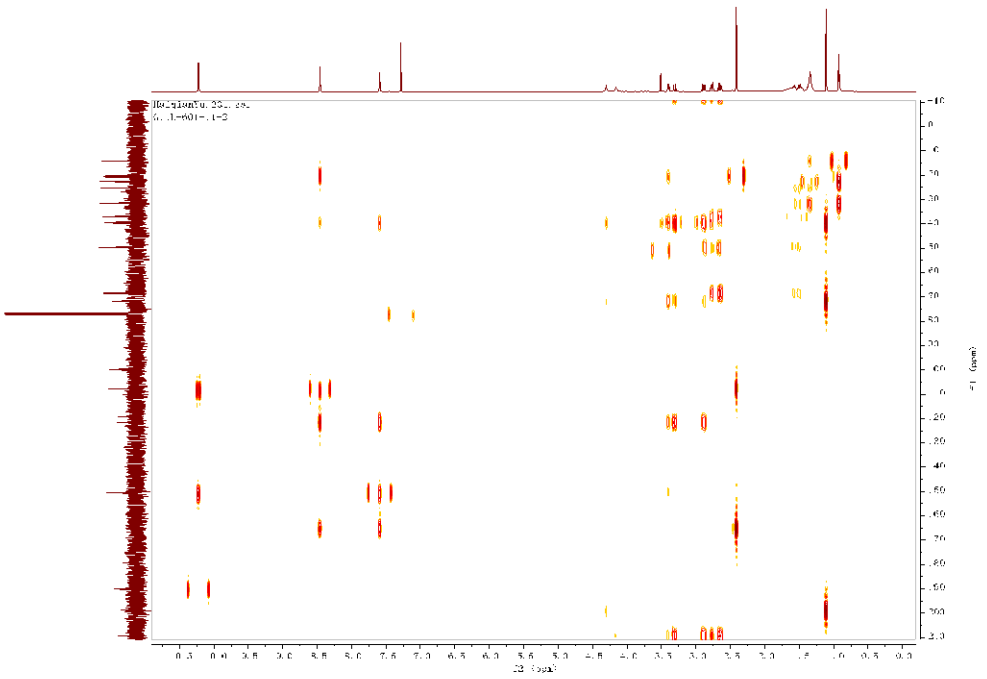

Figure S38. The HMBC (600 MHz, $CDCl_3$) spectrum of compound 5

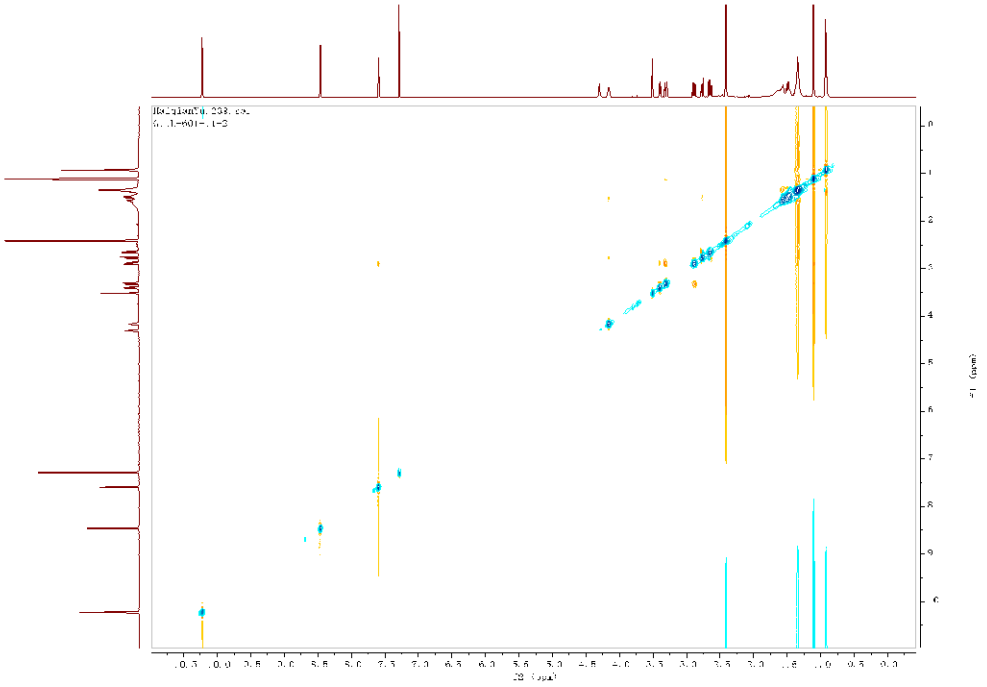

Figure S39. The ROESY (600 MHz, $CDCl_3$) spectrum of compound 5

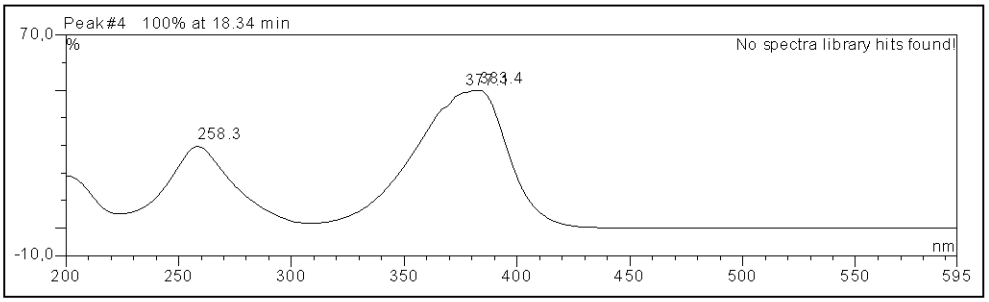

Figure S40. The UV spectrum of compound 5

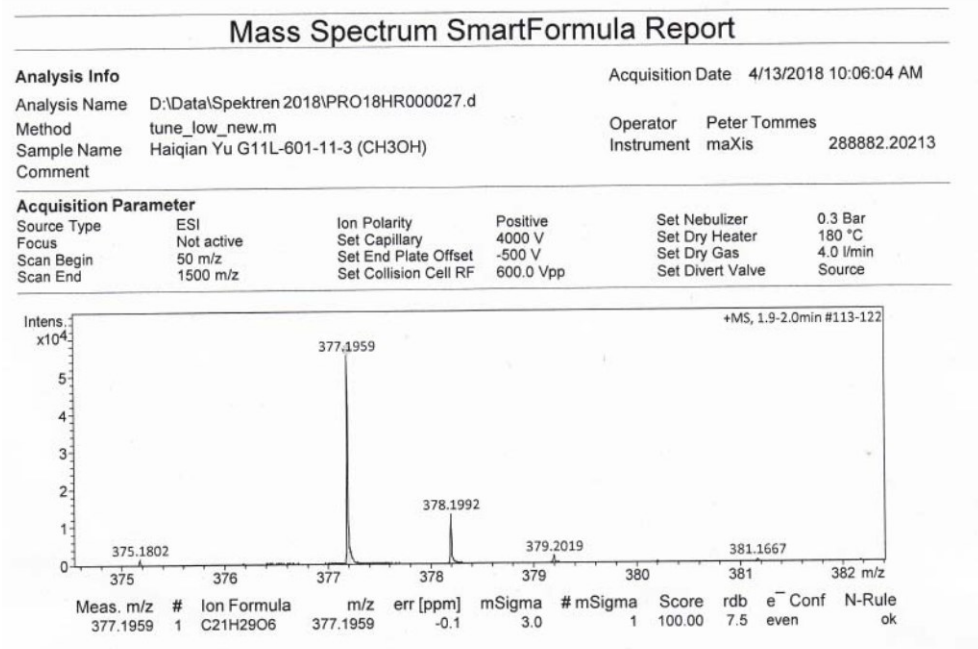

Mass Spectrum SmartFormula Report

Analysis Info

Analysis Name	D:\Data\Spektren 2018\PRO18HR000027.d	Acquisition Date	4/13/2018 10:06:04 AM
Method	tune_low_new.m	Operator	Peter Tommes
Sample Name	Haiqian Yu G11L-601-11-3 (CH3OH)	Instrument	maXis 288882.20213
Comment			

Acquisition Parameter

Source Type	ESI	Ion Polarity	Positive	Set Nebulizer	0.3 Bar
Focus	Not active	Set Capillary	4000 V	Set Dry Heater	180 °C
Scan Begin	50 m/z	Set End Plate Offset	-500 V	Set Dry Gas	4.0 l/min
Scan End	1500 m/z	Set Collision Cell RF	600.0 Vpp	Set Divert Valve	Source

Meas. m/z	#	Ion Formula	m/z	err [ppm]	mSigma	# mSigma	Score	rdb	e⁻ Conf	N-Rule
377.1959	1	C21H29O6	377.1959	-0.1	3.0	1	100.00	7.5	even	ok

Figure S41. The HRESIMS of compound 6

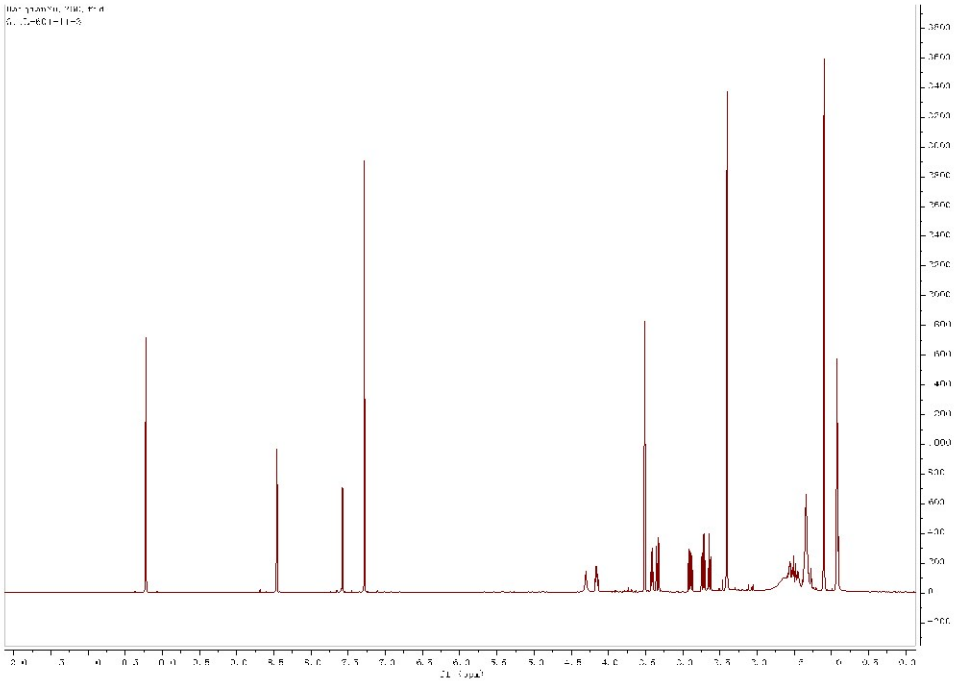

Figure S42. The ^{1}H NMR (600 MHz, $CDCl_3$) spectrum of compound 6

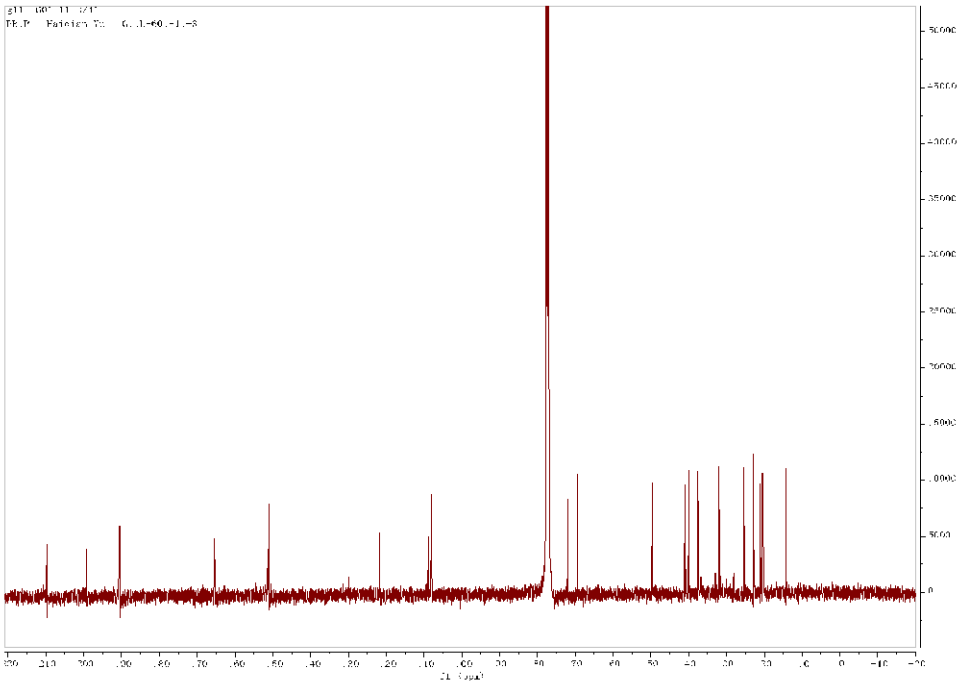

Figure S43. The ^{13}C NMR (150 MHz, $CDCl_3$) spectrum of compound 6

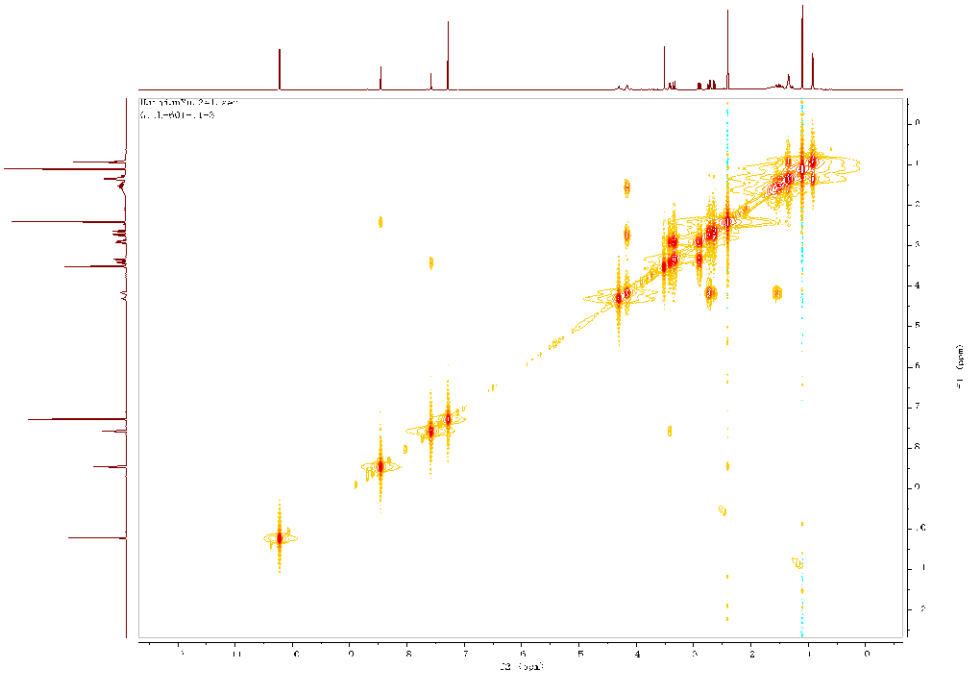

Figure S44. The COSY (600 MHz, $CDCl_3$) spectrum of compound 6

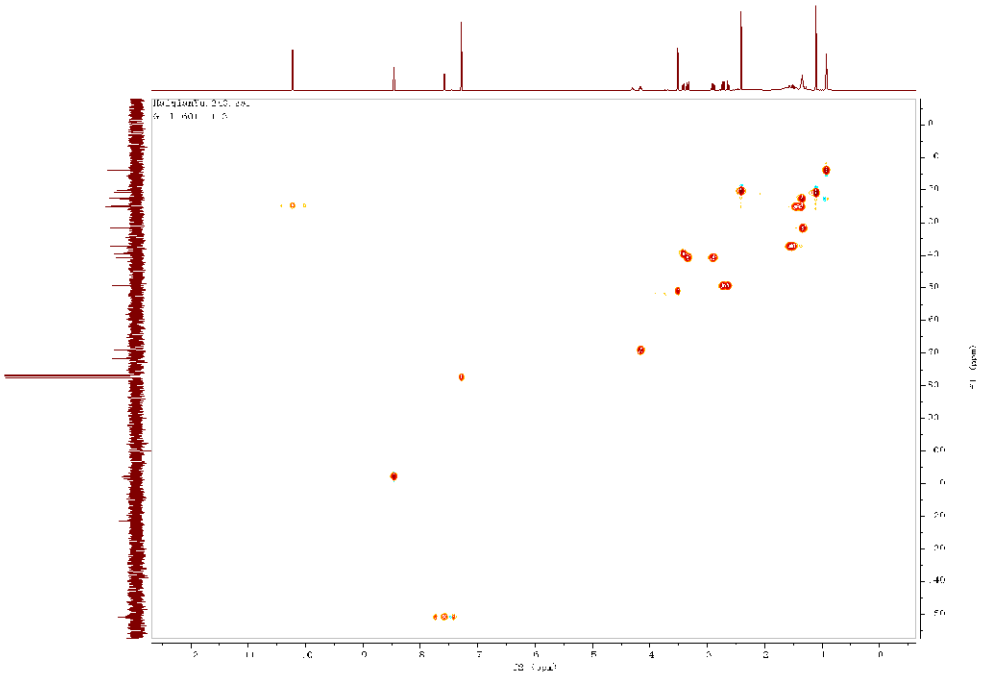

Figure S45. The HSQC (600 MHz, $CDCl_3$) spectrum of compound 6

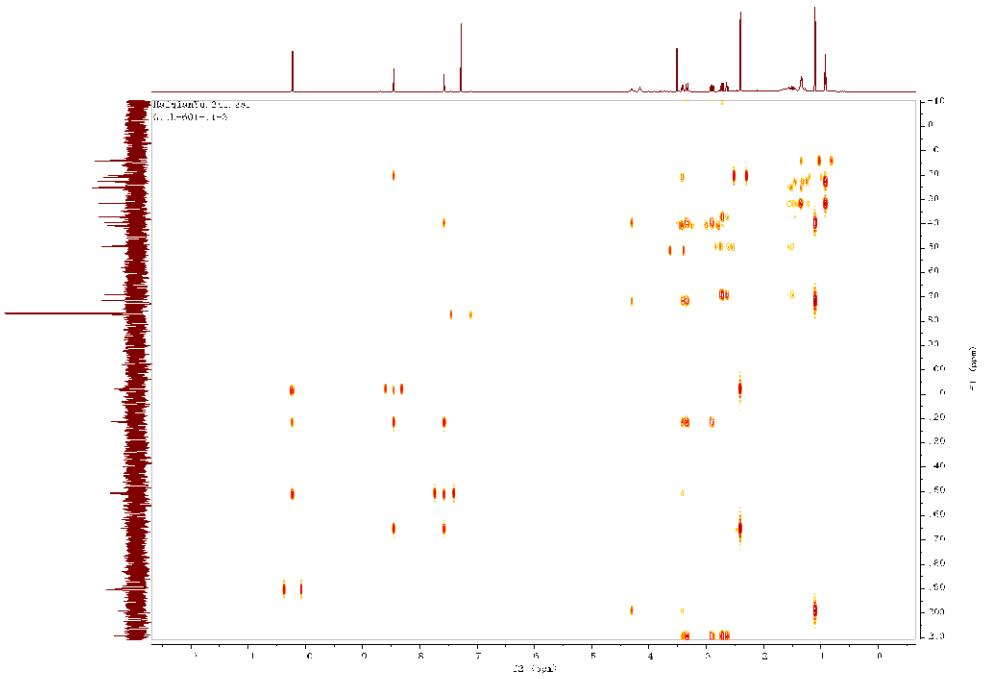

Figure S46. The HMBC (600 MHz, $CDCl_3$) spectrum of compound 6

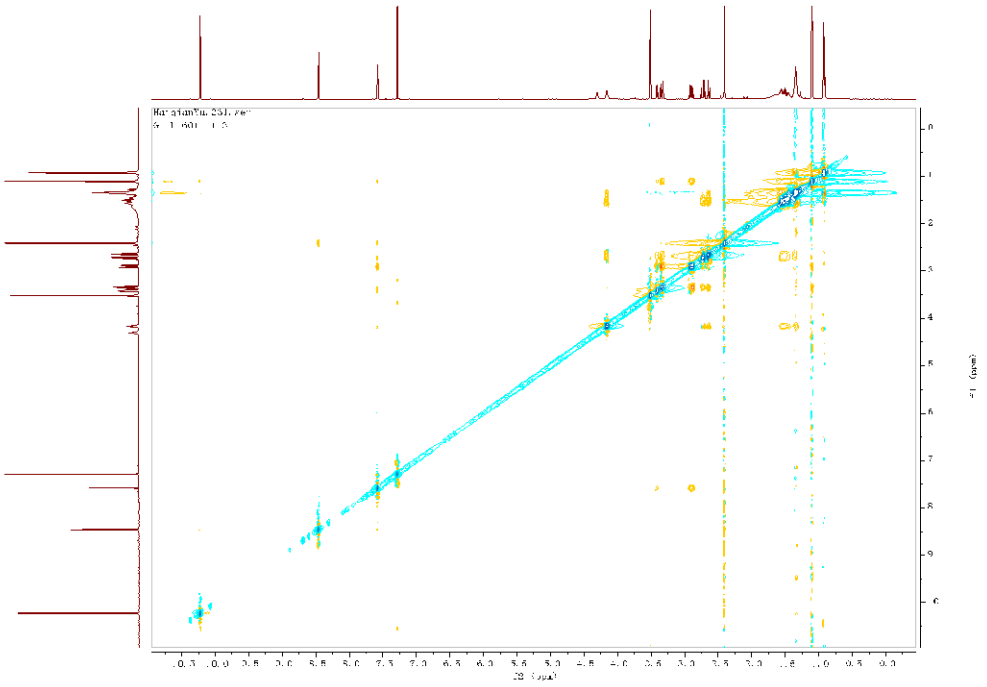

Figure S47. The ROESY (600 MHz, $CDCl_3$) spectrum of compound 6

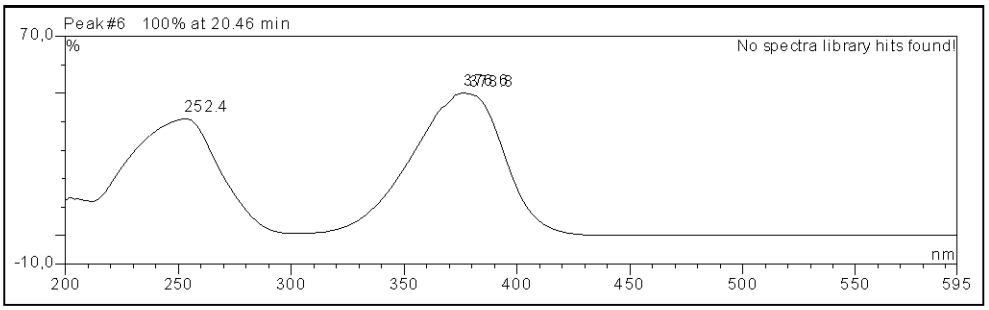

Figure S48. The UV spectrum of compound 6

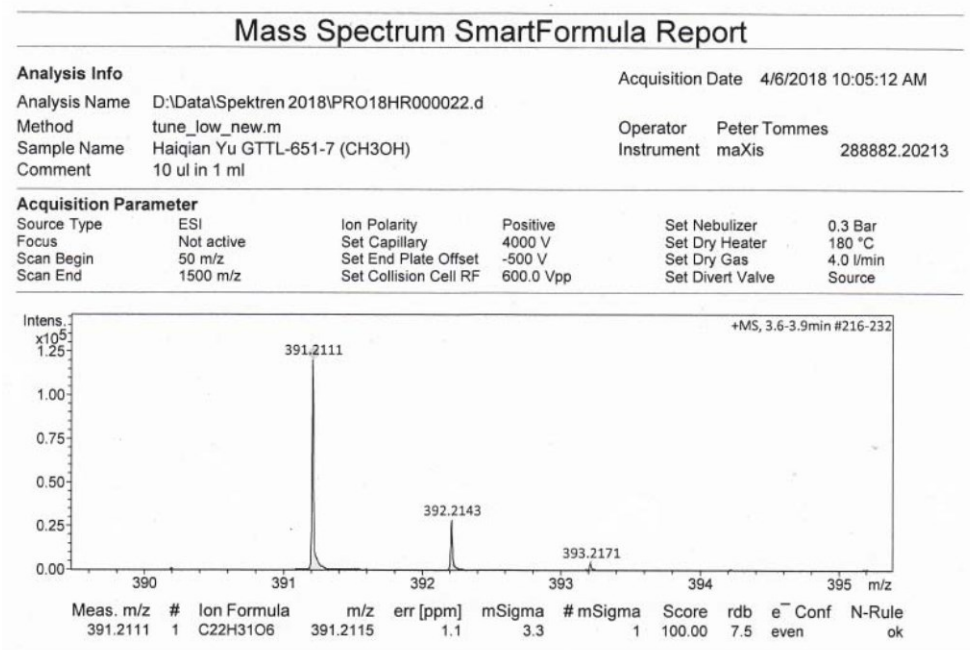

Figure S49. The HRESIMS of compound 7

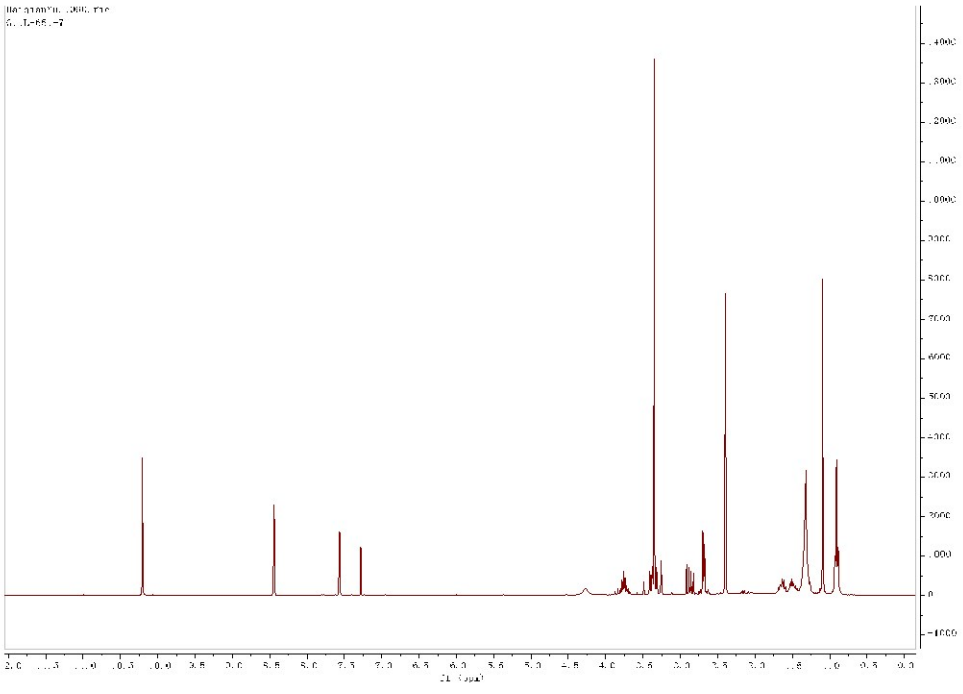

Figure S50. The ^{1}H NMR (300 MHz, $CDCl_3$) spectrum of compound 7

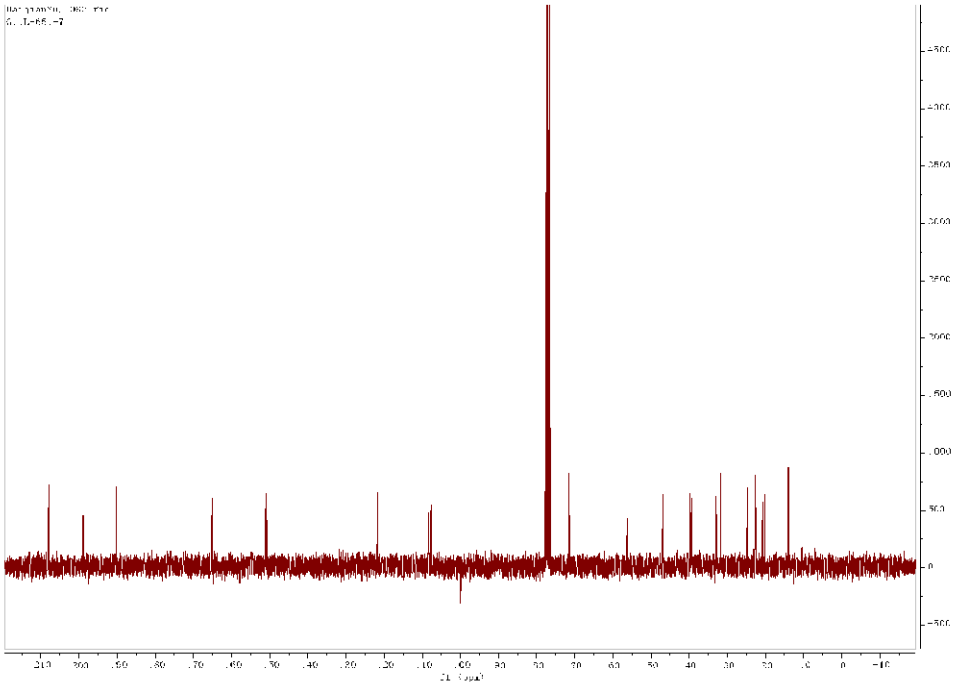

Figure S51. The ^{13}C NMR (75 MHz, $CDCl_3$) spectrum of compound 7

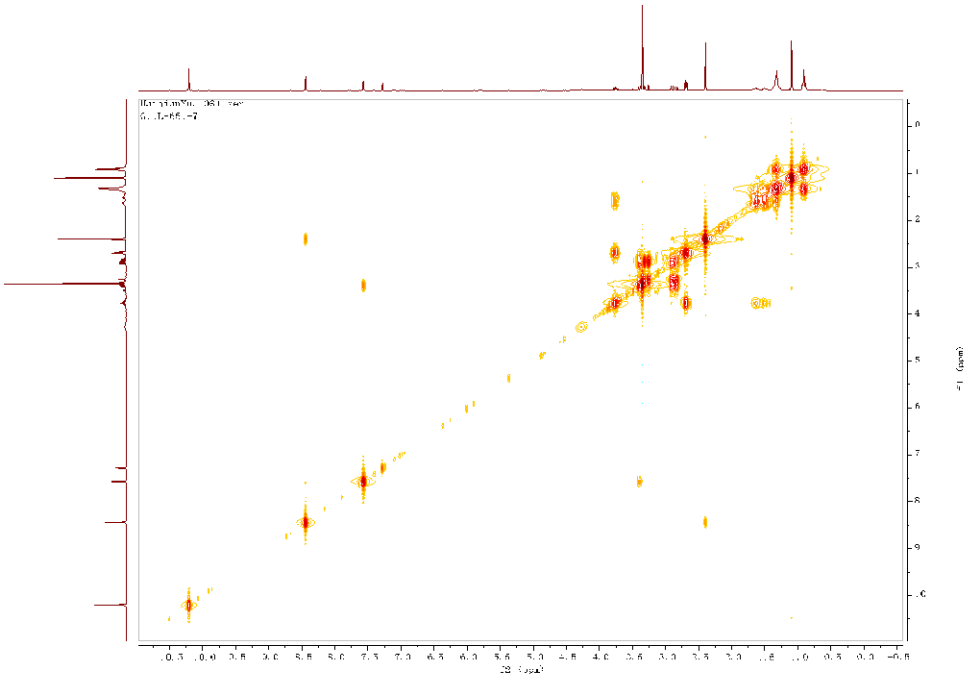

Figure S52. The COSY (300 MHz, $CDCl_3$) spectrum of compound 7

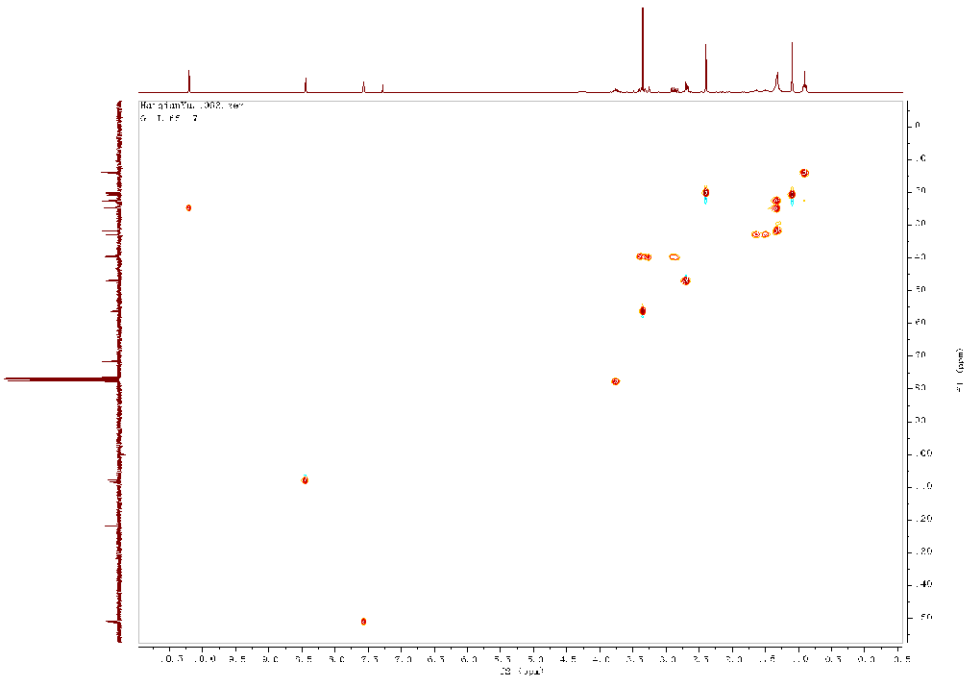

Figure S53. The HSQC (300 MHz, $CDCl_3$) spectrum of compound 7

Figure S54. The HMBC (300 MHz, $CDCl_3$) spectrum of compound 7

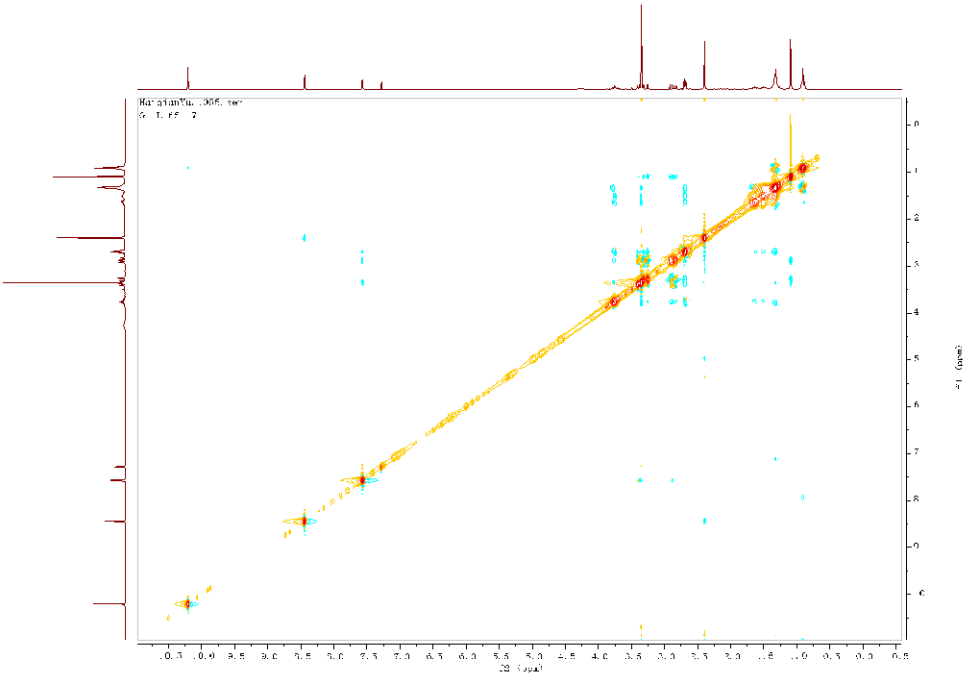

Figure S55. The ROESY (300 MHz, $CDCl_3$) spectrum of compound 7

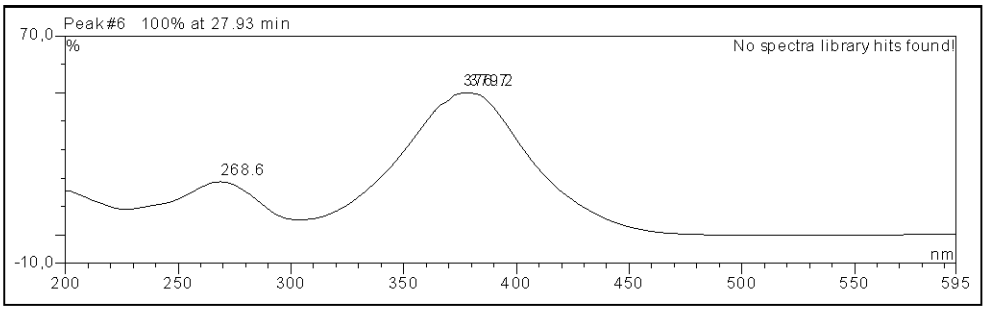

Figure S56. The UV spectrum of compound 7

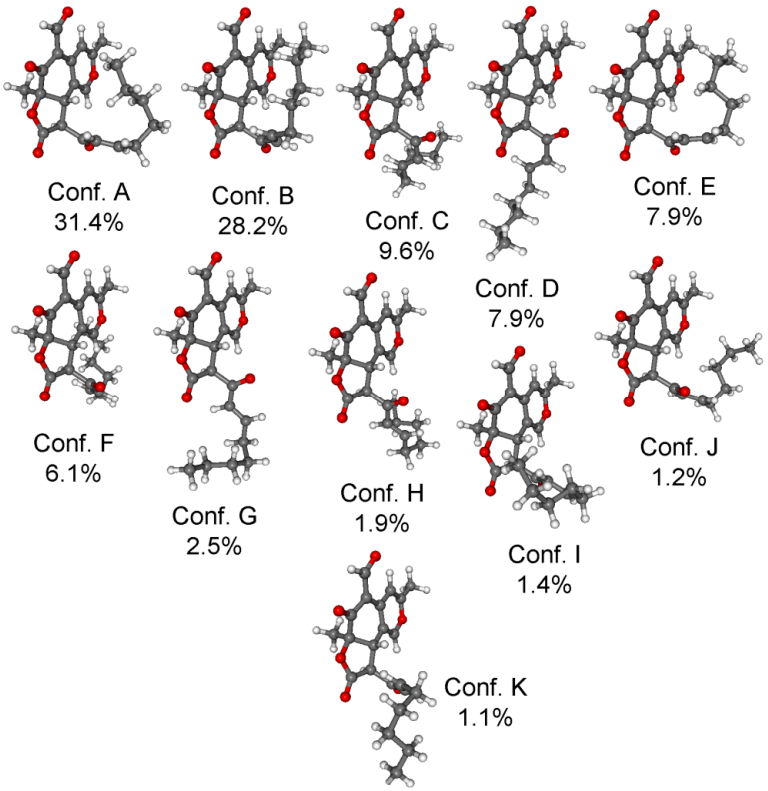

Figure S57. Structure and population of the low-energy B97D/TZVP PCM/MeCN conformers (> 1%) of (7*R*,8*S*,12*S*)-1.

Table S1. Boltzmann populations and optical rotations of the low-energy conformers of (7*R*,8*S*,12*S*)-1 computed at various levels for the B3LYP/6-31G(d) reoptimized MMFF conformers.

Conformer	Boltzmann population	B3LYP/TZVP	BH&HLYP/TZVP	PBE0/TZVP
Conf. A	69.86 %	438.48	409.24	437.21
Conf. B	21.11 %	176.36	161.57	182.60
Conf. C	8.46 %	319.58	328.65	324.36
Average	N/A	372.71	349.80	373.55

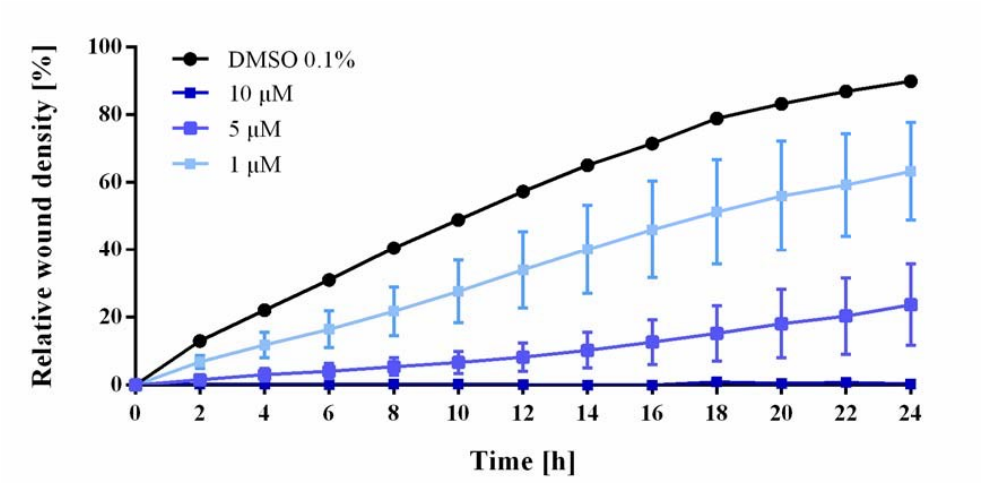

Figure S58. Time course of tumor cell migration. Cell migration in the presence of compound 1 was evaluated at concentrations 1, 5 and 10 µM. Images were taken every two hours for a time period of 24 hours. Data represent increasing relative wound density in percentage calculated with the IncuCyte ZOOM® software. Error bars show ±SEM.

A)

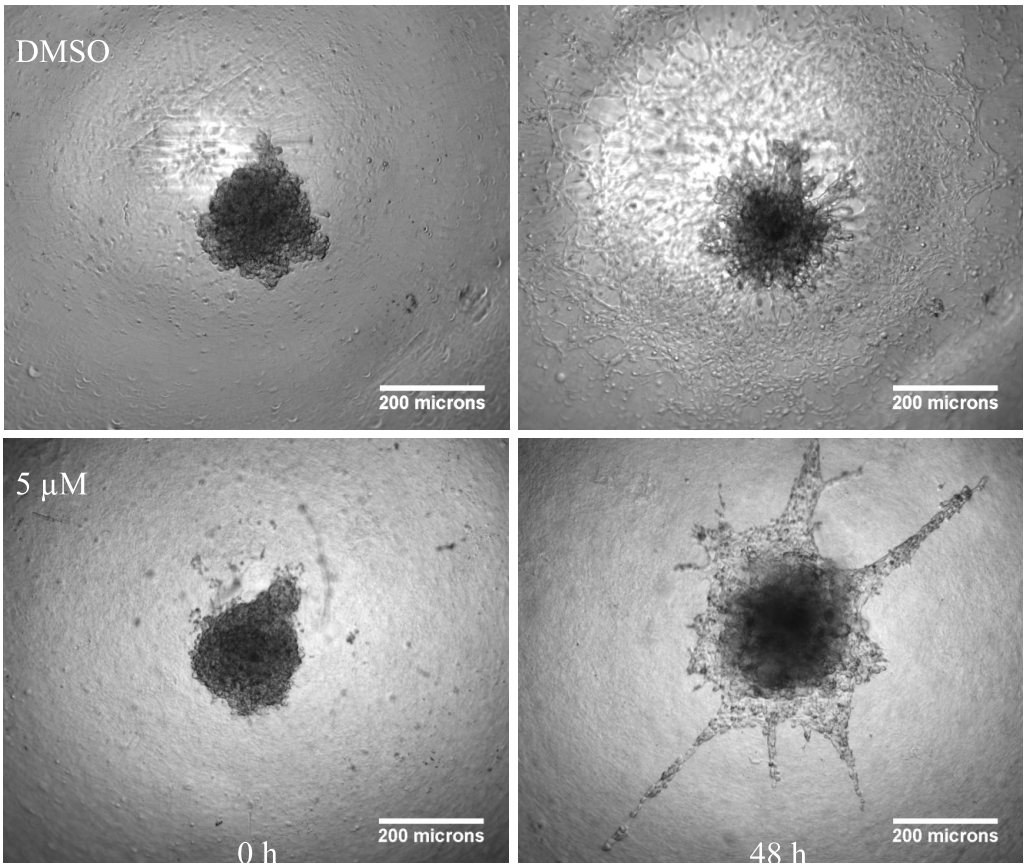

B)

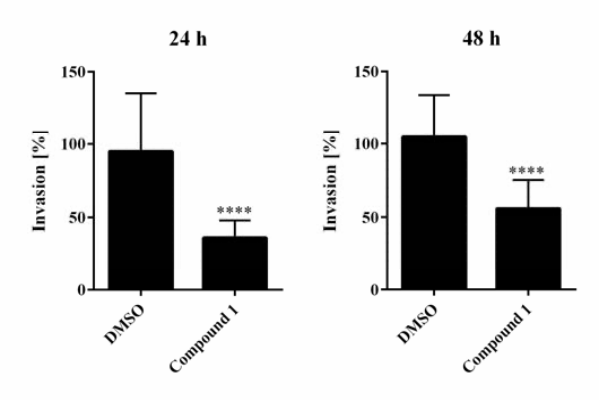

Figure S59. Compound 1 inhibits invasion into the 3D extracellular matrix. Representative images of invasion into matrigel are shown in A). Spheroids

were generated with 3,000 cells/well of MDA-MB-231 cells supplemented with 0.25 % matrigel in an ultra-low-attachment (ULA) plate. After 72 hours of spheroid formation, a mix of matrigel and collagen R solution (ratio of 1:1) was used for embedding the spheroids. Invasion of cells into the surrounding matrix was recorded every day for a time range of 48 hours and quantification of invasion was performed with ImageJ Fiji in B). Compound 1 was tested at 5 µM. Invasion, shown in percentage, was normalized to DMSO control at the specified time points. Error bars show ±SEM. Four stars represent a significance of p< 0.0001. Scale bars in white represent 200 µm in length.

3 Azaphilone pigments and macrodiolides from the coprophilous fungus *Coniella fragariae*

Published in: “Fitoterapia”

Contribution: first author, conducting most of the experiments, literature research, manuscript writing.

Fitoterapia 137 (2019) 104249

Contents lists available at ScienceDirect

Fitoterapia

journal homepage: www.elsevier.com/locate/fitote

Azaphilone pigments and macrodiolides from the coprophilous fungus *Coniella fragariae*

Haiqian Yu[a], Julia Sperlich[b], Simon-Patrick Höfert[c], Christoph Janiak[c], Nicole Teusch[b,d], Fabian Stuhldreier[e], Sebastian Wesselborg[e], Chenyin Wang[f], Matthias U. Kassack[f], Haofu Dai[g], Zhen Liu[a,*], Peter Proksch[a,*]

[a] Institute of Pharmaceutical Biology and Biotechnology, Heinrich-Heine-Universität Düsseldorf, Universitätsstrasse 1, 40225 Düsseldorf, Germany
[b] Bio-Pharmaceutical Chemistry and Molecular Pharmacology, Faculty of Applied Natural Sciences, Technische Hochschule Köln, Chempark, 51368 Leverkusen, Germany
[c] Institute of Inorganic and Structural Chemistry, Heinrich-Heine-Universität Düsseldorf, Universitätsstrasse 1, 40225 Düsseldorf, Germany
[d] Department of Biomedical Sciences, Faculty of Human Sciences, University of Osnabrueck, Barbarastrasse 22, 49076 Osnabrück, Germany
[e] Institute for Molecular Medicine I, Medical Faculty, Heinrich-Heine-Universität Düsseldorf, Universitätsstrasse 1, 40225 Düsseldorf, Germany
[f] Institute of Pharmaceutical and Medicinal Chemistry, Heinrich-Heine-Universität Düsseldorf, Universitätsstrasse 1, 40225 Düsseldorf, Germany
[g] Key Laboratory of Biology and Genetic Resources of Tropical Crops, Ministry of Agriculture, Institute of Tropical Bioscience and Biotechnology, Chinese Academy of Tropical Agricultural Sciences, Haikou 571101, China

ARTICLE INFO

Keywords:
Coniella fragariae
Azaphilones
Pyrenophorin
Cytotoxicity

ABSTRACT

Two azaphilone pigments (**1** and **2**), two dihydrobenzofurans (**3** and **4**), two macrodiolides (**5** and **6**), and a dimeric alkyl aromatic constituent (**7**) were isolated from the goose dung-derived fungus *Coniella fragariae*. Compounds **1–3** proved to be new natural products. Coniellins H and I (**1** and **2**) feature a tetracyclic core and an aldehyde group at C-5, which is unusual for azaphilone derivatives. The X-ray structure of pyrenophorin (**5**) is reported for the first time. Pyrenophorin (**5**) showed strong cytotoxicity against several cancer cell lines with IC_{50} values ranging from 0.07 to 7.8 μM.

1. Introduction

Secondary metabolites of fungi are known for their high structural diversity and pronounced biological activities [1]. Azaphilones as a large group of fungal pigments assembled via the polyketide pathway are found in numerous species of fungi including the genera *Penicillium, Aspergillus, Talaromyces, Chaetomium, and Monascus* [2,3]. The structures of azaphilones are based on a highly oxygenated pyranoquinone bi- or tri-cyclic core, which is responsible for their red or yellow colors [2,3]. Several azaphilones have been reported to show pronounced bioactivities. Peyronellone B exhibited a strong hypoxia-protective effect [4]. Penicilone B displayed potent antibacterial activity against two strains of methicillin-resistant *Staphylococcus aureus* with MIC values of 3.13 μg/mL [5]. *epi*-Isochromophilone II showed strong cytotoxicity against three renal carcinoma cell lines ACHN, 786-O and OS-RC-2 with IC_{50} values of 4.4, 3.0 and 3.9 μM [6].

In our previous study, a series of new azaphilones was isolated from the goose dung-derived fungus *Coniella fragariae* [7]. Fungi of the genus *Coniella* (syn. *Pilidiella* and *Schizoparme*) are generally known as plant-pathogenic fungi [8]. However, chemical investigations of these fungi have rarely been conducted. In continuation of our previous study on *C. fragariae*, we report now two new azaphilone pigments, coniellins H (**1**) and I (**2**), and a new dihydrobenzofuran, conielldihydrobenzofuran (**3**) as well as four known compounds including a further dihydrobenzofuran (**4**), two macrodiolides (**5** and **6**) and a dimeric alkyl aromatic constituent (**7**) (Fig. 1). The structure elucidation of the new compounds and their cytotoxic activities are discussed in this paper.

2. Results and discussion

The molecular formula of **1** was determined as $C_{23}H_{28}O_7$ based on the HRMS data, indicating 10 degrees of unsaturation. The ^{13}C NMR data of **1** (Table 1) combined with HSQC data indicated the presence of three carbonyls at δ_C 204.7 (C-13), 196.6 (C-6) and 191.1 (C-10), an ester carbonyl at δ_C 169.0 (C-21), and four olefinic carbons at δ_C 170.3 (C-3), 99.0 (C-4), 154.9 (C-4a) and 115.1 (C-5), accounting for 6 degrees of unsaturation. Thus, compound **1** was suggested to be a tetracyclic natural product. The HMBC correlations from Me-11 (δ_H 2.16) to C-3 and C-4, from H-4 (δ_H 7.24) to C-5, C-4a and C-8a, from H-10 (δ_H 10.06) to C-4a and C-5, from Me-9 (δ_H 1.35) to C-6, C-7 and C-8, from

* Corresponding authors.
E-mail address: zhenfeizi0@sina.com (Z. Liu).

https://doi.org/10.1016/j.fitote.2019.104249
Received 21 May 2019
Available online 25 June 2019
0367-326X/ © 2019 Elsevier B.V. All rights reserved.

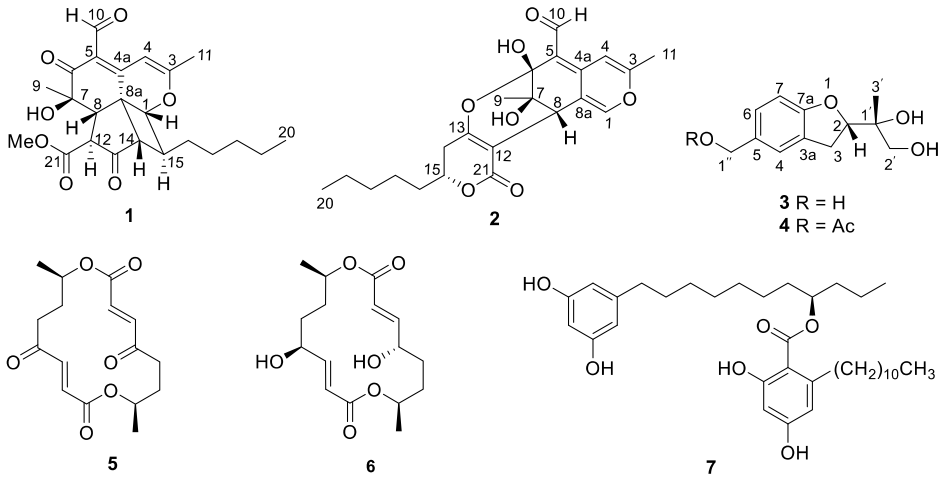

Fig. 1. Structures of isolated compounds.

Table 1
^{1}H and ^{13}C NMR Data of Compounds **1** and **2**.

Position	**1**[a]		**2**[b]	
	δ_C, type	δ_H, (J in Hz)	δ_C, type	δ_H, (J in Hz)
1	80.6, CH	4.86, d (4.8)	146.8, CH	7.47, s
3	170.3, C		160.9, C	
4	99.0, CH	7.24, s	101.2, CH	6.77, s
4a	154.9, C		147.8, C	
5	115.1, C		111.4, C	
6	196.6, C		104.1, C	
7	74.1, C		67.4, C	
8	50.5, CH	3.51, d (11.2)	39.3, CH	3.69, s
8a	42.0, C		121.6, C	
9	21.6, CH_3	1.35, s	19.3, CH_3	1.36, s
10	191.1, CH	10.06, s	188.5, CH	9.94, s
11	22.1, CH_3	2.16, s	20.0, CH_3	2.24, s
12	58.7, CH	3.13, dd (11.2, 1.2)	102.7, C	
13	204.7, C		164.6, C	
14	63.5, CH	3.00, dd (8.9, 1.2)	31.6, CH_2	2.46, ddd (17.0, 11.1, 1.3) 2.32, dd (17.0, 4.2)
15	43.3, CH	3.09, m	75.5, CH	4.25, m
16	28.4, CH_2	1.63, m 1.55, m	34.7, CH_2	1.75, m 1.57, m
17	25.9, CH_2	1.28, m	24.5, CH_2	1.45, m 1.34, m
18	31.5, CH_2	1.27, m	31.4, CH_2	1.27, m
19	22.4, CH_2	1.29, m	22.4, CH_2	1.29, m
20	14.0, CH_3	0.89, t (7.0)	13.9, CH_3	0.87, t (7.0)
21	169.0, C		166.0, C	
6-OH				9.01, s
21-OMe	53.3, CH_3	3.83, s		

[a] Recorded at 300 MHz (^{1}H) and 75 MHz (^{13}C) in $CDCl_3$.
[b] Recorded at 600 MHz (^{1}H) and 150 MHz (^{13}C) in $CDCl_3$.

H-8 (δ_H 3.51) to C-6, C-4a and C-1, and from H-1 (δ_H 4.86) to C-3 and C-8 indicated the presence of a pyranoquinone bicyclic ring, in which two methyl groups are attached to C-3 and C-7 and an aldehyde group is connected to C-5. A third cyclopentanone ring was established from the COSY correlation between H-8 and H-12 (δ_H 3.13) together with the HMBC correlations from H-12 to C-13, and from H-14 (δ_H 3.00) to C-13, C-8 and C-4a. The HMBC correlations from H-8, H-12 and a methoxy group (δ_H 3.83) to C-21 confirmed the attachment of a methoxycarbonyl group to C-12. The remaining signals accounted for a *n*-hexanyl side chain from C-15 to C-20 based on the COSY correlations

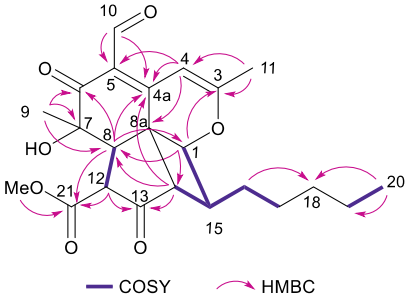

Fig. 2. COSY and key HMBC correlations of compound **1**.

between H-15/H_{ab}-16/H_{ab}-17 and between H_{ab}-19 and Me-20 as well as on the HMBC correlations from H_{ab}-16 to Me-18 and from Me-20 to C-18 and C-19. In addition, the COSY correlations between H-14/H-15/H-1 and the HMBC correlation from H-1 to C-14 indicated the presence of a fourth cyclobutane ring. Thus, the planar structure of **1** was elucidated as shown (Fig. 2), representing a new tetracyclic azaphilone derivative, for which the trivial name coniellin H is proposed.

The NOE correlations between H-14/H-1, H-1/H-8, H-8/H-14 suggested that these protons were proximate in space (Fig. 3). The large coupling constant (11.2 Hz) between H-8 and H-12 indicated that these two protons are oriented on the opposite sides of the cyclopentanone ring. In addition, the NOE correlations from Me-9 to both H-8 and H-12

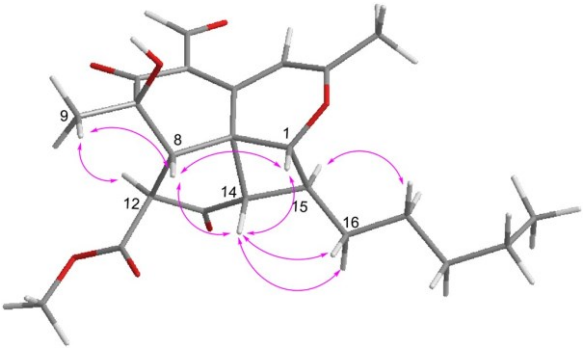

Fig. 3. Key ROESY correlations of compound **1**.

Table 2
^{1}H and ^{13}C NMR Data of Compound **3**.[a]

Position	δ_C, type	δ_H, (J in Hz)
2	85.7, CH	4.81, dd (9.6, 8.3)
3	30.2, CH_2	3.26, dd (16.0, 8.3) 3.20, dd (16.0, 9.6)
3a	127.4, C	
4	124.4, CH	7.21, d (1.8)
5	133.5, C	
6	127.5, CH	7.10, dd (8.1, 1.8)
7	109.0, CH	6.74, d (8.1)
7a	159.0, C	
1′	73.6, C	
2′	67.0, CH_2	3.78, d (11.0) 3.54, d (11.0)
3′	19.3, CH_3	1.20, s
1″	65.3, CH_2	4.60, s

[a] recorded at 600 MHz (^{1}H) and 150 MHz (^{13}C) in $CDCl_3$.

assigned Me-9 on the α-face of the cyclohexenone ring. Furthermore, H-14 exhibited NOE correlations to H_{ab}-16 whereas H-15 showed NOE correlations to H_{ab}-17, indicating opposite orientation between H-14 and H-15. The absolute configuration at C-7, C-8, and C-12 in **1** is suggested to be identical to that of the previously reported coniellin A (Fig. 8) based on the close biogenetic relationship of both compounds [7]. Thus, the stereochemistry of **1** was determined as shown.

Coniellin I (**2**) had the molecular formula $C_{22}H_{26}O_7$ as determined by the HRMS data, corresponding to ten degrees of unsaturation. The ^{1}H and ^{13}C NMR data of **2** (Table 2) were similar to those of **1**, suggesting structural similarity between both compounds. For instance, the correlations in the HMBC spectrum of **2** from Me-11 (δ_H 2.24) to C-3 and C-4, from H-4 (δ_H 6.77) to C-5 and C-8a, from H-10 (δ_H 9.94) to C-5 and C-6, from 6-OH (δ_H 9.01) to C-5, C-6 and C-7, from Me-9 (δ_H 1.36) to C-6, C-7 and C-8, from H-8 (δ_H 3.69) to C-4a, C-8a and C-1, and from H-1 (δ_H 7.47) to C-3, C-4a, C-8a and C-8 established a pyranoquinone bicyclic ring similar to that in **1** except for the presence of a double bond at C-1/C-8a and a hydroxy group at C-6 in **2**. A third α,β-unsaturated δ-lactone ring was deduced from the COSY correlation between H-15/H_{ab}-14 as well as from the HMBC correlations from H-8 to C-12, C-13 and C-21, from H_{ab}-14 to C-12 and C-13, and from H-15 to C-21. The COSY correlations between H-15/H_{ab}-16/H_{ab}-17/H_{ab}-18 and between H_{ab}-19 and Me-20 along with the HMBC correlations from Me-20 to C-18 and C-19 indicated the attachment of a *n*-pentanyl side chain at C-15. The above NMR data accounted for nine degrees of unsaturation, suggesting the presence of a fourth ring in **2**. Based on the chemical shifts of C-6 (δ_C 104.1) and C-13 (δ_C 164.6) and the molecular formula of **2**, an ether bridge between C-6 and C-13 was suggested. Thus, the planar structure of **2** was elucidated as shown (Fig. 4).

The relative configuration of **2** was determined by NOE correlations and coupling constants. In the ROESY spectrum, Me-19 exhibited

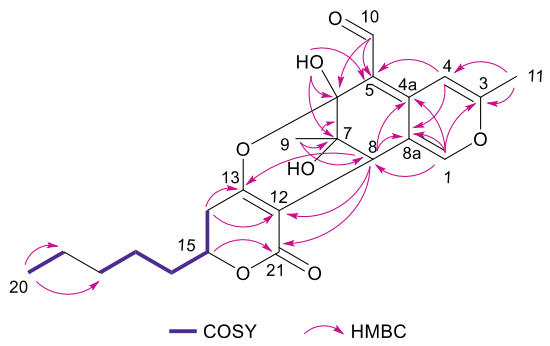

Fig. 4. COSY and key HMBC correlations of compound **2**.

correlations to 6-OH, H-8 and H_b-14 (δ_H 2.32), indicating that 6-OH and H-8 were on the same side and Me-9 was on the α-face of the cyclohexene ring whereas 7-OH was on the opposite side (Fig. 5). In addition, the NOE correlation from H-15 to H_b-14 and H_b-16 (δ_H 1.57) together with the coupling constants between H-15 to H_{ab}-14 ($^{2}J_{H\text{-}15/Ha\text{-}14}$ = 11.1 Hz, $^{2}J_{H\text{-}15/Hb\text{-}14}$ = 4.2 Hz) suggested that H-15 and H_b-14 were on the same side of the lactone ring whereas H_a-14 was on the opposite side. Based on the biogenetic relationship between **2** and coniellin A (Fig. 8), whose absolute configuration has been determined by ECD calculations [7], compound **2** is suggested to share the same absolute configuration at C-7 and C-8. Accordingly, the absolute configuration of **2** was assigned as 6*R*,7*R*,8*R*,15*R*.

The molecular formula of **3** was established as $C_{12}H_{16}O_4$, suggesting five degrees of unsaturation. The ^{13}C NMR spectrum of **3** (Table 2) showed six olefinic carbons at δ_C 127.4 (C-3a), 124.4 (C-4), 133.5 (C-5), 127.5 (C-6), 109.0 (C-7) and 159.0 (C-7a), three methylene groups at δ_C 30.2 (C-3), 67.0 (C-2′) and 65.3 (C-1″), an oxygenated methine at δ_C 85.7 (C-2), a non-protonated carbon at δ_C 73.6 (C-1′), at and a methyl group at δ_C 19.3 (C-3′). An ABX benzene ring system was detected at δ_H 7.21 (d, J = 1.8 Hz, 1H, H-4), 7.10 (dd, J = 8.1, 1.8 Hz, 1H, H-6), 6.74 (d, J = 8.1 Hz, 1H, H-7). A dihydrobenzofuran bicyclic core was established by the COSY correlations between H-2/H_{ab}-3, and H-6/H-7 in addition to the HMBC correlations from H-2 to H-7a, from H_{ab}-3 to C-3a and C-7a, from H-4 to C-3, C-6 and C-7a, from H-6 to C-4 and C-7a, and from H-7 to C-3a and C-5. Furthermore, the HMBC correlations from Me-3′ to C-2, C-1′ and C-2′, from H_{ab}-2′ to C-2, C-1′ and C-3′, and from H_{ab}-1″ to C-4, C-5 and C-6 indicated the attachment of a 1,2-dihydroxyisopropyl group and a hydroxymethyl group at C-2 and C-5, respectively. Thus, the planar structure of **3** was elucidated as shown (Fig. 6), for which the trivial name conielldihydrobenzofuran is proposed.

The absolute configuration of **3** was suggested to be (2*S*,1′*R*) by comparison of its ^{13}C NMR data and optical rotation (Table 3) with those of (2*R*,1′*S*)-, (2*S*,1′*R*)-, (2*R*,1′*R*)-, and (2*S*,1′*S*)-2,3-dihydro-2-(1′,2′-dihydroxy-1′-methylethyl)-6- methoxybenzofuran [9,10].

The four known compounds were identified as 5-(1″-acetyloxymethylene)-2-(1,2-dihydroxyisopropyl)-2,3-dihydrobenzofuran (**4**) [11], pyrenophorin (**5**) [12], pyrenophorol (**6**) [13], and 15-dehydroxyintegracin B (**7**) [14] based on their NMR and MS data as well as by comparison with the literature. Here, the absolute configuration of the C_2-symmetric ring in pyrenophorin (**5**) with *R*-configuration at C-6 and the symmetry-related C-6′ is reported for the first time using X-ray analysis (Fig. 7).

All isolated compounds (**1–7**) were tested for their cytotoxicity against the MDA-MB-231 human breast cancer cell line (Table 4). Only pyrenophorin (**5**) showed cytotoxicity with an IC_{50} value of 7.8 μM. Pyrenophorin (**5**) as well as the analogue pyrenophorol (**6**) were further tested against additional cell lines (Table 3). Pyrenophorin (**5**) showed significant cytotoxicity against A2780 *cis*-platin sensitive and *cis*-platin resistant cells, Ramos cells, and against Jurkat J16 cells with IC_{50} values of 0.5, 0.9, 0.6, and 0.07 μM, respectively. Pyrenophorol (**6**) in contrast was inactive. Comparison of the structures of pyrenophorin (**5**) and pyrenophorol (**6**) indicated the importance of the α,β-unsaturated ketone unit of **5** for cytotoxicity.

Coniellins H and I (**1** and **2**) feature a tetracyclic core and an aldehyde group at C-5, which is unusual for azaphilone derivatives. A proposed biosynthetic pathway is shown in Fig. 8. The azaphilone intermediate A is formed through esterification of a β-ketoacid (from the FAS pathway) to the polyketide chromophore (from the PKS pathway) followed by a C-8/C-12 Knoevenagel cyclization and reduction [15]. Hydrolysis of intermediate A gives the lactone ring-opened product B. From the intermediate B, coniellin H (**1**) is obtained by elimination of 15-OH, [2 + 2]cycloaddition and methylation. The second branch of the pathway from intermediate B to dihydropyrone C is suggested to be catalysed by type III PKS [16]. Then attack of OH-13 to the carbonyl at C-6 affords the hemiketal group of coniellin H (**2**).

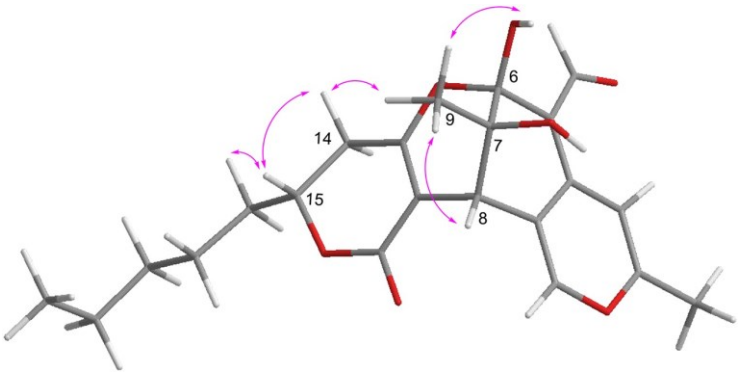

Fig. 5. Key ROESY correlations of compound **2**.

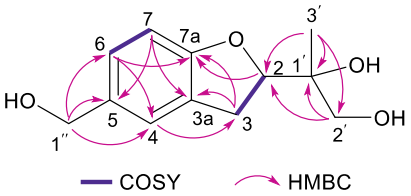

Fig. 6. COSY and key HMBC correlations of compound **3**.

Table 3
Comparison of ^{13}C NMR data in $CDCl_3$ and optical rotation in $CHCl_3$.

	3	2*R*,1′*S*	2*S*,1′*R*	2*R*,1′*R*	2*S*,1′*S*
C-2	85.7	86.13		88.60	
C-1′	73.6	73.76		73.17	
C-2′	67.0	66.96		68.73	
[α] in $CHCl_3$	+17	−27.6	+27.9	−21.2	+20.3

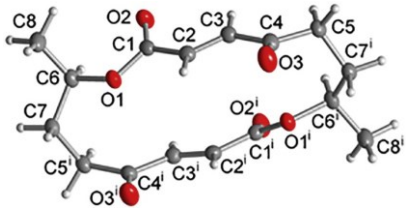

Fig. 7. Molecular structure of compound **5**; the ring lies on the special position around a twofold proper rotation axis (C_2) (symmetry code: $-x + 1$, $-y + 1$, z).

Table 4
Cytotoxity (IC_{50}, μM) of pyrenophorin (**5**) and pyrenophorol (**6**).

	MDA-MB-231	*cis*-platin sensitive A2780	*cis*-platin resistant A2780	Ramos	Jurkat J16
Pyrenophorin (**5**)	7.8	0.5	0.9	0.6	0.07
Pyrenophorol (**6**)	> 100	> 100	> 100	> 100	> 100
STS [a]	0.039	–	–	0.037	0.059
cDDP [b]	–	2.1	11.1	–	–

[a] Staurosporin as positive control.
[b] *cis*-Diammindichloridoplatin as positive control.

3. Experimental section

3.1. General experimental procedures

1D and 2D NMR spectra were recorded with Bruker Avance III 300 or 600 spectrometers. Mass spectra were obtained by a LC-MS HP1100 Agilent Finnigan LCQ Deca XP Thermoquest and HRESIMS data were recorded on a Bruker Daltonics UHR-QTOF Maxis 4G mass spectrometer. Optical rotations were measured with a JASCO P-2000 polarimeter. HPLC analysis was performed using a Dionex UltiMate-3400SD system coupled with a LPG-3400SD Pump, a photodiode array detector (DAD3000RS) and a Knauer Eurospher C_{18} analytical column (125 × 4 mm, 5 μm). Semi-preparative HPLC was performed with a Lachrom-Merck Hitachi system (UV detector L-7400, pump L-7100, 300 × 8 mm Knauer Eurospher-100 C_{18} column). Column chromatography was carried out using Sephadex LH-20, Merck MN Silica gel 60 M or LiChroprep RP-18 as stationary phases. Plates precoated with Merck silica gel F254 were used for TLC with detection under 254 and 365 nm followed by spraying with anisaldehyde reagent.

3.2. Identification, cultivation and isolation

In September 2016, goose (*Anser anser*) dung was collected at the North Sea coast close to Garding, Germany. The fungus was identified as *C. fragariae* (GenBank No. KJ710465.1) by DNA amplification and sequencing of its ITS region [17]. The fungus was fermented on rice medium in 50 Erlenmeyer flasks (each containing 100 g of rice and 110 mL of demineralized water, autoclaved at 121 °C for 20 min) for two weeks at 20 °C under static conditions. 500 mL EtOAc were added to each flask to terminate fermentation followed by shaking for 8 h at 150 rpm. 52 g EtOAc crude extract was divided into a *n*-hexane fraction and a MeOH fraction (27 g) by liquid-liquid separation. The MeOH fraction was separated by vacuum liquid chromatography on a RP-18 column (60 × 200 mm) using a solvent gradient (from 100% H_2O to 100% MeOH) to give seven fractions (Fr.1 to Fr.7). Compound **5** (100 mg) was obtained from Fr.1 (4.1 g) as needle crystals. The rest of Fr.1 was fractionated on a silica gel column (30 × 600 mm) eluted with a gradient of CH_2Cl_2 and MeOH (1:0 to 8:2) to give 6 subfractions (Fr.1.1 to Fr.1.6). Fr.1.2 was purified by semipreparative HPLC using 30% MeOH-H_2O to afford **6** (4.8 mg). Fr.1.5 was separated by semi-preparative HPLC using 25% MeOH-H_2O to give **3** (5.1 mg) and **4** (4.7 mg). Fr.2 (0.6 g) was subjected to a Sephadex LH-20 column (20 × 1000 mm) with MeOH as mobile phase, followed by separation using semipreparative HPLC to give **2** (5.8 mg). Fr.4 (0.9 g) was fractionated on a silica gel column (30 × 300 mm) with *n*-hexane and EtOAc as mobile phase to give three subtractions (Fr.4.1 to Fr.4.3). Fr.4.3 was separated by semipreparative HPLC using 50% MeOH-H_2O to afford **1** (5.0 mg). Fr.6 (2.6 g) was subjected to a silica column

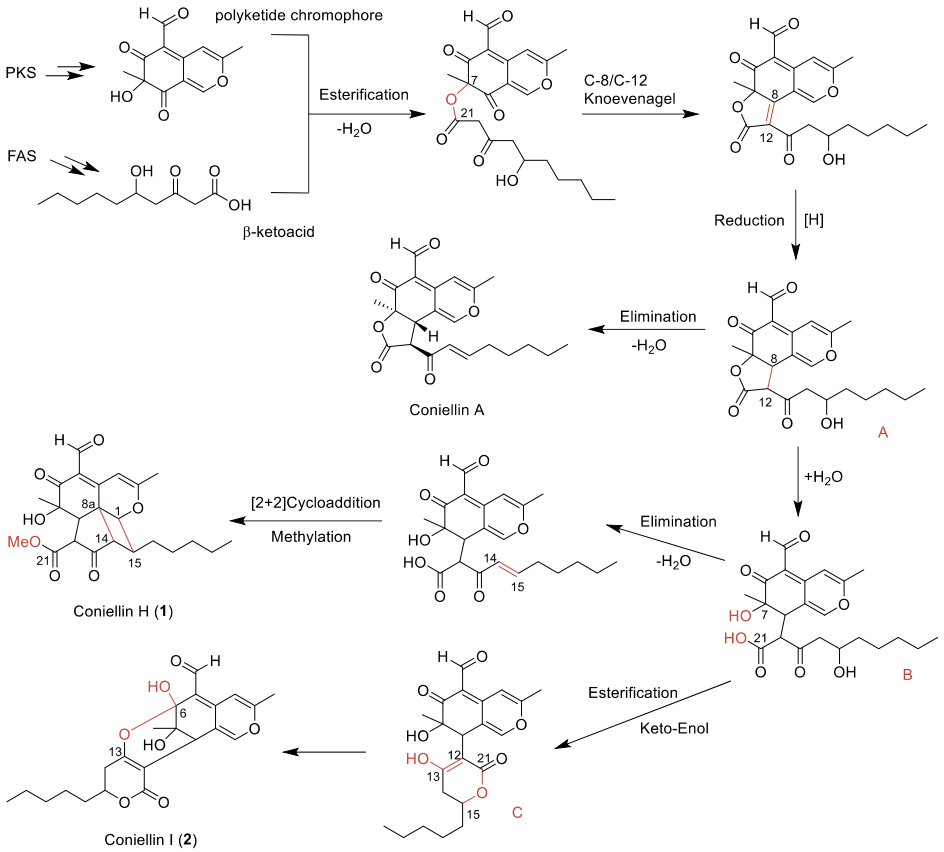

Fig. 8. Proposed biosynthetic pathway for compounds **1** and **2**.

(30 × 600 mm) using a gradient of *n*-hexane and EtOAc, followed by purification with semipreparative HPLC using 80% MeOH-H_2O to give **7** (3.2 mg).

Coniellin H (1): brown amorphous solid; [α]20*D* +413 (*c* 0.1, $CHCl_3$); UV (MeOH) λ_{max} 258, 384 nm; ^1H and ^{13}C NMR data, Table 1; HRESIMS *m/z* 417.1905 $[M + H]^+$ (calcd for $C_{23}H_{29}O_7$, 417.1908).

Coniellin I (2): brown amorphous solid; [α]20*D* -482 (*c* 0.1, $CHCl_3$); UV (MeOH) λ_{max} 259, 384 nm; ^1H and ^{13}C NMR data, Table 1; HRESIMS *m/z* 403.1794 $[M + H]^+$ (calcd for $C_{22}H_{27}O_7$, 403.1757).

Coniellidihydrobenzofuran (3): colorless powder; [α]20*D* +17 (*c* 0.1, $CHCl_3$); UV (MeOH) λ_{max} 230, 283 nm; ^1H and ^{13}C NMR data, Tables 2; HRESIMS *m/z* 247.0941 $[M + Na]^+$ (calcd for $C_{12}H_{16}NaO_4$, 247.0941).

3.3. X-ray crystallographic analysis of compound 5

Data Collection: compound **5** was measured with a Bruker Kappa APEX2 CCD diffractometer with a microfocus tube using Cu Kα radiation (λ = 0.71073 Å). For data collection APEX2, for cell refinement and data reduction SAINT [18], and for experimental absorption correction SADABS were used [19]. The structure was solved by intrinsic phasing using SHELXT [20]. refinement was done by full-matrix least-squares on F^2 using SHELXL-2016/6 [21]. The hydrogen atoms were positioned geometrically (with C-H = 0.95 Å for aromatic and aliphatic CH, 1.00 Å for tertiary CH, 0.99 Å for CH_2 and 0.98 Å for CH_3) and refined using riding models (AFIX 43, 13, 23, 137, respectively), with $U_{iso}(H) = 1.2U_{eq}$ (CH, CH_2) and 1.5 U_{eq} (CH_3).

The absolute structure of **5** was solved using anomalous dispersion from Cu Kα, resulting in a Flack parameter of x = 0.12 [4] using Parsons quotient method [22,23].

All graphics were drawn using DIAMOND [24]. The analyses of hydrogen bonds (inter- and intramolecular) as well as π-π and CH-π interactions were done using PLATON for Windows [25–28]. The structural data has been deposited in the Cambridge Crystallographic Data Center (CCDC No. 1914503).

Crystal Data of ***5****:* $C_{16}H_{20}O_6$, M = 308.32, orthorhombic system, space group $P2_12_12$, a = 9.8268(14) Å, b = 15.824(2) Å, c = 5.1127(7) Å, V = 795.0(2) Å^3, Z = 2, D_{calc} = 1.288 g/cm^3, crystal size 0.26 × 0.10 × 0.10 mm, μ(Cu Kα) = 0.82 mm^{-1}, 5.3° < θ < 66.5°, N_t = 5254, N = 1383 (R_{int} = 0.025), R_1 = 0.026, wR_2 = 0.067, S = 1.08, Flack parameter = 0.12(4).

3.4. Cytotoxicity assay

Cytotoxicity tests using the human breast cancer cell line MDAMB-231, the cisplatin sensitive and resistant human ovarian cancer cell line A2780, the adult lymphoblastic leukemia T cells Jurkat J16, or Burkitt's lymphoma B cells (Ramos) were carried out as described before [7,29].

Acknowledgment

P.P. and S.W. want to thank the DFG (GRK 2158) and the Manchot Foundation for support.

Appendix A. Supplementary data

Supplementary data to this article can be found online at https://doi.org/10.1016/j.fitote.2019.104249.

References

[1] G.F. Bills, J.B. Gloer, Biologically active secondary metabolites from the fungi, Microbiol. Spectrum 4 (2016) 1–32.
[2] N. Osmanova, W. Schultze, N. Ayoub, Azaphilones: a class of fungal metabolites with diverse biological activities, Phytochem. Rev. 9 (2010) 315–342.
[3] J.M. Gao, S.X. Yang, J.C. Qin, Azaphilones: chemistry and biology, Chem. Rev. 113 (2013) 4755–4811.
[4] T.X. Li, R.H. Liu, X.B. Wang, J. Luo, J.G. Luo, L.Y. Kong, M.H. Yang, Hypoxia-protective azaphilone adducts from *Peyronellaea glomerata*, J. Nat. Prod. 81 (2018) 1148–1153.
[5] W.X. Wang, S. Kusari, M. Spiteller, H. Laatsch, C. Golz, C. Strohmann, P. Kusari, O. Kayser, Antibacterial azaphilones from an endophytic fungus, *Colletotrichum* sp. BS4, J. Nat. Prod. 79 (2016) 704–710.
[6] X. Luo, X. Lin, H. Tao, J. Wang, J. Li, B. Yang, X. Zhou, Y. Liu, Isochromophilones A-F, cytotoxic chloroazaphilones from the marine mangrove endophytic fungus *Diaporthe* sp. SCSIO 41011, J. Nat. Prod. 81 (2018) 934–941.
[7] H. Yu, J. Sperlich, A. Mandi, T. Kurtan, H. Dai, N. Teusch, Z.Y. Guo, K. Zou, Z. Liu, P. Proksch, Azaphilone derivatives from the fungus *Coniella fragariae* inhibit NF-κB activation and reduce tumor cell migration, J. Nat. Prod. 81 (2018) 2493–2500.
[8] L.V. Alvarez, J.Z. Groenewald, P.W. Crous, Revising the *Schizoparmaceae*: *Coniella* and its synonyms *Pilidiella* and *Schizoparme*, Stud. Mycol. 85 (2016) 1–34.
[9] R. Tovar-Miranda, R. Cortes-Garcia, N.F. Santos-Sanchez, P. Joseph-Nathan, Isolation, total synthesis, and relative stereochemistry of a dihydrofurocoumarin from *Dorstenia contrajerva*, J. Nat. Prod. 61 (1998) 1216–1220.
[10] R. Tovar-Miranda, R. Cortes-Garcia, P. Joseph-Nathan, Synthesis and absolute configuration of the four possible stereoisomers of prandiol, Tetrahedron Asymmetry 13 (2002) 1147–1152.
[11] J.H. Ding, T. Feng, Z.H. Li, L. Li, J.K. Liu, Twelve new compounds from the basidiomycete *Boreostereum vibrans*, Nat. Prod. Bioprospect. 2 (2012) 200–205.
[12] M.A. Kastanias, M. Chrysayi-Tokousbalides, Bioactivity of the fungal metabolite (8*R*,16*R*)-(−)-pyrenophorin on graminaceous plants, J. Agric. Food Chem. 53 (2005) 5943–5947.
[13] W. Zhang, K. Krohn, H. Egold, S. Draeger, B. Schulz, Diversity of antimicrobial pyrenophorol derivatives from an endophytic fungus, *Phoma* sp, Eur. J. Org. Chem. (2008) 4320–4328.
[14] H.L. Liu, X.Y. Huang, J. Li, G.R. Xin, Y.W. Guo, Absolute configurations of integracins A, B, and 15′-dehydroxy-integracin B, Chirality 24 (2012) 459–462.
[15] W. Chen, R. Chen, Q. Liu, Y. He, K. He, X. Ding, L. Kang, X. Guo, N. Xie, Y. Zhou, Y. Lu, R.J. Cox, I. Molnar, M. Li, Y. Shao, F. Chen, Orange, red, yellow: biosynthesis of azaphilone pigments in *Monascus* fungi, Chem. Sci. 8 (2017) 4917–4925.
[16] T. Aizawa, S.Y. Kim, S. Takahashi, M. Koshita, M. Tani, Y. Futamura, H. Osada, N. Funa, Alkyldihydropyrones, new polyketides synthesized by a type III polyketide synthase from *Streptomyces reveromyceticus*, J. Antibiot. 67 (2014) 819–823.
[17] J. Kjer, A. Debbab, A.H. Aly, P. Proksch, Methods for isolation of marine-derived endophytic fungi and their bioactive secondary products, Nat. Protoc. 5 (2010) 479–490.
[18] Apex2, Data Collection Program for the CCD Area-detector System; SAINT, Data Reduction and Frame Integration Program for the CCD Area-detector System, Bruker Analytical X-ray Systems, Madison, WI, USA, 1997–2012.
[19] G.M. Sheldrick, SADABS: Area-Detector Absorption Correction, University of Goettingen, Germany, 1996.
[20] G.M. Sheldrick, SHELXT - integrated space-group and crystal-structure determination, Acta Crystallogr. A. 71 (2015) 3–8.
[21] G.M. Sheldrick, Crystal structure refinement with SHELXL, Acta Crystallogr. C. 71 (2015) 3–8.
[22] H.D. Flack, G. Bernardinelli, Absolute structure and absolute configuration, Acta Crystallogr. A. 55 (1999) 908–915.
[23] H.D. Flack, On enantiomorph-polarity estimation, Acta Crystallogr. A. 39 (1983) 876–881.
[24] K. Brandenburg, Diamond (Version 3.2), Crystal and Molecular Structure Visualization, Bonn, Germany (2009).
[25] A.L. Spek, Structure validation in chemical crystallography, Acta Crystallogr. D. 65 (2009) 148–155.
[26] A.L. Spek, Single-crystal structure validation with the program PLATON, J. Appl. Crystallogr. 36 (2003) 7–13.
[27] A.L. Spek, PLATON - a Multipurpose Crystallographic Tool, Utrecht University, Utrecht, The Netherlands, 2008.
[28] L.J. Farrugia, Windows Implementation, Version 40608, University of Glasgow, Scotland, 2008.
[29] A. Mokhlesi, F. Stuhldreier, K.W. Wex, A. Berscheid, R. Hartmann, N. Rehberg, P. Sureechatchaiyan, C. Chaidir, M.U. Kassack, R. Kalscheuer, H. Brötz-Oesterhelt, S. Wesselborg, B. Stork, G. Daletos, P. Proksch, Cyclic cystine-bridged peptides from the marine sponge *Clathria basilana* induce apoptosis in tumor cells and depolarize the bacterial cytoplasmic membrane, J. Nat. Prod. 80 (2017) 2941–2952.

Supporting Information

Azaphilone pigments and macrodiolides from the coprophilous fungus *Coniella fragariae*

Haiqian Yu [a], Julia Sperlich [b], Simon-Patrick Höfert [c], Christoph Janiak [c], Nicole Teusch [b,d], Fabian Stuhldreier [e], Sebastian Wesselborg [e], Chenyin Wang [f], Matthias U. Kassack [f], Haofu Dai [g], Zhen Liu [a,*], Peter Proksch [a,*]

[a]Institute of Pharmaceutical Biology and Biotechnology, Heinrich-Heine-Universität Düsseldorf, Universitätsstrasse 1, 40225 Düsseldorf, Germany

[b]Bio-Pharmaceutical Chemistry and Molecular Pharmacology, Faculty of Applied Natural Sciences, Technische Hochschule Köln, Chempark, 51368 Leverkusen, Germany

[c]Institute of Inorganic and Structural Chemistry, Heinrich-Heine-Universität Düsseldorf, Universitätsstrasse 1, 40225 Düsseldorf, Germany

[d]Department of Biomedical Sciences, Faculty of Human Sciences, University of Osnabrueck, Barbarastrasse 22, 49076 Osnabrück, Germany

[e]Institute for Molecular Medicine I, Medical Faculty, Heinrich-Heine-Universität Düsseldorf, Universitätsstrasse 1, 40225 Düsseldorf, Germany

[f]Institute of Pharmaceutical and Medicinal Chemistry, Heinrich-Heine-Universität Düsseldorf, Universitätsstrasse 1, 40225 Düsseldorf, Germany

[g]Key Laboratory of Biology and Genetic Resources of Tropical Crops, Ministry of Agriculture, Institute of Tropical Bioscience and Biotechnology, Chinese Academy of Tropical Agricultural Sciences, Haikou 571101, China

Table of Contents

Figure S1. The HRESIMS of compound **1**·····3
Figure S2. The ^{1}H NMR (300 MHz, $CDCl_3$) spectrum of compound **1**·····3
Figure S3. The ^{13}C NMR (75 MHz, $CDCl_3$) spectrum of compound **1**·····4
Figure S4. The COSY (300 MHz, $CDCl_3$) spectrum of compound **1**·····4
Figure S5. The HSQC (300 MHz, $CDCl_3$) spectrum of compound **1**·····5
Figure S6. The HMBC (300 MHz, $CDCl_3$) spectrum of compound **1**·····5
Figure S7. The ROESY (300 MHz, $CDCl_3$) spectrum of compound **1** ·····6
Figure S8. The UV spectrum of compound **1**·····6
Figure S9. The HRESIMS of compound **2**·····7
Figure S10. The ^{1}H NMR (600 MHz, $CDCl_3$) spectrum of compound **2**·····7
Figure S11. The ^{13}C NMR (150 MHz, $CDCl_3$) spectrum of compound **2**·····8
Figure S12. The COSY (600 MHz, $CDCl_3$) spectrum of compound **2** ·····8
Figure S13. The HSQC (600 MHz, $CDCl_3$) spectrum of compound **2** ·····9
Figure S14. The HMBC (600 MHz, $CDCl_3$) spectrum of compound **2** ·····9
Figure S15. The ROESY (600 MHz, $CDCl_3$) spectrum of compound **2**·····10
Figure S16. The UV spectrum of compound **2**·····10
Figure S17. The HRESIMS of compound **3** ·····11
Figure S18. The ^{1}H NMR (600 MHz, $CDCl_3$) spectrum of compound **3**·····11
Figure S19. The ^{13}C NMR (150 MHz, $CDCl_3$) spectrum of compound **3**·····12
Figure S20. The COSY (600 MHz, $CDCl_3$) spectrum of compound **3** ·····12
Figure S21. The HSQC (600 MHz, $CDCl_3$) spectrum of compound **3** ·····13
Figure S22. The HMBC (600 MHz, $CDCl_3$) spectrum of compound **3** ·····13
Figure S23. The UV spectrum of compound **3**·····14

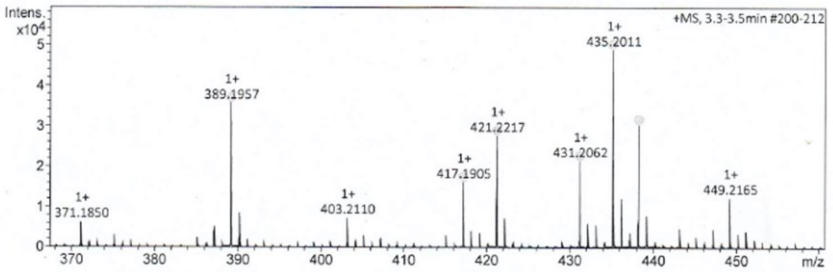

Meas. m/z	#	Ion Formula	m/z	err [ppm]	mSigma	# mSigma	Score	rdb	e¯ Conf	N-Rule
389.1957	1	C22H29O6	389.1959	0.4	7.8	1	100.00	8.5	even	ok
417.1905	1	C23H29O7	417.1908	0.7	102.4	1	100.00	9.5	even	ok
	2	C22H26N4NaO3	417.1897	-1.9	106.9	2	62.33	11.5	even	ok
421.2217	1	C23H33O7	421.2221	0.9	10.3	1	100.00	7.5	even	ok
	2	C22H30N4NaO3	421.2210	-1.7	12.8	2	80.61	9.5	even	ok
431.2062	1	C24H31O7	431.2064	0.6	23.2	1	100.00	9.5	even	ok
	2	C23H28N4NaO3	431.2054	-1.9	27.3	2	69.23	11.5	even	ok
435.2011	1	C23H31O8	435.2013	0.5	13.1	1	100.00	8.5	even	ok
	2	C22H28N4NaO4	435.2003	-2.0	19.2	2	48.15	10.5	even	ok
	3	C23H24N8Na	435.2016	1.1	26.2	3	50.18	15.5	even	ok
438.2483	1	C23H36NO7	438.2486	0.7	3.7	1	100.00	6.5	even	ok
	2	C22H33N5NaO3	438.2476	-1.8	6.9	2	74.55	8.5	even	ok

Figure S1. The HRESIMS of compound **1**

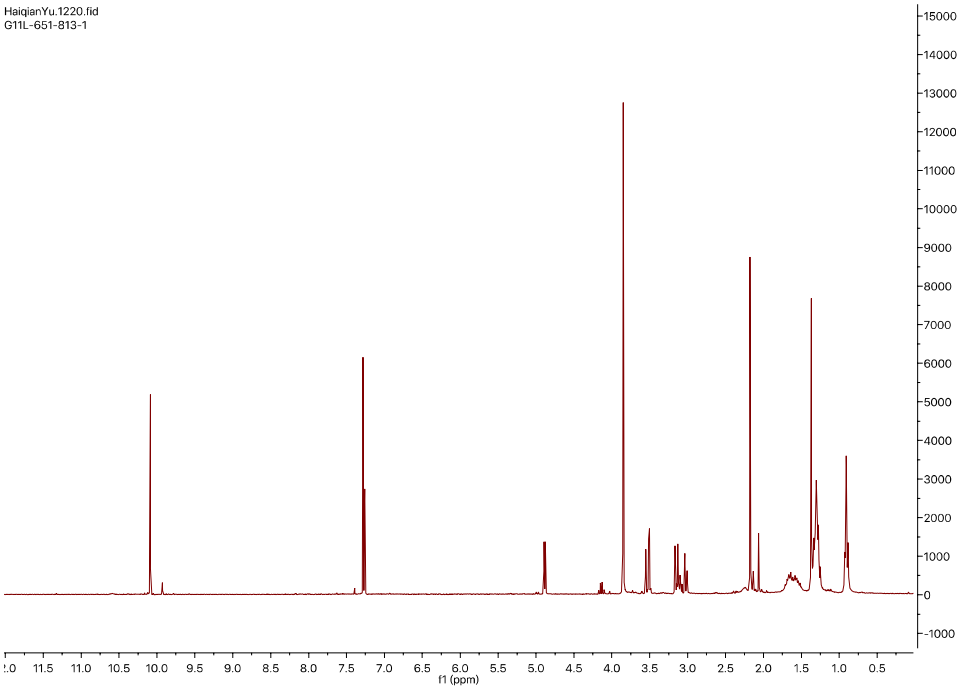

Figure S2. The ^{1}H NMR (300 MHz, $CDCl_3$) spectrum of compound **1**

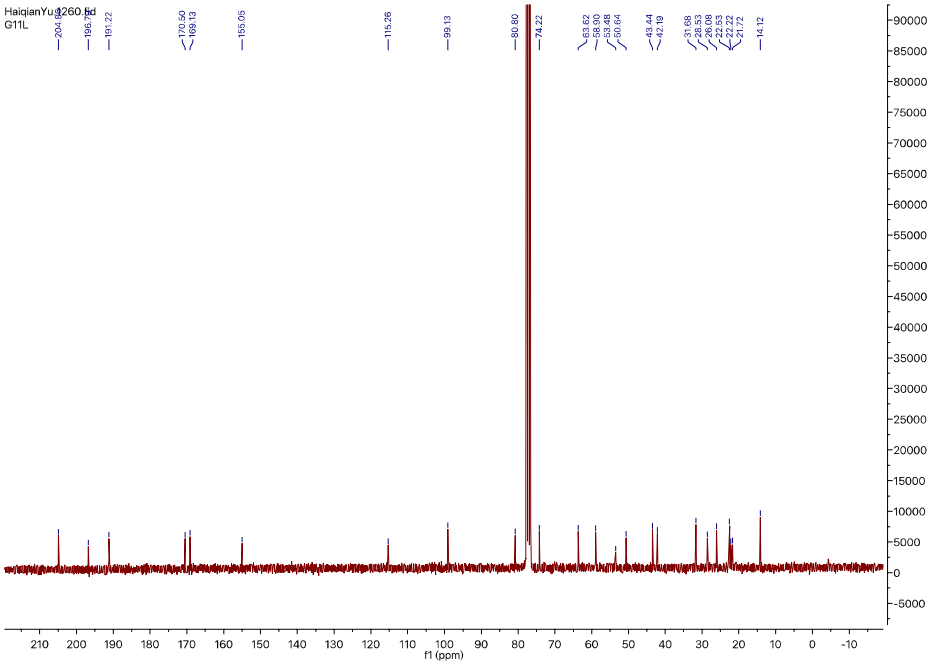

Figure S3. The ^{13}C NMR (75 MHz, $CDCl_3$) spectrum of compound **1**

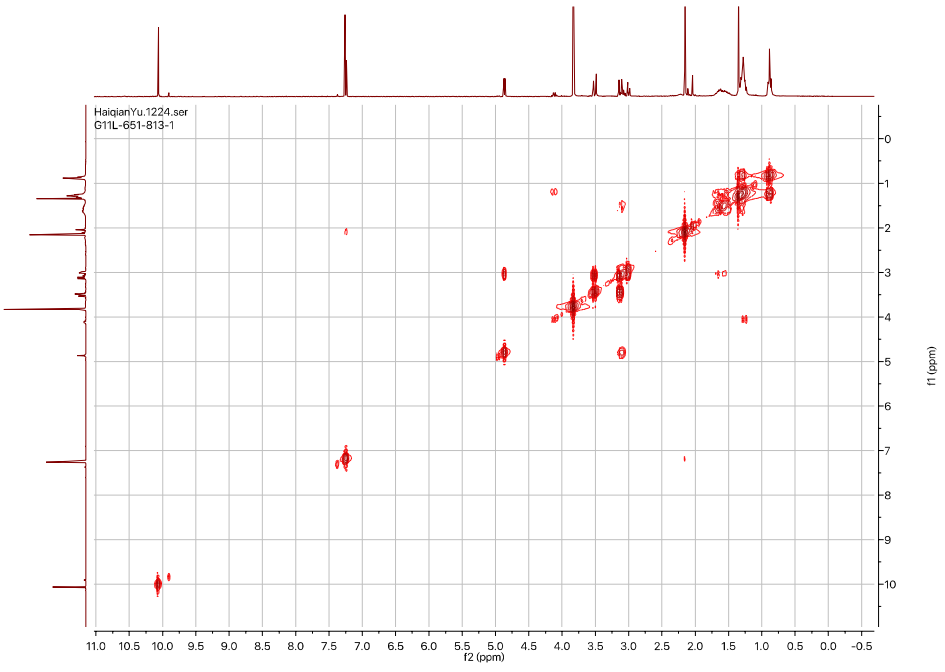

Figure S4. The COSY (300 MHz, $CDCl_3$) spectrum of compound **1**

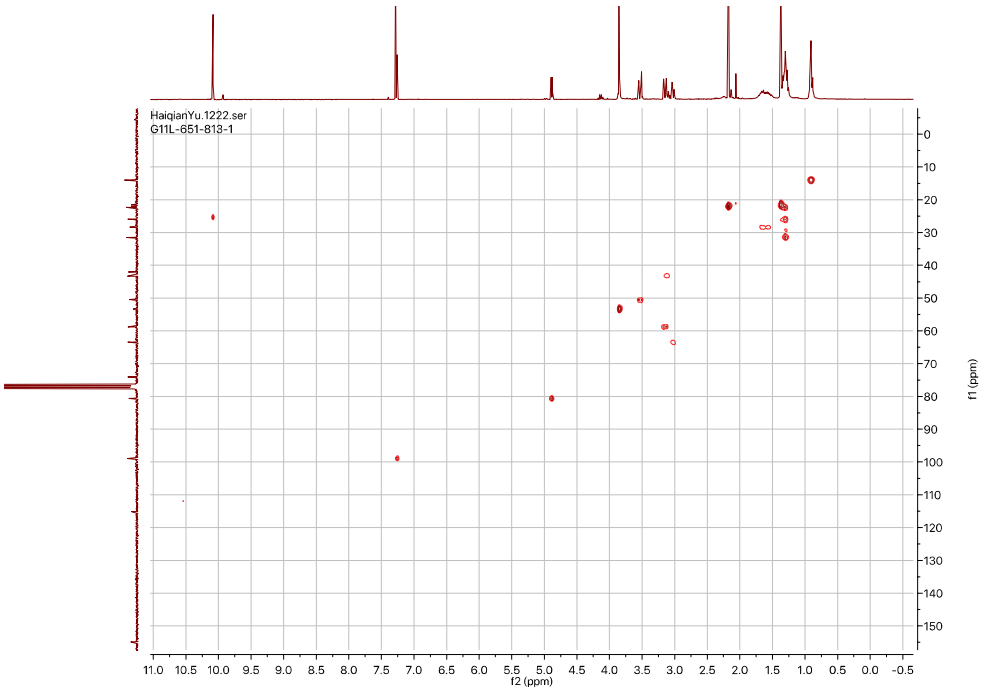

Figure S5. The HSQC (300 MHz, $CDCl_3$) spectrum of compound **1**

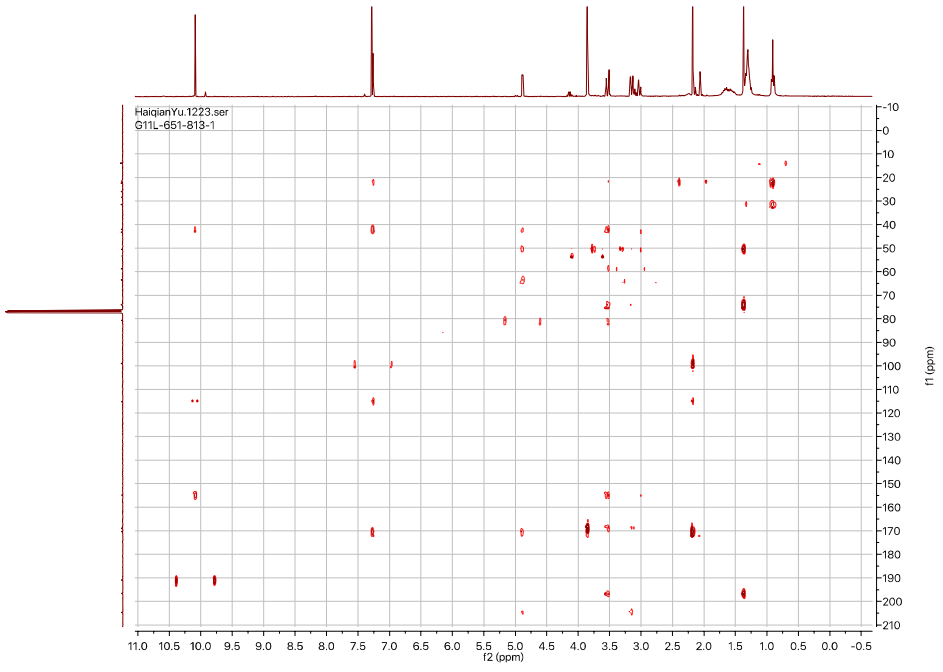

Figure S6. The HMBC (300 MHz, $CDCl_3$) spectrum of compound **1**

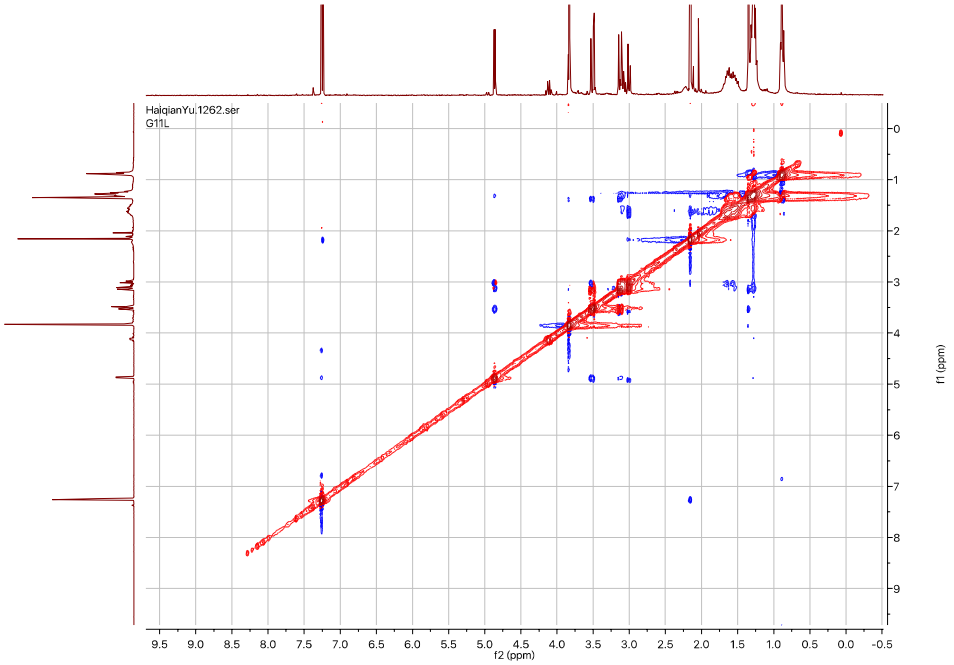

Figure S7. The ROESY (300 MHz, $CDCl_3$) spectrum of compound **1**

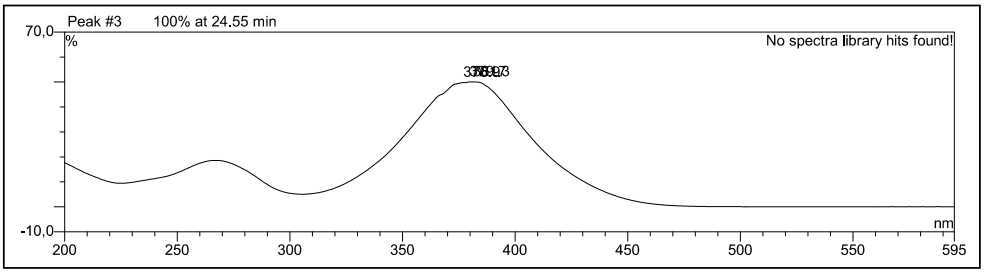

Figure S8. The UV spectrum of compound **1**

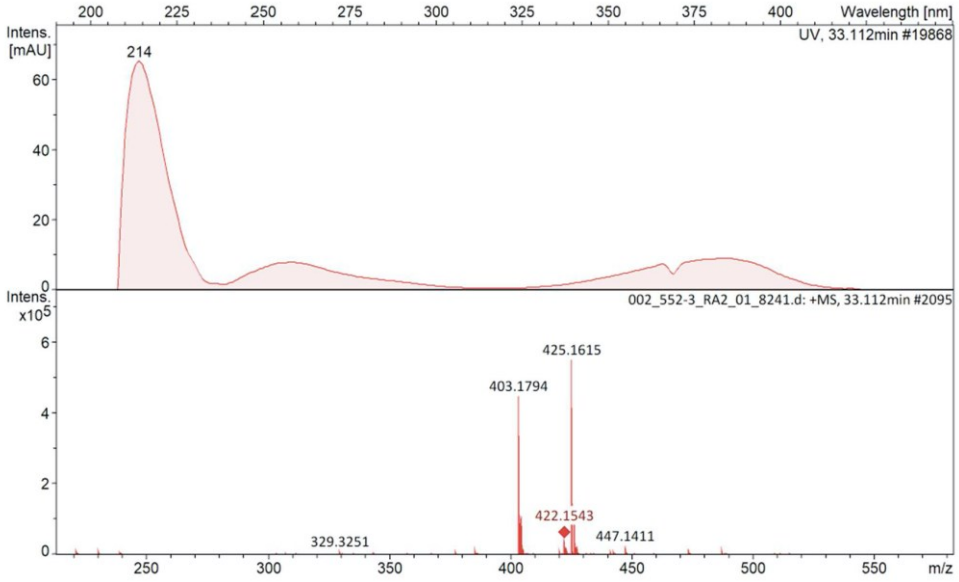

Figure S9. The HRESIMS of compound **2**

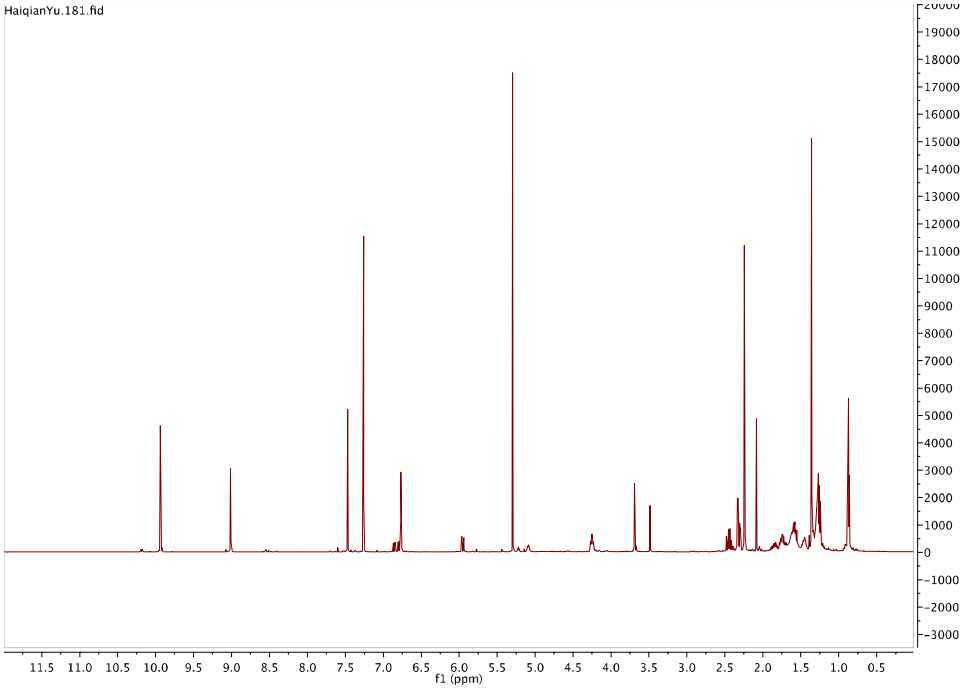

Figure S10. The ^{1}H NMR (600 MHz, $CDCl_3$) spectrum of compound **2**

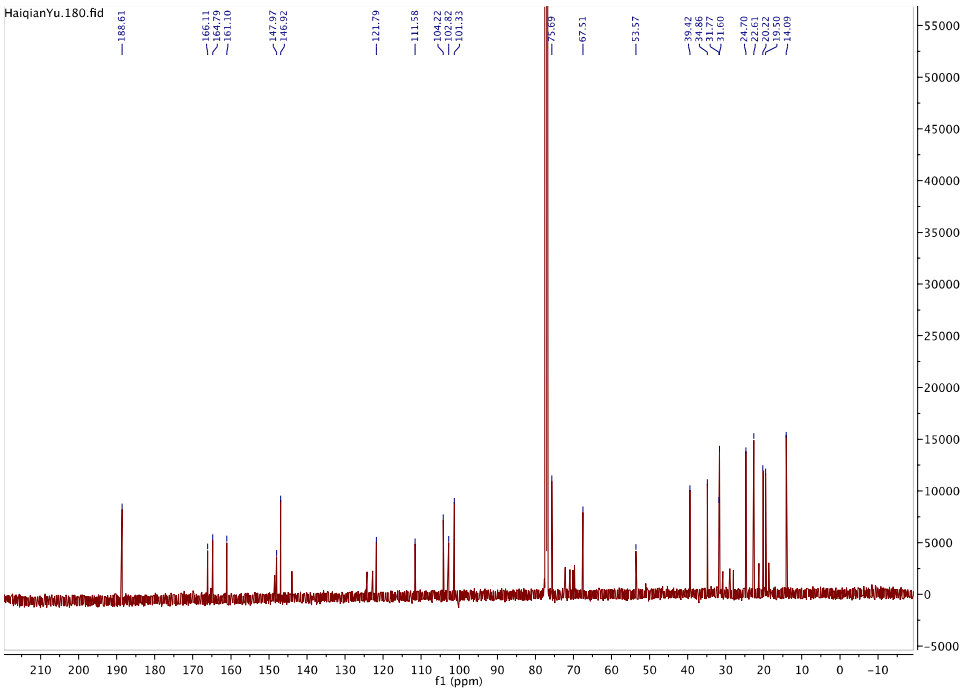

Figure S11. The ^{13}C NMR (150 MHz, $CDCl_3$) spectrum of compound **2**

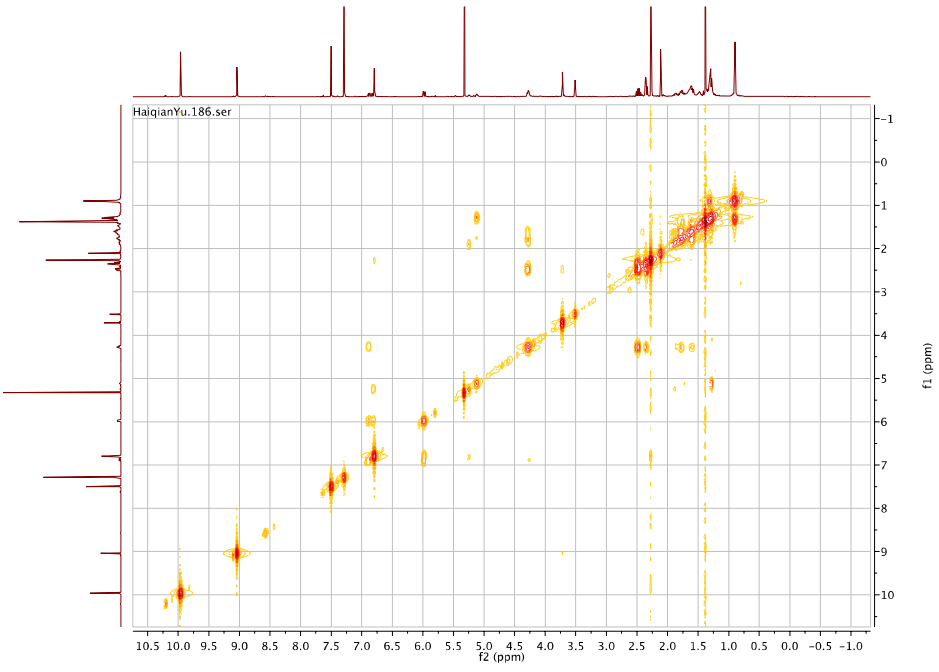

Figure S12. The COSY (600 MHz, $CDCl_3$) spectrum of compound **2**

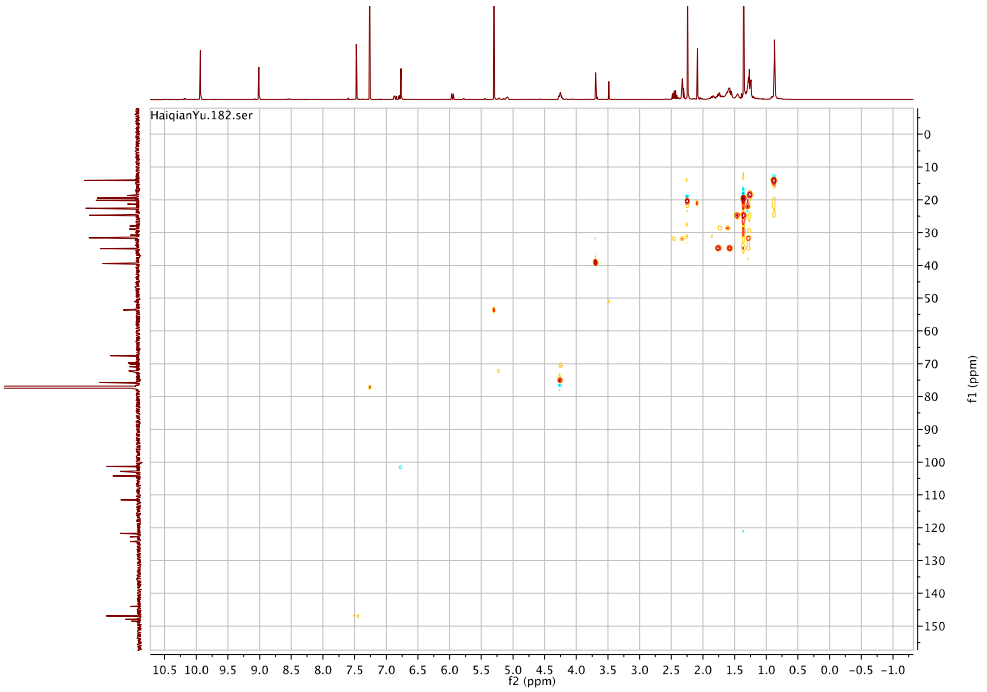

Figure S13. The HSQC (600 MHz, $CDCl_3$) spectrum of compound **2**

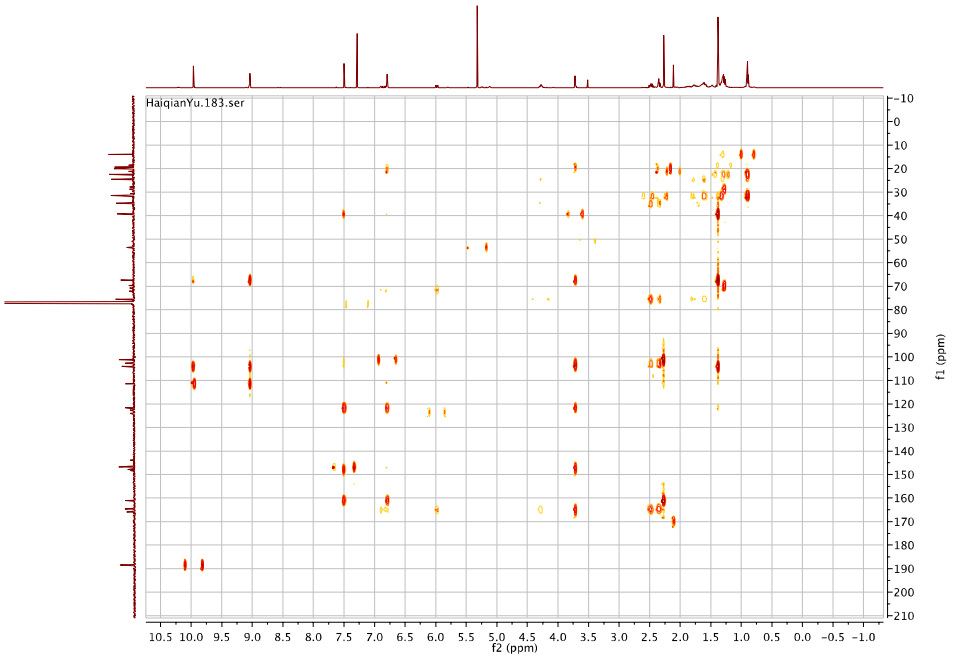

Figure S14. The HMBC (600 MHz, $CDCl_3$) spectrum of compound **2**

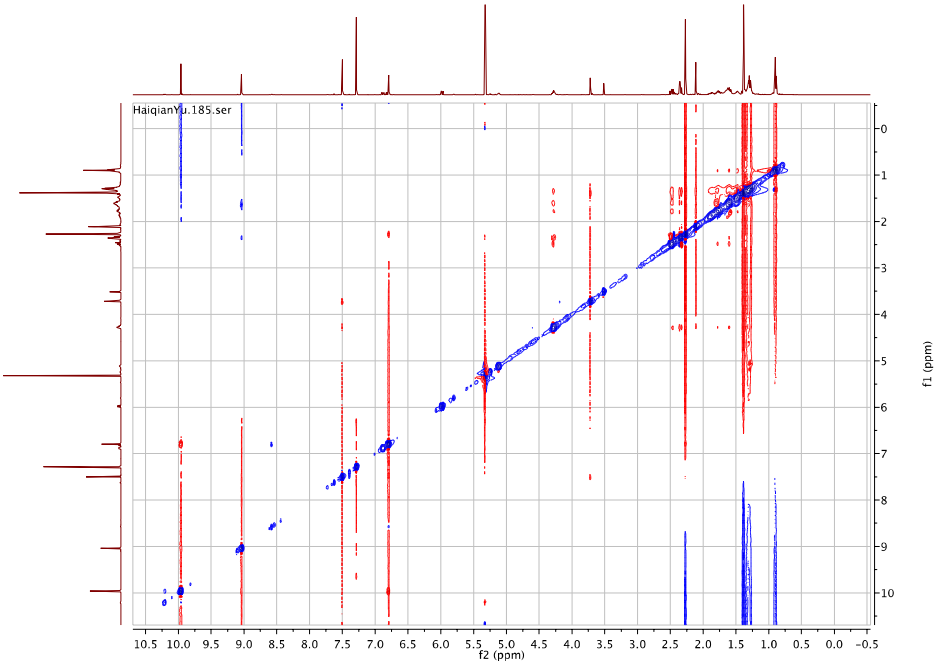

Figure S15. The ROESY (600 MHz, $CDCl_3$) spectrum of compound **2**

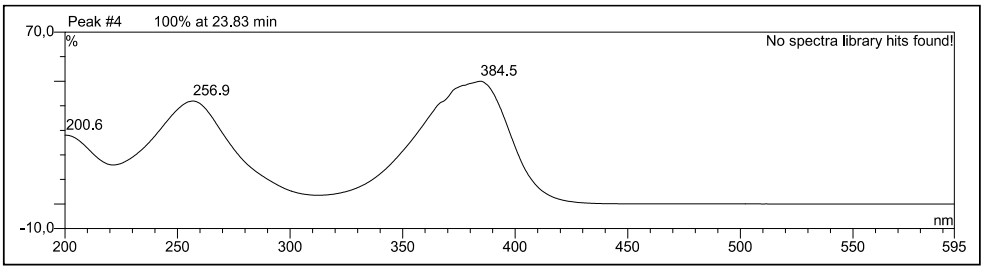

Figure S16. The UV spectrum of compound **2**

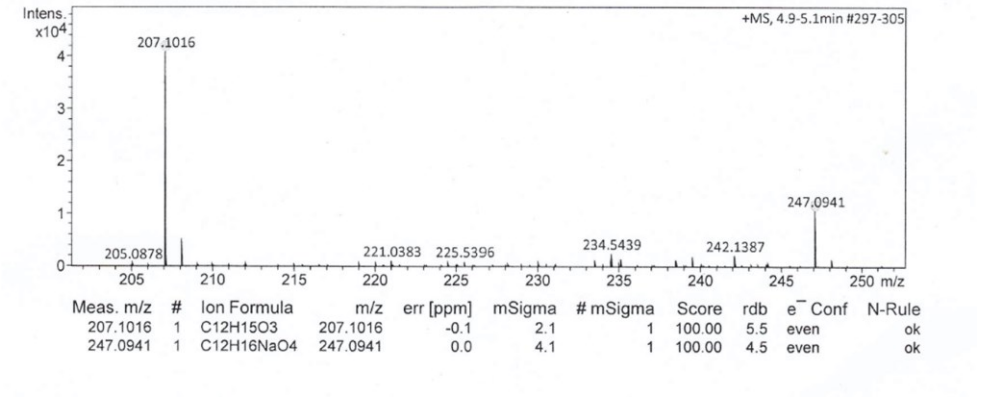

Meas. m/z	#	Ion Formula	m/z	err [ppm]	mSigma	# mSigma	Score	rdb	e⁻ Conf	N-Rule
207.1016	1	C12H15O3	207.1016	-0.1	2.1	1	100.00	5.5	even	ok
247.0941	1	C12H16NaO4	247.0941	0.0	4.1	1	100.00	4.5	even	ok

Figure S17. The HRESIMS of compound **3**

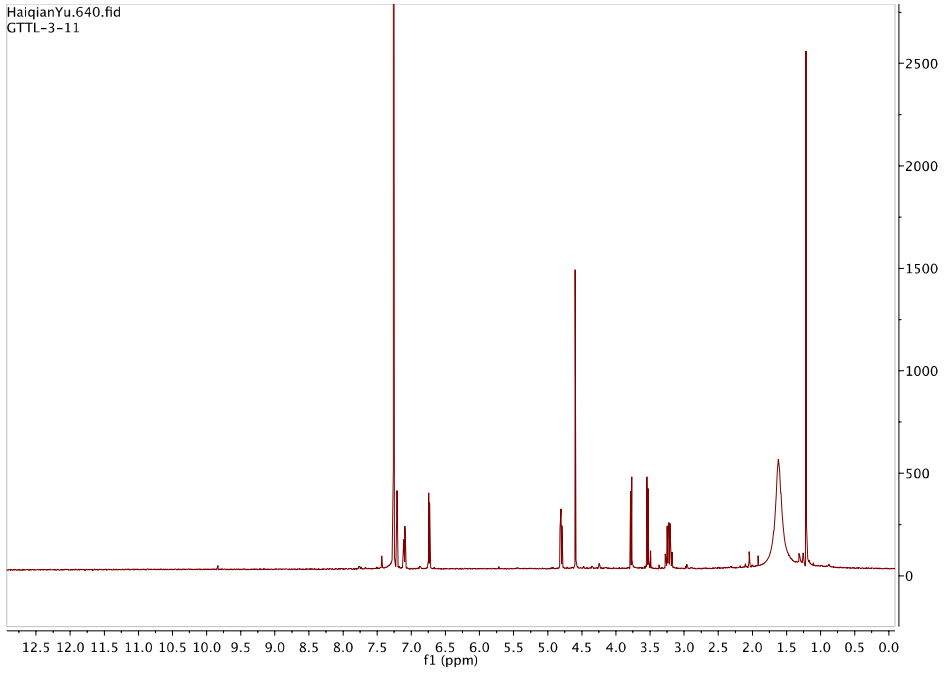

Figure S18. The ^{1}H NMR (600 MHz, $CDCl_3$) spectrum of compound **3**

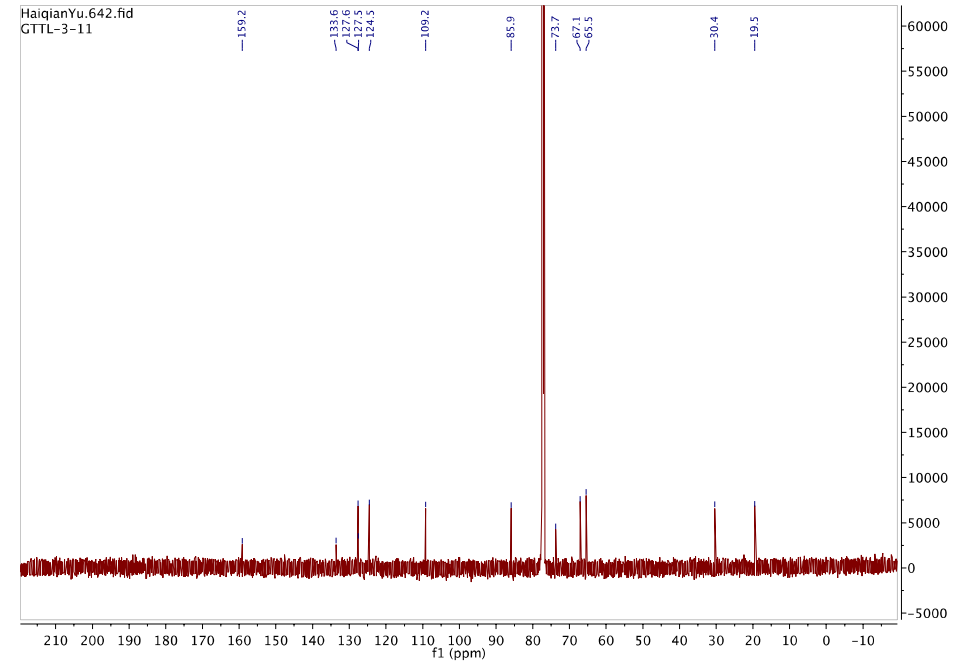

Figure S19. The ^{13}C NMR (150 MHz, $CDCl_3$) spectrum of compound **3**

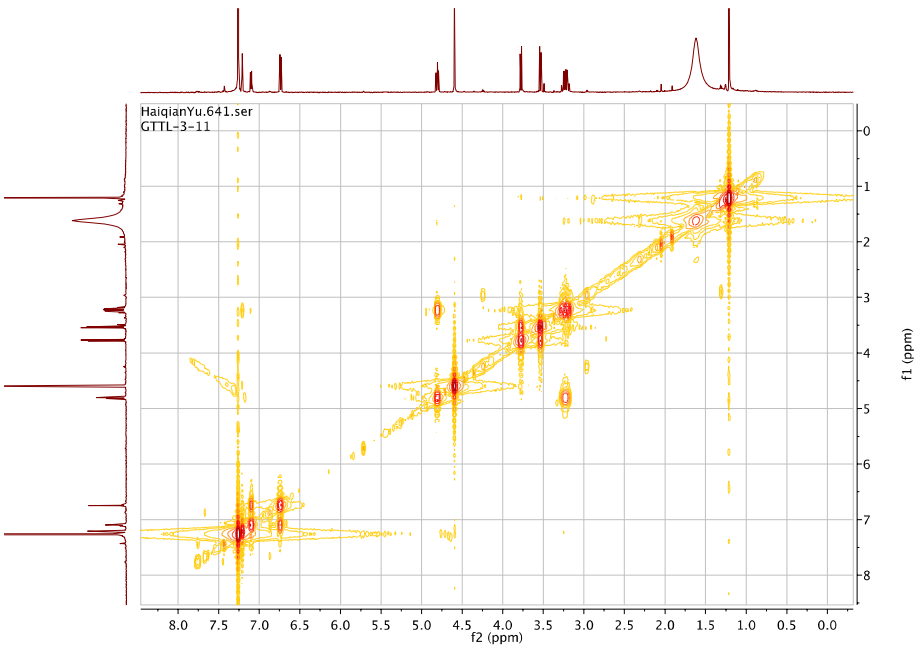

Figure S20. The COSY (600 MHz, $CDCl_3$) spectrum of compound **3**

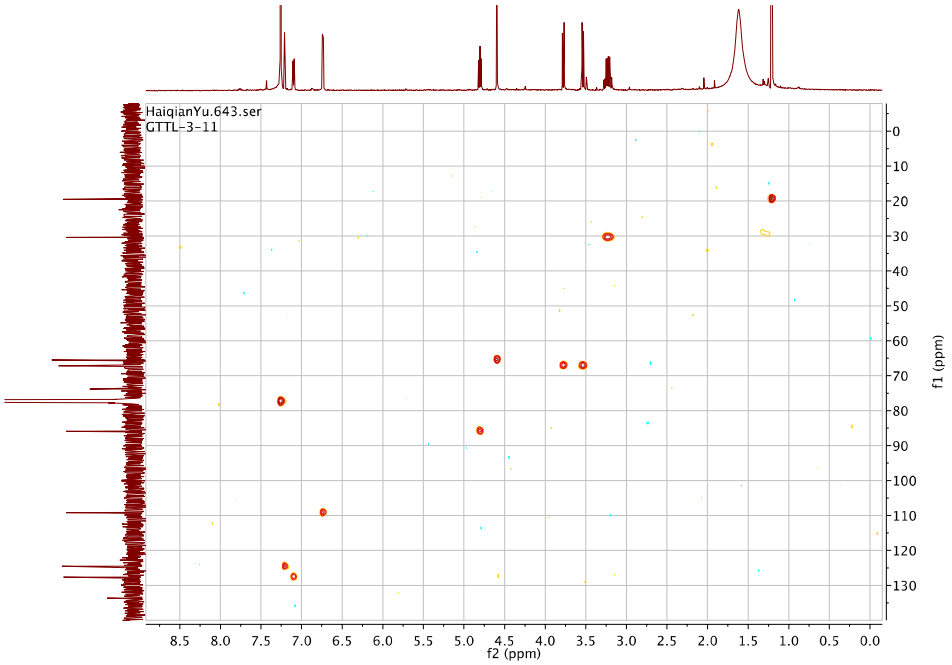

Figure S21. The HSQC (600 MHz, $CDCl_3$) spectrum of compound **3**

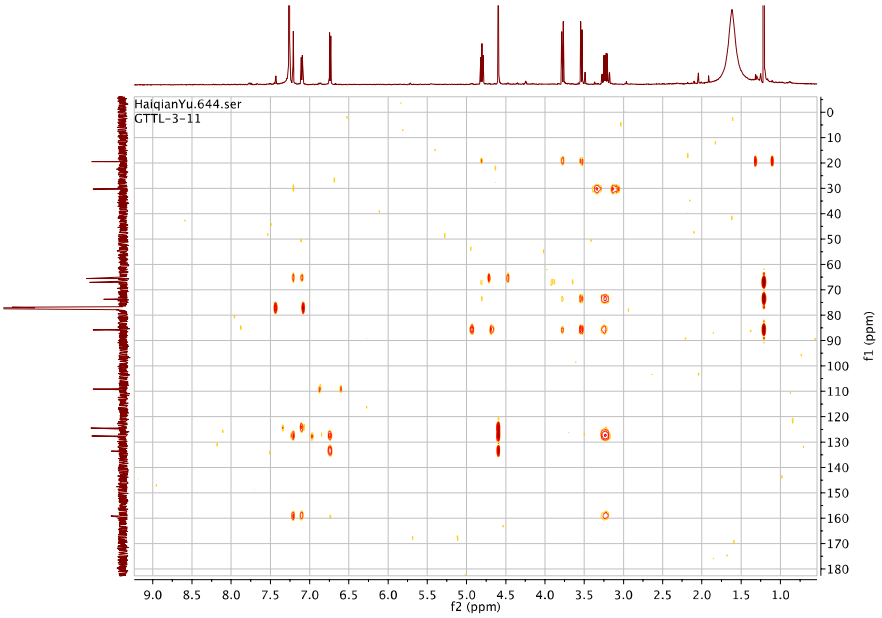

Figure S22. The HMBC (600 MHz, $CDCl_3$) spectrum of compound **3**

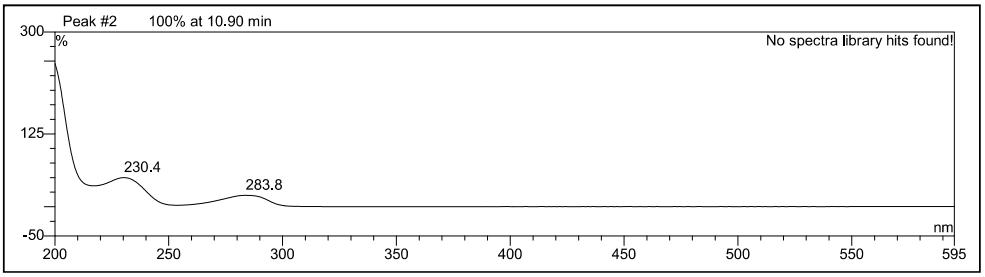

Figure S23. The UV spectrum of compound **3**

4 Polyketides and Nitrogenous Metabolites from The Endophytic Fungus *Phomopsis* sp. D15a2a

Published in: “Tetrahedron Letters”.

Contribution: first author, conducting most of the experiments, literature research, manuscript writing

Tetrahedron Letters 60 (2019) 151325

Contents lists available at ScienceDirect

Tetrahedron Letters

journal homepage: www.elsevier.com/locate/tetlet

Polyketides and nitrogenous metabolites from the endophytic fungus *Phomopsis* sp. D15a2a

Haiqian Yu [a], Simon-Patrick Höfert [b], Mariam Moussa [a], Christoph Janiak [b], Werner E.G. Müller [c], Blessing O. Umeokoli [a,d], Haofu Dai [e], Zhen Liu [a,*], Peter Proksch [a,*]

[a] Institute of Pharmaceutical Biology and Biotechnology, Heinrich-Heine-Universität Düsseldorf, Universitätsstrasse 1, 40225 Düsseldorf, Germany
[b] Institute of Inorganic and Structural Chemistry, Heinrich-Heine-Universität Düsseldorf, Universitätsstrasse 1, 40225 Düsseldorf, Germany
[c] Institute of Physiological Chemistry, Universitätsmedizin der Johannes-Gutenberg-Universität Mainz, 55128 Mainz, Germany
[d] Department of Pharmaceutical and Medicinal Chemistry, Nnamdi Azikiwe University, Awka, Nigeria
[e] Key Laboratory of Biology and Genetic Resources of Tropical Crops, Ministry of Agriculture, Institute of Tropical Bioscience and Biotechnology, Chinese Academy of Tropical Agricultural Sciences, Haikou 571101, China

ARTICLE INFO

Article history:
Received 23 August 2019
Revised 22 October 2019
Accepted 24 October 2019
Available online 25 October 2019

Keywords:
Phomopsis sp.
Endophytic fungus
Polyketide
Peptide

ABSTRACT

Three new polyketides, phomopones A–C (**1–3**), one new cyclic tetrapeptide, 18-hydroxydihydrotentoxin (**4**), and a new amide, 6-hydroxyenamidin (**5**) together with a known derivative, enamindin (**6**) were obtained from the endophytic fungus *Phomopsis* sp. D15a2a isolated from the plant *Alternanthera bettzickiana*. The structures of the new compounds were elucidated by 1D, 2D NMR and HRMS data. The absolute configurations of the isolated metabolites were determined either by X-ray crystallography, Marfey's method or by converting the compounds to Mosher esters.

© 2019 Elsevier Ltd. All rights reserved.

Introduction

Fungi of genus *Phomopsis* have been reported as endophytes, saprobes, plant pathogens, animal pathogens and are even known to infect humans [1]. They have been rather well investigated due to their production of structurally diverse metabolites. *Phomopsis.* sp. TJ507A, an endophyte obtained from the medicinal plant *Phyllanthus glaucus* (Phyllanthaceae), yielded a series of protoilludane, illudalane and botryane sesquiterpenoids, of which some showed β-site amyloid precursor protein cleaving enzyme 1 (BACE1) inhibitory activities [2]. From the endophytic fungus *Phomopsis* sp. YE3250, seven polyoxygenated cyclohexenoids, phomopoxides A–G, were isolated with promising α-glycosidase inhibitory activity [3]. Four furanones, phomopsolidones A–D, were isolated from *Phomopsis* sp. DC275 and two of them exhibited antibacterial activity against *Bacillus subtilis* with MIC values of 0.1 ng [4]. In this study, the endophytic fungus *Phomopsis* sp. D15a2a, that was isolated from leaves of *Alternanthera bettzickiana* (Amaranthaceae) collected in Anambra state of Nigeria, was investigated with regard to its secondary metabolites. The EtOAc extract of *Phomopsis* sp. following fermentation on solid rice medium yielded three new polyketides, phomopones A–C (**1–3**), a new cyclic tetrapeptide, 18-hydroxydihydrotentoxin (**4**), and a new amide, 6-hydroxyenamidin (**5**) in addition to a known derivative, enamindin (**6**) (Figure 1) [5].

Results and discussion

Compound **1** had the molecular formula of $C_{10}H_{14}O_3$ with four degrees of unsaturation as established from the HRESIMS data. The ^{13}C NMR data of **1** (Table 1) showed one carbonyl at δ_C 199.9 (C-1), two olefinic carbons at δ_C 173.6 (C-5) and 109.6 (C-6), two oxygenated methines at δ_C 75.5 (C-9) and 72.4 (C-2), a methyl at δ_C 20.5 (C-10) and four aliphatic methylenes, accounting for two degrees of unsaturation. The remaining two degrees of unsaturation suggested a bicyclic structure for compound **1**. Two spin systems from C-2 to C-4 and from C-7 to C-10 were established from the COSY correlations between H-2/ H-3ab/H-4ab and between H-7ab/H-8ab/H-9/Me-10 (Figure 2). The HMBC correlations from H-2 and H-3ab to C-1, from H-3ab to C-5, from H-4ab to C-5 and C-6, from H-7ab to C-1, C-5 and C-6, and from H-8ab to C-6 indicated the presence of an α,β-unsaturated ketone and linkages between C-1/C-2, C-4/C-5, and C-6/C-7. The location of a hydroxy group at

* Corresponding authors.
E-mail addresses: zhenfeizi0@sina.com (Z. Liu), proksch@uni-duesseldorf.de (P. Proksch).

https://doi.org/10.1016/j.tetlet.2019.151325
0040-4039/© 2019 Elsevier Ltd. All rights reserved.

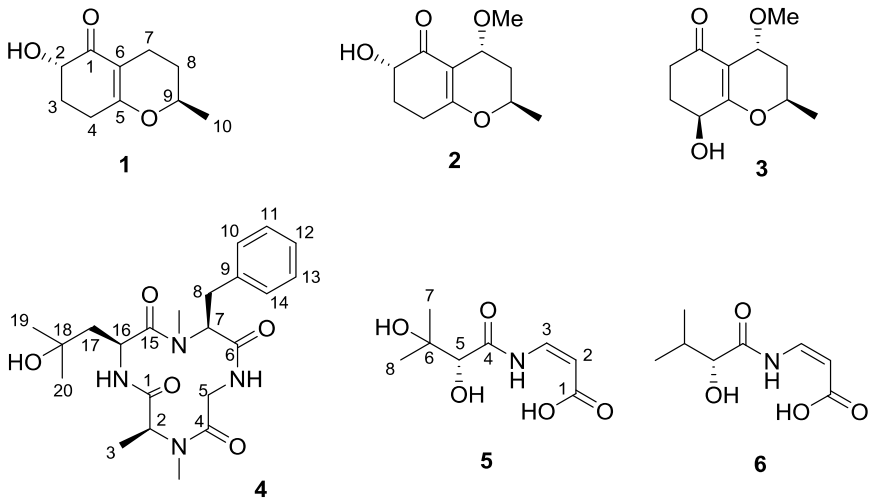

Figure 1. Structures of isolated compounds from *Phomopsis* sp.

Table 1
^{1}H and ^{13}C NMR Data of Compounds 1–3.

position	**1** [a]		**2** [b]		**3** [a]	
	δ_C, type	δ_H, (*J* in Hz)	δ_C, type	δ_H, (*J* in Hz)	δ_C, type	δ_H, (*J* in Hz)
1	199.9, C		199.1, C		199.3, C	
2	72.4, CH	4.03, dd (12.0, 5.2)	72.5, CH	4.01, dd (12.0, 5.0)	34.4, C	2.54, ddd (16.9, 7.9, 4.7) 2.38, ddd (16.9, 8.8, 4.9)
3	30.8, CH_2	2.23, dddd (12.0, 5.2, 5.2, 3.2) 1.84, dddd (12.0, 12.0, 12.0, 5.0)	30.1, CH_2	2.23, dddd (12.0, 5.0, 5.0, 3.3) 1.86, dddd (12.0, 12.0, 12.0, 5.0)	30.6, CH_2	2.20, dddd (13.3, 7.9, 4.9, 4.4) 1.92, dddd (13.3, 8.8, 7.2, 4.7)
4	28.3, CH_2	2.59, br ddd (17.5, 12.0, 5.2) 2.42, br ddd (17.5, 5.0, 3.2)	28.4, CH_2	2.64, ddd (17.7, 12.0, 5.0) 2.48, ddd (17.7, 5.0, 3.3)	67.2, CH	4.38, dd (7.2, 4.4)
5	173.6, C		176.2, C		175.4, C	
6	109.6, C		110.9, C		112.7, C	
7	18.2, CH_2	2.25, m 2.22, m	67.6, CH	4.14, dd (3.0, 2.4)	67.4, CH	4.22, dd (3.1, 2.3)
8	28.6, CH_2	1.95, dddd (13.8, 5.8, 4.6, 2.8) 1.53, dddd (13.8, 9.3, 9.3, 5.6)	34.0, CH_2	2.12, ddd (14.5, 2.4, 2.4) 1.39, ddd (14.5, 12.6, 3.0)	33.9, CH_2	2.13, ddd (14.5, 2.3, 2.3) 1.40, ddd (14.5, 12.6, 3.1)
9	75.5, CH	4.23, dqd (9.3, 6.4, 2.8)	71.8, CH	4.34, dqd (12.6, 6.3, 2.4)	71.8, CH	4.30, dqd (12.6, 6.3, 2.3)
10	20.5, CH_3	1.33, d (6.4)	20.8, CH_3	1.39, d (6.3)	20.7, CH_3	1.45, d (6.3)
7-OMe			56.6, CH_3	3.37, s	56.8, CH_3	3.36, s,

[a] Measured in CD_3OD at 600 (^{1}H) and 150 MHz (^{13}C); [b] Measured in CD_3OD at 300 (^{1}H) and 75 MHz (^{13}C).

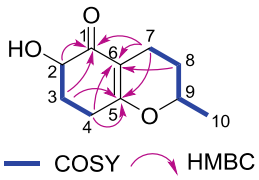

Figure 2. COSY and key HMBC correlations of compound **1**.

C-2 and an ether linkage between C-5 and C-9 were deduced from the molecular formula of **1**, the chemical shifts of C-2, C-5 and C-9 in addition to the weak HMBC correlation from Me-10 to C-5. Thus, the planar structure of **1** was elucidated as shown and the trivial name phomopone A was given to **1**. The relative and absolute configuration of **1** was determined by X-ray diffraction analysis (Figure 3).

The molecular formula of compound **2** was determined as $C_{11}H_{16}O_4$ by the HRESIMS data. The NMR data of **2** (Table 1) were similar to those of **1** except for the replacement of an aliphatic methylene by an oxygenated methine (δ_C 67.6 and δ_H 4.14) and

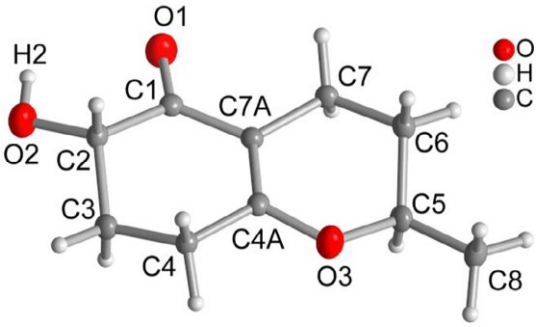

Figure 3. Molecular structure of compound **1** from X-ray diffraction analysis.

an additional methoxy group (δ_C 56.6 and δ_H 3.37) in **2**. The COSY correlations between the protons of this additional methine and H-8ab, H-8ab/H-9, and between H-9/Me-10, together with the HMBC correlations from the protons of this additional methine to C-1 (δ_C

199.1), C-5 (δ_C 176.2) and C-6 (δ_C 110.9) indicated the location of this additional oxygenated methine group at C-7. Furthermore, the attachment of the additional methoxy group at C-7 was confirmed by the HMBC correlations from the protons of the methoxy group to C-7 and in turn from H-7 to the carbon of the methoxy group. The remaining structure of **2** was elucidated to be identical to that of **1** after detailed analysis of the 2D NMR spectra of **2**. Compound **2** is suggested to share the same absolute configurations at C-2 and C-9 as **1** in consideration of the close biogenetic relationship between both compounds. The large value of $^3J_{H\text{-}9/H\text{-}8b}$ (12.6 Hz) and the small values of $^3J_{H\text{-}9/H\text{-}8a}$ (2.4 Hz), $^3J_{H\text{-}7/H\text{-}8a}$ (2.4 Hz) and $^3J_{H\text{-}7/H\text{-}8b}$ (3.0 Hz) indicated diaxial orientation of H-9 and H-8b and equatorial orientation of H-8a and H-7, implying that H-7 and H-9 were on different sides of the ring. Thus, the configuration of **2** was tentatively assigned as 2*S**,7*R**,9*R**.

Compound **3** shared the same molecular formula as **2** as evident from the HRESIMS data. Comparison of the ^{1}H and ^{13}C NMR data of **2** and **3** (Table 1) revealed that both compounds exhibit almost identical signals in the cyclic ether ring whereas the chemical shifts of the oxygenated methine in the cyclohexenone ring in **3** were obviously shifted (δ_C 67.2 and δ_H 4.38 in **3** while δ_C 72.5 and δ_H 4.01 in **2**). In addition, the protons of this oxygenated methine showed HMBC correlations to C-5 and C-6 in **3** rather than to C-1 in **2**, confirming the attachment of a hydroxy group at C-4 in **3** rather than at C-2 in **2**. Based on the similar chemical shifts and coupling constants, **3** was suggested to share the same (7*R**,9*R**) configuration as **2**. The relatively small coupling constants between H-4 and H-3ab (7.2 and 4.4 Hz) in **3** were more comparable to those of H-4b (5.0 and 3.3 Hz) rather than to those of H-4a (12.0 and 5.0 Hz) in **2**, suggesting equatorial orientation of H-4 in **3** and hence (4*S**) configuration for **3**.

Compound **4** was isolated as a white powder. Its molecular formula of $C_{22}H_{32}N_4O_5$ with 9 degrees of unsaturation was deduced from the HRESIMS data. The ^{1}H NMR data of **4** displayed signals of five methyls, three methylenes, three aliphatic methines, and five aromatic methines. The presence of carbonyls at δ_C 169–172 together with α-protons/carbons at δ_H 4.78 (H-5a), 4.49 (H-16), 4.44 (H-7), 4.03 (H-2), 3.37 (H-5b), and δ_C 61.8 (C-7), 55.9 (C-2), 46.8 (C-16), 44.2 (C-5) suggested compound **4** to be a peptide.

Table 2
^{1}H and ^{13}C NMR Data of Compound 4.

amino acid	position	δ_C, type	δ_H, (*J* in Hz)
N-Methyl-Ala	1	170.4, C	
	2	55.9, C	4.03, q (7.1)
	3	15.4, CH_3	1.34, d (7.1)
	2-NCH_3	29.5, CH_3	2.65, s
Gly	4	170.4, C	
	5	44.2, CH_2	4.78, br d (15.4)
			3.37, d (15.4)
	5-NH		8.04, br s
N-Methyl-Phe	6	169.2, C	
	7	61.8, CH	4.44, d (11.0)
	8	33.7, CH_2	3.41, d (14.6)
			2.91, dd (14.6, 11.0)
	9	137.9, C	
	10, 14	128.1, CH	7.20, d (7.6)
	11, 13	128.6, CH	7.28, t (7.6)
	12	126.5, CH	7.19, d (7.6)
	7-NCH_3	30.6, CH_3	2.69, s
γ-OH-Leu	15	171.6, C	
	16	46.8, CH	4.49, m
	17	44.9, CH_2	2.11, dd (14.3, 4.9)
			1.35, m
	18	68.1, C	
	19	29.5, CH_3	0.92, s
	20	28.9, CH_3	0.90, s
	16-NH		8.14, br s
	18-OH		4.14, s

Measured in DMSO d_6 at 600 (^{1}H) and 150 MHz (^{13}C).

The ^{1}H and ^{13}C NMR data of **4** (Table 2) resembled those of dihydrotentoxin [6,7] except for the replacement of an aliphatic methine of the latter by an oxygenated carbon of the former at δ_C 68.1 (C-18) and an additional hydroxy group at δ_H 4.14 (18-OH). The HMBC correlations from Me-19 (δ_H 0.92) and Me-20 (δ_H 0.90) to C-18 and C-17 (δ_C 44.9), from 18-OH to C-17, C-18, C-19 (δ_C 29.5) and C-20 (δ_C 28.9), and from H-17ab (δ_H 2.11 and 1.35) to C-15 (δ_C 171.6), along with the COSY correlations between H-17ab/H-16/16-NH, indicated the replacement of leucine as in dihydrotentoxin by a γ-OH-Leu residue in **4**. Detailed analysis of 2D NMR data of **4** confirmed that the remaining structure of **4** was identical to that of dihydrotentoxin. Thus, compound **4** was identified as 18-hydroxydihydrotentoxin, representing a new cyclotetrapeptide. The absolute configuration of **4** was determined by Marfey's reaction employing the rule that D-FDAA-D-amino acid or L-FDAA-L-amino acid elute earlier during HPLC analysis compared to L-FDAA-D-amino acid or D-FDAA-L-amino acid. [8,9] Comparison of the retention time of the resulting L-FDAA- and D-FDAA-amino acid derivatives [L-FDAA-*N*-Methyl-Ala (35.66 min), D-FDAA-*N*-Methyl-Ala (38.86 min); L-FDAA-18-hydroxy-Leu (47.64 min), D-FDAA-18-hydroxy-Leu (56.15 min); L-FDAA-*N*-Methyl-Phe (85.17 min), D-FDAA-*N*-Methyl-Phe (85.80 min)] revealed that all amino acid residues in **4** were of the L-form.

The molecular formula of compound **5** was determined to be $C_8H_{13}NO_5$ according to the HRESIMS data, indicating the presence of an additional oxygen atom when compared to the co-isolated known compound, enamindin (**6**). [5] The ^{1}H and ^{13}C NMR data of **5** (Table 3) were similar to those of enamindin (**6**). However, the presence of an oxygenated carbon at δ_C 73.3 (C-6) and the observation that the methyl groups (Me-7 and Me-8) resonated as a singlet in **5** rather than as a doublet in **6** indicated the presence of an additional hydroxy group at C-6. This was further confirmed by the HMBC correlations from Me-7 and Me-8 (both at δ_H 1.23) to C-6 and C-5 (δ_C 78.9), and from H-5 (δ_H 3.92) to C-7 (δ_C 25.9), C-8 (δ_C 25.5), and C-4 (δ_C 173.9). The remaining structure of **5** including the configuration of the double bond was elucidated to be identical to enamindin (**6**) after detailed analysis of the 2D NMR spectra. Thus, compound **5** was determined to be 6-hydroxyenamidin. Due to the limited amount of **5**, Mosher's reaction was carried out for **6**, whose absolute configuration had not been reported in the previous publication. [5] Calculation of differences of chemical shifts between the resulting methylated (*R*)- and (*S*)-MPA esters of **6** led to the assignment of the absolute configuration of C-5 as *R* (Figure 4). Considering the close biogenetic relationship and similarity of optical rotation between **5** and **6**, compound **5** was suggested to have the same *R* configuration at C-5.

All isolated compounds were tested for their cytotoxicity against the L5178Y mouse lymphoma cell line but proved to be inactive when tested at a concentration of 10 μM.

In conclusion, three new polyketides, phomopones A – C (**1–3**), a new cyclic tetrapeptide, 18-hydroxydihydrotentoxin (**4**), and a new amide, 6-hydroxyenamidin (**5**) together with a known derivative, enamindin (**6**) were isolated from the rice medium fermenta-

Table 3
^{1}H and ^{13}C NMR Data of Compound 5.

	δ_C, type	δ_H, (*J* in Hz)
1	171.1, C	
2	99.0, CH	5.18, d (9.0)
3	137.3, CH	7.44, d (9.0)
4	173.9, C	
5	78.9, CH	3.92, s
6	73.3, C	
7	25.9, CH_3	1.23, s
8	25.5, CH_3	1.23, s

Measured in CD_3OD at 300 (^{1}H) and 75 MHz (^{13}C).

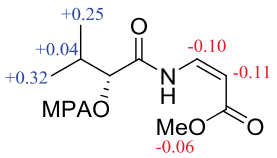

Figure 4. $\Delta\delta^{RS}$ (δ_R – δ_S) values of methylated (*R*)- and (*S*)-MPA esters of **6**.

tion of *Phomopsis* sp. The absolute configurations of those compounds were determined by X-ray crystallography, Marfey's method or Mosher's reaction.

Declaration of Competing Interest

The authors declare that they have no known competing financial interests or personal relationships that could have appeared to influence the work reported in this paper.

Acknowledgements

This work is funded by the Deutsche Forschungsgemeinschaft (DFG, German Research Foundation) – 270650915/GRK 2158 and the Manchot Foundation.

Appendix A. Supplementary data

Supplementary data to this article can be found online at https://doi.org/10.1016/j.tetlet.2019.151325.

References

[1] D. Udayanga, X. Liu, E.H.C. McKenzie, E. Chukeatirote, A.H.A. Bahkali, K.D. Hyde, Fungal Divers. 50 (2011) 189.
[2] S. Xie, Y. Wu, Y. Qiao, Y. Guo, J. Wang, Z. Hu, Q. Zhang, X. Li, J. Huang, Q. Zhou, Z. Luo, J. Liu, H. Zhu, Y. Xue, Y. Zhang, J. Nat. Prod. 81 (2018) 1311–1320.
[3] R. Huang, B.-G. Jiang, Y.-T. Wang, S.-S. Liu, K.-X. Zheng, S.-H. Wu, X.-N. Li, J. He, J. Agric. Food Chem. 66 (2018) 1140–1146.
[4] M.-L. Goddard, N. Mottier, J. Jeanneret-Gris, D. Christen, R. Tabacchi, E. Abou-Mansour, J. Agric. Food Chem. 62 (2014) 8602–8607.
[5] H. Mandavid, A.M.S. Rodrigues, L.S. Espindola, V. Eparvier, D. Stien, J. Nat. Prod. 78 (2015) 1735–1739.
[6] W.L. Meyer, L.F. Kuyper, D.W. Phelps, A.W. Cordes, J. Chem. Soc. Chem. Comm. (1974) 339–340.
[7] E. La Kim, J.L. Li, B. Xiao, J. Hong, E.S. Yoo, W.D. Yoon, J.H. Jung, Chem. Pharm. Bull. 60 (2012) 1590–1593.
[8] S. Vijayasarathy, P. Prasad, L.J. Fremlin, R. Ratnayake, A.A. Salim, Z. Khalil, R.J. Capon, J. Nat. Prod. 79 (2016) 421–427.
[9] M. Frank, F.C. Özkaya, W.E.G. Müller, A. Hamacher, M.U. Kassack, W. Lin, Z. Liu, P. Proksch, Mar. Drugs 17 (2019) 99.

Supporting Information

Polyketides and Nitrogenous Metabolites from The Endophytic Fungus *Phomopsis* sp. D15a2a

Haiqian Yu [a], Simon-Patrick Höfert [b], Mariam Moussa [a], Christoph Janiak [b], Werner E. G. Müller [c], Blessing O. Umeokoli [a d], Haofu Dai [e], Zhen Liu [a,*], Peter Proksch [a,*]

[a] Institute of Pharmaceutical Biology and Biotechnology, Heinrich-Heine-Universität Düsseldorf, Universitätsstrasse 1, 40225 Düsseldorf, Germany

[b] Institute of Inorganic and Structural Chemistry, Heinrich-Heine-Universität Düsseldorf, Universitätsstrasse 1, 40225 Düsseldorf, Germany

[c] Institute of Physiological Chemistry, Universitätsmedizin der Johannes-Gutenberg-Universität Mainz, 55128 Mainz, Germany

[d] Department of Pharmaceutical and Medicinal Chemistry, Nnamdi Azikiwe University, Awka, Nigeria

[e] Key Laboratory of Biology and Genetic Resources of Tropical Crops, Ministry of Agriculture, Institute of Tropical Bioscience and Biotechnology, Chinese Academy of Tropical Agricultural Sciences, Haikou 571101, China

*Corresponding authors.

Tel.: +49 211 81 14163; fax: +49 211 81 11923;

e-mail: zhenfeizi0@sina.com (Z. Liu),

proksch@uni-duesseldorf.de (P. Proksch)

Table of Contents

Figure S1. Asymmetric unit of 1, showing the crystallographically independent molecules. 10

Figure S2. Section of the packing diagram of 1 showing the complementary intermolecular H-bonds (orange dashed line) connecting the two symmetry non-equivalent molecules. 10

Figure S3. Section of the packing diagram of 1 showing the relative position of the two symmetry-independent molecules in the asymmetric unit with their respective intermolecular H-bonds (orange dashed lines). 11

Table S1. Fractional atomic coordinates and isotropic or equivalent isotropic displacement parameters ($Å^2$) for 1 11

Table S2. Atomic displacement parameters ($Å^2$) for 1 13

Table S3. Geometric parameters (Å, º) for 1 14

Table S4. Hydrogen-bond geometry (Å, º) for 1 16

Figure S4. The HRESIMS of compound 1 18

Figure S5. The ^{1}H NMR (600 MHz, CD_3OD) spectrum of compound 1 18

Figure S6. The ^{13}C NMR (150 MHz, CD_3OD) spectrum of compound 1 19

Figure S7. The COSY (600 MHz, CD_3OD) spectrum of compound 1 19

Figure S8. The HSQC (600 MHz, CD_3OD) spectrum of compound 1 20

Figure S9. The HMBC (600 MHz, CD_3OD) spectrum of compound 1 20

Figure S10. The ROESY (600 MHz, CD_3OD) spectrum of compound 1 21

Figure S11. The UV spectrum of compound 1 21

Figure S12. The HRESIMS of compound 2 22

Figure S13. The ^{1}H NMR (300 MHz, CD_3OD) spectrum of compound 2 22

Figure S14. The ^{13}C NMR (75 MHz, CD_3OD) spectrum of compound 2 23

Figure S15. The COSY (300 MHz, CD_3OD) spectrum of compound 2 23

Figure S16. The HSQC (300 MHz, CD_3OD) spectrum of compound 2 24

Figure S17. The HMBC (300 MHz, CD_3OD) spectrum of compound 2 24

Figure S18. The ROESY (300 MHz, CD_3OD) spectrum of compound 2 25

Figure S19. The UV spectrum of compound 2 25

Figure S20. The HRESIMS of compound 3 26

Figure S21. The ^{1}H NMR (600 MHz, CD_3OD) spectrum of compound 3 26

Figure S22. The ^{13}C NMR (150 MHz, CD_3OD) spectrum of compound 3 27

Figure S23. The COSY (600 MHz, CD_3OD) spectrum of compound 3 27

Figure S24. The HSQC (600 MHz, CD_3OD) spectrum of compound 3 28
Figure S25. The HMBC (600 MHz, CD_3OD) spectrum of compound 3 28
Figure S26. The ROESY (300 MHz, CD_3OD) spectrum of compound 3 29
Figure S27. The UV spectrum of compound 3 29
Figure S28. The HRESIMS of compound 4.....30
Figure S29. The ^1H NMR (600 MHz, DMSO-d_6) spectrum of compound 4 30
Figure S30. The ^{13}C NMR (150 MHz, DMSO-d_6) spectrum of compound 4 31
Figure S31. The COSY (600 MHz, DMSO-d_6) spectrum of compound 4 31
Figure S32. The HSQC (600 MHz, DMSO-d_6) spectrum of compound 4.....32
Figure S33. The HMBC (600 MHz, DMSO-d_6) spectrum of compound 4.....32
Figure S34. The ROESY (600 MHz, DMSO-d_6) spectrum of compound 4.....33
Figure S35. The UV spectrum of compound 4 33
Figure S36. The HPLC chromatogram of Marfey's reaction with L-FDAA.....34
Figure S37. The HPLC chromatogram of Marfey's reaction with D-FDAA 34
Figure S38. The HRESIMS of compound 5.....35
Figure S39. The ^1H NMR (300 MHz, CD_3OD) spectrum of compound 5.....35
Figure S40. The ^{13}C NMR (75 MHz, CD_3OD) spectrum of compound 5.....36
Figure S41. The COSY (300 MHz, CD_3OD) spectrum of compound 5.....36
Figure S42. The HSQC (300 MHz, CD_3OD) spectrum of compound 5 37
Figure S43. The HMBC (300 MHz, CD_3OD) spectrum of compound 5 37
Figure S44. The ROESY (300 MHz, CD_3OD) spectrum of compound 5 38
Figure S45. The UV spectrum of compound 5 38
Figure S46. The HRESIMS of compound 6.....39
Figure S47. The ^1H NMR (600 MHz, CD_3OD) spectrum of compound 6.....39
Figure S48. The ^{13}C NMR (150 MHz, CD_3OD) spectrum of compound 6.....40
Figure S49. The HMBC (600 MHz, CD_3OD) spectrum of compound 6 40
Figure S50. The UV spectrum of compound 6 41
Figure S51. The ^1H NMR (600 MHz, CD_3OD) spectrum of (*S*)-MPA ester of compound 6.....41
Figure S52. The ^1H NMR (600 MHz, CD_3OD) spectrum of (*R*)-MPA ester of compound 6.....42

Experimental Section

General Experimental Procedures. Optical rotations were measured on a JASCO P-2000 polarimeter. NMR data were obtained by Bruker Avance III 300 or Bruker Avance III 600 spectrometers. HRESIMS data were recorded on a Bruker Daltonics UHR-QTOF Maxis 4G mass spectrometer. HPLC analysis was carried out using a Dionex UltiMate-3400SD system (a LPG-3400SD pump and a DAD3000RS photodiode array detector) coupled with a Knauer Eurospher C18 analytical column (125 × 4 mm, 5 μm). Semipreparative HPLC was performed on a Lachrom-Merck Hitachi system (a L7100 pump and a L7400 UV detector) using a 300 × 8 mm Knauer Eurospher C18 column. Column chromatography was carried out using Merck silica gel 60M (0.04–0.063 mm), Merck RP C18 (0.04–0.063 mm) or Sephadex LH-20 (Sigma). For TLC analysis, plates precoated with Merck silica gel F254 were used with detection under 254 and 365 nm or by spraying the plates with anisaldehyde reagent followed by heating.

Fungal Material. The fungus was isolated from leaves of *Alternanthera bettzickiana* collected in Anambra state, Nigeria in 2015 and was identified as *Phomopsis* sp. (GenBank accession number JQ341095.1) by DNA amplification and sequencing of its ITS region as described before.[1] The fungus was cultivated for two weeks on solid rice medium in 20 Erlenmeyer flasks (1 L each, 100 g of rice and 110 mL of demineralized water per flasks, autoclaved at 121°C for 20 min before inoculation).

Extraction and Isolation. The culture was extracted by adding 500 mL EtOAC

per flask with shaking at 150 rpm for 8 h. The extract was evaporated to dryness to yield 14.6 g of crude extract followed by fractionation on a RP C18 column (60 × 200 mm) using a solvent gradient (from 100% H_2O to 100% MeOH) to give seven fractions (Fr.1 to Fr.7). Fr.1 (0.05 g) was purified by semipreparative HPLC to give **5** (1.0 mg). Fr.2 (0.65 g) was subjected to a Sephadex LH-20 column (20 × 500 mm) with MeOH, and then purified by semipreparative HPLC to yield **3** (6.0 mg). Fr.3 (0.54 g) was subjected to a Sephadex LH-20 column (20 × 500 mm) with CH_2Cl_2-MeOH (1:1) as mobile phase to afford **6** (300 mg). Fr.4 (0.61 g) was subjected to a silica gel column (30 × 500 mm) eluted with a gradient of *n*-hexane and EtOAC (from 9:1 to 1:1) to give **1** (4.6 mg) and **2** (9.6 mg). Fr.6 (0.64 g) was subjected to a Sephadex LH-20 column (20 × 500 mm) eluted with CH_2Cl_2-MeOH (1:1), followed by purification using semipreparative HPLC to afford **4** (5.0 mg).

*Phomopone A (**1**):* colorless crystal; $[\alpha]_D^{20}$ +65 (*c* 0.1, MeOH); UV(MeOH) λ_{max} 266 nm; ^1H and ^{13}C NMR data, Table 1; HRESIMS *m/z* 183.1017 $[M + H]^+$ (calcd for $C_{10}H_{15}O_3$, 183.1016).

*Phomopone B (**2**):* white amorphous powder; $[\alpha]_D^{20}$ +62 (*c* 0.1, MeOH); UV(MeOH) λ_{max} 258 nm; ^1H and ^{13}C NMR data, Table 1; HRESIMS *m/z* 235.0941 $[M + Na]^+$ (calcd for $C_{11}H_{16}NaO_4$, 235.0941).

*Phomopone C (**3**):* white amorphous powder; $[\alpha]_D^{20}$ +71 (*c* 0.1, MeOH); UV(MeOH) λ_{max} 257 nm; ^1H and ^{13}C NMR data, Table 1; HRESIMS *m/z* 235.0942 $[M + Na]^+$ (calcd for $C_{11}H_{16}NaO_4$, 235.0941).

*18-Hydroxydihydrotentoxin (**4**):* white amorphous powder; $[\alpha]_D^{20}$ -66 (*c* 0.1,

MeOH); UV(MeOH) λ_{max} 206 nm; ^{1}H and ^{13}C NMR data, Table 2; HRESIMS *m/z* 433.2452 $[M + H]^+$ (calcd for $C_{22}H_{33}N_4O_5$, 433.2445).

*6-Hydroxyenamidin (**5**):* light yellow oil; $[\alpha]_D^{20}$ +34 (*c* 0.1, MeOH); UV(MeOH) λ_{max} 268 nm; ^{1}H and ^{13}C NMR data, Table 3; HRESIMS *m/z* 204.0866 $[M + H]^+$ (calcd for $C_8H_{14}NO_5$, 204.0866).

Preparation and Analysis of Marfey's Derivatives of 4. Compound **4** (0.2 mg) was dissolved in two sealed glass vials with 0.2 mL of 6N HCl and hydrolyzed at 110 °C for 12 h. The solution was evaporated to dryness and added with 20 μL of 1M aqueous sodium bicarbonate solution each and 100 μL of a 1% acetone solution of L-FDAA (1-fluoro-2, 4-dinitrophenyl-5-L-alanine amide) or D-FDAA, respectively. The mixtures were kept at 40°C for 3 h and occasionally shaken by hand. The resulting products were analyzed by Knauer Eurospher C18 analytical column (125 × 4 mm, 5 μm) using a gradient of MeOH and water containing 0.1% formic acid (from 10% to 65%) as solvent at a flow rate of 1 mL/min.

Synthesis of (*R*)- and (*S*)-MPA Esters of 6. Compound **6** (5.0 mg) was dissolved in 2 mL dry $CHCl_3$ with *N*,*N*′-dicyclohexylcarbodiimide (40 mg), 4-dimethylaminopyridine (16 mg), (*R*)- or (*S*)-α-methoxyphenylacetic acid (15 mg) at room temperature and the reaction solution was continuously stirring for 8 h. After vacuum 1 mL MeOH was added. After purification with semipreparative HPLC, the methylated (*R*)- and (*S*)-MPA esters of **6** were obtained.

X-ray Crystallographic Analysis of 1. Under a polarizing microscope, suitable crystals were carefully selected and placed in protective oil. A crystal of sufficient

quality was measured with a Bruker Kappa APEX2 CCD diffractometer with microfocus tube using Cu-K_α radiation (λ = 1.54178 Å). For data collection APEX2,[2] for cell refinement SAINT,[2] and for experimental absorption correction SADABS was used.[3] The structure was solved with SHELXT by intrinsic phasing and refined with SHELXL-2017 by full-matrix least-squares on F^2.[4,5] All hydrogen atoms were positioned geometrically (with C–H = 0.95 Å for aromatic CH, 1.00 Å for tertiary CH, 0.99 Å for CH_2 and 0.98 Å for CH_3) and refined using riding models (AFIX 43, 13, 23 and 137) with U_{iso} (H) = 1.2U_{eq} (CH, CH_2) and 1.5U_{eq} (CH_3). The hydrogen atoms for OH were found and refined free with U_{iso}(H) = 1.5U_{eq}. The absolute structure of **1** was determined by anomalous dispersion from Cu-K_α radiation. The resulting negative Flack parameter of x = –0.01(7) made a bayesian statistics analysis of Bijvoet pair differences necessary.[6-8] The drawing of all graphics was done in DIAMOND.[9] The analyses of hydrogen bonds and Bijvoet pairs was done in PLATON for Windows.[10-13] The structure has been deposited in the Cambridge Crystallographic Data Centre (CCDC No. 1946592).

Crystal Data of ***1***: $C_{10}H_{14}O_3$, M = 182.21, monoclinic system, space group $P2_1$, a = 5.8533(5) Å, b = 18.3626(16) Å, c = 8.6312(8) Å, V = 923.66(14) Å^3, Z = 4, D_{calc} = 1.310 g/cm^3, crystal size 0.10 × 0.05 × 0.02 mm, μ(Cu-Ka) = 0.79 mm^{-1}, 4.8° < θ < 66.2°, N_t = 10570, N = 2909 (R_{int} = 0.034), R_1 = 0.035, wR_2 = 0.095, S = 1.10, Flack parameter x = –0.01(7), Hooft parameter = 0.01(6), probability for correct absolute structure $P2$(true) = 1.000, probability for wrong absolute structure $P3$(false) = 0.4·10^{-61}.

X-ray structure solution and refinement for a crystal of (2R,6S)-6-hydroxy-2-methyl-2,3,4,6,7,8-hexahydro-5H-chromen-5-one (phomopone A, **1**) reveals two crystallographically independent molecules in the asymmetric unit, that is, $Z' = 2$ (Figure S1). The origin for the presence of two symmetry-independent molecules appears to be the formation of a complementary hydrogen-bonded pair with an $R_2^2(10)$-motif in the Etter-notation (Figures S2 and S3).[14-16]

REFERENCES

1. Kjer, J.; Debbab, A.; Aly, A. H.; Proksch, P. *Nature Protocols* **2010**, *5*, 479-490.

2. Apex2, Data Collection Program for the CCD Area-Detector System; SAINT, Data Reduction, Frame Integration Program for the CCD Area-Detector System; Bruker Analytical X-ray Systems: Madison, WI, USA **1997 – 2012**.

3. Sheldrick, G. Program for Empirical Absorption Correction of Area Detector Data, University of Göttingen, Germany, 1996.

4. Sheldrick, G. M. *Acta Crystallogr. Sect. A* **2015,** *7* , 3-8.

5. Sheldrick, G. M. *Acta crystallogr. Sect. C* **2015,** *71*, 3-8.

6. Flack, H. D.; Bernardinelli, G. *Acta Crystallogr. Sect. A* **1999,** *55*, 908–915.

7. Flack, H. D. *Acta Crystallogr., Sect. A* **1983,** *39*, 876–881.

8. Hooft, R. W. W.; Straver, L. H.; Spek, A. L. *J. Appl. Crystallogr.* **2008,** *41*, 96–103.

9. Brandenburg, K., Diamond (Version 3.2), Crystal and Molecular Structure Visualization, Bonn, Germany **2009**.

10. Spek, A. L. *Acta Crystallogr. Sect. D* **2009,** *65*, 148–155.

11. Spek, A. L. *J. Appl. Crystallogr.* **2003,** *36*, 7–13.

12. Spek, A. L. PLATON - A Multipurpose Crystallographic Tool, Utrecht, The Netherlands **2008**.

13. Farrugia, L. J. Windows implementation, Version 40608, Glasgow, Scotland **2008**.

14. Etter, M. C. *Accounts Chem. Res.* 1990, 23, 120-126.

15. Etter, M. C. *J. Phys. Chem.* 1991, 95, 4601-4610.

16. Etter, M. C.; MacDonald, J. C.; Bernstein, *J. Acta Crystallogr B* 1990, *46*, 256-262.

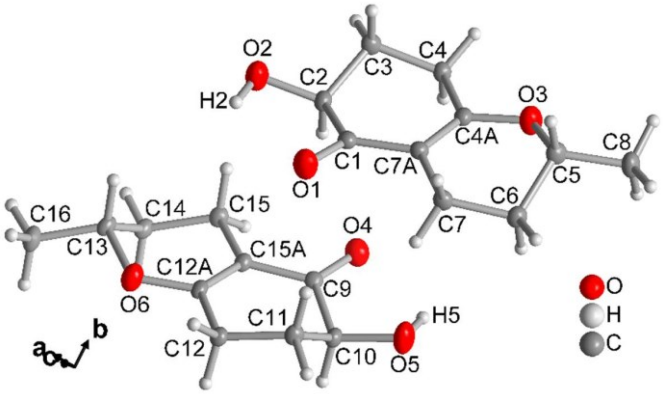

Figure S1. Asymmetric unit of 1, showing the crystallographically independent molecules.

In the asymmetric unit the symmetry-independent molecules were arranged to have their center of gravity within the unit cell.

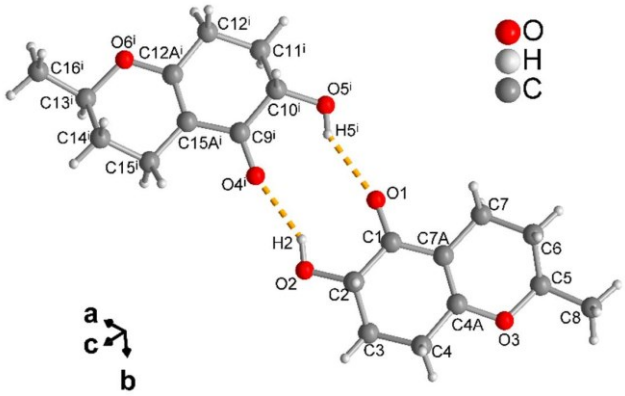

Figure S2. Section of the packing diagram of 1 showing the complementary intermolecular H-bonds (orange dashed line) connecting the two symmetry non-equivalent molecules.

Details for the intermolecular H-bonds:

O2-H2 0.83(4) Å, H2···O4^{i} 2.12(4) Å, O2···O4^{i} 2.860(3) Å, O2-H2···O4^{i} 150(4)°.

O5^{i}-H5^{i} 0.80(4) Å, H5^{i}···O1 2.19(4) Å, O5^{i}···O1 2.892(3) Å, O5^{i}-H5^{i}···O1 148(4)°.

Symmetry code: (i) 1+x, y, z.

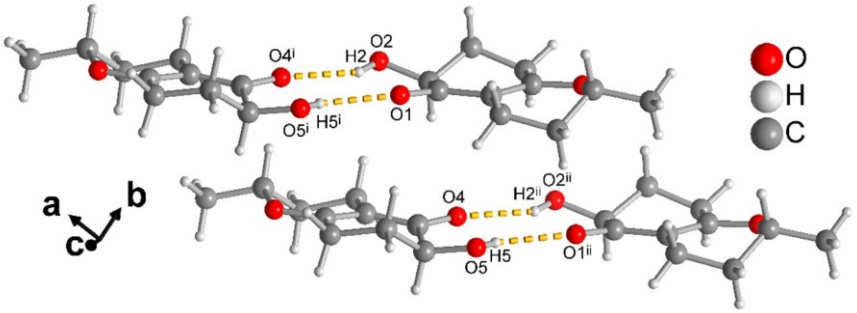

Figure S3. Section of the packing diagram of 1 showing the relative position of the two symmetry-independent molecules in the asymmetric unit with their respective intermolecular H-bonds (orange dashed lines).

Symmetry codes: (i) 1+x, y, z, (ii) -1+x, y, z.

Table S1. Fractional atomic coordinates and isotropic or equivalent isotropic displacement parameters (Å²) for 1

	x	*y*	*z*	U_{iso}*/U_{eq}
O1	1.1082 (4)	0.51982 (10)	0.4865 (2)	0.0351 (5)
O2	1.2130 (4)	0.58742 (11)	0.7617 (2)	0.0346 (5)
H2	1.270 (7)	0.550 (2)	0.728 (5)	0.052*
O3	0.4794 (3)	0.67658 (10)	0.3579 (2)	0.0306 (5)
C1	0.9711 (5)	0.56616 (13)	0.5216 (3)	0.0273 (6)
C2	0.9911 (5)	0.59637 (14)	0.6869 (3)	0.0287 (6)
H2A	0.882594	0.568454	0.747355	0.034*
C3	0.9201 (5)	0.67546 (16)	0.6870 (3)	0.0319 (6)
H3A	1.027974	0.704820	0.630917	0.038*
H3B	0.926352	0.693459	0.795398	0.038*
C4	0.6776 (5)	0.68428 (14)	0.6085 (3)	0.0274 (6)
H4A	0.566751	0.663092	0.675885	0.033*
H4B	0.642084	0.736749	0.595210	0.033*
C5	0.4644 (6)	0.65307 (15)	0.1954 (3)	0.0325 (7)
H5A	0.588534	0.677646	0.142775	0.039*
C4A	0.6515 (5)	0.64746 (13)	0.4527 (3)	0.0257 (6)

C6	0.4976 (5)	0.57186 (15)	0.1867 (3)	0.0329 (7)
H6A	0.481756	0.556137	0.076509	0.039*
H6B	0.378074	0.546828	0.240877	0.039*
C7	0.7333 (5)	0.55099 (15)	0.2617 (3)	0.0303 (6)
H7A	0.739582	0.497801	0.280261	0.036*
H7B	0.851191	0.563512	0.190900	0.036*
C8	0.2352 (6)	0.67922 (18)	0.1221 (3)	0.0394 (7)
H8A	0.217065	0.664972	0.012246	0.059*
H8B	0.227336	0.732374	0.130229	0.059*
H8C	0.112288	0.657307	0.176236	0.059*
C7A	0.7826 (5)	0.59079 (13)	0.4135 (3)	0.0257 (6)
O4	0.5436 (3)	0.47434 (10)	0.7368 (2)	0.0296 (4)
O5	0.4515 (4)	0.40842 (11)	0.4594 (2)	0.0331 (5)
H5	0.384 (7)	0.439 (2)	0.502 (5)	0.050*
O6	1.2163 (3)	0.33487 (10)	0.85209 (19)	0.0273 (4)
C9	0.6729 (5)	0.42391 (13)	0.7094 (3)	0.0230 (5)
C10	0.6132 (5)	0.37523 (14)	0.5691 (3)	0.0271 (6)
H10	0.542185	0.329774	0.606709	0.032*
C11	0.8254 (5)	0.35376 (15)	0.4952 (3)	0.0282 (6)
H11A	0.897310	0.397635	0.454032	0.034*
H11B	0.783708	0.320371	0.407000	0.034*
C12	0.9956 (5)	0.31629 (14)	0.6135 (3)	0.0252 (6)
H12A	0.941584	0.266212	0.631895	0.030*
H12B	1.146219	0.312711	0.570565	0.030*
C13	1.2821 (5)	0.37499 (15)	0.9966 (3)	0.0266 (6)
H13	1.363487	0.420561	0.970086	0.032*
C12A	1.0244 (4)	0.35639 (14)	0.7652 (3)	0.0227 (5)
C14	1.0727 (5)	0.39564 (15)	1.0764 (3)	0.0273 (6)
H14A	1.119872	0.422751	1.173232	0.033*
H14B	0.990603	0.351101	1.104427	0.033*
C15	0.9146 (5)	0.44267 (14)	0.9685 (3)	0.0275 (6)
H15A	0.765877	0.449116	1.012908	0.033*

H15B	0.984139	0.491335	0.957710	0.033*
C16	1.4488 (5)	0.32671 (17)	1.0912 (3)	0.0354 (7)
H16A	1.373347	0.280762	1.113564	0.053*
H16B	1.500930	0.351117	1.189100	0.053*
H16C	1.580937	0.316771	1.032535	0.053*
C15A	0.8762 (5)	0.40672 (14)	0.8112 (3)	0.0228 (5)

Table S2. Atomic displacement parameters (Å^2) for 1

	U^{11}	U^{22}	U^{33}	U^{12}	U^{13}	U^{23}
O1	0.0346 (12)	0.0348 (10)	0.0348 (10)	0.0107 (9)	-0.0033 (9)	-0.0064 (8)
O2	0.0329 (13)	0.0355 (11)	0.0332 (10)	0.0084 (9)	-0.0081 (9)	-0.0055 (8)
O3	0.0328 (11)	0.0325 (10)	0.0253 (9)	0.0085 (8)	-0.0043 (8)	-0.0043 (7)
C1	0.0263 (16)	0.0244 (13)	0.0308 (14)	-0.0006 (11)	0.0011 (11)	-0.0002 (10)
C2	0.0261 (16)	0.0310 (14)	0.0280 (13)	0.0020 (11)	-0.0023 (11)	0.0002 (11)
C3	0.0378 (17)	0.0308 (14)	0.0263 (13)	0.0024 (12)	-0.0017 (11)	-0.0031 (11)
C4	0.0292 (16)	0.0281 (12)	0.0245 (12)	0.0041 (11)	-0.0001 (11)	-0.0019 (10)
C5	0.0387 (18)	0.0351 (15)	0.0229 (13)	0.0025 (12)	-0.0009 (11)	-0.0029 (11)
C4A	0.0239 (15)	0.0264 (13)	0.0264 (13)	-0.0009 (11)	0.0007 (11)	0.0012 (10)
C6	0.0349 (18)	0.0336 (14)	0.0290 (13)	0.0020 (12)	-0.0029 (12)	-0.0050 (11)
C7	0.0356 (18)	0.0272 (13)	0.0276 (14)	0.0039 (11)	-0.0001 (12)	-0.0043 (10)
C8	0.0406 (18)	0.0423 (16)	0.0330 (14)	0.0116 (14)	-0.0080 (12)	-0.0031 (13)
C7A	0.0281 (16)	0.0234 (12)	0.0255 (12)	0.0008 (11)	0.0015 (11)	-0.0020 (10)
O4	0.0287 (11)	0.0308 (9)	0.0290 (9)	0.0055 (8)	0.0018 (8)	-0.0005 (7)
O5	0.0308 (12)	0.0417 (11)	0.0251 (9)	0.0114 (9)	-0.0072 (8)	-0.0050 (8)
O6	0.0228 (11)	0.0355 (10)	0.0229 (8)	0.0037 (8)	-0.0020 (7)	-0.0035 (7)
C9	0.0249 (15)	0.0238 (12)	0.0208 (11)	-0.0007 (10)	0.0046 (10)	0.0008 (9)
C10	0.0244 (15)	0.0307 (13)	0.0249 (12)	0.0007 (11)	-0.0037 (11)	-0.0003 (10)
C11	0.0313 (17)	0.0318 (13)	0.0212 (12)	0.0024 (11)	0.0004 (11)	-0.0049 (10)
C12	0.0211 (15)	0.0291 (13)	0.0253 (12)	0.0006 (10)	0.0024 (11)	-0.0019 (10)
C13	0.0250 (16)	0.0342 (14)	0.0200 (11)	-0.0047 (11)	-0.0008 (10)	-0.0032 (10)
C12A	0.0184 (15)	0.0289 (13)	0.0205 (11)	-0.0029 (10)	0.0007 (10)	0.0022 (9)
C14	0.0270 (16)	0.0343 (14)	0.0202 (11)	-0.0044 (11)	-0.0003 (10)	0.0003 (10)

C15	0.0277 (17)	0.0316 (13)	0.0232 (13)	0.0013 (11)	0.0016 (11)	-0.0037 (10)
C16	0.0274 (17)	0.0499 (17)	0.0277 (14)	0.0055 (14)	-0.0030 (11)	0.0012 (12)
C15A	0.0206 (14)	0.0274 (12)	0.0203 (11)	-0.0011 (10)	0.0014 (10)	-0.0005 (9)

Table S3. Geometric parameters (Å, º) for 1

O1—C1	1.227 (3)	O4—C9	1.233 (3)
O2—C2	1.406 (3)	O5—C10	1.413 (3)
O2—H2	0.82 (4)	O5—H5	0.80 (4)
O3—C4A	1.348 (3)	O6—C12A	1.350 (3)
O3—C5	1.462 (3)	O6—C13	1.468 (3)
C1—C7A	1.449 (4)	C9—C15A	1.448 (4)
C1—C2	1.525 (4)	C9—C10	1.519 (3)
C2—C3	1.511 (4)	C10—C11	1.501 (4)
C2—H2A	1.0000	C10—H10	1.0000
C3—C4	1.524 (4)	C11—C12	1.523 (4)
C3—H3A	0.9900	C11—H11A	0.9900
C3—H3B	0.9900	C11—H11B	0.9900
C4—C4A	1.500 (4)	C12—C12A	1.498 (3)
C4—H4A	0.9900	C12—H12A	0.9900
C4—H4B	0.9900	C12—H12B	0.9900
C5—C6	1.507 (4)	C13—C16	1.502 (4)
C5—C8	1.507 (4)	C13—C14	1.509 (4)
C5—H5A	1.0000	C13—H13	1.0000
C4A—C7A	1.355 (4)	C12A—C15A	1.352 (4)
C6—C7	1.518 (4)	C14—C15	1.519 (4)
C6—H6A	0.9900	C14—H14A	0.9900
C6—H6B	0.9900	C14—H14B	0.9900
C7—C7A	1.505 (3)	C15—C15A	1.507 (3)
C7—H7A	0.9900	C15—H15A	0.9900
C7—H7B	0.9900	C15—H15B	0.9900
C8—H8A	0.9800	C16—H16A	0.9800
C8—H8B	0.9800	C16—H16B	0.9800

C8—H8C	0.9800	C16—H16C	0.9800
C2—O2—H2	109 (3)	C10—O5—H5	109 (3)
C4A—O3—C5	116.1 (2)	C12A—O6—C13	117.62 (19)
O1—C1—C7A	122.3 (2)	O4—C9—C15A	122.1 (2)
O1—C1—C2	119.2 (2)	O4—C9—C10	119.7 (2)
C7A—C1—C2	118.4 (2)	C15A—C9—C10	118.1 (2)
O2—C2—C3	110.8 (2)	O5—C10—C11	110.9 (2)
O2—C2—C1	112.0 (2)	O5—C10—C9	111.7 (2)
C3—C2—C1	110.7 (2)	C11—C10—C9	110.8 (2)
O2—C2—H2A	107.7	O5—C10—H10	107.7
C3—C2—H2A	107.7	C11—C10—H10	107.7
C1—C2—H2A	107.7	C9—C10—H10	107.7
C2—C3—C4	110.3 (2)	C10—C11—C12	110.4 (2)
C2—C3—H3A	109.6	C10—C11—H11A	109.6
C4—C3—H3A	109.6	C12—C11—H11A	109.6
C2—C3—H3B	109.6	C10—C11—H11B	109.6
C4—C3—H3B	109.6	C12—C11—H11B	109.6
H3A—C3—H3B	108.1	H11A—C11—H11B	108.1
C4A—C4—C3	111.3 (2)	C12A—C12—C11	112.2 (2)
C4A—C4—H4A	109.4	C12A—C12—H12A	109.2
C3—C4—H4A	109.4	C11—C12—H12A	109.2
C4A—C4—H4B	109.4	C12A—C12—H12B	109.2
C3—C4—H4B	109.4	C11—C12—H12B	109.2
H4A—C4—H4B	108.0	H12A—C12—H12B	107.9
O3—C5—C6	110.1 (2)	O6—C13—C16	105.7 (2)
O3—C5—C8	106.3 (2)	O6—C13—C14	110.7 (2)
C6—C5—C8	114.1 (3)	C16—C13—C14	114.5 (2)
O3—C5—H5A	108.7	O6—C13—H13	108.6
C6—C5—H5A	108.7	C16—C13—H13	108.6
C8—C5—H5A	108.7	C14—C13—H13	108.6
O3—C4A—C7A	124.2 (2)	O6—C12A—C15A	124.1 (2)

O3—C4A—C4	111.9 (2)	O6—C12A—C12	111.2 (2)
C7A—C4A—C4	123.9 (2)	C15A—C12A—C12	124.7 (2)
C5—C6—C7	110.2 (2)	C13—C14—C15	109.7 (2)
C5—C6—H6A	109.6	C13—C14—H14A	109.7
C7—C6—H6A	109.6	C15—C14—H14A	109.7
C5—C6—H6B	109.6	C13—C14—H14B	109.7
C7—C6—H6B	109.6	C15—C14—H14B	109.7
H6A—C6—H6B	108.1	H14A—C14—H14B	108.2
C7A—C7—C6	110.0 (2)	C15A—C15—C14	109.5 (2)
C7A—C7—H7A	109.7	C15A—C15—H15A	109.8
C6—C7—H7A	109.7	C14—C15—H15A	109.8
C7A—C7—H7B	109.7	C15A—C15—H15B	109.8
C6—C7—H7B	109.7	C14—C15—H15B	109.8
H7A—C7—H7B	108.2	H15A—C15—H15B	108.2
C5—C8—H8A	109.5	C13—C16—H16A	109.5
C5—C8—H8B	109.5	C13—C16—H16B	109.5
H8A—C8—H8B	109.5	H16A—C16—H16B	109.5
C5—C8—H8C	109.5	C13—C16—H16C	109.5
H8A—C8—H8C	109.5	H16A—C16—H16C	109.5
H8B—C8—H8C	109.5	H16B—C16—H16C	109.5
C4A—C7A—C1	119.6 (2)	C12A—C15A—C9	119.0 (2)
C4A—C7A—C7	121.6 (2)	C12A—C15A—C15	121.2 (2)
C1—C7A—C7	118.8 (2)	C9—C15A—C15	119.8 (2)

Table S4. Hydrogen-bond geometry (Å, º) for 1

D—H···*A*	*D*—H	H···*A*	*D*···*A*	*D*—H···*A*
O2—H2···O1	0.82 (4)	2.28 (4)	2.700 (3)	112 (3)
O2—H2···O4^{i}	0.82 (4)	2.12 (4)	2.860 (3)	150 (4)
C2—H2*A*···O4	1.00	2.63	3.504 (3)	147
C4—H4*A*···O2^{ii}	0.99	2.66	3.602 (3)	160
C8—H8*A*···O2^{iii}	0.98	2.59	3.530 (3)	161
O5—H5···O1^{ii}	0.80 (4)	2.19 (4)	2.892 (3)	148 (4)

O5—H5···O4	0.80 (4)	2.25 (4)	2.692 (3)	116 (3)
C11—H11*A*···O1	0.99	2.56	3.474 (3)	153
C13—H13···O4^{i}	1.00	2.56	3.367 (3)	138
C16—H16*B*···O5^{iv}	0.98	2.60	3.513 (3)	155

Symmetry codes: (i) *x*+1, *y*, *z*; (ii) *x*-1, *y*, *z*; (iii) *x*-1, *y*, *z*-1; (iv) *x*+1, *y*, *z*+1.

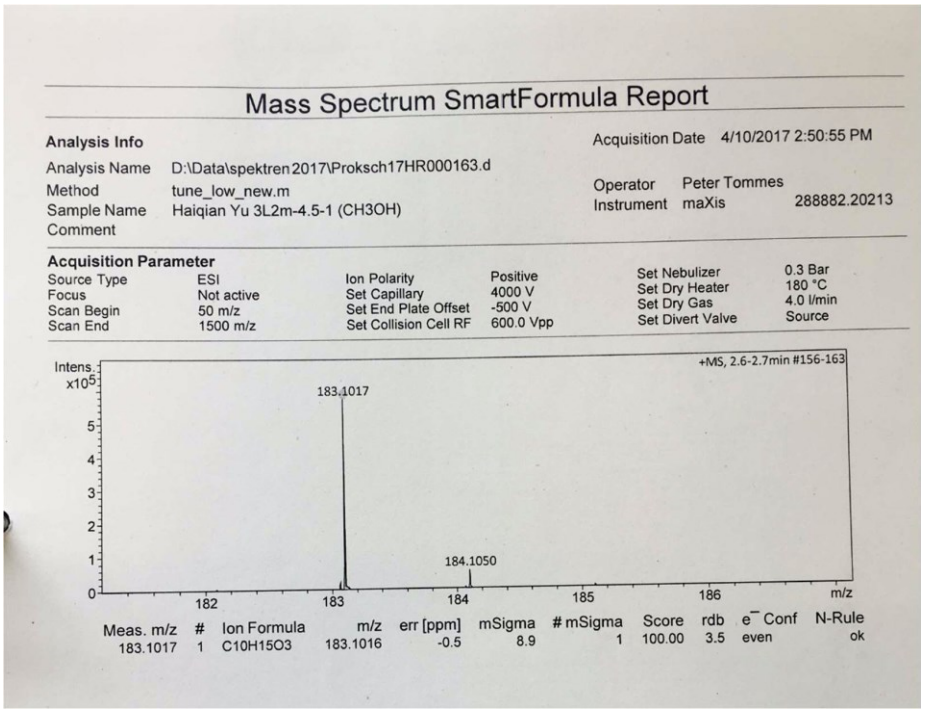

Figure S4. The HRESIMS of compound 1

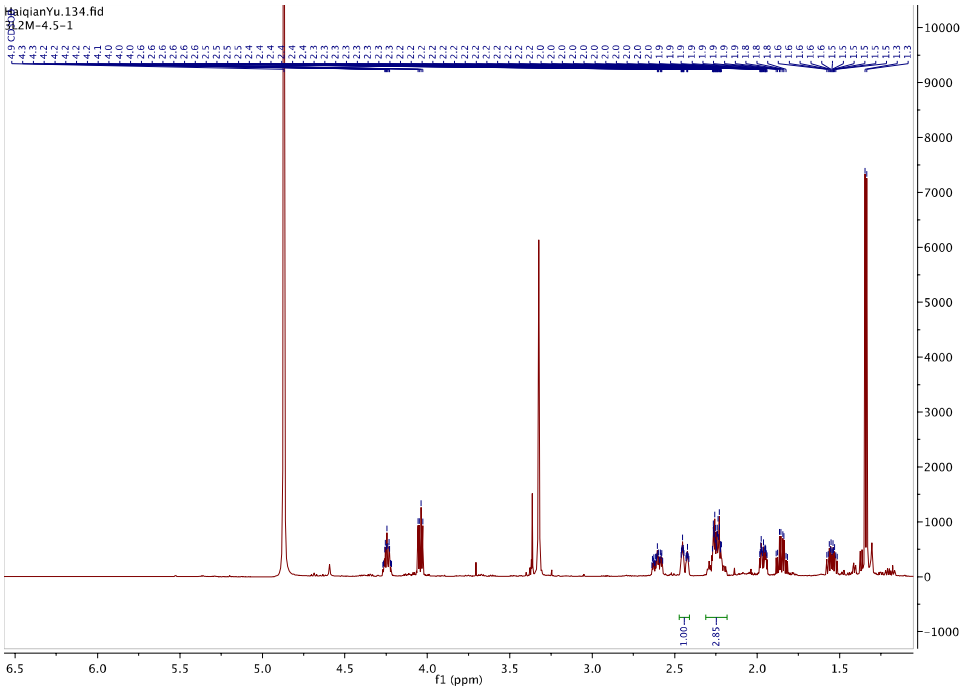

Figure S5. The ^{1}H NMR (600 MHz, CD_3OD) spectrum of compound 1

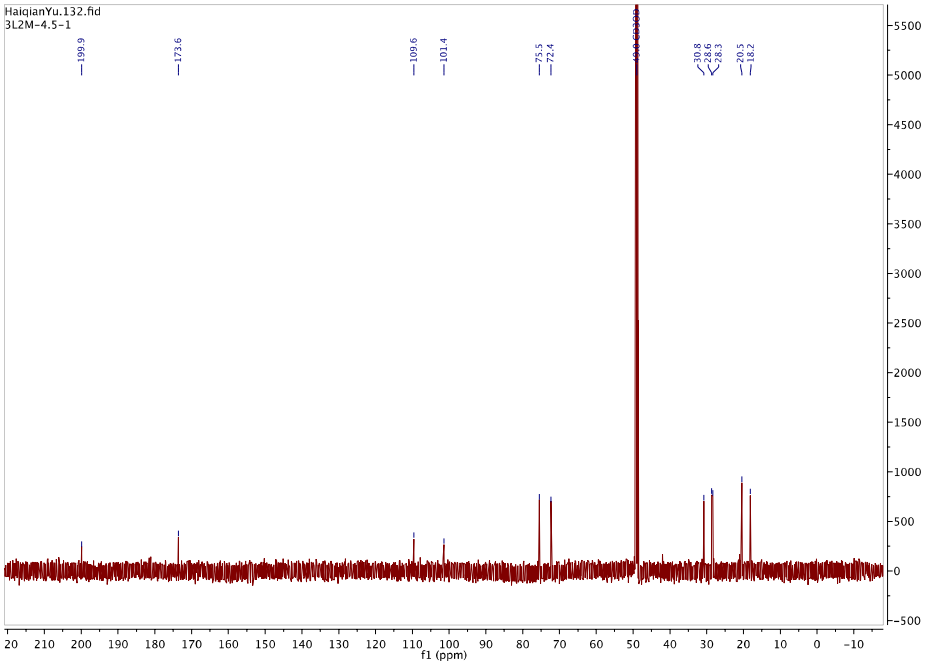

Figure S6. The ^{13}C NMR (150 MHz, CD_3OD) spectrum of compound 1

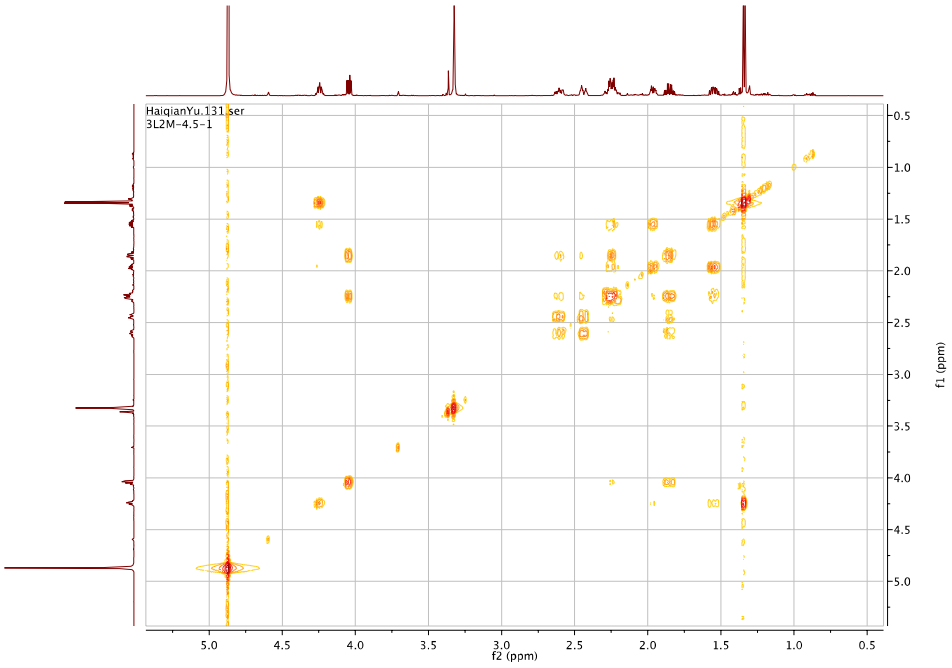

Figure S7. The COSY (600 MHz, CD_3OD) spectrum of compound 1

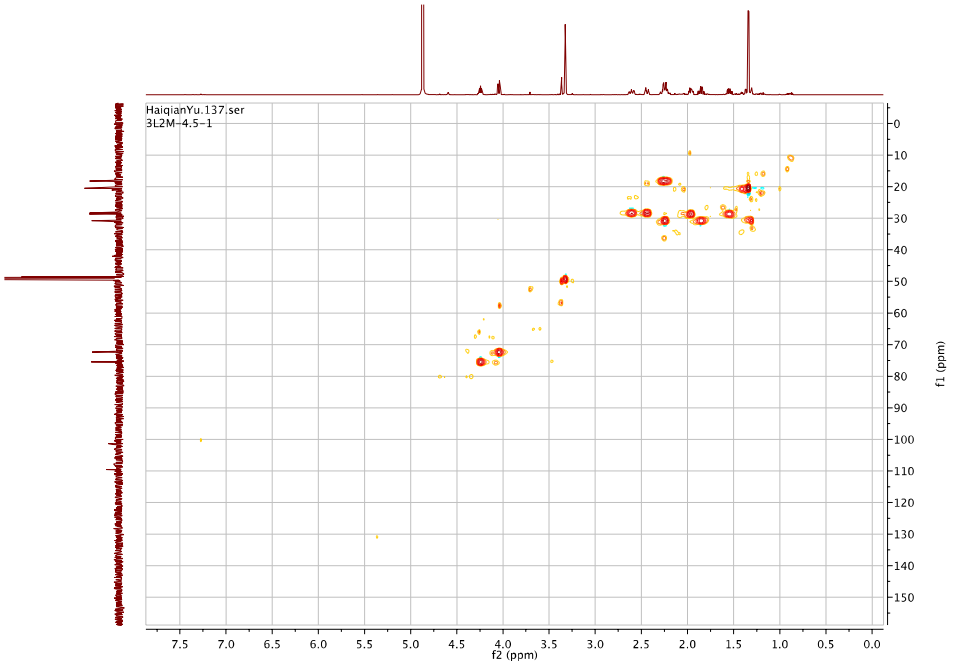

Figure S8. The HSQC (600 MHz, CD_3OD) spectrum of compound 1

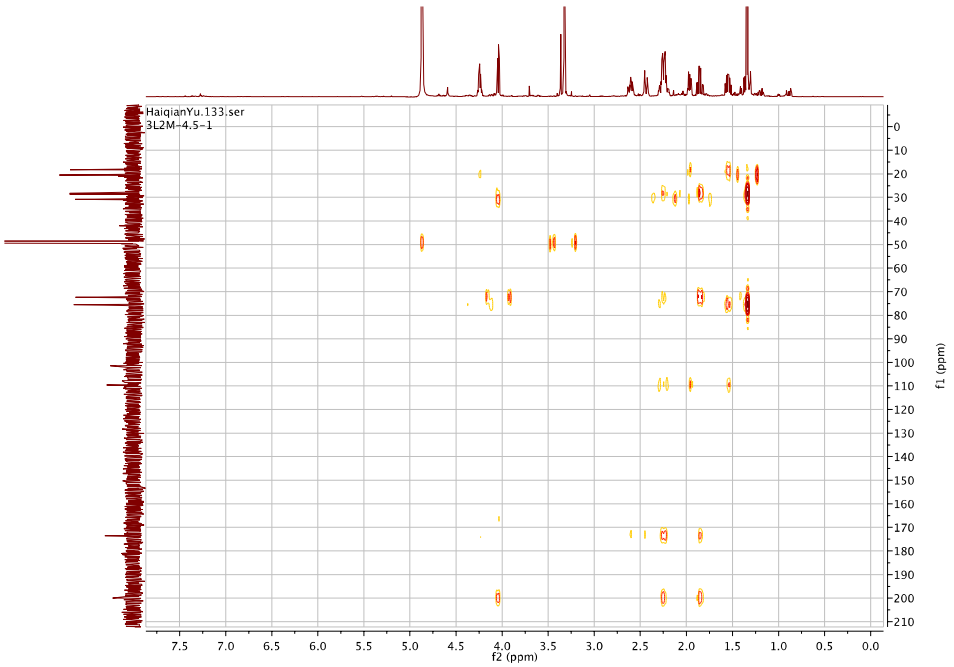

Figure S9. The HMBC (600 MHz, CD_3OD) spectrum of compound 1

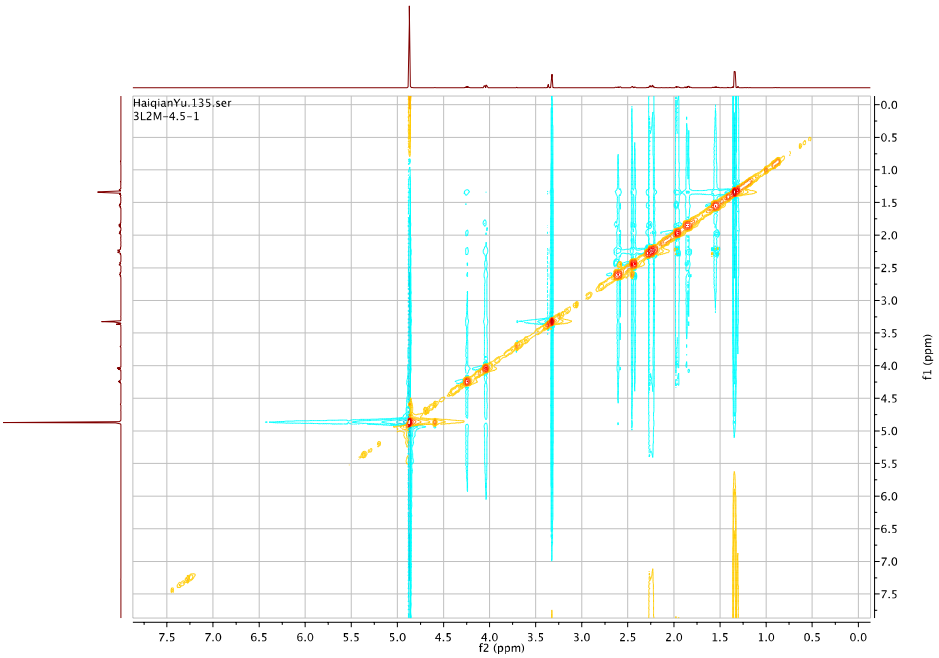

Figure S10. The ROESY (600 MHz, CD_3OD) spectrum of compound 1

Figure S11. The UV spectrum of compound 1

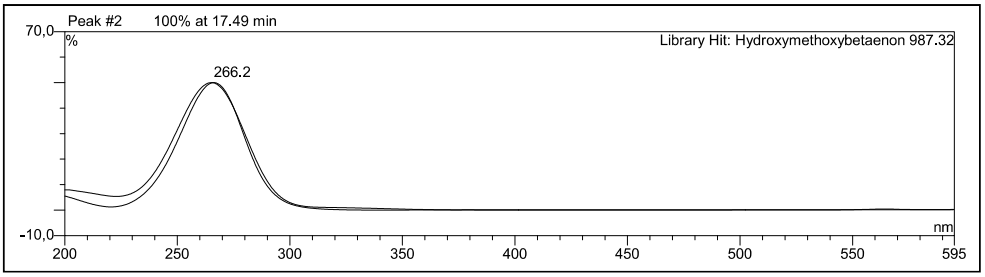

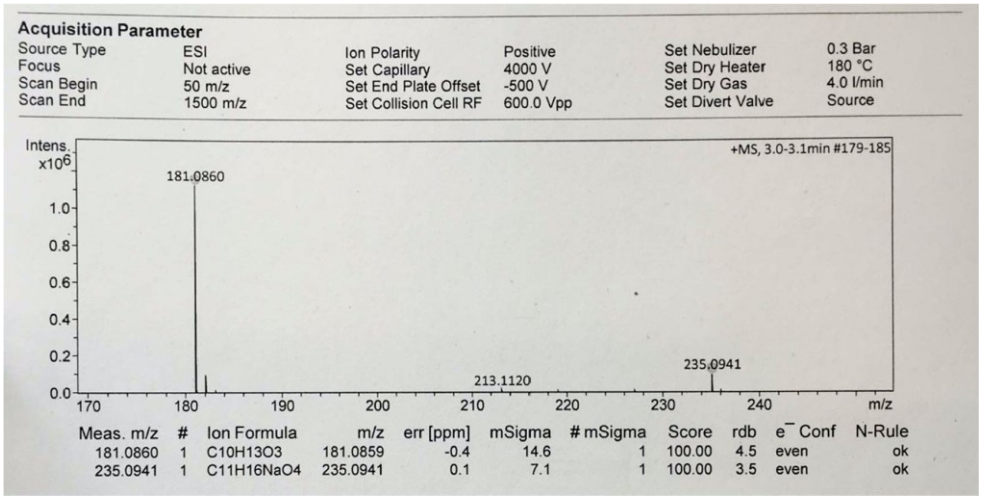

Figure S12. The HRESIMS of compound 2

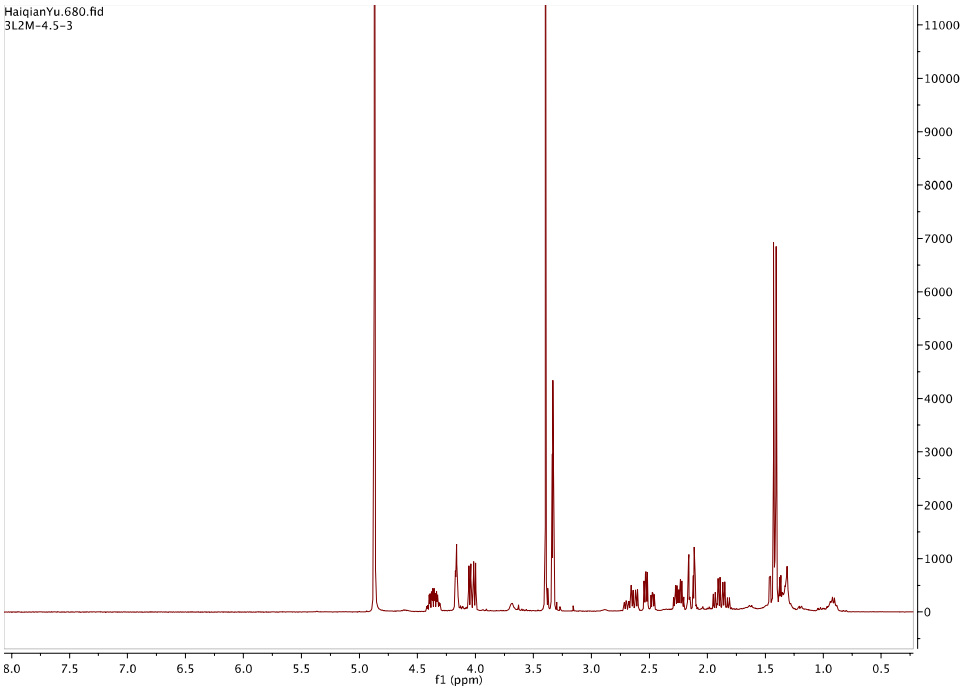

Figure S13. The ^{1}H NMR (300 MHz, CD_3OD) spectrum of compound 2

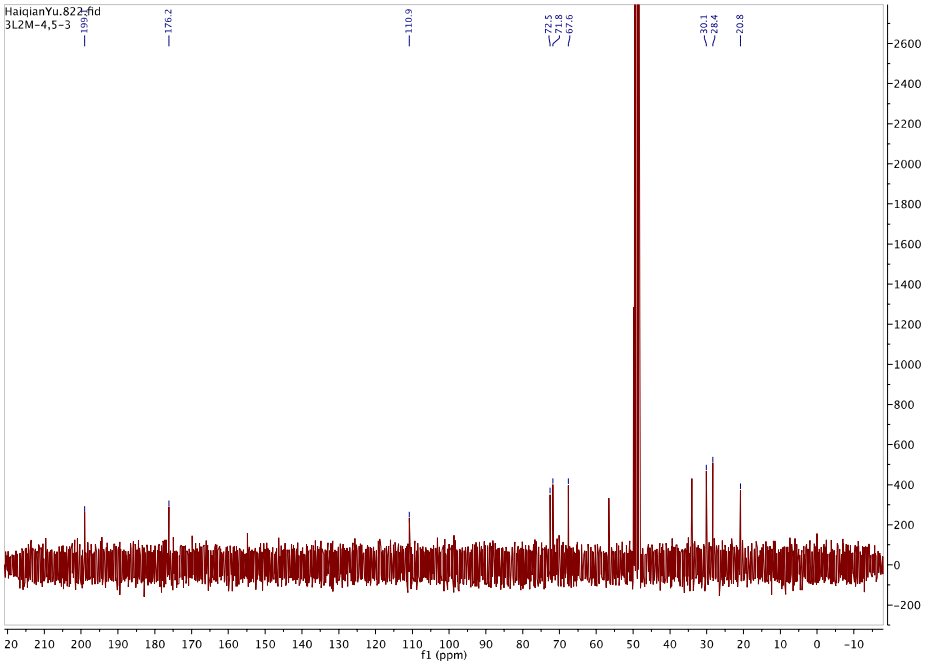

Figure S14. The ^{13}C NMR (75 MHz, CD_3OD) spectrum of compound 2

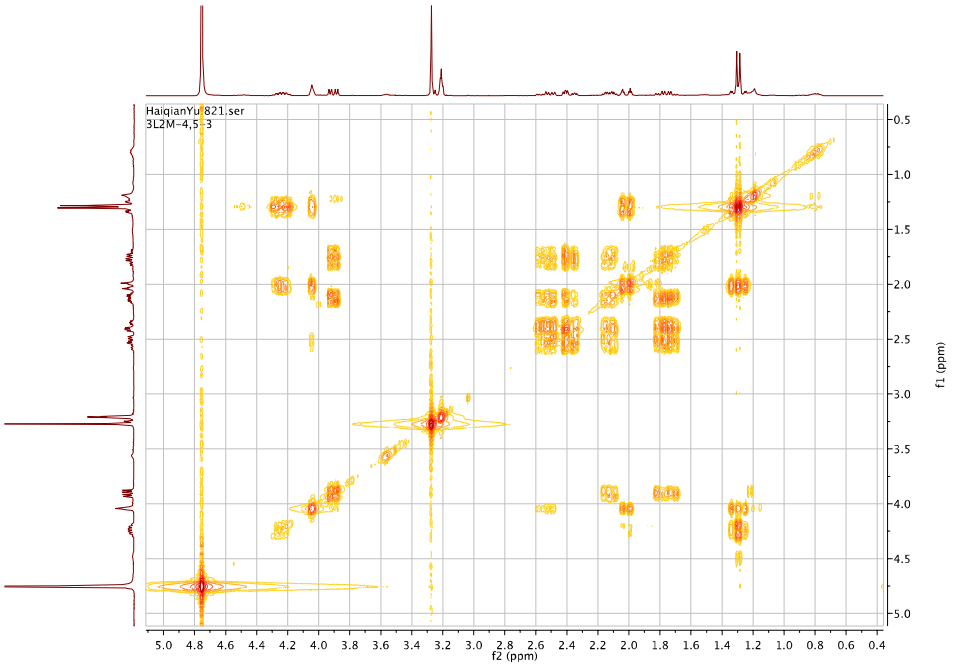

Figure S15. The COSY (300 MHz, CD_3OD) spectrum of compound 2

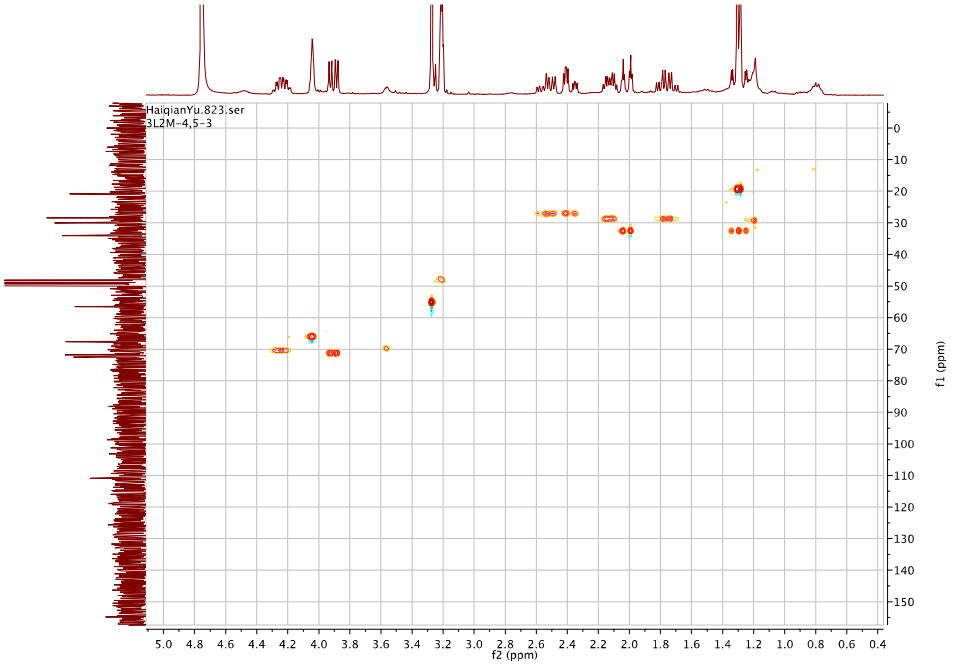

Figure S16. The HSQC (300 MHz, CD_3OD) spectrum of compound 2

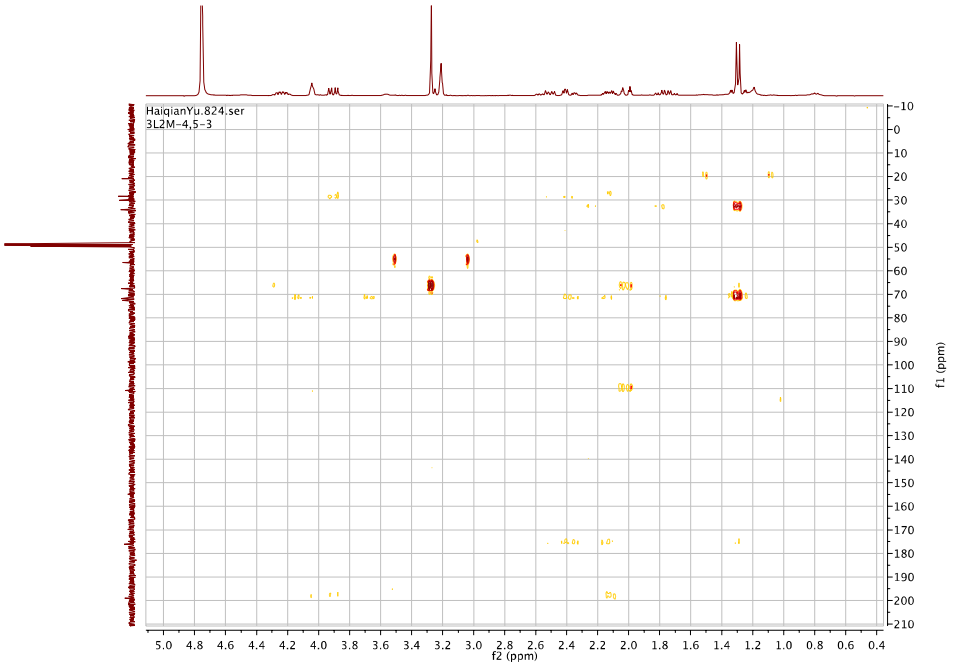

Figure S17. The HMBC (300 MHz, CD_3OD) spectrum of compound 2

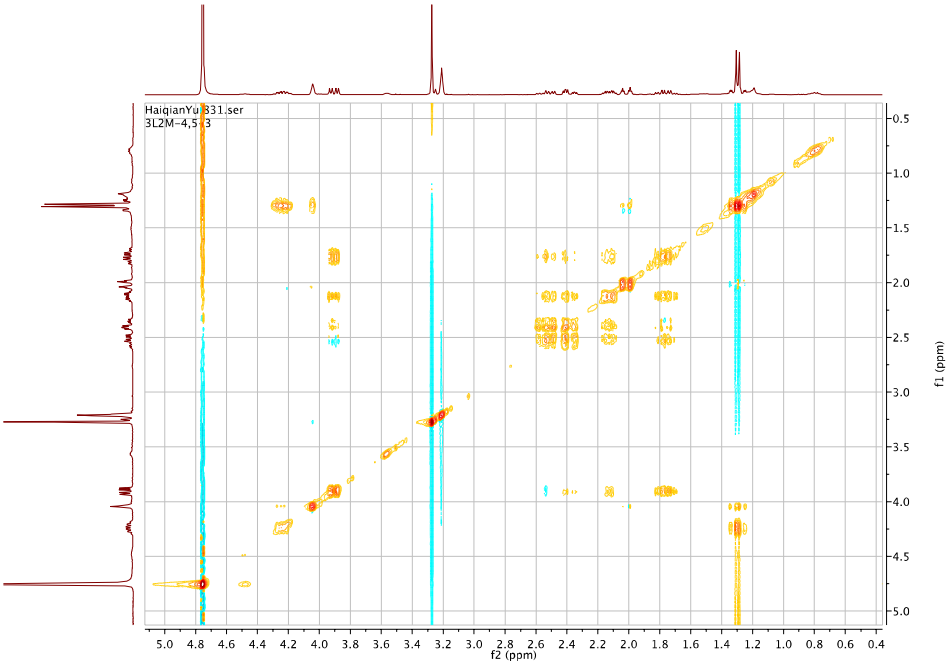

Figure S18. The ROESY (300 MHz, CD_3OD) spectrum of compound 2

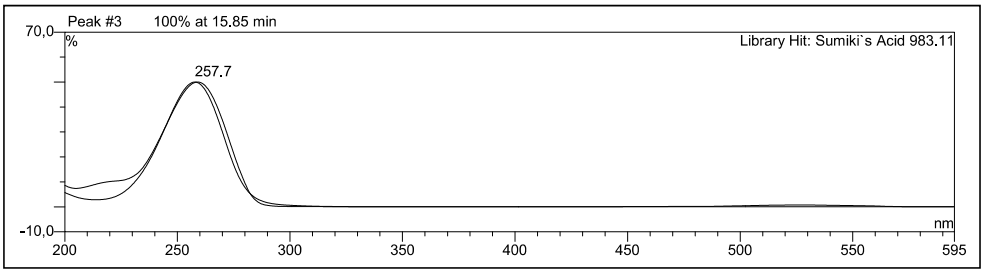

Figure S19. The UV spectrum of compound 2

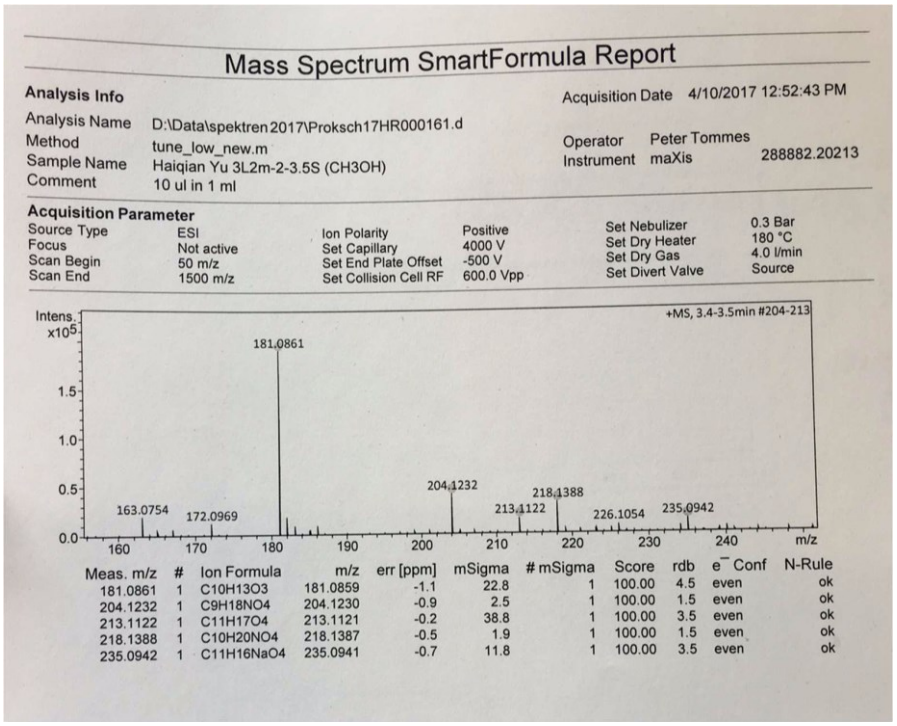

Mass Spectrum SmartFormula Report

Analysis Info

Analysis Name	D:\Data\spektren 2017\Proksch17HR000161.d	Acquisition Date	4/10/2017 12:52:43 PM
Method	tune_low_new.m	Operator	Peter Tommes
Sample Name	Haiqian Yu 3L2m-2-3.5S (CH3OH)	Instrument	maXis 288882.20213
Comment	10 ul in 1 ml		

Acquisition Parameter

Source Type	ESI	Ion Polarity	Positive	Set Nebulizer	0.3 Bar
Focus	Not active	Set Capillary	4000 V	Set Dry Heater	180 °C
Scan Begin	50 m/z	Set End Plate Offset	-500 V	Set Dry Gas	4.0 l/min
Scan End	1500 m/z	Set Collision Cell RF	600.0 Vpp	Set Divert Valve	Source

Meas. m/z	#	Ion Formula	m/z	err [ppm]	mSigma	# mSigma	Score	rdb	e⁻ Conf	N-Rule
181.0861	1	C10H13O3	181.0859	-1.1	22.8	1	100.00	4.5	even	ok
204.1232	1	C9H18NO4	204.1230	-0.9	2.5	1	100.00	1.5	even	ok
213.1122	1	C11H17O4	213.1121	-0.2	38.8	1	100.00	3.5	even	ok
218.1388	1	C10H20NO4	218.1387	-0.5	1.9	1	100.00	1.5	even	ok
235.0942	1	C11H16NaO4	235.0941	-0.7	11.8	1	100.00	3.5	even	ok

Figure S20. The HRESIMS of compound 3

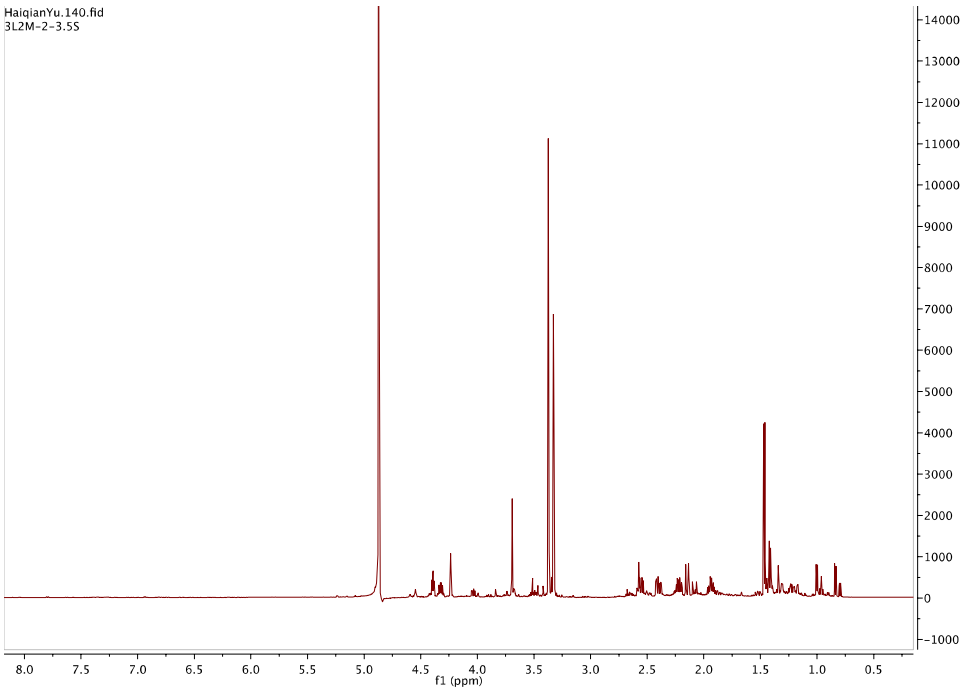

Figure S21. The ^{1}H NMR (600 MHz, CD_3OD) spectrum of compound 3

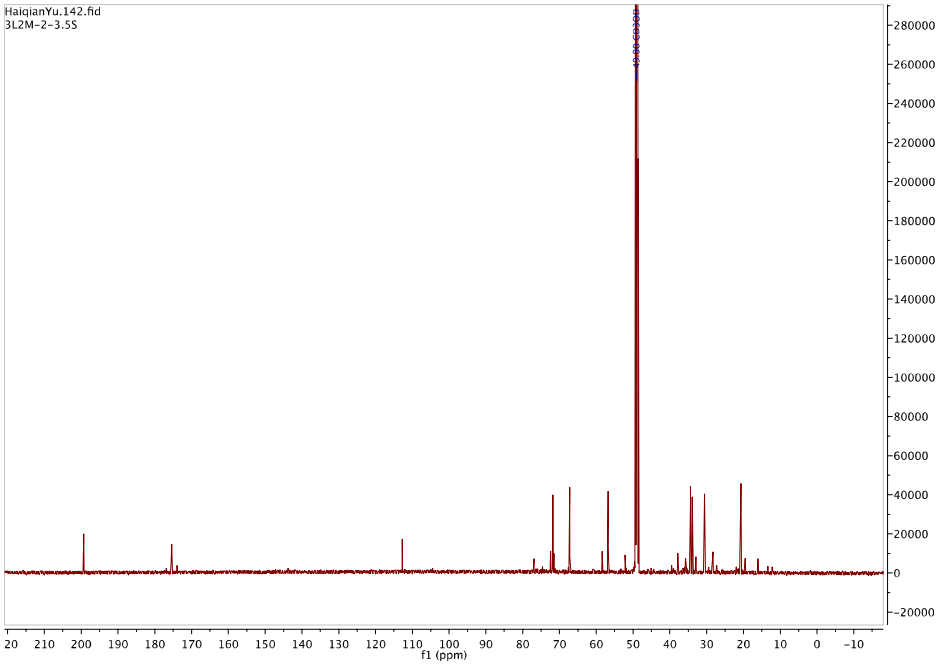

Figure S22. The ^{13}C NMR (150 MHz, CD_3OD) spectrum of compound 3

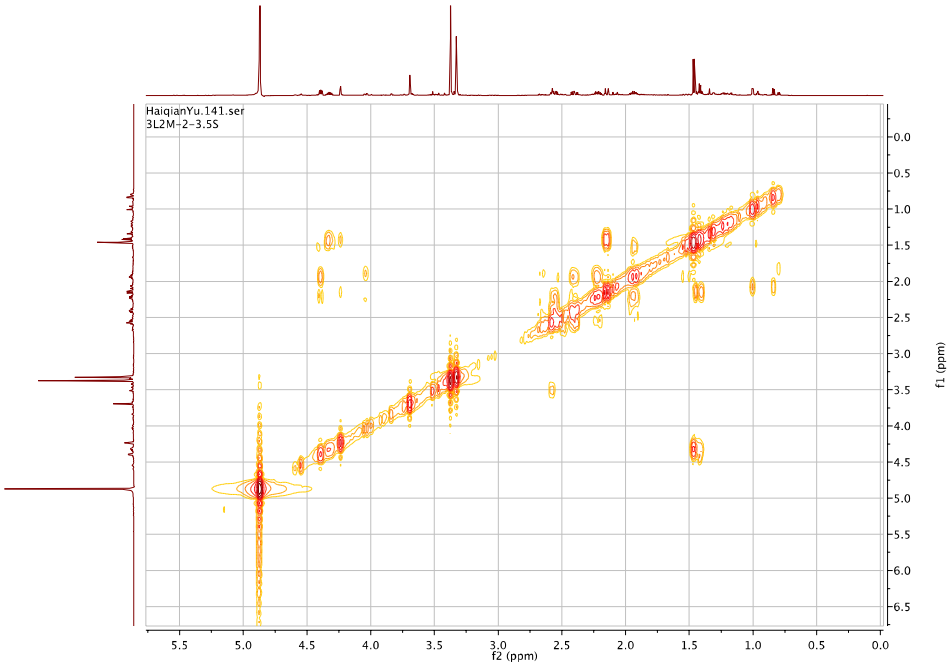

Figure S23. The COSY (600 MHz, CD_3OD) spectrum of compound 3

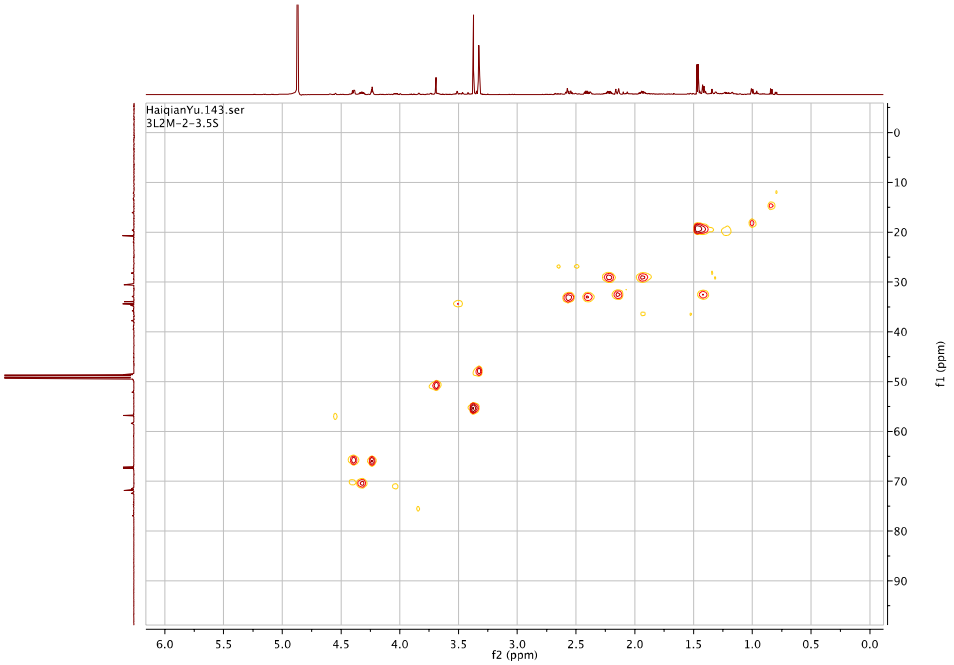

Figure S24. The HSQC (600 MHz, CD_3OD) spectrum of compound 3

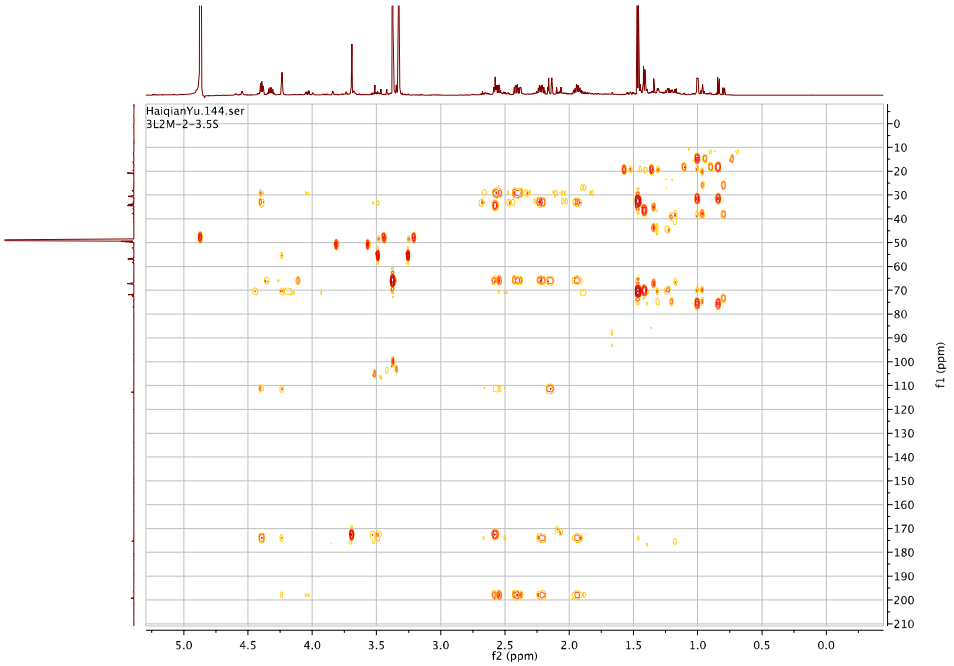

Figure S25. The HMBC (600 MHz, CD_3OD) spectrum of compound 3

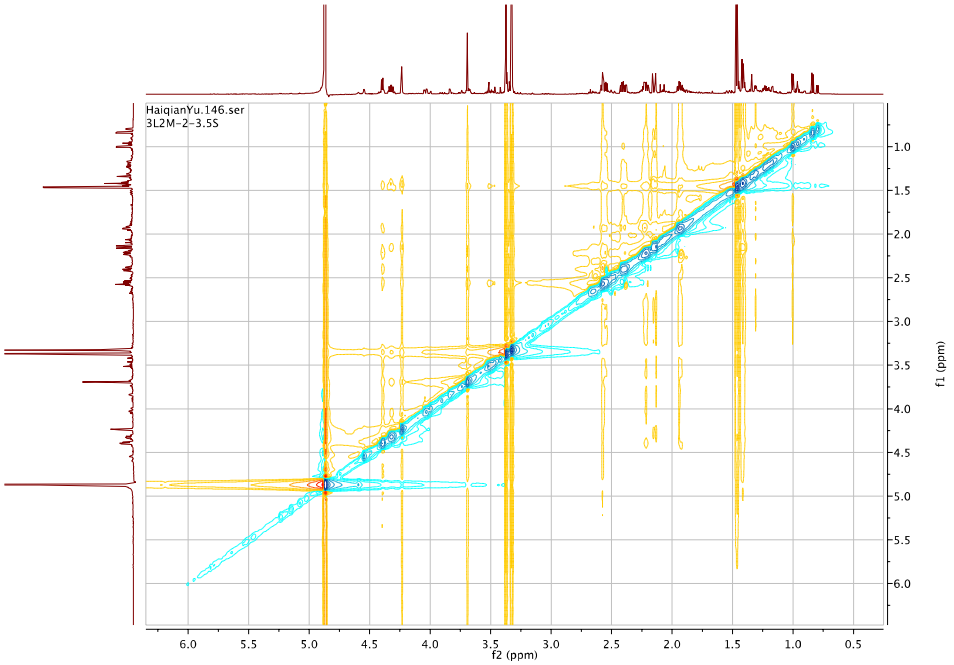

Figure S26. The ROESY (300 MHz, CD_3OD) spectrum of compound 3

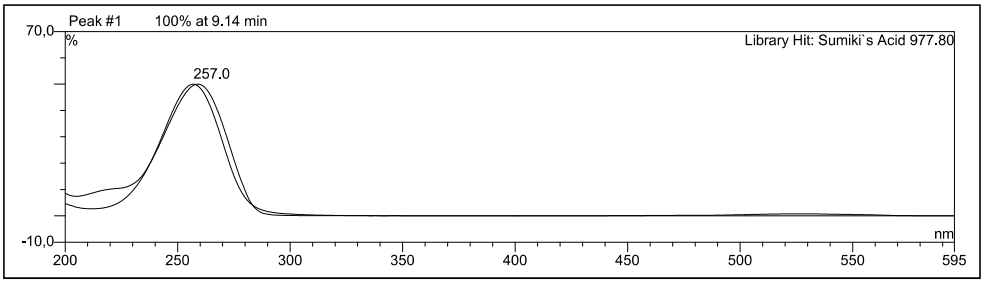

Figure S27. The UV spectrum of compound 3

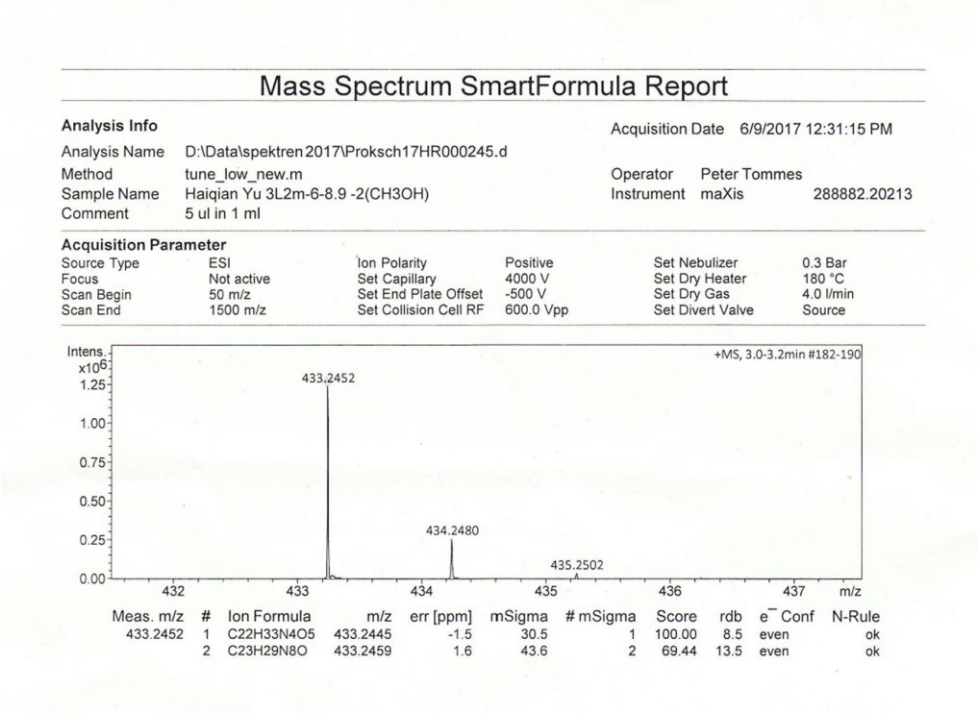

Figure S28. The HRESIMS of compound 4

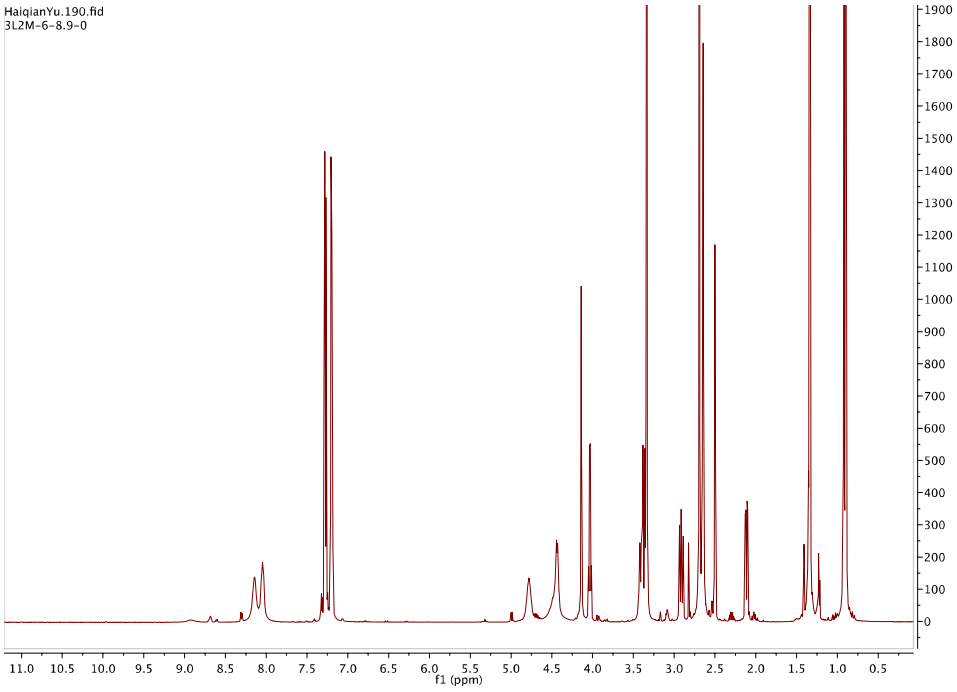

Figure S29. The ^{1}H NMR (600 MHz, DMSO-d_6) spectrum of compound 4

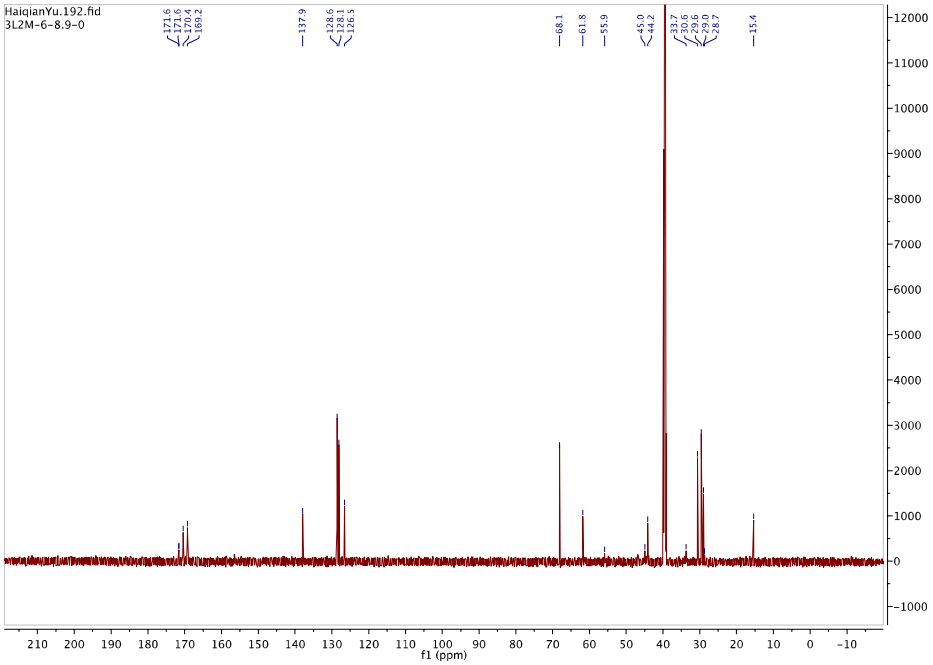

Figure S30. The ^{13}C NMR (150 MHz, DMSO-d_6) spectrum of compound 4

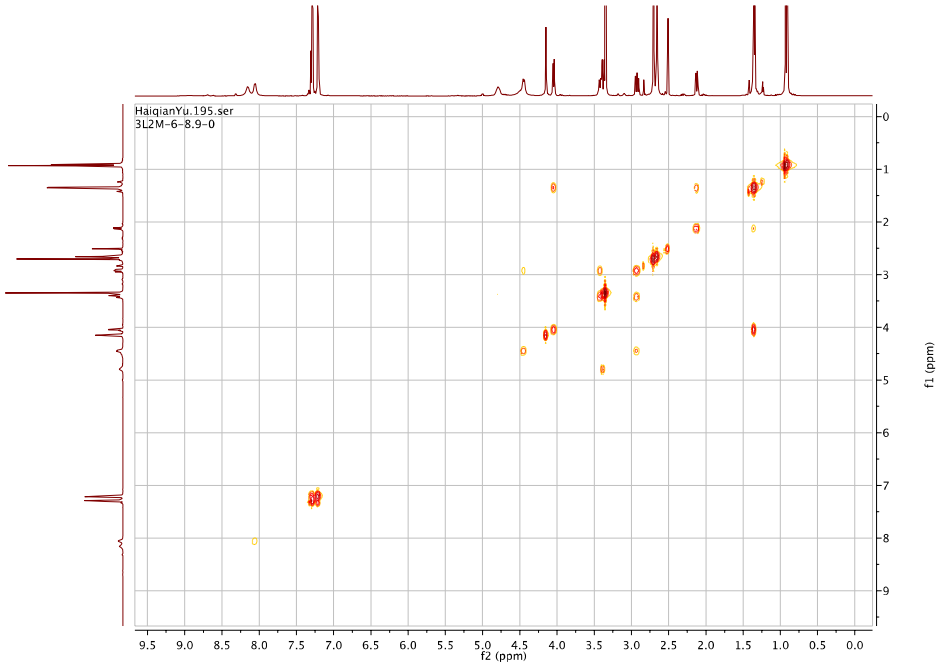

Figure S31. The COSY (600 MHz, DMSO-d_6) spectrum of compound 4

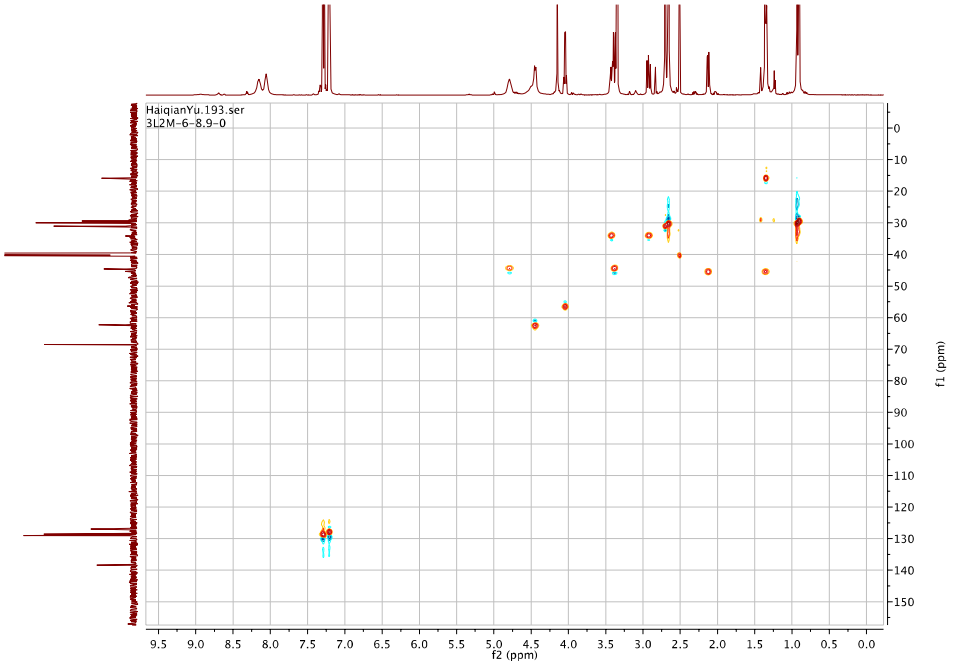

Figure S32. The HSQC (600 MHz, DMSO-d_6) spectrum of compound 4

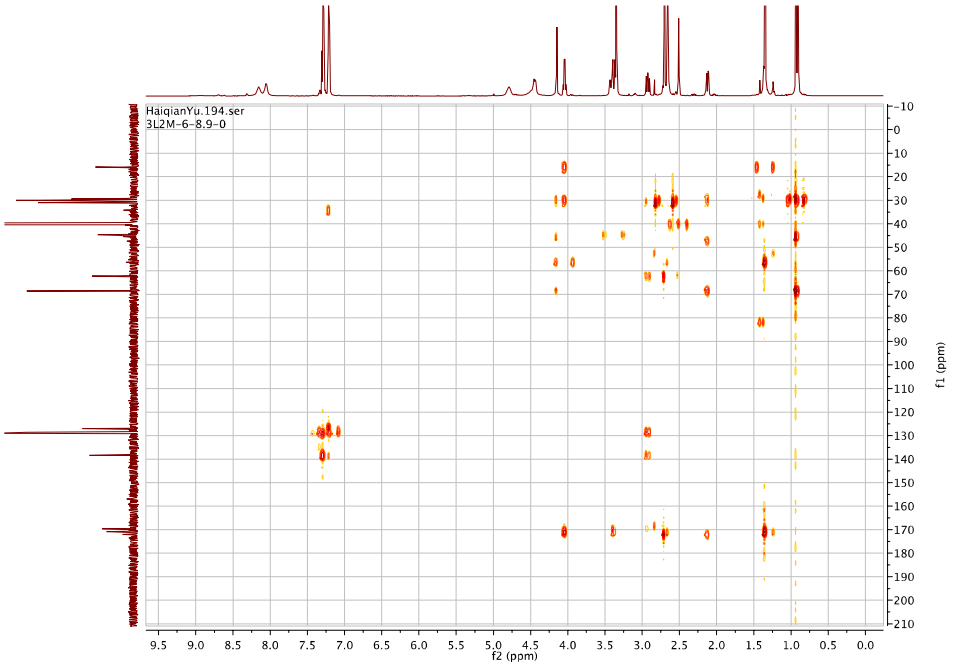

Figure S33. The HMBC (600 MHz, DMSO-d_6) spectrum of compound 4

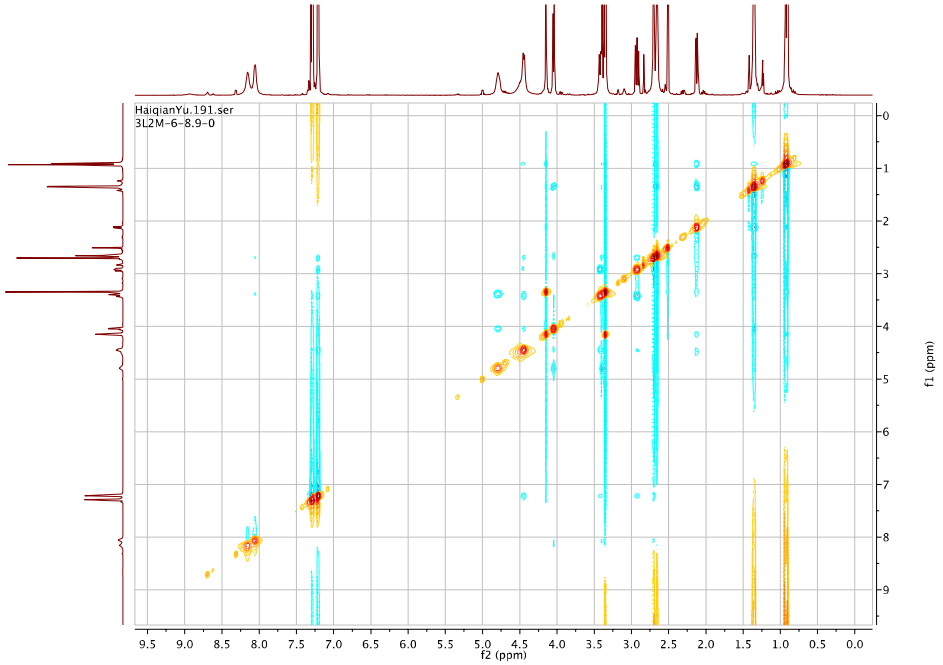

Figure S34. The ROESY (600 MHz, DMSO-d_6) spectrum of compound 4

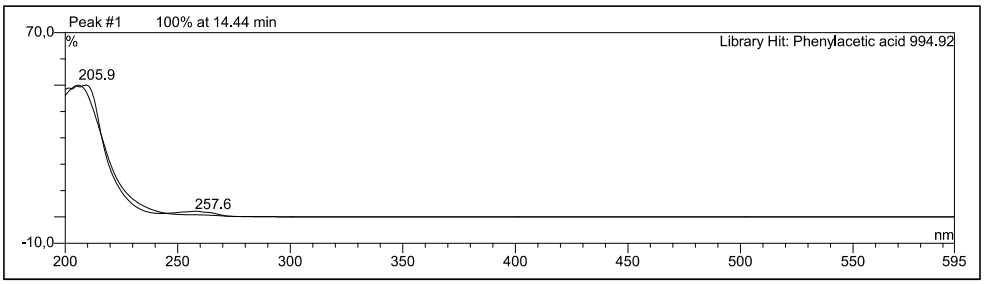

Figure S35. The UV spectrum of compound 4

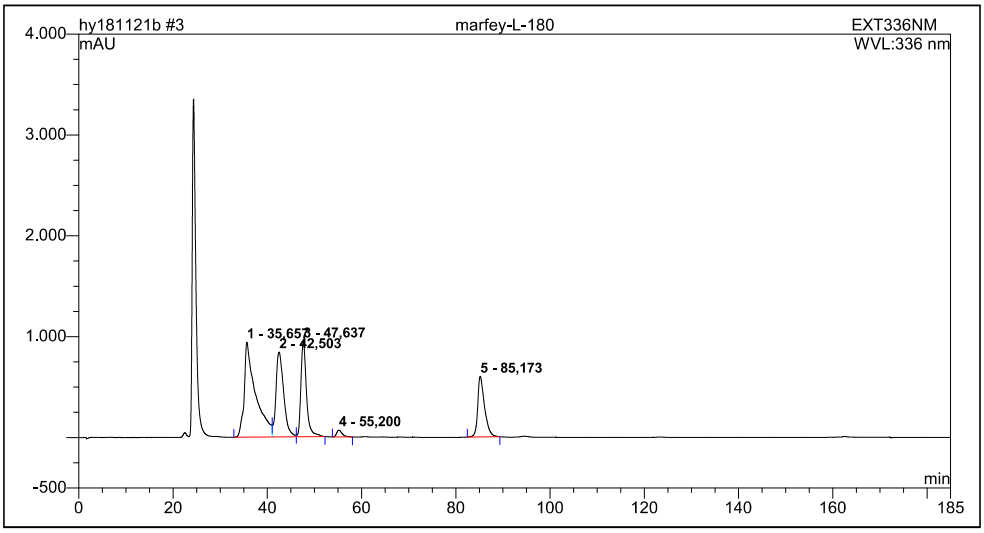

Figure S36. The HPLC chromatogram of Marfey's reaction with L-FDAA

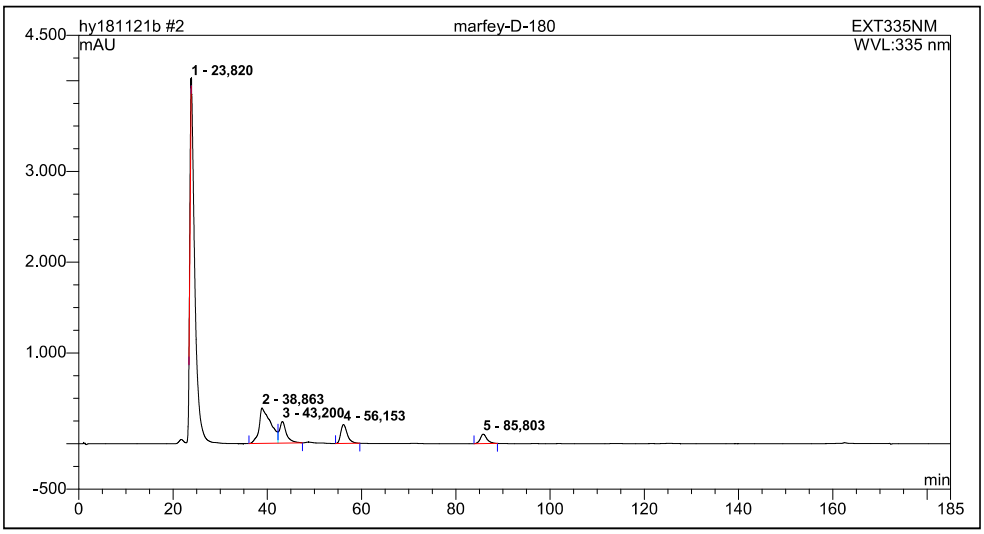

Figure S37. The HPLC chromatogram of Marfey's reaction with D-FDAA

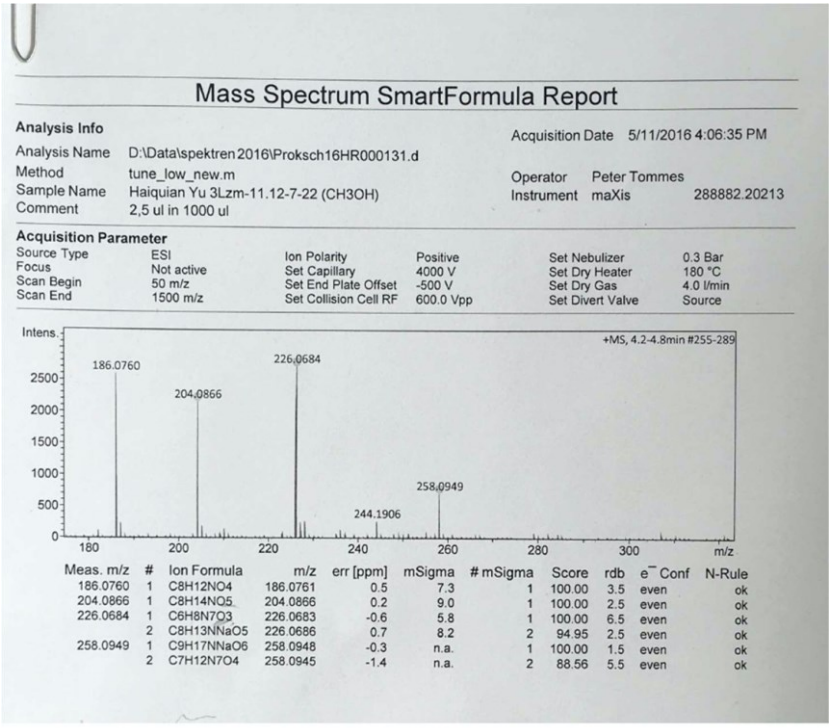

Mass Spectrum SmartFormula Report

Analysis Info

Analysis Name	D:\Data\spektren 2016\Proksch16HR000131.d	Acquisition Date	5/11/2016 4:06:35 PM
Method	tune_low_new.m	Operator	Peter Tommes
Sample Name	Haiquian Yu 3Lzm-11.12-7-22 (CH3OH)	Instrument	maXis 288882.20213
Comment	2,5 ul in 1000 ul		

Acquisition Parameter

Source Type	ESI	Ion Polarity	Positive	Set Nebulizer	0.3 Bar
Focus	Not active	Set Capillary	4000 V	Set Dry Heater	180 °C
Scan Begin	50 m/z	Set End Plate Offset	-500 V	Set Dry Gas	4.0 l/min
Scan End	1500 m/z	Set Collision Cell RF	600.0 Vpp	Set Divert Valve	Source

Meas. m/z	#	Ion Formula	m/z	err [ppm]	mSigma	# mSigma	Score	rdb	e⁻ Conf	N-Rule
186.0760	1	C8H12NO4	186.0761	0.5	7.3	1	100.00	3.5	even	ok
204.0866	1	C8H14NO5	204.0866	0.2	9.0	1	100.00	2.5	even	ok
226.0684	1	C6H8N7O3	226.0683	-0.6	5.8	1	100.00	6.5	even	ok
	2	C8H13NNaO5	226.0686	0.7	8.2	2	94.95	2.5	even	ok
258.0949	1	C9H17NNaO6	258.0948	-0.3	n.a.	1	100.00	1.5	even	ok
	2	C7H12N7O4	258.0945	-1.4	n.a.	2	88.56	5.5	even	ok

Figure S38. The HRESIMS of compound 5

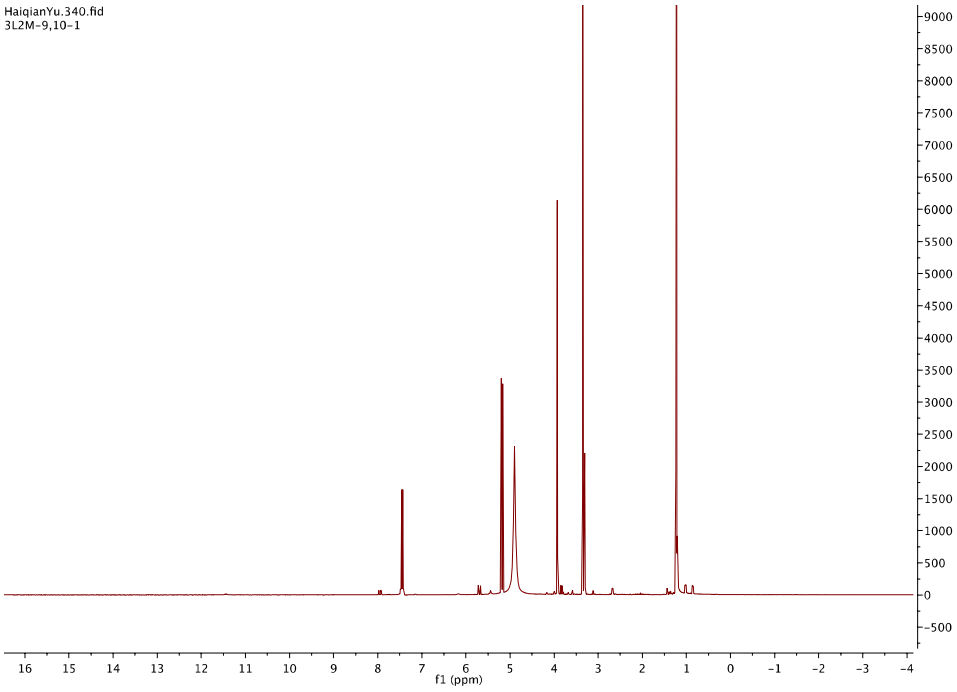

Figure S39. The ^{1}H NMR (300 MHz, CD_3OD) spectrum of compound 5

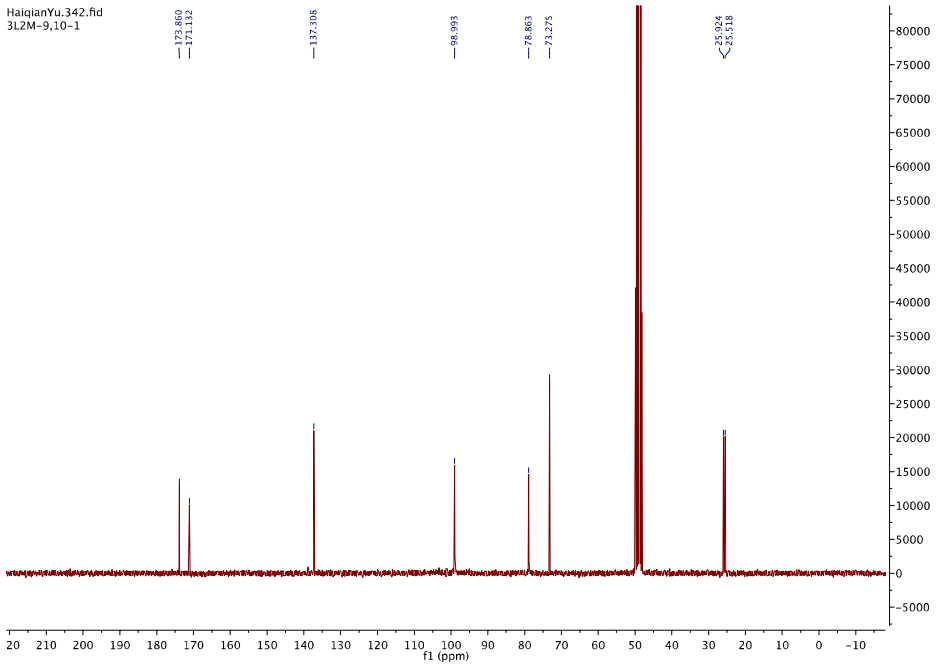

Figure S40. The ^{13}C NMR (75 MHz, CD_3OD) spectrum of compound 5

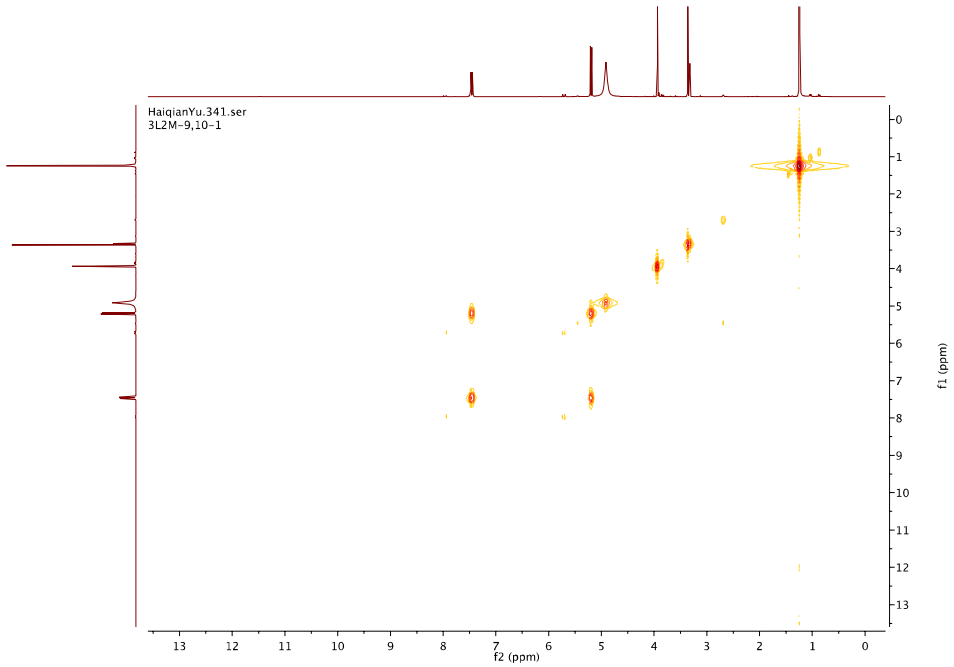

Figure S41. The COSY (300 MHz, CD_3OD) spectrum of compound 5

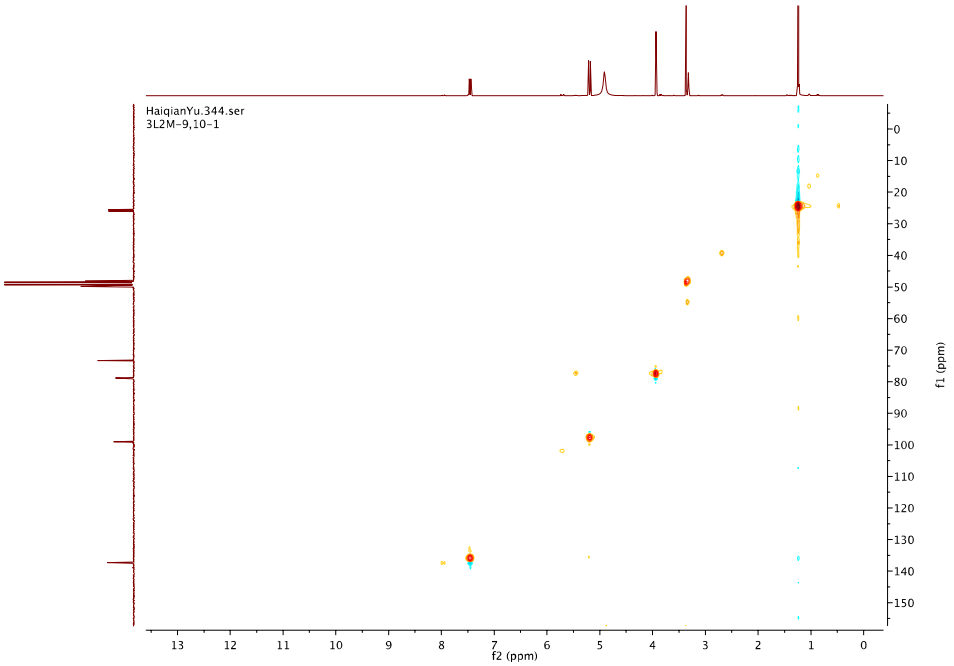

Figure S42. The HSQC (300 MHz, CD_3OD) spectrum of compound 5

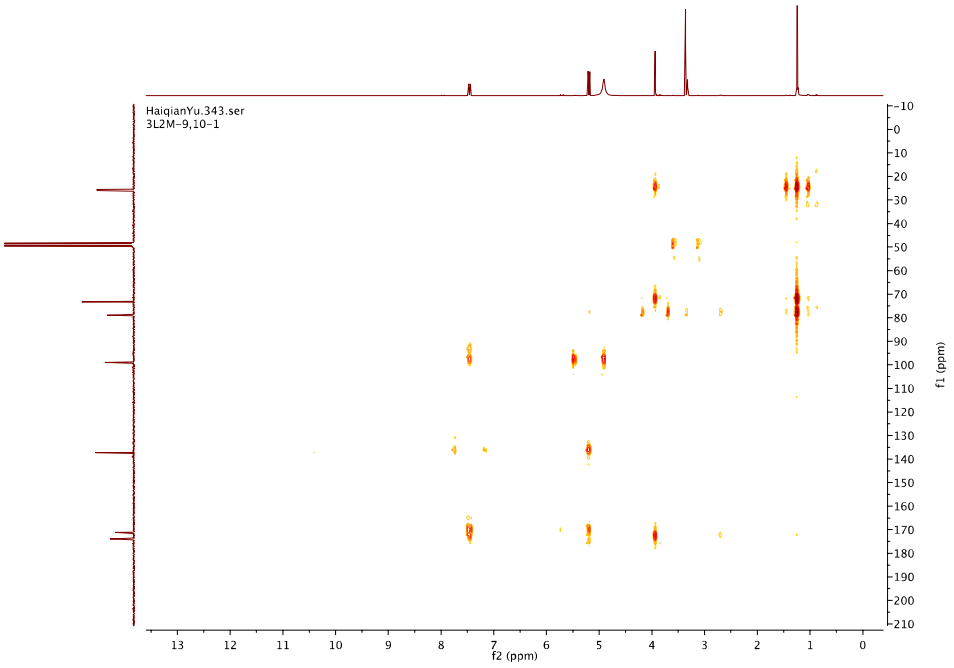

Figure S43. The HMBC (300 MHz, CD_3OD) spectrum of compound 5

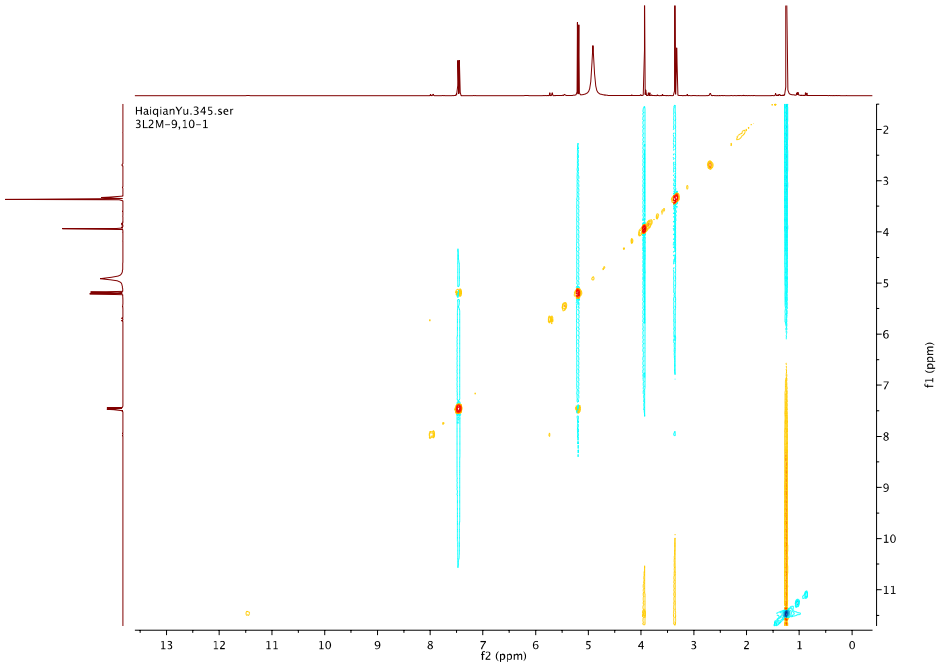

Figure S44. The ROESY (300 MHz, CD_3OD) spectrum of compound 5

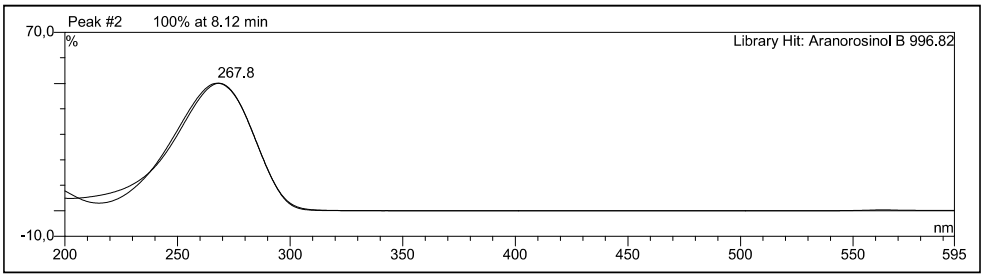

Figure S45. The UV spectrum of compound 5

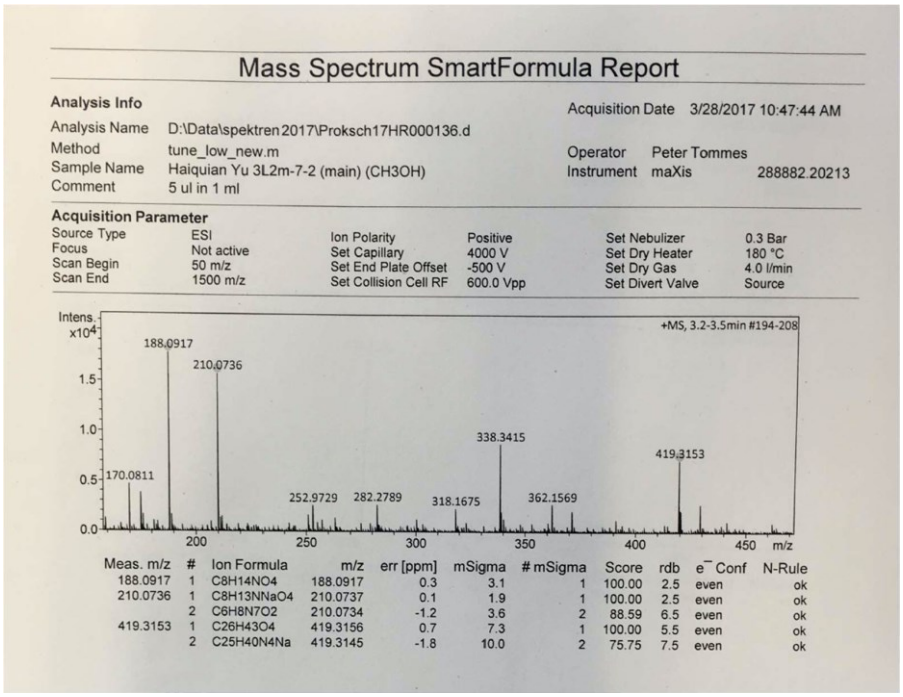

Mass Spectrum SmartFormula Report

Analysis Info

Analysis Name	D:\Data\spektren 2017\Proksch17HR000136.d	Acquisition Date	3/28/2017 10:47:44 AM
Method	tune_low_new.m	Operator	Peter Tommes
Sample Name	Haiquian Yu 3L2m-7-2 (main) (CH3OH)	Instrument	maXis 288882.20213
Comment	5 ul in 1 ml		

Acquisition Parameter

Source Type	ESI	Ion Polarity	Positive	Set Nebulizer	0.3 Bar
Focus	Not active	Set Capillary	4000 V	Set Dry Heater	180 °C
Scan Begin	50 m/z	Set End Plate Offset	-500 V	Set Dry Gas	4.0 l/min
Scan End	1500 m/z	Set Collision Cell RF	600.0 Vpp	Set Divert Valve	Source

Meas. m/z	#	Ion Formula	m/z	err [ppm]	mSigma	# mSigma	Score	rdb	e⁻ Conf	N-Rule
188.0917	1	C8H14NO4	188.0917	0.3	3.1	1	100.00	2.5	even	ok
210.0736	1	C8H13NNaO4	210.0737	0.1	1.9	1	100.00	2.5	even	ok
	2	C6H8N7O2	210.0734	-1.2	3.6	2	88.59	6.5	even	ok
419.3153	1	C26H43O4	419.3156	0.7	7.3	1	100.00	5.5	even	ok
	2	C25H40N4Na	419.3145	-1.8	10.0	2	75.75	7.5	even	ok

Figure S46. The HRESIMS of compound 6

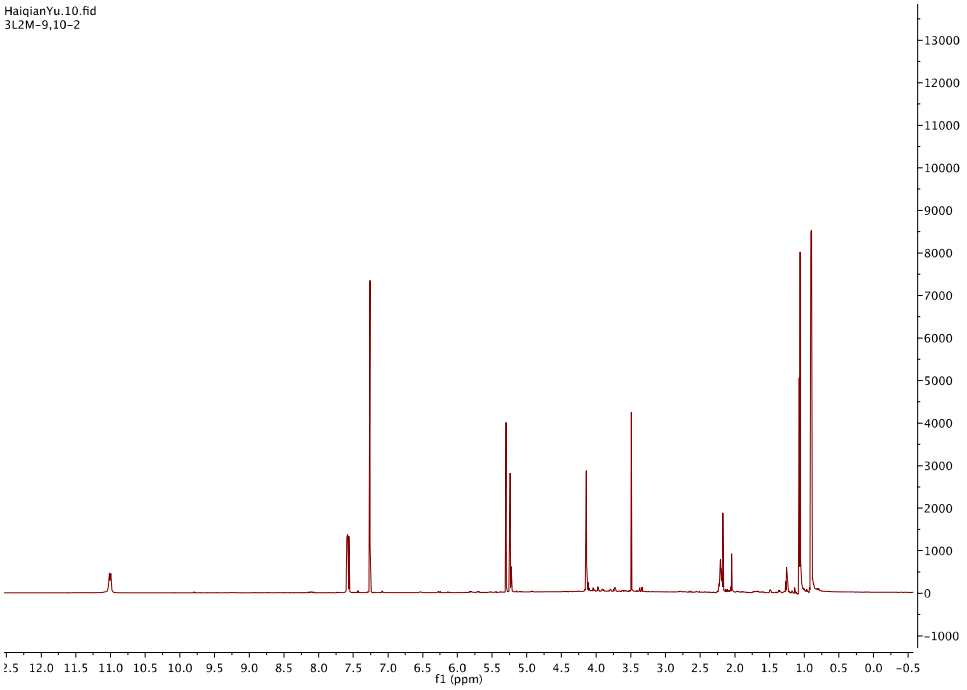

Figure S47. The ^{1}H NMR (600 MHz, CD_3OD) spectrum of compound 6

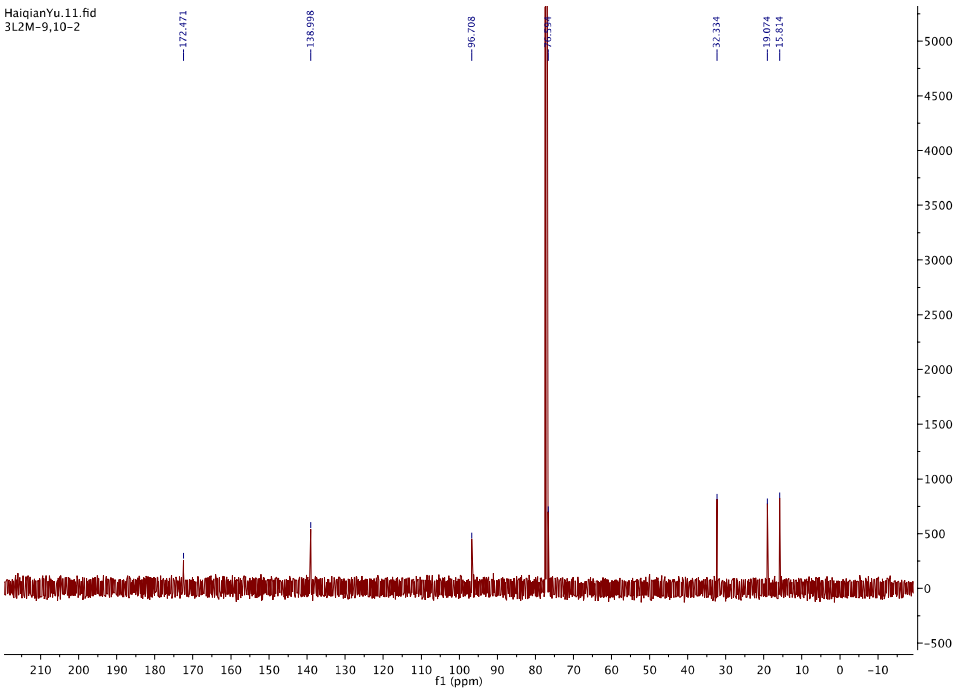

Figure S48. The ^{13}C NMR (150 MHz, CD_3OD) spectrum of compound 6

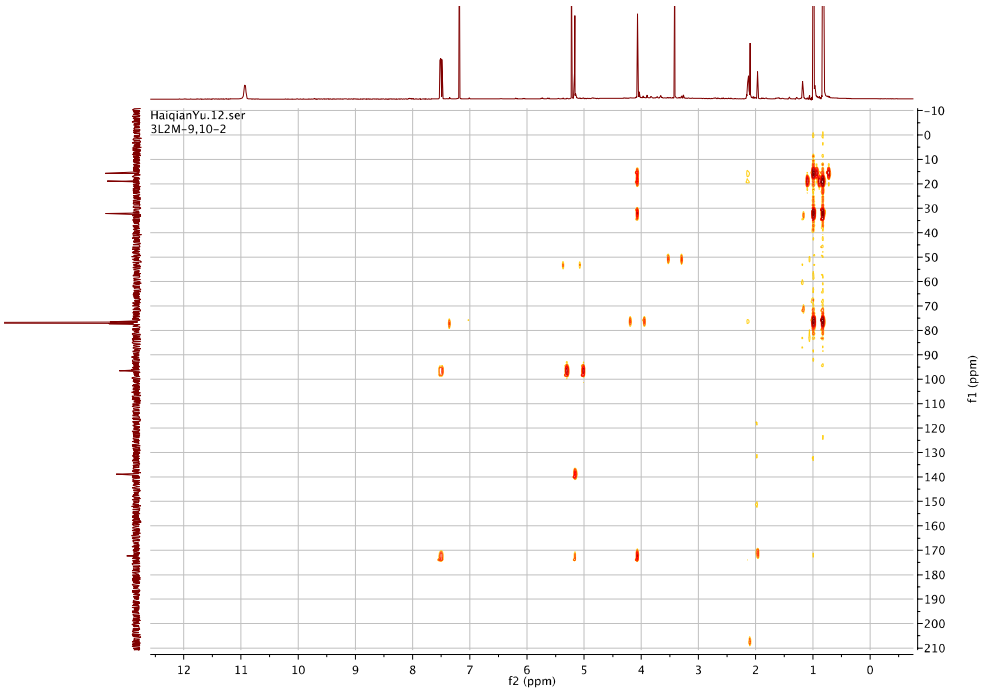

Figure S49. The HMBC (600 MHz, CD_3OD) spectrum of compound 6

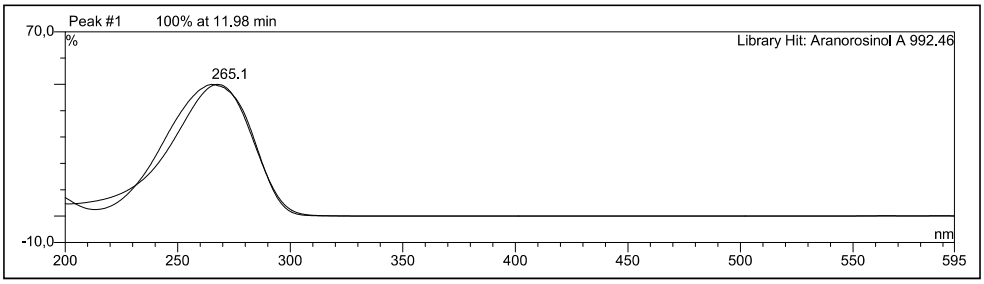

Figure S50. The UV spectrum of compound 6

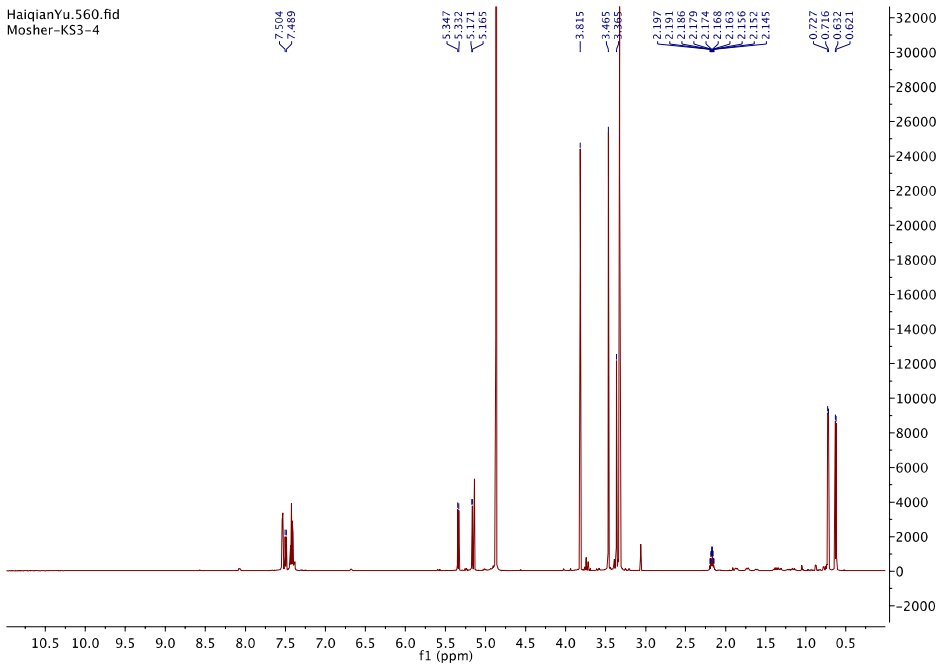

Figure S51. The ^{1}H NMR (600 MHz, CD_3OD) spectrum of (*S*)-MPA ester of compound 6.

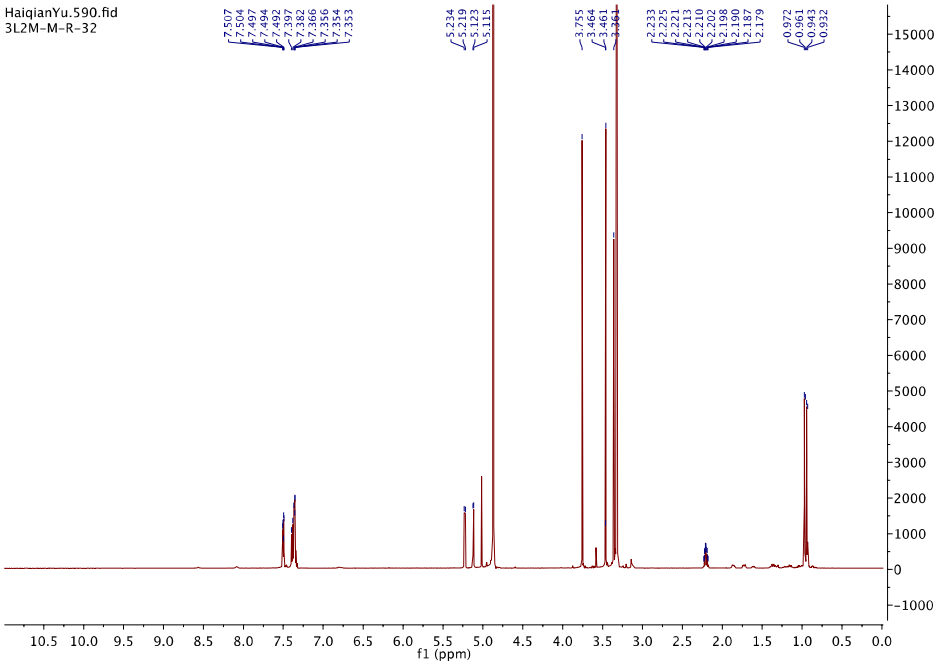

Figure S52. The ^{1}H NMR (600 MHz, CD_3OD) spectrum of (*R*)-MPA ester of compound 6.

5 Discussion

5.1 Chemical Constituents of the Fungus *Coniella fragariae*

Fungi of the genus *Coniella* (synonyms *Pilidiella* and *Schizoparme*) are reported to be plant pathogens and most published reports focus on the biology of *Coniella*, agriculture, or as a target for anti-fungal studies. (Alvarez, Groenewald et al. 2016) In the current study, the fungus was isolated from goose (*Anser anser*) dung that was collected from the North Sea coast close to Garding, Germany. Based on the reports that *Coniella fragariae* is a typical plant pathogen, the true source of the fungus likely consists of plants that had been eaten by the geese. Investigation of the natural products of *Coniella fragariae* in this dissertation (Chapter 2 and 3) showed that metabolites from this fungus included azaphilones, macrodiolides and integracins.

The most interesting metabolites isolated from this fungal strain were the new azaphilones, which are unusual due to the aldehyde group present at position C-5. The main metabolite, coniellin A, led to Nf-κB inhibition and reduced tumor cell migration in the human breast tumor MDA-MB-231 cells. Additionally, two macrodiolides, pyrenophorin (Kastanias and Chrysayi-Tokousbalides 2005) and pyrenophorol (Zhang, Krohn et al. 2008), were isolated from this fungus. Pyrenophorin is cytotoxic against several cancer cell lines at the nanomolar level.

5.1.1 **Macrodiolides**

Pyrenophorin and pyrenophorol are structurally related natural products. Pyrenophorin was reported for the first time as a fungal metabolite isolated from a culture of *Pyrenophora avenae* in 1961.(Ishibashi 1961) Later, pyrenophorol was isolated from the fungus *Byssochlamys nivea*. (Kis, Furger et al. 1969) However, the absolute configurations of both compounds had not been established before. In 1976, as an antibiotic candidate, pyrenophorin was chemically synthesized as a racemic mixture. (Colvin, Purcell et al. 1976) Two years later, the absolute configuration of pyrenophorin was determined via chemical synthesis. (Seuring and Seebach 1978) Because of the strong antibiotic and anti-fungal activity, as well as the challenging chiral synthesis, several recent publications focus on the stereoselective synthesis of pyrenophorin. (Ramakrishna, Sreenivasulu et al. 2016, Costa, Martins et al. 2017)

A variety of bioactivities of pyrenophorin-type macrodiolides has been reported, such as anti-fungal, [McMullin, Green et al. 2015] antibacterial, [Ishibashi 1961] selective phytotoxic, [Sugawara and Strobel 1986, Kastanias and Chrysayi-Tokousbalides 2005] and anthelmintic (abomasum nematodes) activities. [Kind, Zeeck et al. 1996] However, no reports on the cytotoxicity of pyrenophorin have yet been published.

In this study, two macrodiolides were elucidated based on NMR, MS, and optical rotation data. The absolute configuration of pyrenophorin was confirmed via X-ray measurement. Both compounds were tested for their cytotoxicity and antibacterial activity. Pyrenophorin showed antibacterial activity with a MIC value of 6.25 µM against *Mycobacterium tuberculosis*, 1.56 µM against *Staphylococcus aureus* ATCC 700699 and 6.25 µM against *Enterococcus faecalis* ATCC 29212. However, pyrenophorol was not active against these bacteria. In cytotoxicity tests with different cancer cell lines, pyrenophorin showed strong cytotoxicity with an IC_{50} value of 0.6 μM against the Ramos B cell line and 0.065 μM against the Jurkat J16 T cell line (72 hours), IC_{50} values of 0.5 μM and 0.9 μM in *cis*-platin sensitive and resistant A2780 human ovarian cancer cell lines (72 hours), and with an IC_{50} value of 7.8 μM in the MDA-MB-231 human breast cancer cell line (24 hours). However, pyrenophorol was completely inactive against the tested cell lines. During further tests, pyrenophorin did not activate the caspase-3 pathway even at concentration up to 30 μM in the Ramos B cell line and Jurkat J16 T cell line. Thus, pyrenophorin is proposed to work through a caspase-independent type of cell death, that does not trigger the apoptosis pathways.

Considering the antibacterial, cytotoxic, and toxic activities against fungi and nematodes, the structural differences between pyrenophorin and pyrenophorol are the only reasons for the contrasting bioactivates. Pyrenophorin has two carbonyl groups at positions 4 and 4', while pyrenophorol has two hydroxy groups at the same positions. Pyrenophorin is assumed to be more active in hetero-Michael addition reactions. Based on the primary activity-structure relationship, the proposed Michael reaction is probably the reason for the strong cytotoxicity of pyrenophorin. However, even though unsaturated carbonyls together with Michael acceptors show broad bioactivity, they have largely been ignored due to their presumed indiscriminate reactivity. [Jackson, Widen et al. 2017]

5.1.2 **Azaphilones**

5.1.2.1 Structures of Azaphilones

Azaphilones are introduced in Chapter 1.4 already. Compared to the majority of published azaphilone structures, all azaphilones isolated during this study exhibit unusual aldehyde moieties at C-5. Although few examples exist in the literature of compounds showing a similar side chain, examples include austdiol and its derivatives from *Aspergillus ustus* (Vleggaar, Steyn et al. 1974) and pitholides A and B from the marine fungus *Pithomyces* sp.. (Wang, Borgeson et al. 1997) Coniellin H is the only reported azaphilone that contains a four-membered ring. Based on the chemical similarity of the structures, a proposed biosynthetic pathway suggests that coniellin H is a [2 + 2] cycloaddition product. The four chiral centers of coniellin H and the configurations of the two double bonds in coniellin A support this presumption. The carbon scaffold or side chain-connections via carbon bonds at position C-4a are extremely rare in azaphilones. Until now, only coniellin H and bromophilones A and B exhibit scaffold- or side chain-linkage at carbon 4a. (Frank, Hartmann et al. 2019)

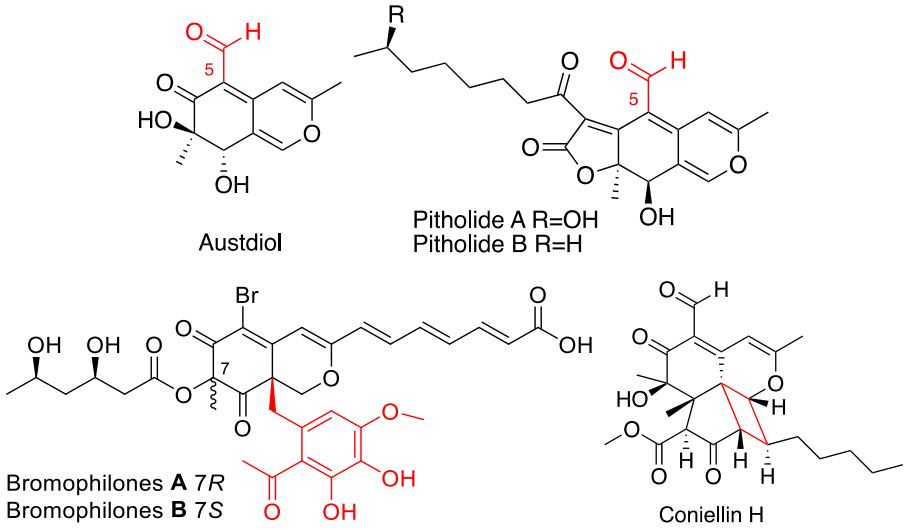

5.1.2.2 Azaphilone Pigments

Some azaphilone pigments were discovered from the fungal genus *Monascus*, including monascin, (Shi, Liao et al. 2012) rubropunctatin, (Zheng, Zhang et al. 2016) and rubropunctamine (Patakova 2013). The fungal genus *Hypoxyloideae* (*Xylariaceae*) has also been reported to

produce azaphilone pigments. (Stadler and Fournier 2006) The structures of the azaphilone pigments that give rise to different colors are due to the aromatic system and the exchangeability of oxygen with nitrogen in the core structure. (Chen, Chen et al. 2017) The nitrogen present at position 2 contributes to the color in some azaphilones, such as amination of the orange pigments rubropuncatatin and monascorubrin with NH_3 which leads to the red pigments rubropunctamine and monascorubramine. (Chen, Chen et al. 2017)

Monascus sp. from red mold rice was first characterized as an azaphilone pigment producer. (Chen, He et al. 2015) Monascus pigments consist mainly of azaphilones and have been used for over 2,000 years in East Asia but are still forbidden in Europe and the USA.(Dufossé, Galaup et al. 2005) In a SKLM (Ständige Senatskommission zur gesundheitlichen Bewertung von Lebensmitteln, Permanent Senate Commission on Food Safety) report, red mold rice was not considered safe for food or food supplements due to insufficient availability of data regarding the safety and constituents. (Steinberg, E. Appel et al. 2013) Some pure azaphilone pigment substances show cytotoxicity, (Hsu, Hsu et al. 2011) anti-fungal activity, (Cheng, Wu et al. 2011) and inhibition of NO production. (Wu, Cheng et al. 2011) The variety of bioactivities could be a risk in the food industry, but several reports have shown that *Monascus purpureus* fermented foods were non-toxic and may even have additional health benefits. (Klimek, Wang et al. 2009, Mohan Kumari, Akhilender Naidu et al. 2009, Puttananjaiah, Dhale et al. 2019)

In this study, coniellin H and I were the only pigments isolated from *Coniella fragariae.* Coniellin H is a four-membered ring compound with a brown color. Coniellin I is a pH-dependent pigment that has a rose-violet color in solution; the color was stable at pH values below 7. However, when the pH was above 7, the rose-violet color was lost and the solution turned light yellow. Based on the structure, the proposed changes from hemiketal at C-6 to the keto-form result in the loss of the aromatic system.

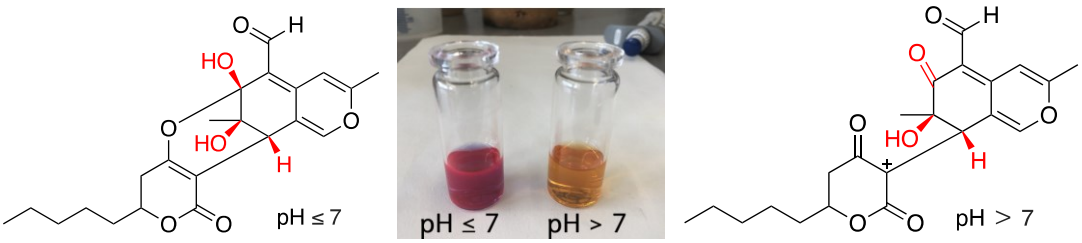

5.1.2.3 Bioactivities of Azaphilones

Azaphilones have a variety of chemical derivatives and may be valuable for drug discovery due to their diverse bioactivities, such as cytotoxic, anti-HIV, antibacterial, anti-fungal, and nematicidal activities. (Khurana, Sharma et al. 2017) Especially for anticancer research, azaphilones show strong and wide-ranging activity in different cell lines. For examples, (−)-berkelic acid from the fungus *Penicillium* sp. displayed strong cytotoxicity against ovarian cancer OVCAR-3 cells with a GI_{50} value of 91 nM. (Stierle, Stierle et al. 2006) Chaetomugilin I from the fungus *Chaetomium globosum* exhibited cytotoxicity that was similarly strong compared to the positive control fluorouracil in several cancer cell lines. (Muroga, Yamada et al. 2009) In this study, all azaphilones were evaluated for their cytotoxicity, together with inhibition of Nf-**κ**B and tumor cell migration in the human breast cancer cell line MDA-MB-231. Coniellin A exhibited the strongest Nf-**κ**B inhibition with an IC_{50} value of 4.4 µM compared to other azaphilone derivatives. From the bioactivity and structures of these azaphilones, coniellin A, B, and C indicate that a C-14/C-15 double bond is important for Nf-**κ**B inhibition. Coniellin E and F are both 15-epimers, coniellin F is *R* configurated while coniellin E is *S* configurated. Coniellin E is more active with regard to reducing cell viability and with regard to Nf-**κ**B inhibition. When comparing the compounds coniellin A-C and E-G, the lactone ring located at C-7/8 proved to be less important for Nf-**κ**B inhibition than a side chain at C-12. Coniellin H and I, which have a different skeleton compared to coniellin A, did not show cytotoxicity and inhibition of Nf-**κ**B.

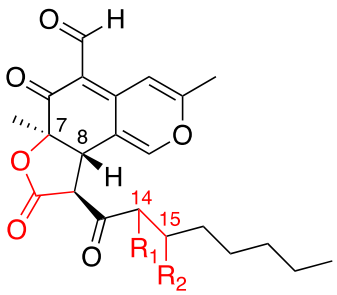

Groups in red color show influence on Nf-**κ**B inhibition and cytotoxicity

5.2 Chemical Constituents of the Fungus *Phomopsis* sp. D15a2a

Endophytic fungi improve the host's adaptability and modulate the growth of host plants through the production of phytohormones, such as abscisic acid derivatives. (Tan and Zou 2001, Siewers, Kokkelink et al. 2006) Fungi also contribute their bioactive metabolites to the host's chemical defenses, such as ergot alkaloids (Schiff 2006) and taxol. (Kasaei, Mobini-Dehkordi et al. 2017)

In this study, the fungus *Phomopsis* sp. D15a2a was isolated from a leaf of *Alternanthera bettzickiana.* No reports exist on the metabolites of this fungal strain. One paper introduced the fungus when it was found in the plant *Diospyros crassiflora* but no natural products from this fungus were described . *(Douanla-Meli and Langer 2012)* In this study, five new compounds were isolated from the EtOAc extract which was obtained following fermentation of the fungus on solid rice medium. These metabolites include three types of compounds: koniginin derivatives, pantothenic acid derivatives, and tentoxin derivatives.

5.2.1 **Koninginin Derivatives**

The first koninginin derivative, koninginin A was isolated in 1989 from *Trichoderma koningii* and showed weak inhibition of wheat coleoptile growth. (Cutler, Himmelsbach et al. 1989) Later, koninginin B was isolated together with koninginin A from the same fungus. (Cutler, Himmelsbach et al. 1991) Starting with koninginin A, the derivatives have been named and published. To date, koninginins R and S are the last fungal metabolites reported from *Trichoderma koningii* in 2017.(Hu, Li et al. 2017) Also the marine derived fungus *Trichoderma reusei* produces trichodermatides B–D, which share the same core structure as the koninginins. (Sun, Tian et al. 2008) This kind of compounds was also isolated from *Emericella nidulans,(Tarawneh, Leon et al. 2013) Trichoderma neokongii, (Zhou, Li et al. 2014) Trichoderma applanatum, (Chen, Wu et al. 2018)* and *Trichoderma koningiopsis.(Liu, Yang et al. 2016, Liu, Yang et al. 2016, Hu, Li et al. 2017)* In this study, koninginin derivatives were isolated from the genus *Phomopsis* for the first time.

All koninginin derivatives are formed by a two-ring core polyketide structure together with a fatty acid derived side chain. Polyketide metabolites linked to fatty acid side

chains are common in fungal metabolites, such as azaphilones (Gao, Yang et al. 2013) and koninginins, due to the close relationship of polyketide biosynthesis and fatty acid biosynthesis. (Cronan and Thomas 2009) In this study, three new koninginin metabolites with a methyl group instead of a fatty side chain were isolated from *Phomopsis* sp. D15a2a. From the database Sci-Finder, (Sci-Finder) koninginin-type compounds with a methyl group have only been obtained by chemical synthesis previously. Phomopones are the first examples obtained as natural products.

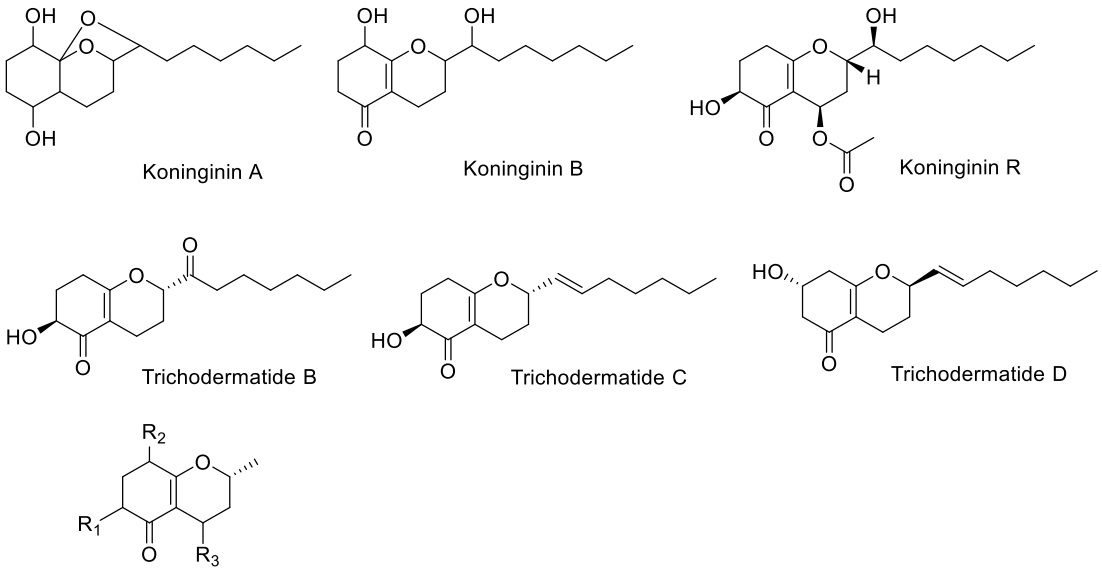

5.2.2 **Pantothenic Acid Derivatives**

Enamidin and 3'-hydroxy-enamidin were isolated in this study. Enamidin was reported without assigning its configuration as a new fungal metabolite from the endophytic fungus *Diaporthe* (sexual stage of *Phomopsis*) sp. SNB-GSS10. Enamidin and 3'-hydroxy-enamidin are structurally similar to pantothenic acid and CJ-15,801 which was reported as an antibiotic. (Saliba and Kirk 2005) However, neither of the former compounds was active in antibacterial tests against *Staphylococcus aureus*. The mode of action for CJ-15,801 has been reported to be similar to sulfonamide antibiotics and based on the key hydroxymethyl group. (van der Westhuyzen, Hammons et al. 2012) This reported mode of action also suggests that the lack of antibacterial activity of enamidin and 3'-hydroxy-enamidin is due to the loss of the hydroxymethyl group.

The absolute configurations for both compounds were determined by Mosher's reactions and comparison of their optical rotation. Calculations of differences of

chemical shifts between the resulting methylated (*R*)- and (*S*)-MPA esters of methyl-enamidin led to the assignment of the absolute configuration of methyl-enamidin as *R*. Comparison of the optical rotation of enamidin (+60.7 c 0.1, MeOH), 3'-hydroxy-enamidin (+34.0 c 0.1, MeOH), CJ-15,801 (+47.7 c 0.44, MeOH), *R*-form of pantothenic acid (+37.5), and *S*-form of pantothenic acid (-56.3), (Sugie, Dekker et al. 2001) indicate that enamidin and 3'-hydroxy-enamidin are present in the *R*-form. The results following the Mosher's reactions result and the comparison of the optical rotation of Enamidin and 3'-hydroxy-enamidin to published similar structures CJ-15,801 and *R*-pantothenic acid showed agreement in the configuration determination. In the cytotoxicity tests against the L5178Y mouse lymphoma cell line, both compounds enamidin and 3'-hydroxy-enamidin were inactive.

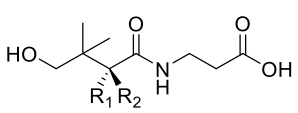

R_1=OH *R*-pantothenic acid
R_2=OH *S*-pantothenic acid

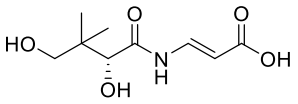

CJ-15,801

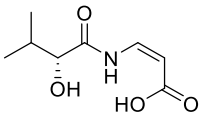

enamidin

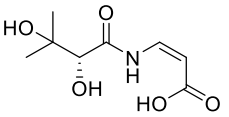

3'-hydroxy-enamidin

5.2.3 **Tentoxin Derivatives**

Tentoxin was reported in 1970 as a cyclic tetrapeptide that was isolated from the fungus *Alternaria tenuis*. (Saad, Halloin et al. 1970) Later, in 1974 crystal measurements elucidated the structure.(Meyer, Kuyper et al. 1974) Tentoxin shows plant toxicity due to the inhibition of energy transfer that was equal to the positive control ATPase inhibitor DCCD (N,N'-dicyclohexylcarbodiimide). (Dahse, Matorin et al. 1986) Tentoxin tetrapeptides have mostly been isolated from the fungal genus *Alternaria*, but derivatives have also been reported from *Phoma* and *Auxarthron*.*(La Kim, Lin Li et al. 2012, Li, Yue et al. 2017)*

18-hydroxydihydrotentoxin was isolated from *Phomopsis* as a new metabolite. The hydroxyl group that is linked with γ-OH-Leu at C-18 of compound 18-hydroxydihydrotentoxin, at a similar position to that in 3'-hydroxy-enamidin suggests that the hydroxylation reactions are catalyzed by the same enzyme. The compound was inactive in the anti-bacterial test against *Staphylococcus aureus* and cytotoxicity tests against the L5178Y mouse lymphoma cell line.

5.3 Conclusion

The results of this dissertation describe the chemical constituents of two fungi. From the fermentation of *Coniella fragariae* on solid rice media, eleven metabolites including a series of new azaphilones were obtained. From the endophytic fungus *Phomopsis* sp. D15a2a, six compounds were isolated.

Two pigments, coniellin H and I, contribute to the azaphilone structural diversity. Furthermore, coniellin I is the first reported pH-independent pigment belonging to the azaphilone group. The phomopones are the first naturally occurring koninginin-type compounds featuring a methyl group instead of a fatty acid derived side chain. In the bioactivity study, metabolites from *Coniella fragariae* showed activity as NF-κB inhibitors and as inhibitors of tumor cell migration. Based on the bioactivity data and chemical differences, structure activity relationships are proposed. The two macrodiolides, pyrenophorin and pyrenophorol, have contrasting cytotoxic and antibacterial activities, which we propose are due to structural differences of α, β-unsaturated carbonyl related to their reactivity as Michael acceptors.

6 References

Adelin, E., M.-T. Martin, S. Cortial, P. Retailleau, S. Lumyong and J. Ouazzani (2013). "Bioactive polyketides isolated from agar-supported fermentation of Phomopsis sp. CMU-LMA, taking advantage of the scale-up device, Platotex." Phytochemistry (Elsevier) **93**: 170-175.

Akay, S., G. Ekiz, F. Kocabas, E. E. Hames-Kocabas, K. S. Korkmaz and E. Bedir (2014). "A new 5,6-dihydro-2-pyrone derivative from Phomopsis amygdali, an endophytic fungus isolated from hazelnut (Corylus avellana)." Phytochemistry Letters **7**: 93-96.

Alvarez, L. V., J. Z. Groenewald and P. W. Crous (2016). "Revising the Schizoparmaceae: Coniella and its synonyms Pilidiella and Schizoparme." Stud Mycol **85**: 1-34.

Aly, A. H., A. Debbab and P. Proksch (2011). "Fifty years of drug discovery from fungi." Fungal Diversity **50**(1): 3-19.

Andolfi, A., A. Boari, M. Evidente, A. Cimmino, M. Vurro, G. Ash and A. Evidente (2015). "Gulypyrones A and B and Phomentrioloxins B and C Produced by Diaporthe gulyae, a Potential Mycoherbicide for Saffron Thistle (Carthamus lanatus)." J Nat Prod **78**(4): 623-629.

Andrioli, W. J., R. Conti, M. J. Araujo, R. Zanasi, B. C. Cavalcanti, V. Manfrim, J. S. Toledo, D. Tedesco, M. O. de Moraes, C. Pessoa, A. K. Cruz, C. Bertucci, J. Sabino, D. N. Nanayakkara, M. T. Pupo and J. K. Bastos (2014). "Mycoleptones A-C and polyketides from the endophyte Mycoleptodiscus indicus." J Nat Prod **77**(1): 70-78.

Arunpanichlert, J., V. Rukachaisirikul, S. Phongpaichit, O. Supaphon and J. Sakayaroj (2016). "Xylariphilone: a new azaphilone derivative from the seagrass-derived fungus Xylariales sp. PSU-ES163." Nat Prod Res **30**(1): 46-51.

Arunrattiyakorn, P., N. Suwannasai, T. Aree, S. Kanokmedhakul, H. Ito and H. Kanzaki (2014). "Biotransformation of α-mangostin by Colletotrichum sp. MT02 and Phomopsis euphorbiae K12." J. Mol. Catal. B: Enzym. **102**: 174-179.

Balba, H. (2007). "Review of strobilurin fungicide chemicals." J Environ Sci Health B **42**(4): 441-451.

Barbero, M., E. Artuso and C. Prandi (2018). "Fungal Anticancer Metabolites: Synthesis Towards Drug Discovery." Curr Med Chem **25**(2): 141-185.

Bridge, P. and B. Spooner (2001). "Soil fungi: diversity and detection." Plant and Soil **232**(1-2): 147-154.

Butler, M. S. (2004). "The role of natural product chemistry in drug discovery." J Nat Prod **67**(12): 2141-2153.

Cai, R., S. Chen, Z. Liu, C. Tan, X. Huang and Z. She (2017). "A new alpha-pyrone from the mangrove endophytic fungus Phomopsis sp. HNY29-2B." Nat Prod Res **31**(2): 124-130.

Cao, F., J. K. Yang, Y. F. Liu, H. J. Zhu and C. Y. Wang (2016). "Pleosporalone A, the first azaphilone characterized with aromatic A-ring from a marine-derived Pleosporales sp. fungus." Nat Prod Res **30**(21): 2448-2452.

Caro, Y., L. Anamale, M. Fouillaud, P. Laurent, T. Petit and L. Dufosse (2012). "Natural hydroxyanthraquinoid pigments as potent food grade colorants: an overview." Natural Products and Bioprospecting **2**(5): 174-193.

Çeliker, N. M., A. Uysal, B. Çetinel and D. Poyraz (2012). "Crown rot on pomegranate caused by Coniella granati in Turkey." Australasian Plant Disease Notes **7**(1): 161-162.

Chang, H.-S., C.-J. Peng, M.-J. Cheng, H.-C. Wu, H.-Y. Chan, S.-Y. Hsieh, G.-F. Yuan and I.-S. Chen (2018). "Chemical Constituents of the Endophytic Fungus Phomopsis asparagi Isolated from the Plant Peperomia sui." Chem. Nat. Compd. **54**(3): 504-508.
Chapla, V. M., M. L. Zeraik, V. F. Ximenes, L. M. Zanardi, M. N. Lopes, A. J. Cavalheiro, D. H. S. Silva, M. C. M. Young, L. M. da Fonseca, V. S. Bolzani and A. R. Araujo (2014). "Bioactive secondary metabolites from Phomopsis sp., an endophytic fungus from Senna spectabilis." Molecules **19**(5): 6597-6608, 6512 pp.
Chen, C., J. Wang, H. Zhu, J. Wang, Y. Xue, G. Wei, Y. Guo, D. Tan, J. Zhang, C. Yin and Y. Zhang (2016). "Chaephilones A and B, two new azaphilone derivatives isolated from Chaetomium globosum." Chem. Biodiversity **13**(4): 422-426.
Chen, C. J., X. X. Liu, W. J. Zhang, L. Y. Zang, G. Wang, S. W. Ng, R. X. Tan and H. M. Ge (2015). "Sesquiterpenoids isolated from an endophyte fungus Diaporthe sp." Rsc Advances **5**(23): 17559-17565.
Chen, H., M. Huang, X. Li, L. Liu, B. Chen, J. Wang and Y. Lin (2018). "Phochrodines A-D, first naturally occurring new chromenopyridines from mangrove entophytic fungus Phomopsis sp. 33." Fitoterapia **124**: 103-107.
Chen, L., G. W. Wu, D. Liu, W. Y. Zhuang and W. B. Yin (2018). "Trichodermatides E and F from fungus Trichoderma applanatum." J Asian Nat Prod Res: 1-7.
Chen, M., N. X. Shen, Z. Q. Chen, F. M. Zhang and Y. Chen (2017). "Penicilones A-D, Anti-MRSA Azaphilones from the Marine-Derived Fungus Penicillium janthinellum HK1-6." J Nat Prod **80**(4): 1081-1086.
Chen, W., R. Chen, Q. Liu, Y. He, K. He, X. Ding, L. Kang, X. Guo, N. Xie, Y. Zhou, Y. Lu, R. J. Cox, I. Molnar, M. Li, Y. Shao and F. Chen (2017). "Orange, red, yellow: biosynthesis of azaphilone pigments in Monascus fungi." Chem Sci **8**(7): 4917-4925.
Chen, W. P., Y. He, Y. X. Zhou, Y. C. Shao, Y. L. Feng, M. Li and F. S. Chen (2015). "Edible Filamentous Fungi from the Species Monascus: Early Traditional Fermentations, Modern Molecular Biology, and Future Genomics." Comprehensive Reviews in Food Science and Food Safety **14**(5): 555-567.
Chen, Y.-S., M.-J. Cheng, Y. Hsiao, H.-Y. Chan, S.-Y. Hsieh, C.-W. Chang, T.-W. Liu, H.-S. Chang and I.-S. Chen (2015). "Chemical constituents of the endophytic fungus Hypoxylon sp. 12F0687 isolated from Taiwanese Ilex formosana." Helv. Chim. Acta **98**(8): 1167-1176.
Cheng, M.-J., M.-D. Wu, I.-S. Chen, M. Tseng and G.-F. Yuan (2011). "Chemical constituents from the fungus Monascus purpureus and their antifungal activity." Phytochemistry Letters **4**(3): 372-376.
Cheng, M.-J., M.-D. Wu, Y.-L. Chen, I.-S. Chen, Y.-S. Su and G.-F. Yuan (2013). "Chemical constituents of red yeast rice fermented with the fungus Monascus pilosus." Chem. Nat. Compd. **49**(2): 249-252.
Cheng, M. J., M. D. Wu, H. Y. Chan, J. J. Chen, Y. C. Cheng, Y. L. Chen, I. S. Chen and G. F. Yuan (2016). "A New Azaphilone Metabolite from the Fungus Monascus ruber." Chemistry of Natural Compounds **52**(2): 231-233.
Cheng, M. J., M. D. Wu, H. Y. Chan, Y. C. Cheng, J. J. Chen, Y. L. Chen, I. S. Chen and G. F. Yuan (2015). "New Metabolite from the Fungus Monascus kaoliang." Chemistry of Natural Compounds **51**(6): 1091-1093.
Cheng, M. J., M. D. Wu, H. Y. Chan, S. Y. Hsieh, J. J. Chen, H. S. Chang, Y. H. Kuo, G. F. Yuan and I. S. Chen (2018). "A NEW BENZENOID DERIVATIVE FROM AN ENDOPHYTIC FUNGUS IN Peperomia sui." Chemistry of Natural Compounds **54**(4): 625-627.

Cheng, M. J., M. D. Wu, H. Y. Chan, S. Y. Hsieh, Y. L. Chen, I. S. Chen, F. L. Chan, J. J. Chen and G. F. Yuan (2015). "Secondary Metabolites Produced by Phomopsis sp 11F0023, an Endophytic Fungus in Eragrostis amabilis." Chemistry of Natural Compounds **51**(3): 431-434.
Chethana, K. W. T., Y. Zhou, W. Zhang, M. Liu, Q. K. Xing, X. H. Li, J. Y. Yan, K. W. T. Chethana and K. D. Hyde (2017). "Coniella vitis sp. nov. Is the Common Pathogen of White Rot in Chinese Vineyards." Plant Dis **101**(12): 2123-2136.
Choi, J. N., J. Kim, K. Ponnusamy, C. Lim, J. G. Kim, M. J. Muthaiya and C. H. Lee (2013). "Identification of a new phomoxanthone antibiotic from Phomopsis longicolla and its antimicrobial correlation with other metabolites during fermentation." J Antibiot (Tokyo) **66**(4): 231-233.
Cimmino, A., A. Andolfi, M. C. Zonno, A. Boari, C. Troise, A. Motta, M. Vurro, G. Ash and A. Evidente (2013). "Phomentrioloxin, a fungal phytotoxin with potential herbicidal activity, and its derivatives: a structure-activity relationship study." J Agric Food Chem **61**(40): 9645-9649.
Cimmino, A., P. Nocera, B. T. Linaldeddu, M. Masi, M. Gorecki, G. Pescitelli, L. Montecchio, L. Maddau and A. Evidente (2018). "Phytotoxic Metabolites Produced by Diaporthella cryptica, the Causal Agent of Hazelnut Branch Canker." J Agric Food Chem **66**(13): 3435-3442.
Colvin, E. W., T. A. Purcell and R. A. Raphael (1976). "Total synthesis of the macrocyclic antibiotic (±)-pyrenophorin." J. Chem. Soc., Perkin Trans. 1(16): 1718-1722.
Costa, M., M. Martins, H. de Araújo and I. Resck (2017). "Synthesis and Expansion of Bicyclic Enol Ether: A Probable Precursor for the Synthesis of Macrolide (±)-Pyrenophorin." Journal of the Brazilian Chemical Society **29**(1): 74-78.
Cronan, J. E. and J. Thomas (2009). Chapter 17 Bacterial Fatty Acid Synthesis and its Relationships with Polyketide Synthetic Pathways. Methods in Enzymology, Academic Press. **459:** 395-433.
Cui, H., M. Ding, D. Huang, Z. Zhang, H. Liu, H. Huang and Z. She (2017). "Chroman-4-one and pyrano[4,3-b]chromenone derivatives from the mangrove endophytic fungus Diaporthe phaseolorum SKS019." RSC Adv. **7**(33): 20128-20134.
Cui, H., Y. Lin, M. Luo, Y. Lu, X. Huang and Z. She (2017). "Diaporisoindoles A-C: Three Isoprenylisoindole Alkaloid Derivatives from the Mangrove Endophytic Fungus Diaporthe sp. SYSU-HQ3." Org Lett **19**(20): 5621-5624.
Cui, H., Y. Liu, J. Li, X. Huang, T. Yan, W. Cao, H. Liu, Y. Long and Z. She (2018). "Diaporindenes A-D: Four Unusual 2,3-Dihydro-1 H-indene Analogues with Anti-inflammatory Activities from the Mangrove Endophytic Fungus Diaporthe sp. SYSU-HQ3." J Org Chem **83**(19): 11804-11813.
Cui, H., J. Yu, S. Chen, M. Ding, X. Huang, J. Yuan and Z. She (2017). "Alkaloids from the mangrove endophytic fungus Diaporthe phaseolorum SKS019." Bioorg Med Chem Lett **27**(4): 803-807.
Cutler, H. G., D. S. Himmelsbach, R. F. Arrendale, P. D. Cole and R. H. Cox (1989). "Koninginin-a - a Novel Plant-Growth Regulator from Trichoderma-Koningii." Agricultural and Biological Chemistry **53**(10): 2605-2611.
Cutler, H. G., D. S. Himmelsbach, B. Yagen, R. F. Arrendale, J. M. Jacyno, P. D. Cole and R. H. Cox (1991). "Koninginin-B - a Biologically-Active Congener of Koninginin a from Trichoderma-Koningii." Journal of Agricultural and Food Chemistry **39**(5): 977-980.

Dahse, I., D. N. Matorin and B. Liebermann (1986). "A comparison of tentoxin action on the delayed fluorescence in chloroplasts of spinach, Chlorella and Anacystis." Biochem. Physiol. Pflanz. **181**(3): 137-146.
Deshmukh, S. K., M. K. Gupta and S. K. Lenka (2019). Endophytic Fungi As the Alternate Source of High-Value Plant Secondary Metabolites. Microbial Diversity in Ecosystem Sustainability and Biotechnological Applications: Volume 2. Soil & Agroecosystems. T. Satyanarayana, S. K. Das and B. N. Johri. Singapore, Springer Singapore**:** 493-532.
Deshmukh, S. K., S. A. Verekar and S. V. Bhave (2014). "Endophytic fungi: a reservoir of antibacterials." Front Microbiol **5**: 715.
Ding, B., Z. Y. Wang, G. P. Xia, X. S. Huang, F. Xu, W. R. Chen and Z. G. She (2017). "Three New Chromone Derivatives Produced by Phomopsis sp HNY29-2B from Acanthus ilicifolius Linn." Chinese Journal of Chemistry **35**(12): 1889-1893.
Ding, B., J. Yuan, X. Huang, W. Wen, X. Zhu, Y. Liu, H. Li, Y. Lu, L. He, H. Tan and Z. She (2013). "New dimeric members of the phomoxanthone family: phomolactonexanthones A, B and deacetylphomoxanthone C isolated from the fungus Phomopsis sp." Mar Drugs **11**(12): 4961-4972.
Douanla-Meli, C. and E. Langer (2012). "Diversity and molecular phylogeny of fungal endophytes associated with Diospyros crassiflora." Mycology **3**(3): 175-187.
Du, F.-Y., X.-M. Li, P. Zhang, C.-S. Li and B.-G. Wang (2014). "Cyclodepsipeptides and Other O-Containing Heterocyclic Metabolites from Beauveria felina EN-135, a Marine-Derived Entomopathogenic Fungus." **12**(5): 2816.
Du, G., Z. C. Wang, W. Y. Hu, K. L. Yan, X. L. Wang, H. M. Yang, H. Y. Yang, Y. H. Gao, Q. Liu and Q. F. Hu (2017). "Three new 3-methyl-2-arylbenzofurans from the fermentation products of an endophytic fungus Phomopsis sp and their anti-TMV activity." Phytochemistry Letters **21**: 287-290.
Dufossé, L., P. Galaup, A. Yaron, S. M. Arad, P. Blanc, K. N. Chidambara Murthy and G. A. Ravishankar (2005). "Microorganisms and microalgae as sources of pigments for food use: a scientific oddity or an industrial reality?" Trends in Food Science & Technology **16**(9): 389-406.
Evidente, A., A. Kornienko, A. Cimmino, A. Andolfi, F. Lefranc, V. Mathieu and R. Kiss (2014). "Fungal metabolites with anticancer activity." Nat Prod Rep **31**(5): 617-627.
Evidente, M., A. Boari, S. Vergura, A. Cimmino, M. Vurro, G. Ash, S. Superchi and A. Evidente (2015). "Structure and Absolute Configuration of Kongiidiazadione, a New Phytotoxic 3-Substituted-5-Diazenylcyclopentendione Produced by Diaporthe Kongii." Chirality **27**(9): 557-562.
Fan, Z., Z. H. Sun, H. X. Liu, Y. C. Chen, H. H. Li and W. M. Zhang (2016). "Perangustols A and B, a pair of new azaphilone epimers from a marine sediment-derived fungus Cladosporium perangustm FS62." J Asian Nat Prod Res **18**(11): 1024-1029.
Frank, M., R. Hartmann, M. Plenker, A. Mándi, T. Kurtán, F. C. Özkaya, W. E. G. Müller, M. U. Kassack, A. Hamacher, W. Lin, Z. Liu and P. Proksch (2019). "Brominated Azaphilones from the Sponge-Associated Fungus Penicillium canescens Strain 4.14.6a." Journal of Natural Products.
Frank, M., H. Niemann, P. Böhler, B. Stork, S. Wesselborg, W. Lin and P. Proksch (2015). "Phomoxanthone A - From Mangrove Forests to Anticancer Therapy." Current Medicinal Chemistry **22**(30): 3523-3532.
Gadd, G. M. (2007). "Geomycology: biogeochemical transformations of rocks, minerals, metals and radionuclides by fungi, bioweathering and bioremediation." Mycol Res **111**(Pt 1): 3-49.

Gao, J.-M., S.-X. Yang and J.-C. Qin (2013). "Azaphilones: Chemistry and Biology." Chemical Reviews **113**(7): 4755-4811.
Gao, Y. H., R. Zheng, J. Li, W. S. Kong, X. Liu, L. Ye, Q. L. Mi, W. S. Kong, M. Zhou, G. Y. Yang, Q. F. Hu, G. Du, H. Y. Yang and X. M. Li (2018). "Three new diphenyl ether derivatives from the fermentation products of an endophytic fungus Phomopsis fukushii." J Asian Nat Prod Res: 1-7.
Goddard, M. L., N. Mottier, J. Jeanneret-Gris, D. Christen, R. Tabacchi and E. Abou-Mansour (2014). "Differential production of phytotoxins from Phomopsis sp. from grapevine plants showing esca symptoms." J Agric Food Chem **62**(34): 8602-8607.
Gomes, R. R., C. Glienke, S. I. Videira, L. Lombard, J. Z. Groenewald and P. W. Crous (2013). "Diaporthe: a genus of endophytic, saprobic and plant pathogenic fungi." Persoonia **31**: 1-41.
Grantina-Ievina, L. and I. Kalniņa (2016). Strawberry crown rot–a common problem in 2015. OF THE 74th SCIENTIFIC CONFERENCE OF THE UNIVERSITY OF LATVIA.
Greve, H., I. E. Mohamed, A. Pontius, S. Kehraus, H. Gross and G. M. Konig (2010). "Fungal metabolites: structural diversity as incentive for anticancer drug development." Phytochemistry Reviews **9**(4): 537-545.
Griffiths, M., R. Wylie, S. Lawson, G. Pegg and J. McDonald (2004). Known or potential threats from pests and diseases to prospective tree species for high value timber plantings in northern Australia.
Grishkan, I., E. Zaady and E. Nevo (2006). "Soil crust microfungi along a southward rainfall gradient in desert ecosystems." European Journal of Soil Biology **42**(1): 33-42.
Gu, B.-B., Y. wu, J. Tang, W.-h. Jiao, L. Li, F. Sun, S.-P. Wang, F. Yang and H.-W. Lin (2018). "Azaphilone and isocoumarin derivatives from the sponge-derived fungus Eupenicillium sp. 6A-9." Tetrahedron Letters **59**(36): 3345-3348.
Haarmann, T., Y. Rolke, S. Giesbert and P. Tudzynski (2009). "Ergot: from witchcraft to biotechnology." Mol Plant Pathol **10**(4): 563-577.
Hemtasin, C., S. Kanokmedhakul, P. Moosophon, K. Soytong and K. Kanokmedhakul (2016). "Bioactive azaphilones from the fungus Penicillium multicolor CM01." Phytochem. Lett. **16**: 56-60.
Hermawati, E., L. D. Juliawaty and E. H. Hakim (2017). "A Quinone Derivative from an Endophytic Fungus Phomopsis sp from Morus cathayana." Records of Natural Products **11**(3): 315-317.
Hetherington, A. C. and H. Raistrick (1931). "On the Production and Chemical Constitution of a New Yellow Colouring Matter, Citrinin, Produced from Glucose by Penicillium citrinum Thom." Philosophical Transactions of the Royal Society B: Biological Sciences **220**(468-473): 269-295.
Hewage, R. T., T. Aree, C. Mahidol, S. Ruchirawat and P. Kittakoop (2014). "One strain-many compounds (OSMAC) method for production of polyketides, azaphilones, and an isochromanone using the endophytic fungus Dothideomycete sp." Phytochemistry **108**: 87-94.
Hsiao, Y., H. S. Chang, T. W. Liu, S. Y. Hsieh, G. F. Yuan, M. J. Cheng and I. S. Chen (2016). "Secondary Metabolites and Bioactivity of the Endophytic Fungus Phomopsis theicola from Taiwanese endemic plant." Records of Natural Products **10**(2): 189-194.
Hsu, Y. W., L. C. Hsu, Y. H. Liang, Y. H. Kuo and T. M. Pan (2011). "New bioactive orange pigments with yellow fluorescence from Monascus-fermented dioscorea." J Agric Food Chem **59**(9): 4512-4518.

Hu, H. B., Y. F. Luo, P. Wang, W. J. Wang and J. Wu (2018). "Xanthone-derived polyketides from the Thai mangrove endophytic fungus Phomopsis sp. xy21." Fitoterapia **131**: 265-271.
Hu, M., Q. L. Li, Y. B. Yang, K. Liu, C. P. Miao, L. X. Zhao and Z. T. Ding (2017). "Koninginins R-S from the endophytic fungus Trichoderma koningiopsis." Nat Prod Res **31**(7): 835-839.
Hu, M., X. Q. Yang, C. P. Wan, B. Y. Wang, H. Y. Yin, L. J. Shi, Y. M. Wu, Y. B. Yang, H. Zhou and Z. T. Ding (2018). "Potential antihyperlipidemic polyketones from endophytic Diaporthe sp. JC-J7 in Dendrobium nobile." Rsc Advances **8**(73): 41810-41817.
Hu, Q., Y. Yang, S. Yang, H. Cao, M. Chunyang, H. Yang, X. Gao and G. Du (2015). "Xanthones from the Fermentation Products of the Endophytic Fungus of Phomopsis amygdali." Chemistry of Natural Compounds **51**(3): 456-459.
Hu, Y., Y. Zhou, Z. Mao, H. Li, F. Chen and Y. Shao (2017). "NAD(+)-dependent HDAC inhibitor stimulates Monascus pigment production but inhibit citrinin." AMB Express **7**(1): 166.
Hu, Z., Y. Wu, S. Xie, W. Sun, Y. Guo, X. N. Li, J. Liu, H. Li, J. Wang, Z. Luo, Y. Xue and Y. Zhang (2017). "Phomopsterones A and B, Two Functionalized Ergostane-Type Steroids from the Endophytic Fungus Phomopsis sp. TJ507A." Org Lett **19**(1): 258-261.
Huang, M., J. Li, L. Liu, S. Yin, J. Wang and Y. Lin (2016). "Phomopsichin A-D; Four New Chromone Derivatives from Mangrove Endophytic Fungus Phomopsis sp. 33." Mar Drugs **14**(11): 215.
Huang, R., B. G. Jiang, X. N. Li, Y. T. Wang, S. S. Liu, K. X. Zheng, J. He and S. H. Wu (2018). "Polyoxygenated Cyclohexenoids with Promising alpha-Glycosidase Inhibitory Activity Produced by Phomopsis sp. YE3250, an Endophytic Fungus Derived from Paeonia delavayi." J Agric Food Chem **66**(5): 1140-1146.
Huang, Z. J., J. X. Yang, F. H. Lei, Z. G. She and Y. C. Lin (2013). "A New Xanthone O-Glycoside from the Mangrove Endophytic Fungus Phomopsis sp." Chemistry of Natural Compounds **49**(1): 27-30.
Hufendiek, P., S. S. M. Stoelben, S. Kehraus, N. Merten, H. Harms, M. Cruesemann, I. Arslan, M. Guetschow, T. Schneider and G. M. Koenig (2017). "Biosynthetic Studies on Acetosellin and Structure Elucidation of a New Acetosellin Derivative." Planta Med. **83**(12/13): 1044-1052.
Ishibashi, K. (1961). Pyrenophorin, an antibiotic, Sankyo Co., Ltd. .
Ito, A., I. Kumagai, M. Maruyama, H. Maeda, A. Tonouchi, T. Nehira, K. Kimura and M. Hashimoto (2016). "Homopetasinic acid isolated from Diaporthe sp strain 1308-05." Tetrahedron Letters **57**(10): 1117-1119.
Jackson, P. A., J. C. Widen, D. A. Harki and K. M. Brummond (2017). "Covalent Modifiers: A Chemical Perspective on the Reactivity of α,β-Unsaturated Carbonyls with Thiols via Hetero-Michael Addition Reactions." Journal of Medicinal Chemistry **60**(3): 839-885.
Jansen, N., B. Ohlendorf, A. Erhard, T. Bruhn, G. Bringmann and J. F. Imhoff (2013). "Helicusin E, isochromophilone X and isochromophilone XI: new chloroazaphilones produced by the fungus Bartalinia robillardoides strain LF550." Mar Drugs **11**(3): 800-816.
Ju, Z.-R., X.-P. Lin, Y.-Q. Tian, J.-F. Wang, J. Liu, Y. Liu, Z.-R. Ju, Y. Wang, S.-H. Xu, M. Li, Z. Tu, Y. Liu and Y. Liu (2017). "Chaetochromones A - C, Three New Polyketides from Mangrove Plant Derived Endophytic Fungus Phomopsis sp. SCSIO 41006." Chem Biodivers **14**(11).

Kanoh, K., S. Kohno, T. Asari, T. Harada, J. Katada, M. Muramatsu, H. Kawashima, H. Sekiya and I. Uno (1997). "(–)-Phenylahistin: A new mammalian cell cycle inhibitor produced by aspergillus ustus." Bioorganic & Medicinal Chemistry Letters **7**(22): 2847-2852.
Kasaei, A., M. Mobini-Dehkordi, F. Mahjoubi and B. Saffar (2017). "Isolation of Taxol-Producing Endophytic Fungi from Iranian Yew Through Novel Molecular Approach and Their Effects on Human Breast Cancer Cell Line." Current Microbiology **74**(6): 702-709.
Kastanias, M. A. and M. Chrysayi-Tokousbalides (2005). "Bioactivity of the Fungal Metabolite (8R,16R)-(-)-Pyrenophorin on Graminaceous Plants." J. Agric. Food Chem. **53**(15): 5943-5947.
Khamthong, N., V. Rukachaisirikul, S. Phongpaichit, S. Preedanon and J. Sakayaroj (2014). "An antibacterial cytochalasin derivative from the marine-derived fungus Diaporthaceae sp PSU-SP2/4." Phytochemistry Letters **10**: 5-9.
Khurana, N., S. B. Sharma, A. A. Jafri and A. M. Sharma (2017). "Azaphilones: their role in various biological activities." Asian J. Biomed. Pharm. Sci. **7**(60): 34-43.
Kim, S. M., S. Son, J. W. Kim, E. S. Jeon, S.-K. Ko, I.-J. Ryoo, K.-S. Shin, H. Hirota, S. Takahashi, H. Osada, J.-H. Jang and J. S. Ahn (2015). "Penidioxolanes A and B, 1,3-Dioxolane Containing Azaphilone Derivatives from Marine-derivedPenicilliumsp. KCB12C078." Natural Product Sciences **21**(4): 231-236.
Kind, R., A. Zeeck, S. Grabley, R. Thiericke and M. Zerlin (1996). "Secondary metabolites by chemical screening .30. Helmidiol, a new macrodiolide from Alternaria alternata." Journal of Natural Products **59**(5): 539-540.
Kis, Z., P. Furger and H. P. Sigg (1969). "Über die Isolierung von Pyrenophorol." Experientia **25**(2): 123-124.
Klimek, M., S. Wang and A. Ogunkanmi (2009). "Safety and efficacy of red yeast rice (Monascus purpureus) as an alternative therapy for hyperlipidemia." P & T : a peer-reviewed journal for formulary management **34**(6): 313-327.
Kongprapan, T., X. Xu, V. Rukachaisirikul, S. Phongpaichit, J. Sakayaroj, J. Chen and X. Shen (2017). "Cytosporone derivatives from the endophytic fungus Phomopsis sp PSU-H188." Phytochemistry Letters **22**: 219-223.
Kornsakulkarn, J., W. Somyong, S. Supothina, N. Boonyuen and C. Thongpanchang (2015). "Bioactive oxygen-bridged cyclooctadienes from endophytic fungus Phomopsis sp. BCC 45011." Tetrahedron **71**(48): 9112-9116.
Kuhnert, E., F. Surup, S. Halecker and M. Stadler (2017). "Minutellins A - D, azaphilones from the stromata of Annulohypoxylon minutellum (Xylariaceae)." Phytochemistry **137**: 66-71.
Kui-Wu, W., W. Shi-Wei, W. Bin and W. Ji-Guang (2014). "Bioactive Natural Compounds from the Mangrove Endophytic Fungi." Mini-Reviews in Medicinal Chemistry **14**(4): 370-391.
La Kim, E., J. Lin Li, B. Xiao, J. Hong, E. Sook Yoo, W. Duk Yoon and J. H. Jung (2012). "A New Cyclic Tetrapeptide from the Jellyfish-derived Fungus Phoma sp." Chemical and Pharmaceutical Bulletin **advpub**.
Le Calvez, T., G. Burgaud, S. Mahe, G. Barbier and P. Vandenkoornhuyse (2009). "Fungal diversity in deep-sea hydrothermal ecosystems." Appl Environ Microbiol **75**(20): 6415-6421.
Li, G., S. Kusari, P. Kusari, O. Kayser and M. Spiteller (2015). "Endophytic Diaporthe sp. LG23 Produces a Potent Antibacterial Tetracyclic Triterpenoid." J Nat Prod **78**(8): 2128-2132.

Li, J., X. Yang, Y. Lin, J. Yuan, Y. Lu, X. Zhu, J. Li, M. Li, Y. Lin, J. He and L. Liu (2014). "Meroterpenes and azaphilones from marine mangrove endophytic fungus Penicillium 303#." Fitoterapia **97**: 241-246.
Li, L., H. Wang, J. Yang, J. Lou, G. Liu, X. Gao, Q. Hu and Y. Ye (2014). "A New Dihydroxanthenone from the Fermentation Products of Endophytic Fungus of Phomopsis amygdali." Asian Journal of Chemistry **26**(24): 8271-8273.
Li, T. X., R. H. Liu, X. B. Wang, J. Luo, J. G. Luo, L. Y. Kong and M. H. Yang (2018). "Hypoxia-Protective Azaphilone Adducts from Peyronellaea glomerata." J Nat Prod **81**(5): 1148-1153.
Li, W., C. Lee, S. H. Bang, J. Y. Ma, S. Kim, Y. S. Koh and S. H. Shim (2017). "Isochromans and Related Constituents from the Endophytic Fungus Annulohypoxylon truncatum of Zizania caduciflora and Their Anti-Inflammatory Effects." J Nat Prod **80**(1): 205-209.
Li, X., Y. Tian, S. X. Yang, Y. M. Zhang and J. C. Qin (2013). "Cytotoxic azaphilone alkaloids from Chaetomium globosum TY1." Bioorg Med Chem Lett **23**(10): 2945-2947.
Li, X. H., X. H. Han, L. L. Qin, J. L. He, Z. X. Cao, Y. C. Gu, D. L. Guo and Y. Deng (2018). "Isochromanes from Aspergillus fumigatus, an endophytic fungus from Cordyceps sinensis." Nat Prod Res: 1-6.
Li, Y., Q. Yue, D. R. Jayanetti, D. C. Swenson, G. A. Bartholomeusz, Z. An, J. B. Gloer and G. F. Bills (2017). "Anti-Cryptococcus Phenalenones and Cyclic Tetrapeptides from Auxarthron pseudauxarthron." J Nat Prod **80**(7): 2101-2109.
Li, Z. J., H. Y. Yang, J. Li, X. Liu, L. Ye, W. S. Kong, S. Y. Tang, G. Du, Z. H. Liu, M. Zhou, G. Y. Yang, Q. F. Hu and X. M. Li (2018). "Isopentylated diphenyl ether derivatives from the fermentation products of an endophytic fungus Phomopsis fukushii." J Antibiot (Tokyo) **71**(3): 359-362.
Liu, K., Y. Yang, C. P. Miao, Y. K. Zheng, J. L. Chen, Y. W. Chen, L. H. Xu, H. L. Guang, Z. T. Ding and L. X. Zhao (2016). "Koningiopisins A-H, Polyketides with Synergistic Antifungal Activities from the Endophytic Fungus Trichoderma koningiopsis." Planta Med **82**(4): 371-376.
Liu, K., Y. B. Yang, J. L. Chen, C. P. Miao, Q. Wang, H. Zhou, Y. W. Chen, Y. Q. Li, Z. T. Ding and L. X. Zhao (2016). "Koninginins N-Q, Polyketides from the Endophytic Fungus Trichoderma koningiopsis Harbored in Panax notoginseng." Nat Prod Bioprospect **6**(1): 49-55.
Liu, Y., Z. Hu, X. Lin, C. Lu and Y. Shen (2013). "A new polyketide from Diaporthe sp. SXZ-19, an endophytic fungal strain of Camptotheca acuminate." Nat Prod Res **27**(22): 2100-2104.
Liu, Z., J. Zhao, X. Liang, X. Lv, Y. Li, J. Qu and Y. Liu (2018). "Dothiorelone derivatives from an endophyte Diaporthe pseudomangiferaea inhibit the activation of human lung fibroblasts MRC-5 cells." Fitoterapia **127**: 7-14.
Lomascolo, A., C. Stentelaire, M. Asther and L. Lesage-Meessen (1999). "Basidiomycetes as new biotechnological tools to generate natural aromatic flavours for the food industry." Trends in Biotechnology **17**(7): 282-289.
Luo, J. G., Y. M. Xu, D. C. Sandberg, A. E. Arnold and A. A. Gunatilaka (2017). "Montagnuphilones A-G, Azaphilones from Montagnulaceae sp. DM0194, a Fungal Endophyte of Submerged Roots of Persicaria amphibia." J Nat Prod **80**(1): 76-81.
Luo, X., X. Lin, H. Tao, J. Wang, J. Li, B. Yang, X. Zhou and Y. Liu (2018). "Isochromophilones A-F, Cytotoxic Chloroazaphilones from the Marine Mangrove Endophytic Fungus Diaporthe sp. SCSIO 41011." J Nat Prod **81**(4): 934-941.

Luo, X. W., J. Yang, F. M. Chen, X. P. Lin, C. M. Chen, X. F. Zhou, S. W. Liu and Y. H. Liu (2018). "Structurally Diverse Polyketides From the Mangrove-Derived Fungus Diaporthe sp SCSIO 41011 With Their Anti-influenza A Virus Activities." Frontiers in Chemistry **6**: 282.
Luo, Y. F., M. Zhang, J. G. Dai, P. Pedpradab, W. J. Wang and J. Wu (2016). "Cytochalasins from mangrove endophytic fungi Phomopsis spp. xy21 and xy22." Phytochemistry Letters **17**: 162-166.
Ma, K.-X., X.-T. Shen, R. Huang, T. Wang, X.-S. Xie, S.-W. Liu, S.-H. Wu and J. He (2014). "Bioactive metabolites produced by the endophytic fungus Phomopsis sp. YM355364." Nat. Prod. Commun. **9**(5): 669-670.
Ma, X., W. Wang, E. Li, F. Gao, L. Guo and Y. Pei (2016). "A new sesquiterpene from the entomogenous fungus Phomopsis amygdali." Nat Prod Res **30**(3): 276-280.
Mandavid, H., A. M. Rodrigues, L. S. Espindola, V. Eparvier and D. Stien (2015). "Secondary Metabolites Isolated from the Amazonian Endophytic Fungus Diaporthe sp. SNB-GSS10." J Nat Prod **78**(7): 1735-1739.
Marmann, A., A. H. Aly, W. H. Lin, B. G. Wang and P. Proksch (2014). "Co-Cultivation-A Powerful Emerging Tool for Enhancing the Chemical Diversity of Microorganisms." Marine Drugs **12**(2): 1043-1065.
McMullin, D. R., B. D. Green and J. D. Miller (2015). "Antifungal sesquiterpenoids and macrolides from an endophytic Lophodermium species of Pinus strobus." Phytochemistry Letters **14**: 148-152.
McMullin, D. R., M. W. Sumarah, B. A. Blackwell and J. D. Miller (2013). "New azaphilones from Chaetomium globosum isolated from the built environment." Tetrahedron Letters **54**(6): 568-572.
Meyer, W. L., L. F. Kuyper, D. W. Phelps and A. W. Cordes (1974). "Structure of the cyclic tetrapeptide tentoxin. Crystal and molecular structure of the dihydro derivative." Journal of the Chemical Society, Chemical Communications(9): 339-340.
Mohan Kumari, H. P., K. Akhilender Naidu, S. Vishwanatha, K. Narasimhamurthy and G. Vijayalakshmi (2009). "Safety evaluation of Monascus purpureus red mould rice in albino rats." Food and Chemical Toxicology **47**(8): 1739-1746.
Muroga, Y., T. Yamada, A. Numata and R. Tanaka (2009). "Chaetomugilins I–O, new potent cytotoxic metabolites from a marine-fish-derived Chaetomium species. Stereochemistry and biological activities." Tetrahedron **65**(36): 7580-7586.
Mycobank. from http://www.mycobank.org/Biolomics.aspx?Table=Mycobank&Rec=92439&Fields=All.
Nakashima, K. I., J. Tomida, T. Kamiya, T. Hirai, Y. Morita, H. Hara, Y. Kawamura, T. Adachi and M. Inoue (2018). "Diaporthols A and B: Bioactive diphenyl ether derivatives from an endophytic fungus Diaporthe sp." Tetrahedron Letters **59**(13): 1212-1215.
Nalli, Y., D. N. Mirza, Z. A. Wani, B. Wadhwa, F. A. Mallik, C. Raina, A. Chaubey, S. Riyaz-Ul-Hassan and A. Ali (2015). "Phialomustin A-D, new antimicrobial and cytotoxic metabolites from an endophytic fungus, Phialophora mustea." Rsc Advances **5**(115): 95307-95312.
Ola, A. R. B., A. Debbab, T. Kurtan, H. Brotz-Oesterhelt, A. H. Aly and P. Proksch (2014). "Dihydroanthracenone metabolites from the endophytic fungus Diaporthe melonis isolated from Annona squamosa." Tetrahedron Letters **55**(20): 3147-3150.
Panthama, N., S. Kanokmedhakul, K. Kanokmedhakul and K. Soytong (2015). "Chemical constituents from the fungus Chaetomium cupreum RY202." Arch. Pharmacal Res. **38**(5): 585-590.

Patakova, P. (2013). "Monascus secondary metabolites: production and biological activity." J Ind Microbiol Biotechnol **40**(2): 169-181.
Puttananjaiah, H., M. Dhale and V. Govindaswamy (2019). Non-Toxic Effect of Monascus purpureus Extract on Lactic Acid Bacteria Suggested Their Application in Fermented Foods.
Ramakrishna, K., R. Sreenivasulu, S. Vidavalur and B. Reddy (2016). "Stereoselective Total Synthesis of (-)-Pyrenophorin." Letters in Organic Chemistry **13**(9): 693-697.
Raudabaugh, D. B., T. Iturriaga, A. Carver, S. Mondo, J. Pangilinan, A. Lipzen, G. F. He, M. Amirebrahimi, I. V. Grigoriev and A. N. Miller (2018). "Coniella lustricola, a new species from submerged detritus." Mycological Progress **17**(1-2): 191-203.
Ren, J., S.-S. Ding, A. Zhu, F. Cao and H.-J. Zhu (2017). "Bioactive Azaphilone Derivatives from the Fungus Talaromyces aculeatus." Journal of Natural Products **80**(8): 2199-2203.
Rodriguez, R. J., J. Henson, E. Van Volkenburgh, M. Hoy, L. Wright, F. Beckwith, Y. O. Kim and R. S. Redman (2008). "Stress tolerance in plants via habitat-adapted symbiosis." ISME J **2**(4): 404-416.
Romano, S., S. A. Jackson, S. Patry and A. D. W. Dobson (2018). "Extending the "One Strain Many Compounds" (OSMAC) Principle to Marine Microorganisms." Marine Drugs **16**(7): 244.
Ronsberg, D., A. Debbab, A. Mandi, V. Vasylyeva, P. Bohler, B. Stork, L. Engelke, A. Hamacher, R. Sawadogo, M. Diederich, V. Wray, W. Lin, M. U. Kassack, C. Janiak, S. Scheu, S. Wesselborg, T. Kurtan, A. H. Aly and P. Proksch (2013). "Pro-apoptotic and immunostimulatory tetrahydroxanthone dimers from the endophytic fungus Phomopsis longicolla." J Org Chem **78**(24): 12409-12425.
Roossinck, M. J. (2011). "The good viruses: viral mutualistic symbioses." Nat Rev Microbiol **9**(2): 99-108.
Ruisi, S., D. Barreca, L. Selbmann, L. Zucconi and S. Onofri (2006). "Fungi in Antarctica." Reviews in Environmental Science and Bio/Technology **6**(1-3): 127-141.
Saad, S. M., J. M. Halloin and D. J. Hagedorn (1970). "Production, purification, and bioassay of tentoxin." Phytopathology **60**(3): 415-418.
Saliba, K. J. and K. Kirk (2005). "CJ-15,801, a fungal natural product, inhibits the intraerythrocytic stage of Plasmodium falciparum in vitro via an effect on pantothenic acid utilization." Mol. Biochem. Parasitol. **141**(1): 129-131.
Sanchez, J. F., Y. M. Chiang, E. Szewczyk, A. D. Davidson, M. Ahuja, C. Elizabeth Oakley, J. Woo Bok, N. Keller, B. R. Oakley and C. C. Wang (2010). "Molecular genetic analysis of the orsellinic acid/F9775 gene cluster of Aspergillus nidulans." Mol Biosyst **6**(3): 587-593.
Sarrocco, S. (2016). "Dung-inhabiting fungi: a potential reservoir of novel secondary metabolites for the control of plant pathogens." Pest Manag Sci **72**(4): 643-652.
Schiff, P. L. (2006). "Ergot and its alkaloids." American Journal of Pharmaceutical Education **70**(5): 98.
Schiff, P. L. (2006). "Ergot and its alkaloids." Am J Pharm Educ **70**(5): 98.
Schloss, S., T. Hackl, C. Herz, E. Lamy, M. Koch, S. Rohn and R. Maul (2017). "Detection of a Toxic Methylated Derivative of Phomopsin A Produced by the Legume-Infesting Fungus Diaporthe toxica." J Nat Prod **80**(6): 1930-1934.
Schmidt-Dannert, C. (2015). Biosynthesis of Terpenoid Natural Products in Fungi. Biotechnology of Isoprenoids. J. Schrader and J. Bohlmann. Cham, Springer International Publishing: 19-61.
Sci-Finder. from https://scifinder.cas.org/scifinder/view/scifinder/scifinderExplore.jsf.

Seuring, B. and D. Seebach (1978). "Syntheses and Determinations of the Absolute-Configurations of Norpyrenophorin, Pyrenophorin, and Vermiculine." Justus Liebigs Annalen Der Chemie(12): 2044-2073.
Shang, Z., R. Raju, A. A. Salim, Z. G. Khalil and R. J. Capon (2017). "Cytochalasins from an Australian Marine Sediment-Derived Phomopsis sp. (CMB-M0042F): Acid-Mediated Intramolecular Cycloadditions Enhance Chemical Diversity." J Org Chem **82**(18): 9704-9709.
Sharma, V., V. Singamaneni, N. Sharma, A. Kumar, D. Arora, M. Kushwaha, S. Bhushan, S. Jaglan and P. Gupta (2018). "Valproic acid induces three novel cytotoxic secondary metabolites in Diaporthe sp., an endophytic fungus from Datura inoxia Mill." Bioorg Med Chem Lett **28**(12): 2217-2221.
Shen, L., Q. Luo, Z. P. Shen, L. Y. Li, X. J. Zhang, Z. Q. Wei, Y. Fu, Y. C. Song and R. X. Tan (2014). "A new cytochalasin from endophytic Phomopsis sp. IFB-E060." Chin J Nat Med **12**(7): 512-516.
Shi, C., L. Yuan, X. Lin and P. J. Zhao (2016). "[Two new lactone derivatives from an endophyte Diaporthe sp. XZ-07 cultivated on Camptotheca acuminata]." Zhongguo Zhong Yao Za Zhi **41**(10): 1860-1863.
Shi, Y.-C., V. H.-C. Liao and T.-M. Pan (2012). "Monascin from red mold dioscorea as a novel antidiabetic and antioxidative stress agent in rats and Caenorhabditis elegans." Free Radical Biology and Medicine **52**(1): 109-117.
Shiono, Y., T. Sasaki, F. Shibuya, Y. Yasuda, T. Koseki and U. Supratman (2013). "Isolation of a phomoxanthone A derivative, a new metabolite of tetrahydroxanthone, from a Phomopsis sp. isolated from the mangrove, Rhizhopora mucronata." Nat Prod Commun **8**(12): 1735-1737.
Siewers, V., L. Kokkelink, J. Smedsgaard and P. Tudzynski (2006). "Identification of an Abscisic Acid Gene Cluster in the Grey Mold Botrytis cinerea." Applied and Environmental Microbiology **72**(7): 4619.
Skellam, E. (2017). "The biosynthesis of cytochalasans." Natural Product Reports **34**(11): 1252-1263.
Son, S., S. K. Ko, J. W. Kim, J. K. Lee, M. Jang, I. J. Ryoo, G. J. Hwang, M. C. Kwon, K. S. Shin, Y. Futamura, Y. S. Hong, H. Oh, B. Y. Kim, M. Ueki, S. Takahashi, H. Osada, J. H. Jang and J. S. Ahn (2016). "Structures and biological activities of azaphilones produced by Penicillium sp. KCB11A109 from a ginseng field." Phytochemistry **122**: 154-164.
Sousa, J. P. B., M. M. Aguilar-Pérez, A. E. Arnold, N. Rios, P. D. Coley, T. A. Kursar and L. Cubilla-Rios (2016). "Chemical constituents and their antibacterial activity from the tropical endophytic fungus Diaporthe sp. F2934." Journal of Applied Microbiology **120**(6): 1501-1508.
Stadler, M. and J. Fournier (2006). "Pigment chemistry, taxonomy and phylogeny of the Hypoxyloideae (Xylariaceae)." Rev Iberoam Micol **23**(3): 160-170.
Steinberg, P., K. E. Appel, M. Baum, H. Brunn, P. Diel, G. Eisenbrand, B. Engeli, J. Hengstler, H.-U. Humpf, D. Lachenmeier, D. Marko, C. Steffen and P. Winterhalter (2013). Toxicological evaluation of red mould rice: An update.
Stierle, A. A., D. B. Stierle, T. Girtsman, T. C. Mou, C. Antczak and H. Djaballah (2015). "Azaphilones from an Acid Mine Extremophile Strain of a Pleurostomophora sp." Journal of Natural Products **78**(12): 2917-2923.
Stierle, A. A., D. B. Stierle and K. Kelly (2006). "Berkelic Acid, A Novel Spiroketal with Selective Anticancer Activity from an Acid Mine Waste Fungal Extremophile." The Journal of Organic Chemistry **71**(14): 5357-5360.

Sugawara, F. and G. A. Strobel (1986). "(–)-Dihydropyrenophorin, a novel and selective phytotoxin produced by Drechslera avenae." Plant Science **43**(1): 1-5.
Sugie, Y., K. A. Dekker, H. Hirai, T. Ichiba, M. Ishiguro, Y. Shioni, A. Sugiura, L. Brennan, J. Duignan, L. H. Huang, J. Sutcliffe and Y. Kojima (2001). "CJ-15,801, a Novel Antibiotic from a Fungus, Seimatosporium sp." The Journal of Antibiotics **54**(12): 1060-1065.
Sun, Y., L. Tian, J. Huang, H. Y. Ma, Z. Zheng, A. L. Lv, K. Yasukawa and Y. H. Pei (2008). "Trichodermatides A-D, novel polyketides from the marine-derived fungus Trichoderma reesei." Org Lett **10**(3): 393-396.
Surup, F., K. I. Mohr, R. Jansen and M. Stadler (2013). "Cohaerins G–K, azaphilone pigments from Annulohypoxylon cohaerens and absolute stereochemistry of cohaerins C–K." Phytochemistry **95**: 252-258.
Tan, R. X. and W. X. Zou (2001). "Endophytes: a rich source of functional metabolites." Nat Prod Rep **18**(4): 448-459.
Tang, J. W., W. G. Wang, A. Li, B. C. Yan, R. Chen, X. N. Li, X. Du, H. D. Sun and J. X. Pu (2017). "Polyketides from the endophytic fungus Phomopsis sp sh917 by using the one strain/many compounds strategy." Tetrahedron **73**(26): 3577-3584.
Tao, M.-H., Y.-C. Chen, X.-Y. Wei, J.-W. Tan and W.-M. Zhang (2014). "Chemical constituents of the endophytic fungus Phomopsis sp. A240 isolated from Taxus chinensis var. mairei." Helv. Chim. Acta **97**(3): 426-430.
Tarawneh, A. H., F. Leon, M. M. Radwan, L. H. Rosa and S. J. Cutler (2013). "Secondary metabolites from the fungus Emericella nidulans." Nat Prod Commun **8**(9): 1285-1288.
Tian, W., Z. Liao, M. Zhou, G. Wang, Y. Wu, S. Gao, D. Qiu, X. Liu, T. Lin and H. Chen (2018). "Cytoskyrin C, an unusual asymmetric bisanthraquinone with cage-like skeleton from the endophytic fungus Diaporthe sp." Fitoterapia **128**: 253-257.
Tribe, H. T. (1998). "The discovery and development of cyclosporin." Mycologist **12**(1): 20-22.
Udayanga, D., X. Z. Liu, E. H. C. McKenzie, E. Chukeatirote, A. H. A. Bahkali and K. D. Hyde (2011). "The genus Phomopsis: biology, applications, species concepts and names of common phytopathogens." Fungal Diversity **50**(1): 189-225.
van der Westhuyzen, R., J. C. Hammons, J. L. Meier, S. Dahesh, W. J. Moolman, S. C. Pelly, V. Nizet, M. D. Burkart and E. Strauss (2012). "The antibiotic CJ-15,801 is an antimetabolite that hijacks and then inhibits CoA biosynthesis." Chem Biol **19**(5): 559-571.
Van Niekerk, J. M., J. Z. Groenewald, G. J. Verkley, P. H. Fourie, M. J. Wingfield and P. W. Crous (2004). "Systematic reappraisal of Coniella and Pilidiella, with specific reference to species occurring on Eucalyptus and Vitis in South Africa." Mycol Res **108**(Pt 3): 283-303.
Verekar, S. A., P. D. Mishra, E. S. Sreekumar, S. K. Deshmukh, H. H. Fiebig, G. Kelter and A. Maier (2014). "Anticancer activity of new depsipeptide compound isolated from an endophytic fungus." J Antibiot (Tokyo) **67**(10): 697-701.
Vleggaar, R., P. S. Steyn and D. W. Nagel (1974). "Constitution and absolute configuration of austdiol, the main toxic metabolite from Aspergillus ustus." Journal of the Chemical Society, Perkin Transactions 1(0): 45-49.
Von Höhnel, F. (1918). "Dritte vorlaufige Mitteilung mycologischer Ergebnisse (Nr. 201-304)." Ber Deut Bot Ges **36**: 309-317.
Wang, C., L. Engelke, D. Bickel, A. Hamacher, M. Frank, P. Proksch, H. Gohlke and M. U. Kassack (2019). "The tetrahydroxanthone-dimer phomoxanthone A is a strong inducer of

apoptosis in cisplatin-resistant solid cancer cells." Bioorganic & Medicinal Chemistry **27**(19): 115044.
Wang, C. Y., J. D. Hao, X. Y. Ning, J. S. Wu, D. L. Zhao, C. J. Kong, C. L. Shao and C. Y. Wang (2018). "Penicilazaphilones D and E: two new azaphilones from a sponge-derived strain of the fungus Penicillium sclerotiorum." Rsc Advances **8**(8): 4348-4353.
Wang, G.-Y.-S., B. M. Borgeson and P. Crews (1997). "Pitholides A-D, polyketides from a marine tunicate-derived culture of Pithomyces sp." Tetrahedron Letters **38**(49): 8449-8452.
Wang, J., G. Bai, Y. Liu, H. Wang, Y. Li, W. Yin, Y. Wang and F. Lu (2015). "Cytotoxic Metabolites Produced by the Endophytic Fungus Aspergillus clavatus." Chemistry Letters **44**(8): 1148-1149.
Wang, P., Y. F. Luo, M. Zhang, J. G. Dai, W. J. Wang and J. Wu (2018). "Three xanthone dimers from the Thai mangrove endophytic fungus Phomopsis sp. xy21." J Asian Nat Prod Res **20**(3): 217-226.
Wang, W., Y. Liao, R. Chen, Y. Hou, W. Ke, B. Zhang, M. Gao, Z. Shao, J. Chen and F. Li (2018). "Chlorinated azaphilone pigments with antimicrobial and cytotoxic activities isolated from the deep sea derived fungus chaetomium sp. NA-S01-R1." Mar. Drugs **16**(2): 61/61-61/11.
Wang, W. X., S. Kusari, H. Laatsch, C. Golz, P. Kusari, C. Strohmann, O. Kayser and M. Spiteller (2016). "Antibacterial Azaphilones from an Endophytic Fungus, Colletotrichum sp. BS4." J Nat Prod **79**(4): 704-710.
Wei, W., J. Gao, Y. Shen, Y. L. Chu, Q. Xu and R. X. Tan (2014). "Immunosuppressive Diterpenes from Phomopsis sp. S12." European Journal of Organic Chemistry **2014**(26): 5728-5734.
Wijeratne, E. M., P. Espinosa-Artiles, R. Gruener and A. A. Gunatilaka (2014). "Thielavialides A-E, nor-spiro-azaphilones, and a bis-spiro-azaphilone from Thielavia sp. PA0001, an endophytic fungus isolated from aeroponically grown Physalis alkekengi." J Nat Prod **77**(6): 1467-1472.
Wijesekera, K., C. Mahidol, S. Ruchirawat and P. Kittakoop (2017). "Metabolite diversification by cultivation of the endophytic fungus Dothideomycete sp. in halogen containing media: Cultivation of terrestrial fungus in seawater." Bioorg Med Chem **25**(11): 2868-2877.
Wu, M.-D., M.-J. Cheng, Y.-J. Yech, Y.-L. Chen, K.-P. Chen, I.-S. Chen, P.-H. Yang and G.-F. Yuan (2011). "Monasnicotinates A-D, four new pyridine alkaloids from the fungal strain Monascus pilosus BCRC 38093." Molecules (Basel, Switzerland) **16**(6): 4719-4727.
Wu, M. D., M. J. Cheng, Y. J. Yech, Y. L. Chen, K. P. Chen, P. H. Yang, I. S. Chen and G. F. Yuan (2013). "Monascusazaphilones A-C, three new azaphilone analogues isolated from the fungus Monascus purpureus BCRC 38108." Nat Prod Res **27**(13): 1145-1152.
Wu, Q., Y. Guo, Z. K. Guo, Y. L. Chu, T. Wang and R. X. Tan (2013). "Two new cytosporones from the culture of endophytic Phomopsis sp." Chemistry of Natural Compounds **48**(6): 938-941.
Wu, S. H., R. Huang, C. P. Miao and Y. W. Chen (2013). "Two new steroids from an endophytic fungus Phomopsis sp." Chem Biodivers **10**(7): 1276-1283.
Xiao, Z. e., S. e. Lin, C. Tan, X. Huang, Z. She, Y. Lu and L. He (2015). "Asperlones A and B, dinaphthalenone derivatives from a mangrove endophytic fungus Aspergillus sp. 16-5C." Mar Drugs **13**(1): 366-378.
Xie, S., Y. Wu, Y. Qiao, Y. Guo, J. Wang, Z. Hu, Q. Zhang, X. Li, J. Huang, Q. Zhou, Z. Luo, J. Liu, H. Zhu, Y. Xue and Y. Zhang (2018). "Protoilludane, Illudalane, and Botryane

Sesquiterpenoids from the Endophytic Fungus Phomopsis sp. TJ507A." J Nat Prod **81**(6): 1311-1320.
Xu, J., H. Tan, Y. Chen, S. Li, Z. Huang, H. Guo, H. Li, X. Gao, H. Liu and W. Zhang (2018). "Lithocarpins A–D: four tenellone-macrolide conjugated [4 + 2] hetero-adducts from the deep-sea derived fungus Phomopsis lithocarpus FS508." Organic Chemistry Frontiers **5**(11): 1792-1797.
Xu, J. L., H. X. Liu, Y. C. Chen, H. B. Tan, H. Guo, L. Q. Xu, S. N. Li, Z. L. Huang, H. H. Li, X. X. Gao and W. M. Zhang (2018). "Highly Substituted Benzophenone Aldehydes and Eremophilane Derivatives from the Deep-Sea Derived Fungus Phomopsis lithocarpus FS508." Mar Drugs **16**(9).
Yan, B. C., W. G. Wang, D. B. Hu, X. Sun, L. M. Kong, X. N. Li, X. Du, S. H. Luo, Y. Liu, Y. Li, H. D. Sun and J. X. Pu (2016). "Phomopchalasins A and B, Two Cytochalasans with Polycyclic-Fused Skeletons from the Endophytic Fungus Phomopsis sp. shj2." Org Lett **18**(5): 1108-1111.
Yang, H.-Y., Y.-Q. Duan, Y.-K. Yang, J. Li, X. Liu, L. Ye, Q.-L. Mi, W.-S. Kong, M. Zhou, G.-Y. Yang, X.-M. Li and Q.-F. Hu (2017). "Three new napthalene derivatives from the endophytic fungus Phomopsis fukushii." Phytochemistry Letters **22**: 266-269.
Yang, H. Y., Y. H. Gao, D. Y. Niu, L. Y. Yang, X. M. Gao, G. Du and Q. F. Hu (2013). "Xanthone derivatives from the fermentation products of an endophytic fungus Phomopsis sp." Fitoterapia **91**: 189-193.
Yang, J. X., S. Qiu, Z. She and Y. Lin (2013). "A new xanthone derivative from the marine fungus Phomopsis sp. (No. SK7RN3G1)." Chemistry of Natural Compounds **49**(2): 246-248.
Yang, J. X., S. X. Qiu, Z. G. She and Y. C. Lin (2014). "A New Isochroman Derivative from the Marine Fungus Phomopsis sp (No. Gx-4)." Chemistry of Natural Compounds **50**(3): 424-426.
Yang, Y. C., H. Y. Yang, Y. K. Li, Y. Q. Ye, Q. F. Hu, X. M. Gao and G. Du (2014). "A New Xanthone from the Fermentation Products of Endophytic Fungus of Phomopsis Species." Asian Journal of Chemistry **26**(15): 4591-4593.
Yang, Z. J., J. W. Ding, K. S. Ding, D. J. Chen, S. Cen and M. Ge (2013). "Phomonaphthalenone A: A novel dihydronaphthalenone with anti-HIV activity from Phomopsis sp HCCB04730." Phytochemistry Letters **6**(2): 257-260.
Yedukondalu, N., P. Arora, B. Wadhwa, F. A. Malik, R. A. Vishwakarma, V. K. Gupta, S. Riyaz-Ul-Hassan and A. Ali (2017). "Diapolic acid A-B from an endophytic fungus, Diaporthe terebinthifolii depicting antimicrobial and cytotoxic activity." J Antibiot (Tokyo) **70**(2): 212-215.
Yin, G.-P., Y.-R. Wu, M.-H. Yang, T.-X. Li, X.-B. Wang, M.-M. Zhou, J.-L. Lei and L.-Y. Kong (2017). "Citrifurans A-D, Four Dimeric Aromatic Polyketides with New Carbon Skeletons from the Fungus Aspergillus sp." Org. Lett. **19**(15): 4058-4061.
Youn, U. J., T. Sripisut, E. J. Park, T. P. Kondratyuk, N. Fatima, C. J. Simmons, M. M. Wall, D. Sun, J. M. Pezzuto and L. C. Chang (2015). "Determination of the absolute configuration of chaetoviridins and other bioactive azaphilones from the endophytic fungus Chaetomium globosum." Bioorg Med Chem Lett **25**(21): 4719-4723.
Yu, H., J. Sperlich, A. Mandi, T. Kurtan, H. Dai, N. Teusch, Z. Y. Guo, K. Zou, Z. Liu and P. Proksch (2018). "Azaphilone Derivatives from the Fungus Coniella fragariae Inhibit NF-kappaB Activation and Reduce Tumor Cell Migration." J Nat Prod **81**(11): 2493-2500.

Yuan, L., W. Z. Huang, G. Du, X. M. Gao, H. Y. Yang, Q. F. Hu and Y. H. Ma (2015). "Isolation of Xanthones from the Fermentation Products of the Endophytic Fungus of Phomopsis amygdali." Chemistry of Natural Compounds **51**(3): 460-463.
Zhan, F., X. Y. Li, L. W. Wu, T. Yang, Y. P. Han and G. Y. Li (2013). "Cytochalasins from the endophytic fungus Phomopsis sp cib-109." Chemistry of Natural Compounds **49**(4): 696-698.
Zhang, D., J. Zhao, X. Wang, L. Zhao, H. Liu, Y. Wei, X. You, S. Cen and L. Yu (2018). "Peniazaphilin A, a new azaphilone derivative produced by Penicillium sp. CPCC 400786." J Antibiot (Tokyo) **71**(10): 905-907.
Zhang, L.-h., Y. Long, X.-l. Lei, J.-y. Xu, Z.-j. Huang, Z.-g. She, Y.-c. Lin, J. Li and L. Liu (2016). "Azaphilones isolated from an alga-derived fungus Penicillium sp. ZJ-27." Phytochem. Lett. **18**: 180-186.
Zhang, Q., H. Q. Li, S. C. Zong, J. M. Gao and A. L. Zhang (2012). "Chemical and Bioactive Diversities of the Genus Chaetomium Secondary Metabolites." Mini-Reviews in Medicinal Chemistry **12**(2): 127-148.
Zhang, W., K. Krohn, H. Egold, S. Draeger and B. Schulz (2008). "Diversity of antimicrobial pyrenophorol derivatives from an endophytic fungus, Phoma sp." European Journal of Organic Chemistry(25): 4320-4328.
Zhang, W., L. Xu, L. Yang, Y. Huang, S. Li and Y. Shen (2014). "Phomopsidone A, a novel depsidone metabolite from the mangrove endophytic fungus Phomopsis sp. A123." Fitoterapia **96**: 146-151.
Zhang, Y., F. Hao, N. Liu, Y. Xu, A. Jia, Z. Yang, X. Xia and C. Liu (2013). "Stereochemical determination of a new and cytotoxic euphane triterpenoid from the plant endophytic fungus Phomopsis chimonanthi." J Antibiot (Tokyo) **66**(11): 679-682.
Zhang, Z. X., X. Q. Yang, Q. Y. Zhou, B. Y. Wang, M. Hu, Y. B. Yang, H. Zhou and Z. T. Ding (2018). "New Azaphilones from Nigrospora oryzae Co-Cultured with Beauveria bassiana." Molecules **23**(7): 1816.
Zhao, D.-L., C.-L. Shao, Q. Zhang, K.-L. Wang, F.-F. Guan, T. Shi and C.-Y. Wang (2015). "Azaphilone and diphenyl ether derivatives from a gorgonian-derived strain of the fungus Penicillium pinophilum." J. Nat. Prod. **78**(9): 2310-2314.
Zheng, Y., Y. Zhang, D. Chen, H. Chen, L. Lin, C. Zheng and Y. Guo (2016). "Monascus Pigment Rubropunctatin: A Potential Dual Agent for Cancer Chemotherapy and Phototherapy." J Agric Food Chem **64**(12): 2541-2548.
Zhou, Q. Y., X. Q. Yang, Z. X. Zhang, B. Y. Wang, M. Hu, Y. B. Yang, H. Zhou and Z. T. Ding (2018). "New azaphilones and tremulane sesquiterpene from endophytic Nigrospora oryzae cocultured with Irpex lacteus." Fitoterapia **130**: 26-30.
Zhou, S. L., M. Wang, H. G. Zhao, Y. H. Huang, Y. Y. Lin, G. H. Tan and S. L. Chen (2016). "Penicilazaphilone C, a new antineoplastic and antibacterial azaphilone from the Marine Fungus Penicillium sclerotiorum." Arch Pharm Res **39**(12): 1621-1627.
Zhou, X.-X., J. Li, Y.-H. Yang, Y. Zeng and P.-J. Zhao (2014). "Three new koninginins from Trichoderma neokongii 8722." Phytochemistry Letters **8**: 137-140.
Zhou, X. M., A. F. MacKenzie, C. A. Madramootoo and D. L. Smith (1999). "Effects of stem-injected plant growth regulators, with or without sucrose, on grain production, biomass and photosynthetic activity of field-grown corn plants." Journal of Agronomy and Crop Science-Zeitschrift Fur Acker Und Pflanzenbau **183**(2): 103-110.

7 List of abbreviations

$[\alpha]^{20}_{D}$	specific rotation at the sodium d-line
μg	microgram
μL	microliter
μM	micromolar
A2780 CisR	cisplatin resistance, human ovarian cancer cell line
A2780 Sens	cisplatin sensitive, humane ovarian cancer cell line
BC	Before Christ
br	broad
CD	circular dichroism
CD_3OD	deuterated methanol
$CDCl_3$	deuterated chloroform
CH_2Cl_2	dichloromethane
$CHCl_3$	chloroform
Cl	chlorine
cm	centimeter
COSY	correlation spectroscopy
d	doublet
DCM	dichloromethane
dd	doublet of doublet signal
DMSO	dimethyl sulfoxide
ECD	electronic circular dichroism
EI	electron impact ionization
ESI	electron spray ionization
et al.	et altera (and others)
EtOAc	ethyl acetate
g	gram
HCl	hydrochloric acid
HMBC	heteronuclear multiple bond connectivity
HPLC	high performance liquid chromatography
HPLC-MS	liquid chromatography-mass
HRESIMS	high-resolution electrospray ionisation mass spectrometry hz
HR-MS	high resolution mass spectrometry
HSQC	heteronuclear single quantum coherence
Hz	herz
IC_{50}	half maximal inhibitory concentration
ITS	internal transcriber spacers
L	liter
LC	liquid chromatography
LC/MS	liquid chromatography-mass spectrometery

m	multiplet
M	molar
m/z	mass per charge
MeOD	deuterated methanol
MeOH	methanol
mg	milligram
MHz	mega hertz
MIC	minimum inhibitory concentration
min	minute
mL	milliliter
mm	millimeter
MS	mass spectrometry
MTT	3-(4,5-dimethylthiazol-2-yl)-2,5-diphenyltetrazolium bromide
MW	molecular weight
NF-κB	nuclear factor kappa-light-chain-enhancer of activated b-cells
nM	nanomolar
NMR	nuclear magnetic resonance
NOE	nuclear Overhauser effect
NOESY	nuclear Overhauser and exchange spectroscopy
PCR	polymerase chain reaction
PKS	polyketide synthase
ppm	parts per million
q	quartet signal
ROESY	rotating frame Overhauser enhancement spectroscopy
RP 18	reversed phase c 18
s	singlet
sp.	species (singular)
t	triplet
TDDFT	time-dependent density functional theory
TFA	trifluoroacetic acid
TLC	thin layer chromatography
UV	ultra-violet
VLC	vacuum liquid chromatography

8 Acknowledgements

Foremost, I would express my heartfelt appreciation to my supervisor Prof. Dr. Dres. h.c. Peter Proksch offer me the opportunity to join research group in Institute Pharmaceutical Biology and Biotechnology, Heinrich-Heine University, Duesseldorf. Also, express gratitude to Prof. Proksch for the scientific training, guidance, and support, as well as his support for me to join the DFG GRK2158 program and got finical support from Manchot Foundation.

I would express my thankfulness to Co-supervisor Prof. Dr. Rainer Kalscheuer, (Institute of Pharmaceutical Biology and Biotechnology, Henrich-Heine University Duesseldorf) for evaluation my doctorate research and collaboration in the antimicrobial assays.

My special thanks to Prof. Dr. Haofu Dai (Key Laboratory of Biology and Genetic Resources of Tropical Crops, Ministry of Agriculture, Institute of Tropical Bioscience and Biotechnology, Chinese Academy of Tropical Agricultural Sciences) for accepting me as a master student in his groups and help me applying join the research group of Prof Proksch.

I wish to give my special thanks to Dr. Zhen Liu for sharing the knowledge, elucidating NMR, and correcting manuscript and dissertation. Also, thanks to Dr Marian Frank, a warm-hearted colleague who helped me a lot.

In the scientific collaboration, I would thank Prof. Dr. Nicole Teusch (Institut für gesundheitsforschung und bildung, Universität Osnabrück) and Dr. Julia Sperlich for bioactivity test. Thanks for Prof. Dr. Tibor Kurtán (Department of Organic Chemistry, University of Debrecen, Hungary) for helping in CD measurement. Thanks for Prof. Dr. Matthias Kassackand and Chenyin Wang (Institute of Pharmaceutical and Medicinal Chemistry, Heinrich-Heine-University) for the cytotoxicity test. Thanks for Prof. Dr. Christoph Janiak and Simon-Patrick Höfert (Institute of Inorganic and Structural Chemistry, Heinrich-Heine-University) in the X-ray measurement. Thanks for Prof. Sebastian Wesselborg and Fabian Stuhldreier (Institut für Molekulare Medizin I, Heinrich-Heine-University) in the cytotoxicity test.

I would extend deep appreciate for the suggestion and advises to Prof. Dr. Bingui Wang, (Laboratory of Experimental Marine Biology, Institute of Acknowledgements II Oceanology, Chinese Academy of Science, Qingdao, P. R. China), Prof. Dr. Wenhan Lin (National Research Laboratories of Natural and Biomimetic Drugs, Peking University, Health Science Center, Beijing, P. R. China)

I would like to express my appreciation to our secretary Claudia Eckelskemper, our technicians Waltraud Schlag, Simone Miljanovic, Katja Friedrich, Simone Mönninghoff-Pützer, Linda Wiegand, Heike Goldbach-Gecke (Institute of Pharmaceutical Biology and Biotechnology, Heinrich-Heine University) for her various help and assistance for the help to solve my problems during the living and study whenever needed. My deep thanks to Dr. Martina Holz in GRK2158 for organizing the conference, industry visit, and joining the workshop.

Special thanks to my best friend Nam Michael Tran-Cong. We have several trips and join the symposium together. Special thanks to Dr. Hao Wang for helping my NMR analysis and take care when beginning work in the lab. Special thanks to Dr. Yang Liu for suggestions in and out of the institute.

I also thanks to my collages and friends: Dr. Amin Mokhlesi, Dr. Catalina Perez Hemphill, Dr. Elena Ancheeva, Dr. Feng Pan, Dr. Georgios Daletos, Dr. Rini Muharini, Dr. Sergi Akone, Dr. Shuai Liu, Dina EI-Kashef, Harwoko, Kim Le, Lin Wang, Imke Form, Mariam Moussa, Ni Putu Ariantari, Prof. Han Xiao, Xiaoqin Yu, Ying Gao. We have a nice time together. My great thankful to DFG GRK2158 program and Manchot Foundation for training and supporting.

In the End, I would like deepest gratitude my wife Dr. Yunhua Shi and my son Bingyuan Yu, also with my family. They are forcing and encouraging in the past four years.

To all of you, thank you so much.

9 Curriculum Vitae

Name: Haiqian Yu
Gender: Male.
Nationality: P. R. China.
Adress: Fabriciusstraße 8, 40225 Düsseldorf, Germany
E-Mail: bluebf@live.cn; Haiqian.Yu@hhu.de

Education and Working

From Nov 2015 - present
PhD candidate of natural sciences. Research direction: Natural product chemistry.
Supervisor: Prof. Dr. Dres. h.c. Peter Proksch, Institute of Pharmaceutical Biology and Biotechnology, university Duesseldorf, Germany

From Jul 2013 to Apr 2015
Joint-program (Master), program direction: Natural product chemistry.
Supervisor: Prof. Dr. Haofu Dai, Institute of Tropical Bioscience and Biotechnology, Chinese Academy of Tropical Agricultural Sciences, P. R. China

From Aug 2012 to Jun 2015
Master of science, Majoring in biochemistry and molecular biology, College of Life Sciences, Tarim University, P. R. China

From Jul 2008 to Aug 2012
Working as Technician (2008-2010) and Assistant manager (2010-2012) in Beijing Fluobon Surfactant Institute, P. R. China

From Aug 2005 to Jul 2008
Study in College of Vocation, Beijing University of Chemical Technology, P. R. China

Awards, Joined Program and Conference

Member of research training group 2158 (GRK2158)
Funding by JUERGEN MANCHOT
Awarded the Elsevier Best Poster Prize in the 3rd International PSE Congress on Natural Compounds in Cancer Prevention and Therapy, Naples, Italy.
1st, 2ed, and 3st Symposium of Research Training Group 2158 (GRK2158)

Publication

1. **Yu, H**.; Sperlich, J.; Mandi, A.; Kurtan, T.; Dai, H.; Teusch, N.; Guo, Z. Y.; Zou, K.; Liu, Z.; Proksch, P., Azaphilone Derivatives from the Fungus *Coniella fragariae* Inhibit NF-kappaB Activation and Reduce Tumor Cell Migration. *J Nat Prod* **2018,** *81* (11), 2493-2500.
2. **Yu, H.;** Sperlich, J.; Hofert, S. P.; Janiak, C.; Teusch, N.; Stuhldreier, F.; Wesselborg, S.; Wang, C.; Kassack, M. U.; Dai, H.; Liu, Z.; Proksch, P., Azaphilone pigments and macrodiolides from the coprophilous fungus *Coniella fragariae*. *Fitoterapia* **2019,** *137*, 104249.
3. **Yu H.;** Hofert, S. P.; Moussa M.; Janiak, C.; Müller W. E. G.; Umeokoli B.O.; Dai, H.; Liu, Z.; Proksch, P., Polyketides and Nitrogenous Metabolites from The Endophytic Fungus *Phomopsis* sp. D15a2a. *Tetrahedron Letters* **2019**, 151325.
4. **Yu, H**.; Bai, H.; Mei, W.; Zuo, W.; Wang, H.; Yang, J.; Dai, H., Chemical Constituents from Twigs of *Trigonostemon lutescens* (II). Journal of Tropical and Subtropical Botany 2015, (3), 323-328.
5. **Yu, H**.; Mei, W.; Zuo, W.; Yang, J.; Dai, H., Antibacterial Constituents from Twigs of *Trigonostemon chinensis* Merr.. Chinese Journal of Medicinal Chemistry. 2015, 25 (3), 216-220.
6. Yang, J.; Mei, W.; Dong, W.; **Yu, H.**; Dai, H., GC-MS Analysis of Three Kinds of Agarwood from Vietnam. Chinese Journal of Tropical Crops 2015, (8), 1498-1504.
7. Yang, J.; Mei, W.; **Yu, H**.; Yang, D.; Wang, J.; Li, W.; Dai, H., HPLC fingerprint of Agarwood of *Aquilaria sinensis*. Chinese Traditional and Herbal Drugs 2014, (23), 3456-3461.

8. Yang, J; Mei, W; **Yu, H**; Zuo, W; Dai, H, Determination of Chromones Content in Agarwood by Using UV Spectrophotometry, Journal of Tropical Biology 2014, (4), 400-404.
9. Gao, A.-T.; Xing, H.; Zhou, H.-T.; Cao, A.-Q.; Wu, B.-W.; **Yu, H.-Q**.; Gou, Z.-M.; Xiao, J.-X., Effects of counterion structure on the surface activities of anionic fluorinated surfactants whose counterions are organic ammonium ions. Colloids and Surfaces A: Physicochemical and Engineering Aspects 2014, 459, 31-38.
10. Zhou, H.; Xing, H.; Bao, Y.; **Yu, H**.; Xiao, J., Spreading of aqueous mixtures of sodium perfluorooctanoate and octyl triethylammonium bromide on oil. Journal of Safety and Environment 2011, (2), 200-205.
11. Xing, H.; Zhou, H.-T.; **Yu, H.-Q**.; Gou, Z.-M.; Xiao, J.-X., Participation of Inclusion Complexes in the Surface Adsorbed Layer in Mixtures of α-Cyclodextrin and Cationic−Anionic Hydrogenated and Fluorinated Surfactants: A Surface Tension Proof. Journal of Chemical & Engineering Data 2011, 56 (4), 1423-1432.
12. Zhou, H.; Xing, H.; Gou, Z.; **Yu, H**.; Xiao, J., Surface activity, wetting and foaming properties of trialkyl ammonium perfluorooctanoate China Surfactant Detergent & Cosmetics 2010, (5), 320-325.
13. Zhou, H.; Xing, H.; **Yu, H.**; Wu, J.; Xiao, J., Interactions between sodium perfluoro butane sulfonate and octyl triethylammonium bromide. Chinese Journal of Applied Chemistry, 2010, (5), 572-578.